CHEMICAL REVIEWS

pubs.acs.org/CR

Review

Enzymes' Power for Plastics Degradation

Vincent Tournier,[‖] Sophie Duquesne,[‖] Frédérique Guillamot, Henri Cramail, Daniel Taton,* Alain Marty,* and Isabelle André*

Cite This: https://doi.org/10.1021/acs.chemrev.2c00644

Read Online

ACCESS | Metrics & More | Article Recommendations

ABSTRACT: Plastics are everywhere in our modern way of living, and their production keeps increasing every year, causing major environmental concerns. Nowadays, the end-of-life management involves accumulation in landfills, incineration, and recycling to a lower extent. This ecological threat to the environment is inspiring alternative bio-based solutions for plastic waste treatment and recycling toward a circular economy. Over the past decade, considerable efforts have been made to degrade commodity plastics using biocatalytic approaches. Here, we provide a comprehensive review on the recent advances in enzyme-based biocatalysis and in the design of related biocatalytic processes to recycle or upcycle commodity plastics, including polyesters, polyamides, polyurethanes, and polyolefins. We also discuss scope and limitations, challenges, and opportunities of this field of research. An important message from this review is that polymer-assimilating enzymes are very likely part of the solution to reaching a circular plastic economy.

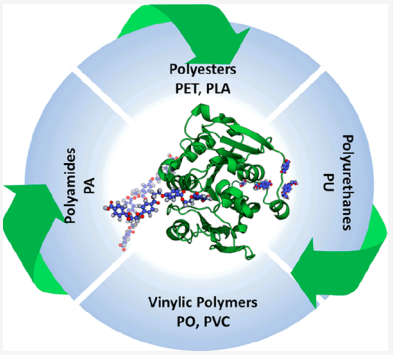

CONTENTS

Special Issue: Bridging the Gaps: Learning from Catalysis across Boundaries

Received: September 19, 2022

1. INTRODUCTION

1.1. Interest and Importance of Polymeric Materials

2020 was the celebration of the centennial anniversary of the first article published by Hermann Staudinger introducing the concept of polymerization.[1] Today, polymeric materials, which are most often coined as "plastics", have become ubiquitous in our modern way of living. They indeed address our needs for energy and new technologies, for construction, health, housing, clothing, packaging, transport, communication, and for our well-being in general. The worldwide polymer market reaches more than 500 million metric tons (Mt) per year, which not only comprises functional and structural polymers (approximately 23 Mt and 370 Mt, respectively), but also rubber products (30 Mt) and man-made fibers as well (>80 Mt). Plastic production has increased by roughly 35% in the past decade and is expected to grow to 700 Mt in 2030, representing 80 kg of plastics per human being.[2] In the past two decades, plastic demand has increased at a rate of approx 5% every year (Figure 1A). Since the 1950s, almost 9 billion tons of plastics have been manufactured, of which approximately 80% has been landfilled, 10−12% has been incinerated, and less than 10% (600 Mt) has been recycled. Figure 1B shows the global generation of plastics in 2019. Roughly 20% of plastics were produced in Europe, while China now appears as the leading plastic producer, accounting for 29% of the total global production. Figure 1C shows the distribution of plastics use in Europe by application area. Unsurprisingly, plastic production is mainly intended for the packaging sector (food and nonfood) accounting for 40% of consumption, far ahead of the automotive, building and construction, electrical and electronic devices, and all other applications.

As far as their physical properties, and in particular their thermomechanical properties are concerned, although this is misnomer, polymeric materials can be divided into three main types, including thermoplastics, thermosets, sometimes called thermosetting plastics, and elastomers.[4] These three families eventually distinguish one from each other by their response to mechanical stress, temperature, and chemical structures (see next section). In fact, elastomers, also known as rubbers, should not be considered as plastics strictly speaking, as they represent a very special class of polymeric materials. Elastomers indeed exhibit a high capability for large elastic deformation under stress, namely, they can be stretched sometimes over a few hundreds of % of their original length, with no deformation.[4−6]

If plastics have conquered so much our daily life, representing most consumed synthetic products in the world, it is mainly because they exhibit remarkable chemical diversity and functionalities, including elasticity, lightness, impact resistance, thermal and electrical conduction, insulating properties, etc.[4−8] In addition, their production cost remains relatively low. 2020 has also seen the entire planet facing the health crisis due to the Covid-19 pandemic. In this context, polymeric materials have shown all their interest but also their limitations. Plastic-made protective or medical equipment, such as face masks, gloves, catheters, protective glass, etc., enable to keep safe or cure millions of people. In the forthcoming global combat against viruses, polymeric materials will continue to play a key role.

Polymers are barely used as such in a given application: they are formulated, processed, and manufactured in the presence of multiple and variable proportions of specific additives, such as plasticizers, antioxidants, pigments, compatibilizers, flame retardants, lubricants, antimicrobial agents, or fillers.[9,10] Obviously, the molecular and macromolecular characteristics of the polymer matrix, sometimes called resin, play a key role in the targeted applications. In practice, the additives are not easily recovered as they are intimately integrated within the polymer matrix. Formulation and processing operations aim at optimizing the performance and physical-chemical properties of polymers. Polymeric materials can also result from the blending of different resins or are in the form of laminates. The resulting materials correspond to what are commonly called "plastics" or "elastomers", as mentioned above. Therefore, it is important to keep in mind that chemical structure and composition of plastics are highly heterogeneous in essence, while research efforts on polymer recycling and/or polymer design most often focuses on one type of polymer chains and not on the complex structure of plastics. At the end, the real content in polymeric chains in a plastic can range from less than 10% to almost 100%, depending on the targeted usage. This heterogeneity should be considered when targeting the end-of-life management and the recycling of this plastic and the perspective to develop scalable and economically viable recycling processes.[11]

1.2. Some Definitions about Polymers, Main Features and Possible Classifications

There are different ways to classify polymers, according to (i) their origin (naturally occurring vs synthetic polymers), (ii) the polymerization method from which they are derived (chain vs step-growth polymerization), (iii) their cost-performance ratios (e.g., commodity vs high performance plastics), and (iv) their structure and the dimensionality of their constitutive chains.[4−7] In the latter case, and as mentioned above, one can distinguish between thermosets, thermoplastics, and elastomers. Thermosets refer to dense three-dimensional (3D) networks that prove infusible and insoluble materials because of an irreversible curing process into a permanent shape. Thermosets cannot be easily recycled due to their permanently cross-linked structure, making them thermally, mechanically, and chemically resistant. A few common thermosets include formo-phenolics, polyepoxides, most of the polyurethanes, or cross-linked materials deriving from unsaturated polyesters. In contrast, thermoplastics are free of covalent bonds between polymeric chains, i.e., they are made of linear chains, enabling them to be potentially recycled. There are two main categories of thermoplastics, namely, amorphous and semicrystalline thermoplastics. The former usually correspond to transparent materials due to the random arrangement of the constitutive chains. Examples of fully amorphous polymers include polystyrene (PS), poly(methyl methacrylate) (PMMA), poly(vinyl chloride) (PVC), or polycarbonate of bisphenol A (PC). For instance, PS and PVC are sought for their resistance at the solid state (high T_g), while polybutadiene is used for its rubber elasticity (low T_g). Semicrystalline polymers are characterized by a degree of crystallinity (X_c) corresponding to the relative content between regularly arranged, cohesive, and organized crystalline domains and nonorganized amorphous domains. These confer semicrystalline materials mechanical reinforce-

https://doi.org/10.1021/acs.chemrev.2c00644
Chem. Rev. XXXX, XXX, XXX−XXX

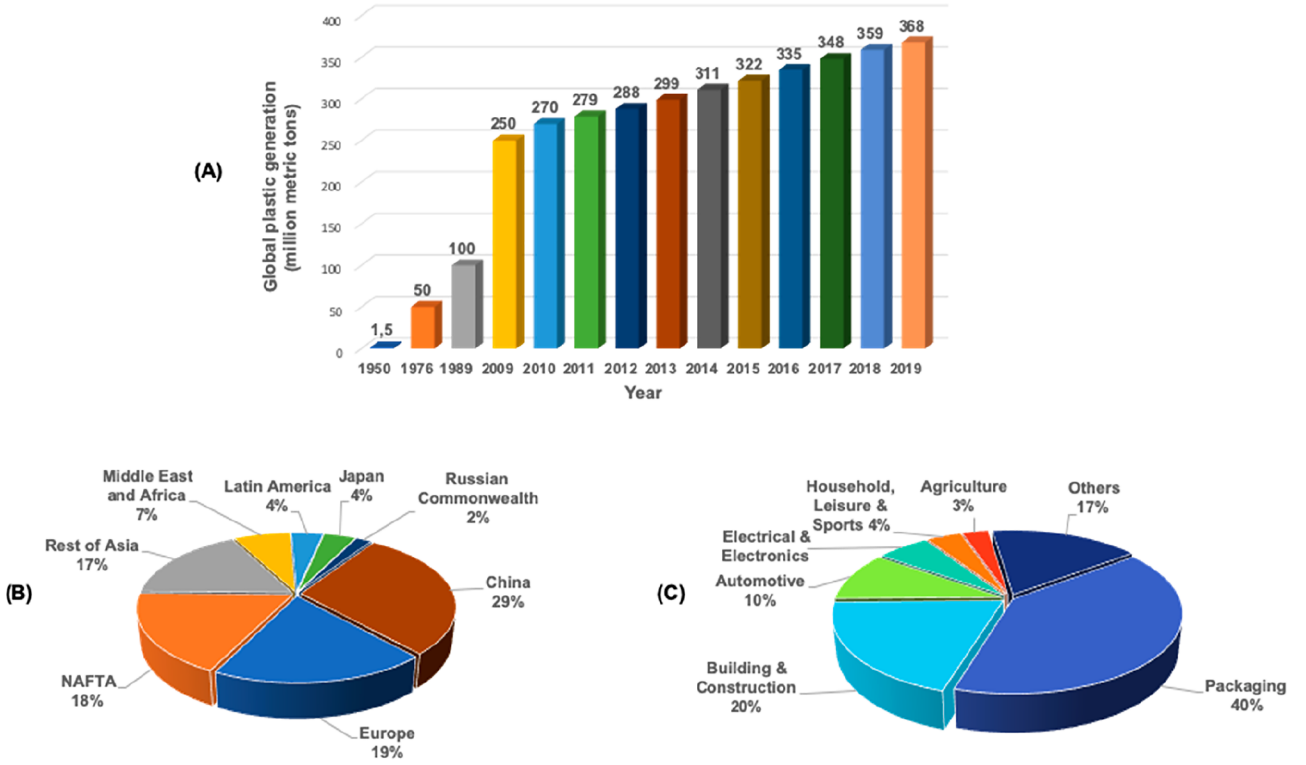

Figure 1. (A) Steady increase in global plastic production during the past 70 years; (B) global production of plastics by region; (C) plastics production by sector in Europe. NAFTA = American Free Trade Agreement Nations, including Mexico, the United States, and Canada, Adapted with permission from ref 3. Copyright 2021 Wiley-VCH.

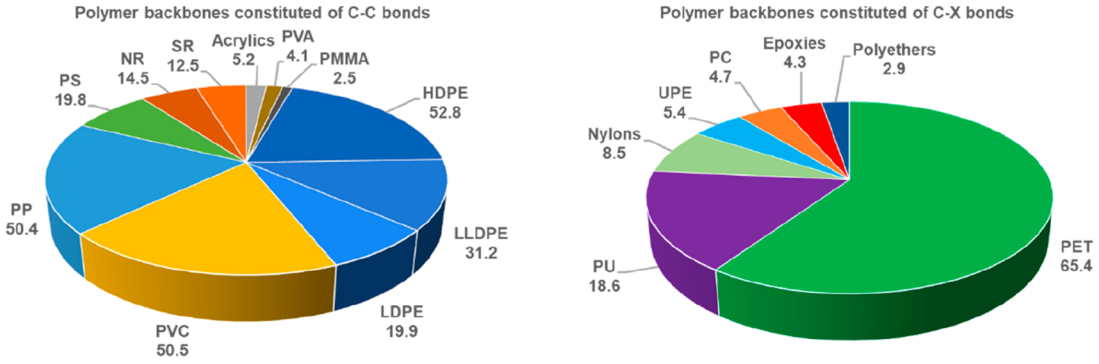

Figure 2. Annual global market size of main plastics in million metric tons (Mt) per year. (left) Polymers constituted of C−C bonds in their macromolecular backbone; (right) polymers linked by C−N and C−O bonds. HDPE = high density polyethylene; LDPE = low density polyethylene; LLDPE = linear low density polyethylene; PVC = poly(vinyl chloride); PP = polypropylene; PS = polystyrene; NR = natural rubber; SR = synthetic rubber; PVA = poly(vinyl alcohol); PMMA = poly(methyl methacrylate); PET = poly(ethylene terephthalate); PU = polyurethanes; UPE = unsaturated polyesters; PC = polycarbonate. Data correspond to years 2016−2019 and were taken from ref 11.

ment and impact resistance while restricting polymer mobility and reducing the permeability to small molecules such as liquids and gas. Typical examples of semicrystalline polymers are (linear) low-density and high-density polyethylenes (LDPE, LLDPE, and HDPE, respectively), isotactic polypropylene (iPP), poly(ethylene terephthalate) (PET), or polyamides (PA).

Another view for classifying polymers from a structural viewpoint is as follows.[11−13] Polymer backbones are most often either linked by sp^3-hybridized C−C bonds or are constituted of functional groups (oxygenated, chlorinated, etc.), i.e., polymers containing C−X linkages (X = O, N in most cases), which mainly define their properties of use (Figure 2). Table 1 summarizes the most prevalent synthetic polymers categorized by polymers linked by C−C bonds and polymers with C−N and C−O-based motifs, along with their chemical structure, properties, and common uses. The materials within each class are further ordered by their global annual consumption amounts.

The glass transition temperature (T_g) and potential for crystallization are among the most important properties to be considered for the final application of the constitutive polymer. Thus, polymer backbone that is flexible can relax quickly, and is characterized by a much lower T_g than room temperature, for applications for instance as rubber or as polyethylene-based plastic bags. In contrast, rigid polymer backbone will relax on longer time scales, giving high T_g materials. All synthetic

https://doi.org/10.1021/acs.chemrev.2c00644
Chem. Rev. XXXX, XXX, XXX−XXX

Table 1. Polymer Constituting the Main Plastics to Be Degraded

Polymer	Abbreviation and code	Chemical Structure	Major uses; common commercial products	T_g (°C)[a]	T_m (°C)[b]	Density (g/cm^3)
Poly(ethylene terephthalate)	PET 1	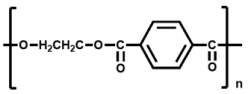	Packaging food and beverages; drink bottles, cups, food containers, textile fibers	80	> 250	1.38-1.40
High-density polyethylene	HDPE 2		Packaging; grocery bags; containers for shampoo, motor oil, detergent bleach	~ -100	135	0.93-0.97
Poly(vinyl chloride)	PVC 3		Building; pipeline tubes, cables, garden furniture, fencing and carpet backing	60-70	-[c]	1.10-1.45
Low-density polyethylene	LDPE 4		Packaging; bags, wrapping films, trays, computer components	~ -100	90-110	0.91-0.94
Polypropylene	PP 5		Packaging; bottle caps, luggage, dishware, furniture, appliances, car parts	-15-18	130-170	0.90-0.92
Polystyrene	PS 6	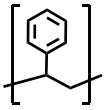	Packaging and building; carryout containers, trays, cups, foam packaging	60-110	-	0.96-1.04
Polyurethanes Polycarbonates, Polyesters, …	Others 7	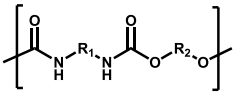	Diverse applications; Multilayer packaging, some food containers, CD's, DVD's, safety glasses	Various	Various	

[a] T_g: glass transition temperature [b] T_m: melting temperature [c] The T_m value of commercial PVC can range from 110 °C to 250−260 °C, depending on the size of the crystallites. The melting and processing behavior of PVC have been discussed in ref 14.

polymers possess a T_g value that is characteristic of the amorphous regions.[4−7]

Polymer chains are of various length, consisting of a few tens to several thousands of repeating units, which make related materials so long-lasting. Namely, polymer molar masses (also called polymer molecular weights), i.e., the number-average molar mass, M_n, the weight-average molar mass, M_w, or the viscometric average molar mass, M_v, which can range from a few thousands to sometimes millions of grams per mole, are key factors that define the properties of the polymer. Thus, increasing the molecular weight gives higher T_g materials. Other structural parameters having a determining role on the macroscopic properties and final application and, consequently, on its ability to be deconstructed and/or recycled, include molecular weight distribution (called dispersity, $Đ$), chemical nature, stereoregularity (tacticity), degree of branching, and/or degree of cross-linking (topology).[4−7]

Topology effect can be best illustrated by the two architecturally different polyethylenes, namely, LDPE and HDPE. Due to the existence of both short and long chain branches in its structure, enabling strain hardening during extensional or elongational flows, LDPE is an ideal candidate for film-forming applications (e.g., plastic bags). In contrast, HDPE exhibits an essentially linear structure and is almost free of branchings. Therefore, its extent of crystallinity is much higher than that of LDPE, which makes HDPE well-adapted for applications as rigid flasks and containers. On the other hand, it is important to distinguish between topologically branched and cross-linked polymers. The former materials remain soluble with, eventually, an improved solubility, relative to linear polymer analogues of same molecular weight. Conversely, cross-linked polymers are 3D networks that do not flow as they are not soluble in any solvents and cannot be reprocessed. Both thermosets and elastomers, e.g., resulting from vulcanization of polydienes, are typical examples of insoluble 3D polymeric networks. Therefore, the knowledge of most of (macro)molecular parameters, such as T_g, T_m, M_n, $Đ$, and some essential chemical and physical properties of the polymers, such as composition, solubility, and thermomechanical properties, are paramount in the perspective of conducting degradability and/or recycling studies.

A great part of plastics, namely, more than 85% fall into seven categories defined by the Society of the Plastics Industry.[2−5,7−13,15] In this frame, one can find the logo of three triangular arrows, called the Möbius strip, with a code number from 1 to 7 in the center, meaning that the plastic is potentially recyclable (Table 1). These codes are supposed to facilitate plastic sorting for the aforementioned recycling (Table 1). The number indicates the specific type of plastic and is used in the following manner: PET (1), HDPE (2),

https://doi.org/10.1021/acs.chemrev.2c00644
Chem. Rev. XXXX, XXX, XXX−XXX

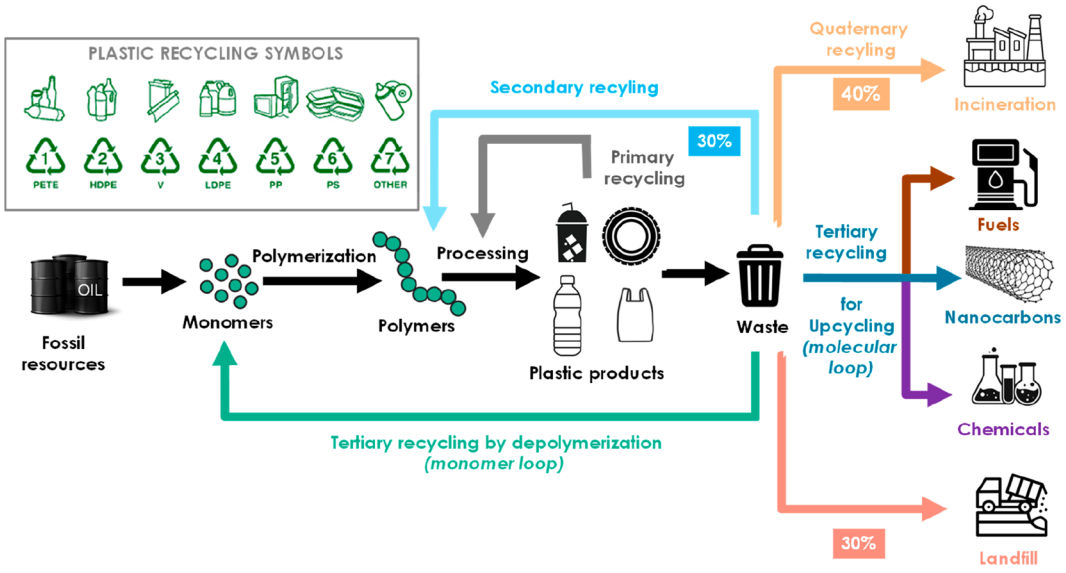

Figure 3. Life cycle of polymeric materials and main recycling technologies.

PVC (3), LDPE (4), PP (5), PS (6). Code 7 is finally used to cover all other types of potentially recyclable plastics, e.g., polycarbonates (PC), polyurethanes (PU), polyamides (PA), and bioplastics such as polylactide (PLA), PMMA, or polyesters different from PET. It is important to note that most of these plastics have long been considered as neither biodegradable nor compostable, with the exception of PLA and now PET (see further).

1.3. Environmental Pollution by Persistent Plastics

Most plastics are still designed mainly for their performance and much less for their degradability and recyclability. Plastics have thus become a threat because of their environmental impact and an inappropriate management of their end-of-life as well.[11−13,15,16] The high chemical stability of the macromolecular structure that make plastics so valuable in many applications is also an obstacle to convert them into new products. Current methods that enable to transform polymeric constitutive chains are indeed poorly selective and very energy demanding. Seeing plastic waste in the environment has thus given the public, and the media, a very negative perception of plastics. Again, this should not overshadow the many benefits that these materials provide: for transportation, clothing, entertainment, health and protection, food without waste, and, more generally, for everyday well-being. Scientists now have a key role to play in finding a solution to the problem of "white pollution".[3,11−13,15−19]

Plastics are typically designed to have a service life of 1−50 years. However, a large part of plastics is for short-term single-use packaging for food, beverages, etc. Of the ∼460 Mt produced in 2019, 40% was for single-use products composed of PE, PP, and PET.[11,12,20,21] However, all plastics are not intended for ephemeral use but remain commonplace for a given period of time in our homes, offices, etc. Electronic equipment, car parts, household appliances, shoe soles, sport equipment, food containers, reusable water bottles, pens, textiles, and other objects are all examples of the perennial use of plastics in our daily lives. Last but not least, the plastics industry employs millions of people all over the world (e.g., more than 1.6 million people in Europe, over 60 000 companies (mostly SMEs), with a turnover of over 360 billion euros in 2018). Yet, the current polymer economy is essentially linear.[2,3,11−13,15−19]

More than a million disposable plastic grocery bags made from fossil fuel are produced per minute worldwide. Some plastics can remain in the environment for several hundreds of years, depending on the type of plastic and its ecosystem.[15,16] During this time, they can be ingested by animals and/or transformed into microparticles and then nanoparticles, whose impact on human health remains uncertain. Paradoxically, indeed, the chemical inertness that makes polymeric materials so stable is also their major drawback, as it is challenging to break them down. For a very long time, plastics were not designed to be degraded until the relatively recent awareness of the problem of their environmental footprint. Most commodity plastics are thus recalcitrant to degradation due to the high chemical stability of their constituting units. This is particularly true for the most prevalent synthetic polymers, namely, those in which polymer chains are all linked by sp^3-hybridized C−C polyolefins (Table 1). In this regard, resistance of synthetic polymers to degradation is reminiscent of that of lignocellulosic biomass in biofuels production, in the sense that plastics, as plant cell walls, are structurally and chemically heterogeneous composites. But, to do without plastics in our daily life is simply illusory, and "elimination of plastics", as advocated by various associations, remains utopian. Plastics are not only comfort tools, they are useful too, from a health and safety point of view, as already mentioned. It is not so much the plastics industry that needs to be destabilized, but rather the end-of-life of these materials that needs to be better managed and optimized. Regulations have been boosted over the past few years toward this end. Thus, to achieve the objective of "plastics circularity", next challenges in polymer science are to develop alternative polymer synthesis methods, and in parallel, more efficient polymer recycling technologies. In the former case, upstream actions and innovative initiatives are needed to deliver polymers that can be better designed for recyclability, reducing our reliance on fossil sources, and increasing their overall biodegradability. These more sustainable, degradable, and easily recyclable polymers are aimed to serve as replacements for nondegradable petroleum-based plastics. On the other hand, through downstream actions with the

https://doi.org/10.1021/acs.chemrev.2c00644
Chem. Rev. XXXX, XXX, XXX−XXX

implementation of much more efficient recycling technologies for mass-produced plastics, also seem essential. Such considerations to build a better plastic future have been taken into account when the partners of the Mix-Up consortium evocated the "6-R" principles (rethink, refuse, reduce, reuse, recycle, replace).[22]

1.4. Recycling Technologies of Commodity Plastics

Approximately 25% of postconsumer waste plastics are landfilled and thus lose their intrinsic value. Another important fraction (roughly 42%) of plastic waste is incinerated for energy recovery. Eventually, less than 30% of plastic waste is collected for recycling and reused in closed loop.[3,11−13,15−19] In fact, recycling options often appear complex and/or costly and/or too energy intensive. As each constitutive polymer of plastics show specific physicochemical properties, the recycling of these plastics cannot be viewed as a one-size-fits-all approach, but rather must be analyzed on a case-by-case basis. A range of technical complexities affect recycling rates, including aspects related to intrinsic chemical or compositional characteristics, such as the presence of additives, fillers, contaminants, including dust, metallic residues, or traces of poly(vinyl alcohol) (PVA) or PVC that can leach acidic catalysts, promoting for instance acidolysis or hydrolysis of PET during extrusion, or biological contaminants, as well as more logistical aspects related to the collection, sorting of these raw materials, their possible hygienization, etc. As mentioned, not all plastic materials should be recycled, and the environmental benefits of recycling must be assessed for each type of material across the entire value chain. Clearly, with the notable exception of PET as detailed further in this review, current recycling approaches do not enable yet a circular plastics economy.

Recycling technologies can eventually be divided into four subcategories that are differentiated by the nature of the recycling processes implemented and the nature of the final products (Figure 3). These methods for polymer recycling are termed primary, secondary, tertiary, and quaternary recycling.[11−13,15−19,23]

In primary recycling, postindustrial scrap polymer feedstocks generated during plastic manufacturing in plants are mixed with the virgin polymer. The resulting mixture is further processed mechanically without any loss of properties, representing a real "closed polymer-to-polymer loop recycling" approach.[24] However, only plastics of the same type can be recycled in this way, and this is achieved with low extent of waste to retain the quality of the virgin plastic product. Primary recycling thus deals with postproduction materials and not with, for instance, postconsumer or contaminated waste. A relevant example is that of PET, which can undergo primary recycling to regenerate recycled PET that can be reused for the production of new containers (e.g., bottles).

Postconsumer plastic waste is treated by secondary mechanical recycling, also referred to as mechanical recycling process, after collection, sorting, and cleaning, producing new plastics with less demanding properties. Consequently, polymers thus recycled are used for downgraded applications and are ultimately landfilled. At the end, both primary recycling and secondary recycling are based on a mechanical melt process.[3,11−13,15−19,23,24] Secondary recycling, and eventually primary recycling as well, require less than half the energy used to generate new plastics, hence both prove less energy-demanding than producing plastics from petroleum products. However, secondary recycling produces plastics of compromised mechanical quality after a few melt cycles compared to the "virgin" plastic. This is due to side reactions such as radical chain scissions and/or couplings/cross-linkings. In addition, pure and clean plastic waste is necessary in these recycling processes. Residual contaminants can diffuse during the melting process and can contribute to alter the properties and the aspect of the recycled polymers, such as elongation at break, toughness, melting point, and color. For these reasons, secondary recycling is often reckoned as a "downcycling" method, the number of reprocessing cycles being dependent on the evolution of the polymer properties. In the particular case of PET, such variations in molecular weights during mechanical reprocessing can be alleviated, in particular by a solid-state postpolycondensation and/or the addition of chain extenders[24] (e.g., oxazolines, isocyanates, epoxides, lactams, hydroxyls, carboxylic acids, phosphites, and phosphates). Therefore, further purification through selective solvent-based extractions can aid achieving chemically pure recycled materials (e.g., the Polyloop process by Solvay for PVC or the Creasolv and PureCycle processes for various plastics).[25−27]

In tertiary recycling, (thermo)chemical or (bio)catalytic processes are implemented to degrade polymer waste as selectively as possible, breaking down the macromolecular structure into value-added smaller molecule products.[3,11−13,15−19,23] These include monomers (monomer loop, Figure 3) or oligomers, and molecular feedstocks, such as syngas (CO and H_2), that can be further employed to design new materials (molecular loop, Figure 3). Typical processes are by hydrolysis, for instance, in the presence of chemical catalysts or enzymes, pyrolysis, and gasification. Depolymerization of plastic waste back to the original monomers, which can be readily repolymerized to produce the same polymer, is likely the most sought-after way of tertiary recycling.[28−30] This "chemical recycling to monomer" (CRM) method indeed allows operating in closed loop under rather mild conditions in some cases. In particular, polar step-growth polymer substrates consisting of C−N or C−O-based units, e.g., polyesters, such as PET, polyamides, and polyurethanes, have been shown to be depolymerized. This is not surprising as these polymers contain carbonyl moieties that can easily undergo chemolysis, for instance, using nucleophiles, thus enabling relatively controlled degradation of the polymer chains. In contrast, chain-growth-derived C−C-based and unfunctionalized commodity polymers, such as PE or iPP, requires energy-intensive pyrolysis, i.e., at high temperature (>400 °C) and/or pressure, and the use of designed transition metal-based catalysts. These severe conditions prove unselective, yielding a broad spectrum of species, including waxes and fuels of different molecular weights. In this regard, and although innovative approaches in this area have been recently reported, pyrolysis is still viewed as a downcycling and not as recycling or upcycling method, as the energetic, environmental, and commercial viability of this process have been questioned. These recycling technologies have been reviewed, discussing possibilities to increase the efficiency of used catalysts or polymer functionalization prior to the thermolysis process.[20,29−38]

Chemical upcycling, sometimes called repurposing, of polymers aims at selectively converting discarded plastics into higher value chemicals, e.g., fuels, or surfactants, or nanostructured carbon-based materials.[33,35,39−42] Chemical upcycling thus holds great promise to reduce our dependency

https://doi.org/10.1021/acs.chemrev.2c00644
Chem. Rev. XXXX, XXX, XXX−XXX

to fossil resources, to save energy, and to eventually reduce the environmental impact of plastic waste.

In addition to some biosynthesized polymers like cellulose or chitin, some synthetic polymers can be biologically degraded into small molecular fragments by microorganisms producing enzymes.[11] Several reviews focused on biological upcycling and valorization of plastic waste by microorganisms or enzymes have been published very recently.[22,31,36−38,43] Analysis of this literature shows, as it will be discussed in detail in this review, that (i) enzymatic degradation of synthetic polymers is generally slow, (ii) the scope of polymer substrates is still limited to certain polymers, again those featuring carbonyl groups in their main chain (PET, PLA, PA), and (iii) enzymes are poorly tolerant to harsh reaction conditions. For instance, enzymatic biocatalysis of plastic is expected to primarily take place under aqueous conditions. As most polymer plastics are not soluble in water, deconstruction of recalcitrant polymers by enzymes should proceed via an interfacial mechanism, if an analogy can be made with the degradation of naturally occurring biopolymers. Many efforts are thus directed toward improvements of enzyme stability to increase the accessible surface area for enzymatic depolymerization of synthetic polymers. Not only do processing conditions matter for efficient biocatalytic recycling, but also structural parameters of the polymer substrate (T_g, T_m, molecular weights, etc.), as already mentioned.

Energy recovery via incineration of postconsumer plastic waste is considered as the fourth recycling technology for end-of-life polymer materials.[2,23,24] This recycling option leverages the high calorific values of plastic waste to produce carbon dioxide and steam energy in the presence of oxygen. Some polymeric materials can only be recycled by this way, for example, those contaminated with biological agents (e.g., viruses, blood, etc.) or complex materials made of multiple layers or incorporating large proportions of additives, for which pretreatment options (separation of the various components from each other) is too costly. However, quaternary recycling recovers only partly the energy used to produce the plastics. In addition, incineration of waste causes serious environmental issues and contributes to greenhouse gas emissions, as it generates several hazardous pollutants and volatile organic compounds and necessitates subsequent cleaning of the incinerator.

1.5. Methods to Probe Plastic (Bio)degradation

Monitoring the degradation process of a polymer is essential to select the most effective conditions and routes. Various analytical methods have been implemented, and they are briefly presented hereafter. First, visual estimation of the macroscopic and morphological state of the material, before and after treatment according to one or the other process discussed above, can first account for some evolution, at least qualitatively: presence of cracks in the sample, change in color, size, and/or shape, etc.[11] A step further, although remaining qualitative, consists in observing whether biofilms can form on the plastic surface upon exposing that plastic either under terrestrial conditions in soil, or under aqueous conditions, in particular inside the marine water. This method helps to anticipate the ability of a plastic for microbial degradation and provides a primary indication that biodegradation can occur.

More accurate assessment about the polymer morphological evolution can be obtained by microscopic analysis techniques, such as scanning electron microscopy (SEM) or atomic force microscopy (AFM). Obviously, many characterization techniques, specific or not of polymeric materials, can provide information about the progress of the biodegradation process by probing the properties of the polymer in relation with its morphology, its dimensional state, and its intimate structure at different scales of observation and analysis (Figure 4). These

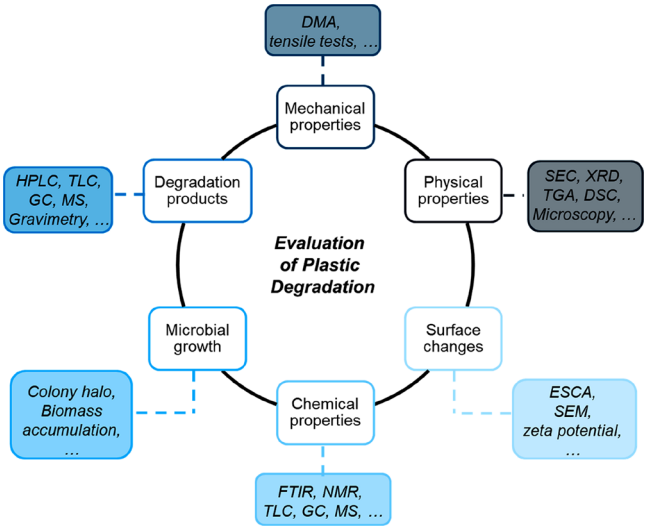

Figure 4. Analytical techniques for monitoring the extent and nature of plastic degradation. DMA, dynamic mechanical analysis; SEC, size exclusion chromatography; XRD, X-ray diffraction; TGA, thermogravimetric analysis; DSC, differential scanning calorimetry; ESCA, electron spectroscopy for chemical analysis; SEM, scanning electron microscopy; FTIR, Fourier transform infrared spectroscopy; NMR, nuclear magnetic resonance; TLC, thin-layer chromatography; GC, gas chromatography; MS, mass spectrometry; HPLC, high performance liquid chromatography.

techniques are routine or more sophisticated and include size exclusion chromatography (SEC), differential scanning colorimetry (DSC), dynamic mechanical analysis (DMA) and other mechanical tests, static and dynamic light scattering (SLS and DLS), X-ray photoelectron spectroscopy (XPS), contact angle measurements and water uptake, Fourier transform infrared spectroscopy (FTIR), ultraviolet−visible (UV−vis) spectroscopy, X-ray diffraction (XRD), or nuclear magnetic resonance (NMR) spectroscopy.[11] For instance, as biocatalytic degradation is expected to cause changes in the chemical structure of the polymer, this can be monitored by FTIR, and/or NMR, and UV−vis spectroscopy, through the appearance and/or disappearance of functional groups. On the other hand, polymer degradation is reflected by a steep decrease of the molecular weight, which can be evidenced by SEC before and after the enzymatic treatment. This is also most often accompanied by weight loss, which can be monitored by gravimetry.

In addition, various analytical methods can be implemented to screen and characterize plastic degrading enzymes and microorganisms. The so-called halo method, which is based on the visualization of a clear halo zone around the spotted sample on immobilized insoluble substrate due to release of soluble monomers, represents around half of the utilized methods. A more quantitative approach consists in following the decrease in turbidity of an emulsion of polymer by visible spectroscopy, upon incubation with a plastic degrading enzyme. The latter method, however, might impact the crystallinity of the treated

https://doi.org/10.1021/acs.chemrev.2c00644
Chem. Rev. XXXX, XXX, XXX−XXX

polymeric sample while not providing any information about product release (monomer or oligomers). Evaluation of weight loss is the other widely used technique.[44] This can be carried out either by precision balance, QCM-D, or SPR.[45] Monitoring released products is a much more accurate and quantitative method, although it is limited to quantify soluble fractions only, thus missing the oligomer formation and endoworking enzymes. This can be followed by more classic analytical methods, including HPLC NMR, titration of released acidic functions (e.g., in the case of PLA or PET depolymerization), but it does not provide any information about the type of depolymerization products. Additional pH variation by monitoring the reaction supernatant can also be instructive.[46]

More specific to PLA, the total organic carbon (TOC) value can be used as an indicator of the content of the water-soluble PLA oligomers and monomer formed by hydrolysis. As a means to evaluate the hydrolysis of polyester films, optical waveguide light mode spectroscopy (OWLS) is based on sensing change in the refractive indices across the sensor-solution interfaces. Other methods qualitatively probing change of the polymer properties, e.g. by viscometry,[47] FTIR,[48] SEC, SEM, AFM[49−53] can be employed. Finally, alteration of the mechanical properties of the polymer by an enzyme can be established by tensile strength and/or stress at break and/or Young modulus measurements.

1.6. General Considerations on Enzymatic Degradation of Polymers

The past decade has witnessed a considerable increase in the number of initiatives by academics and industries for polymer-recycling processes. The development of more efficient (bio)catalytic chemical recycling or upcycling processes of commodity plastics is booming, both in research groups from academia and in industry. Current efforts in this direction appear promising in view of developing closed loop recycling technologies that can be commercially competitive with regard to traditional polymer manufacturing methods. In this context, possibilities to degrade commodity plastics using a biocatalytic approach have been intensively investigated. As already mentioned, however, and as detailed hereafter, this has only been successfully conducted in the case of polymers containing relatively easy to hydrolyze chemical bonds, notably ester or amide moieties, as in the case of PET, PLA, and some PU and PA, which can be recycled or upcycled into well-defined oligomers or monomers or higher-value products. The biorecyclability of polymers can thus be directly correlated to their constitutive chemical bonds.

Enzymes are highly efficient biocatalysts that offer numerous advantages over chemical processes, notably thanks to (i) their high catalytic power, providing acceleration by up to 10^{20} of each elementary reaction step, (ii) their operation in milder reaction conditions (temperature, pH and pressure), (iii) their high selectivity, and (iv) low environmental impact (less energy consumption, reduces waste generation). Enzymes can be thought of as renewable and biodegradable catalysts that can easily be implemented through inexpensive and environmentally benign fermentation processes. Many industries have already exploited the advantages of enzyme catalysis for a broad range of applications in the pharmaceutical, food and beverage, detergent, biofuel, and fine chemistry fields. Enzymes can improve industrial chemical processing by simplifying the conventional chemical synthesis routes and the process economics. Furthermore, biocatalytic processes relying on the utilization of enzymes in their purified form, as part of a cell lysate, or whole cells provide more sustainable and renewable solutions to produce chemical synthons, materials, and energy from waste, feedstocks, or bioresources, and enabling a circular bioeconomy. The global market for enzymes in industrial applications is expected to grow from $6.4 billion in 2021 to $8.7 billion by 2026.[54] This market projection emphasizes the need to discover or to engineer efficient enzymes that can enter biocatalytic processes further optimized at different levels (catalytic activity, stability, expression efficiency, fermentation yields, immobilization, reuse of and recycling of catalysts, etc.) to fulfill industrial operation constraints and commercial needs.

The first microorganism degrading synthetic polymers was reported nearly 50 years ago, with the degradation of polycaprolactone by fungus *Aureobasidium pullulans*.[55] Yet, research in the field has remained quite limited until 2000. Over the past 20 years, with the fossil fuel limitations and the plastic pollution crisis, the research on enzymes or microorganisms able to degrade synthetic polymers has regained considerable interest,[56] even necessitating the development of databases to compile the flood of data and their exploitation.[56,57] It is nowadays well admitted that depolymerization mediated by free enzymes is emerging as an efficient and sustainable alternative for plastic treatment and recycling.[22] However, this approach remains limited to some polyesters (PET and PLA) and the finding of active enzymes for PE, PP, PVC, ether-based PUR, PA, or others still represents an urgent challenge that needs to be tackled.[43] In the following sections, we review depolymerization and controlled degradation methods of polymers utilizing different classes of enzymes. These include serine hydrolases (cutinases (EC 3.1.1.74), lipases (EC 3.1.1.3), and carboxyl ester hydrolases (EC 3.1.1)), oxidases (laccases, peroxidases), etc., depending on the nature of the polymer and the catalytic reaction envisaged. Besides the use of enzymes and microorganisms available in Nature, we will also present and discuss how directed evolution and structure-based engineering have enabled to improve catalytic activity and stability of enzymes, substrate binding in the active site and onto enzyme surface. Most successful approaches to develop performing enzymatic biocatalysis are often multidisciplinary, combining enzyme screening, design, and engineering to biophysical and computational techniques, to provide deeper understanding about the interrelationships between the sequence, the structure, and the function of the enzymes.

Biocatalytic chemical recycling, which is now regarded as part of tertiary recycling, is expected to lead to a transformation of the commercial recycling market, as the intrinsic value of waste materials is retained, in addition to proving energy efficient. In this review, we specifically present advances made in enzyme-based biocatalytic methods for the deconstruction of the most representative polymers. We also discuss scope and limitations, challenges, and opportunities of this field of research. Focus is placed on microbial and enzymatic degradation and/or depolymerization of the most common commodity polymers (Table 1, Figures 1 and 2), namely, polyesters (PET and PLA), and other main polymers such as polyamides (PA), polyurethanes (PU), vinylic polymers, includingpolyolefins (PO), polystyrene (PS), and polyvinyl chloride (PVC). The next section (section 2) deals first with the two polymers that have been the subject of the most enzymatic depolymerization studies, namely PET and

https://doi.org/10.1021/acs.chemrev.2c00644
Chem. Rev. XXXX, XXX, XXX−XXX

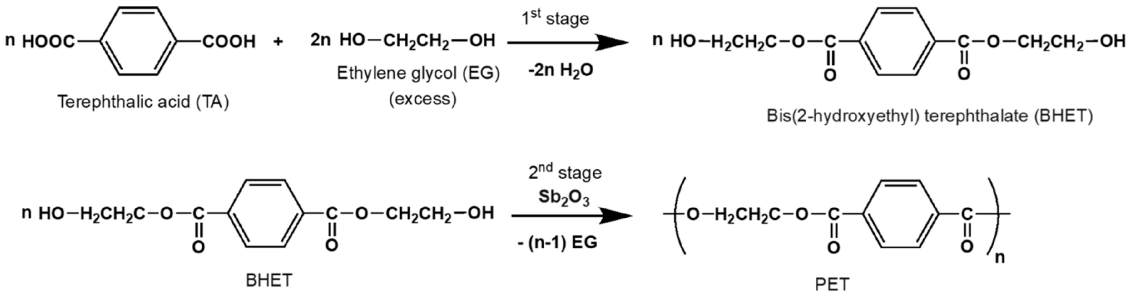

Figure 5. Industrial manufacture of PET via the BHET route.

PLA. Indeed, many enzymes have been discovered, characterized, and optimized for polyester degradation, the ester link being an easily enzyme-catalyzed broken bond. The following section (section 3) is dedicated to biocatalytic degradation of the more recalcitrant polymers, including not only PA, PU, or PUR, but also vinylic polymers, keeping in mind that only a very few (if none) enzymes have been identified yet, the C−C bond, and to some extent, the amide bond, being less accessible to an enzyme activity. Note that due to a very limited literature on the enzymatic degradability of elastomers and most of thermosets, polymers falling into these categories, such as natural or synthetic rubbers, or polyepoxides, will not be considered in this review.

2. ENZYME-CATALYZED DEPOLYMERIZATION OF POLYESTERS

2.1. Polyethylene Terephthalate (PET)

2.1.1. About PET. Poly(ethylene terephthalate) (PET) is a major polymer with about 18% of the world polymer production and is part of the so-called "big five" category with PE, PP, PS, and PVC.[58]

PET is a semiaromatic and semicrystalline polyester exhibiting high mechanical strength, good barrier properties, and high optical clarity, features that justify its main use as textile fibers and packaging. Most of the PET production (98 Mt; *IHS Market in 2021, Market Research Future in 2021 and KPC in 2022)* is for synthetic fibers (around 60%), with bottle production accounting for about 30%. In the case of textile applications, PET is referred to by its common name, polyester, whereas the acronym PET is generally related to packaging.

PET is the most recycled plastic worldwide; it can be identified by its recycling code 1. Recycled PET can be converted to fibers, fabrics, sheets for packaging, and manufacturing automotive parts. Depending on its processing and thermal history, PET may exist either as an amorphous (transparent) or as a semicrystalline material. It can be semirigid to rigid, impact-resistant, very lightweight, and makes a good gas and fair moisture barrier as well as a good barrier to solvents.

Semicrystalline PET might appear transparent or opaque and white, depending on the size of the crystal structures. About 60% crystallization is the upper limit for commercial products, except for polyester fibers. Clear products can be produced by fast cooling molten polymer below T_g to form an amorphous solid. At room temperature, the chains are frozen in place, but if enough heat energy is put back upon heating above T_g, they gain in mobility allowing crystals to nucleate and grow, a process which is known as solid-state crystallization. When allowed to cool slowly, the molten polymer forms a more crystalline material, namely, in the form of spherulites containing many small crystallites when crystallized from an amorphous solid.

Industrially, PET is manufactured via a four-step process (Figure 5). First, bis(2-hydroxyethyl terephthalate), BHET, is synthesized by esterification of ethylene glycol (EG) with terephthalic acid (TA). Transesterification of EG with dimethylterephthalate (DMT) was widely used until the 1960s, but slow reaction rates and high corrosivity rendered this process obsolete. The second and third steps are characterized by the prepolymerization of BHET and subsequent melt condensation to form low-molecular weight PET (suitable for fibers). Finally, solid-state polymerization (SSP) is implemented to access PET of high M_n suitable for drink bottles.[59−61] Antimony-based catalysts, such as Sb_2O_3 or $Sb(OAc)_3$, prove effective for PET synthesis. Two main PET grades are thus produced, namely, fiber-grade PET and bottle-grade PET, which mainly differ in molecular weight and/or intrinsic viscosity. Bottle-grade PET has a molecular weight of 24 000−36 000 g/mol, corresponding to a viscosity index (VI) between 0.75 and 1.00 dL/g, standard bottle grade having an intrinsic viscosity of 0.80 dL/g. Textile fiber-grade PET has a lower molecular weight of 15 000−20 000 g/mol, corresponding to an VI between 0.55 and 0.67 dL/g. PET fiber-grades for technical yarns, such as tire cord, have higher molecular weights, with a VI above 0.95 dL/g. For packaging films, the VI is 0.64 dL/g.

PET properties can be modulated to target specific applications through the synthesis of PET-based copolymers, namely, by copolymerizing the above monomers with other diols or diacids. A common monomer modifier for that purpose is isophthalic acid (IPA), which leads to a replacement of 1,4-*para*-linked terephthalate units by 1,2-*ortho*- or 1,3-*meta*-linkages. Compared to PET, the resulting copolymer chains are kinked, thus affecting their crystallization and eventually lowering their melting point. These copolymers are valuable for molding applications, such as thermoforming, which is used, for example, to make trays or blister packaging from co-PET films or amorphous PET sheets. Crystallization is also important in other applications where mechanical and dimensional stability are requested, such as seat belts. Cyclohexanedimethanol (CHDM) can also be used as a comonomer with EG, which will result in the modification of the crystallization process and will lower the polymer melting temperature. Such PET is referred to as PETG or PET-G for PET glycol-modified. It is a clear amorphous thermoplastic that can be injection-molded, sheet-extruded, or extruded as filament for 3D-printing. PETG can be colored during processing. For PET bottles, film, and packaging applications, around 2% IPA is added to slow down crystallization. As a

https://doi.org/10.1021/acs.chemrev.2c00644
Chem. Rev. XXXX, XXX, XXX−XXX

result, bottles are manufactured via stretch blow molding (SBM) and are both clear and crystalline enough to be an adequate barrier to aromas and even gases, such as carbon dioxide in carbonated beverages. This explains why PET bottles are less crystalline than fibers made with IPA-free PET. For fibers, high crystallinity is sought to obtain heat resistance. Diethylene glycol (DEG) can be added to improve dyeability, color pick-up of yarn or garment. CHDM can be also added for special packaging applications by small number of suppliers (e.g., SK Chemical/Eastman). In the perspective of enzyme-catalyzed depolymerization of PET, it is important to consider that the presence of comonomer units in the copolymer chain emanating from these comonomers can impact the binding of the polymer substrate to the enzyme, and consequently the catalytic efficiency of the reaction.

PET is prone to various types of degradation during processing. Main degradation processes that can occur are hydrolytic, photolytic, and most importantly, thermal. When PET degrades, several events take place, including discoloration, chain scissions resulting in molecular weight reduction, formation of acetaldehyde, and cross-links ("gel" or "fish-eye" formation). Discoloration is due to the formation of various chromophores following prolonged thermal treatment at elevated temperatures. This becomes a problem when the visual expectations for the polymer are very high, such as in packaging applications. The thermal and thermo-oxidative degradation results in poor processability characteristics and performance of the material. Again, one way to alleviate this issue is to resort to a copolymeric material, i.e., by using upstream comonomers such as CHDM or IPA. Thus, the resin can be plastically formed at lower temperatures and/or with lower force. This helps to prevent degradation, reducing the acetaldehyde content of the finished product to a quasi-unnoticeable level. Another way to improve the stability of PET is to use stabilizers, mainly antioxidants such as phosphites. Stabilization at molecular level of the material using nanostructured chemicals has also been considered.[62]

Traditionally, EG and TA are petroleum-based although the synthesis of biobased PET is possible. Bio-PET in circulation is eventually 30% biobased only, corresponding to renewably sourced EG from biomass. The perspective of producing 100% biobased PET thus remains a long-term ambition of the industry, technical constraints associated with renewable TA production still limiting its commercialization. Handling properly PET waste is thus a main concern nowadays. The thermomechanical recycling of PET is well established, but several drawbacks are associated with such a process. Recycling into bottles can only use transparent and pure PET waste. Indeed, no purification step can remove colorants, pigments, titanium dioxide, and it is not possible to use multilayers trays or bottles. It is also limited by eventual material downcycling, with ductility decreasing from 310% to 218%% after only one cycle and to 2.9% after the third cycle.[63] This necessitates recycled PET to be repurposed into lower-value products, such as fibers (72%) in carpeting, which cannot be recycled further.[63,64] Moreover, PET waste streams are easily contaminated by PVC and PLA, rendering the recycled product of low-grade quality, which cannot be mechanically recycled.[24] Nevertheless, there is no competition between thermomechanical and enzymatic recycling, the first one uses transparent bottles, whereas enzymatic recycling can use less expensive waste, colored and opaque bottles, as well as multilayer trays. In the past, the commercial viability of thermomechanical recycling relied on a high and stable oil price (>75$/barrel), but nowadays, a booming demand for r-PET creates an unprecedent price increase trend. Indeed, the r-PET market price is no more correlated to the "virgin" PET market price and is even 44% higher, reaching 2500€ per ton in March 2022 (Source: Icis in 2022).

Another strategy is the chemical recycling to monomer (CRM).[65] After purification, BHET and dimethyl terephthalate (DMT) are the main reaction products. An important limitation of this approach is that DMT is not a common monomer of the PET industry, and consequently it requires to couple a dedicated PET production unit to a recycling unit. Beyond long-term material value retention, the possibility to access higher-value products offers a potential route to decoupling PET recycling from a volatile oil market. There is already an exhaustive body of literature concerning the chemical recycling of PET.[65−69]

2.1.2. Biocatalysts for PET Depolymerization. Nowadays, enzyme-based depolymerization of PET through biotechnological processes is considered as an unambiguous alternative to chemical depolymerization of PET.[70−75] Indeed, chemical methods often require the maintenance of high temperature and pressure, as well as use of toxic reagents.[70,71] In contrast, biological recycling of PET through enzyme-based depolymerization appears to be a more sustainable solution because of mild pH and comparatively lower temperature conditions without the use of hazardous chemicals.[70,76,77] Additionally, the biological catalyst shows a very high selectivity, specifically targeting the polymer ester bonds, thus facilitating the monomers recovery (TA and EG). This can be readily achieved by discoloration, TA precipitation and crystallization, monoethyleneglycol (MEG) distillation after salt separation, and further used for synthesis of virgin PET.[71,73,78] The high specificity toward a given substrate also allows enzyme-based depolymerization to be applicable to PET recycling from blended materials (multilayer trays or sparkling water bottles containing a layer of polyamide) and mixed waste, avoiding intensive sorting.[79] As less intensive sorting of PET waste means a reduced price of the PET waste feedstock, this might be an important consideration for the economic development of such a recycling approach. On the other hand, a reduced purity of PET waste feedstock might increase the cost of post-PET depolymerization waste treatment. It is a complicated task to speculate now on the optimal sorting of PET waste, as it might only be carefully evaluated once highly advanced processes will be in operation, either at demonstration unit scale or at industrial scale.

For decades, PET has been considered as a nondegradable polymer, until Tokiwa and Suzuki reported in 1977 that some lipases, which are extracellular enzymes that usually cleave esters in oils and fats, can attack ester bonds in some aliphatic polyesters and can depolymerize such materials.[80] Nevertheless, such enzymes could not hydrolyze aromatic polyesters. The reason for the missing degradability of aromatic polyesters was later elucidated by Marten et al. These authors indeed showed that the mobility of the polymer chains in the crystalline zones controls the degradability of PET by hydrolases, e.g., lipases.[81,82] Successively, two *Thermomonospora fusca* strains were found able to hydrolyze an aliphatic-aromatic copolyester, the poly(butylene adipate-*co*-terephthalate (PBAT).[83] However, the first breakthrough in enzymatic PET depolymerization was achieved using a cutinase, namely, TfH from the actinomycete *Thermobifida fusca*. A three-week

https://doi.org/10.1021/acs.chemrev.2c00644
Chem. Rev. XXXX, XXX, XXX−XXX

Table 2. Reported PET Hydrolases from *Actinomycetota* Phylum[a]

name	sequence identity with BTA-1 (%)	sequence identity with BTA-2 (%)	alternate name compared to BTA-1 or BTA-2	source	GenBank accession	UniProtKB accession	ref
BTA-1 (TfH)[b]	100	92.3	BTA-1	*Thermobifida fusca* DSM43793	AJ810119.1	Q6A0I4	83,84,92,104
BTA-2	92.3	100	BTA-2	*Thermobifida fusca* DSM43793	AJ810119.1	Q6A0I3	83,84,92,104
Tfu_0882		99.2	BTA-2$^{K112E/S176T}$	*Thermobifida fusca* YX	AAZ54920.1	Q47RJ7	95
Tfu_0883[b]	100		BTA-1	*Thermobifida fusca* YX	AAZ54921.1	Q47RJ6	94,95,105
TfCut1		98.1	BTA-2$^{R68N/A69V/F72L/D75S/N127I}$	*Thermobifida fusca* KW3	CBY05529.1	E5BBQ2	96
*Tf*Cut2 (Cut2-kw3)[b]	99.2		BTA-1$^{S58R/T176S}$	*Thermobifida fusca* KW3	CBY05530.1	E5BBQ3	96
Cut1		99.2	BTA-2$^{K112E/S176T}$	*Thermobifida fusca* NRRL B-8184	JN129499.1	G8GER6	106
Cut2[b]	100		BTA-1	*Thermobifida fusca* NRRL B-8184	JN129500.1	Q6A0I4	106
Thf42_Cut1	97.7		BTA-1$^{S58R/T176S/T205R/A222L/K226R/S234T}$	*Thermobifida fusca* DSM44342	ADV92528.1	E9LVI0	96
TfAXE	98.9		BTA-1$^{S58R/N88S/R268W}$	*Thermobifida fusca* NTU22	ADM47605.1	E0Z5H1	97
Thc_Cut1	100		BTA-1	*Thermobifida cellulosilytica* DSM44535	ADV92526.1	E9LVH8	96
Thc_Cut2[b]		99.2	BTA-2$^{K112E/S176T}$	*Thermobifida cellulosilytica* DSM44535	ADV92527.1	E9LVH9	96
Tha_Cut1	98.5		BTA-1$^{E112P/L177P/W201R/R293C}$	*Thermobifida alba* DSM43185	ADV92525.1	E9LVH7	98
Est1[b]	83.1	85.1		*Thermobifida alba* AHK119	BAI99230.2	D4Q9N1	100,101,107
Est119 (Est2)	82.4	85.1		*Thermobifida alba* AHK119	BAK48590.1	F7IX06	100,101,107
Thh_Est	75.1	75.9		*Thermobifida halotolerans* DSM44931	AFA45122.1	H6WX58	102
Tcur1278	60.8	60.0		*Thermomonospora curvata* DSM43183	ACY96861.1	D1A9G5	108
Tcur0390[b]	60.8	61.0		*Thermomonospora curvata* DSM43183	ACY95991.1	D1A2H1	109
Cut190	64.8	65.5		*Saccharomonospora viridis* AHK190	AB728484.1	W0TJ64	110,111

[a]The sequence identities were calculated based on pairwise alignments of the mature protein sequences, either described or predicted using SignalP 6.0 signal peptide predictor online server.[103] Each mature enzyme has been compared with the first described tandem synthetic polyester hydrolases BTA-1 (TfH) and BTA-2 from *Thermobifida fusca* DSM43793, and only highest sequence identity percentage is mentioned to allocate an alternative protein name presented as a variant of the closest BTA enzyme. Amino acid numbering is performed from the full length of native BTA-1 and BTA-2 proteins (301 amino acids), regardless of their respective mature protein sequences (e.g., BTA-1 and BTA-2, 260 amino acids from position 41 to 301). [b]Higher enzyme activity described than the other one from the tandem enzymes for a specific origin.

enzymatic incubation at 55 °C with an amorphous melt pressed postconsumer PET bottle film (10% crystallinity) conclusively resulted in 50% weight loss of the aromatic polyester.[84]

Since then, numerous enzymatic catalysts able to promote PET depolymerization have been reported. Related enzymes, characterized so far as PET hydrolases, belong mainly to the esterase class (EC 3.1.1., carboxylic ester hydrolases),[85−88] for which a comprehensive database derived from their primary, secondary, and tertiary structures is maintained (CASTLE).[89] More specifically, PET hydrolases have been classified as carboxylesterases (EC 3.1.1.1, carboxyl ester hydrolases, and EC 3.1.1.2, arylesterase), cutinases (EC 3.1.1.74), and lipases (EC 3.1.1.3, triacylglycerol lipase). Finally, in 2016, the PET hydrolase class (EC 3.1.1.101) was created to contemplate the catalytic activity of *Is*PETase.[72,90] To date, no general denomination has been accepted by the scientific community for these enzymatic catalysts, beside their enzymatic classification. Consequently, numerous descriptive names are still in use, such as PET hydrolytic enzymes (PHEs), PET depolymerases, PET hydrolases, or even PETases. In addition, a distinction between PET surface-modifying enzymes and PET hydrolases has been proposed.[85] This enabled better distinguishing of enzymes only capable of PET surface hydrophilization without visible change by scanning electron microscopy (SEM), from PET hydrolases that can significantly degrade the inner block of PET, causing observable change by SEM. It has been proposed, after a comprehensive and elaborate demonstration, that PET hydrolases must ideally display at least two characteristics. First, the protein should exhibit a thermostability higher than 65 °C (preferably above 70 °C or even better 90 °C), which is consistent with the T_g of PET (70−80 °C). Second, an open active site topology is required to enable the binding of more than a single monomer

https://doi.org/10.1021/acs.chemrev.2c00644
Chem. Rev. XXXX, XXX, XXX−XXX

unit (e.g., MHET).[87] Consequently, PET hydrolases meeting these requirements are mainly limited to thermostable cutinases.[91]

2.1.2.1. Bacterial PET Hydrolases from Actinomycetota Phylum. Since the description of TfH, which was the first PET hydrolase identified from the bacterial actinomycete *Thermobifida fusca*,[84] a second PET hydrolase has been characterized in the same DSM43793 strain (Table 2).[92] The latter hydrolase was named BTA-2, while TfH was renamed as BTA-1. Both enzymes are cutinases harboring a signal peptide, cleaved during protein secretion to the extracellular environment. In fact, matured BTA-1 and BTA-2 only differ by 20 amino acids over their 261 amino acids length (92.3% sequence identity). Moreover BTA-1 PET hydrolase was found to be more efficient for PET depolymerization than its homologous protein.[93] At the same time, numerous *Thermobifida fusca* strains have been screened and numerous homologous tandem PET hydrolases have been identified. Tfu_0882 and Tfu_0883 were successfully identified from XY strain,[94,95] TfCut1 and *Tf*Cut2 from KW3 strain,[96] and Cut1 and Cut2 from NRRL B-8184. Nevertheless, only unique PET hydrolases were identified from strains DSM44242 and NTU22, named Thf42_Cut1[96] and TfAXE,[97] respectively. Similarly, tandem PET hydrolases named Thc_Cut1 and Thc_Cut2 were characterized from the species *Thermobifida cellulosilytica*, a member of the *Thermobifida* genus,[96] whereas Tha_Cut1, a unique PET hydrolase, has been described from *Thermobifida alba* DSM43185, another member of the *Thermobifida* genus.[98] When considering protein sequence identities, it appeared that BTA-1, Tfu-0883, Cut2, and Thc_Cut1 were strictly identical, and *Tf*Cut2, TfAXE, Tha_Cut1, and Thf42_Cut1 differed by only two, three, four, and six amino acids from this pool, respectively. They could thus be considered as four closely related independent variants of BTA-1. Similarly, BTA-2 differs by only two amino acids from a set formed by Tfu_0882, Cut1, and Thc_Cut2 (identical all together) and five amino acids from TfCut1 and could be considered as two closely related independent variants of BTA-2. Unfortunately, no consolidated denomination has been accepted by the scientific community yet, rendering difficult the analysis and the comparison of the multiple data produced over the years. For instance, comparison of TfH, *Tf*Cut2, TfCut1, Tfu-0882, and BTA-2 activities[93] could have been more illustrative if written BTA-1, BTA-$1^{S58R/T176S}$, BTA-$2^{R68N/A69V/F72L/D75S/N127I}$, BTA-$2^{K112E/S176T}$, and BTA-2 by considering the nature of the mutated amino acids in relation to a unique protein. Similarly, a recent study comparing Thc_Cut1 and Thc_Cut2[99] could have been more effective if stated as a comparison between BTA-1 and BTA-$2^{K112E/S176T}$ proteins, thus facilitating comparison between research articles. Finally, three less conserved PET hydrolases, but still displaying more than 75% of protein sequence identity with BTA-1 or BTA-2 mature proteins, were identified and characterized from the same *Thermobifida* genus. Effectively, Est119 and Est1, a tandem of PET hydrolases, were found in *Thermobifida alba* strain AHK119[100,101] when a unique PET hydrolase was characterized from *Thermobifida halotolerans* and named Thh_Est[102] (Table 2).

Complementarily, among bacterial thermophilic *Actinomycetota* phylum,[112] three other PET hydrolases were characterized through screening studies, namely, Tcur1278 and Tcur0390 as a tandem of proteins from *Thermomonospora curvata*[113] and Cut190 from *Saccharomonospora viridis*[110] (Table 2). All of these thermophilic PET hydrolases isolated from *Actinomycetes* were carefully described in a dedicated book chapter.[109]

At the same time, many novel PET hydrolases were discovered from various organisms, mainly from bacterial sources and a few from *Eucaryota*. An extensive phylogenetic distribution analysis of plastic-degrading microorganisms has been performed,[44] confirming that the *Actinomycetota* phylum represents a potential source of PET-degrading enzymes. Previously, 853 putative PET hydrolase genes were identified from various databases and metagenomes (108 marine and 25 terrestrial). The respective origins of these PET hydrolase genes indicated an over-representation from *Actinomycetota* and *Pseudomonadota* phyla (mainly in *Beta-*, *Delta-* and *Gamma-protobacteria* classes) regarding terrestrial metagenomes when a *Bacteriodota* phylum origin was mainly observed from marine metagenomes.[114] Similarly, a deep search for cutinases in the carbohydrate esterase family 5 (CE5) of the carbohydrate-active enzymes database (CAZy)[115] and representing over 3000 entries, allowed identifying 151 putative cutinases, 41 from bacterial and 110 from fungal organisms.[116] In view of the intensive efforts to search for new PET hydrolases, and even if considered as particularly rare enzymes,[114,117] the need for specific databases rapidly appeared mandatory. Consequently, the plastics microbial biodegradation database (PMBD) aiming at compiling experimentally verified enzymes able to specifically depolymerize a synthetic polymer was published online.[118] However, this database, with only 22 enzymes listed in June 2022, suffers of a lack of exhaustivity and maintenance regarding already or newly characterized PET hydrolases. Conversely, the plastics-active enzymes database (PAZy), compiling all biochemically characterized active PET hydrolases, currently 41 enzymes, appears more exhaustive.[57] As emphasized previously, only three enzymes out of this database were identified from *Eucaryota*. Another database, called PlasticDB, has been released recently.[56] Extensive developments have been made since its first publication[44] and the web application provides access to consolidated data regarding all microorganisms and proteins related to plastic biodegradation. By June 2022, 50 proteins were referenced under the PET entry. Hopefully, these databases will continue to be updated as they enable to follow the diversity of PET hydrolases regularly reported. In addition, some general guidelines or classifications would also be needed to help a better distinction between PET hydrolases from other PET surface-modifying enzymes at the origin of some discrepancies between databases.

2.1.2.2. Eucaryota PET Hydrolases. To date, only a few PET hydrolases are known to be produced by eucaryotes, more specifically by fungi.[72,85,88] Indeed, even if numerous lipases and cutinases have been reported as being able to degrade various objects in PET,[119] they are globally not considered as PET hydrolases but rather as PET surface-modifying enzymes. As one major use of PET resides in fiber production, fungal enzymes from *Fusarium solani*, *Candida antarctica*, *Aspergillus orizae*, *Cladosporium cladosporoides*, or *Penicillium citrinum* are suitable as antipilling and antigraying agents on polyester textiles where degradation of the inner building block of PET is unfavorable as it weakens the fiber strength.[85,120] Consequently, a very limited number of enzymes are considered as PET hydrolases, mainly because of their low optimal temperature, below 50 °C, which is

https://doi.org/10.1021/acs.chemrev.2c00644
Chem. Rev. XXXX, XXX, XXX−XXX

Table 3. Other Reported PET Hydrolases from Diverse or Unknown Bacterial Origins[a]

name	source	bacterial PET hydrolase type	thermostability T_m or T_{opt} (°C)	UniProtKB accession	ref
	Chloroflexota				
LCC	metagenome from leaf-branch compost	type I	86.2 (T_m)	G9BY57	130
BhrPETase	bacterium HR29	type I	101.0 (T_m)	A0A2H5Z9R5	131,132
	Bacillota				
Cbotu_EstA	*Clostridium botulinum* ATCC3502	na[b]	40.0 (T_{opt})	A5I055	129
BsEstB	*Bacillus subtilis* 4P3-11	na	40.0 (T_{opt})	D7R6G8	128,129
	Pseudomonadota				
*Is*PETase	*Ideonella sakaiensis* strain 201-F6	type IIb	46.0 (T_m)	A0A0K8P6T7	90
PET5 (OaCut)	*Oleispira antarctica* RB-8	type IIa	40.4 (T_m)	R4YKL9	114,137
PET6	*Vibrio gazogenes*	type IIa	nd[b]	A0A1Z2SIQ1	114
PET12	[*Polyangium*] *brachysporum*	type IIb	nd	A0A0G3BI90	114
*Rg*PETase	*Rhizobacter gummiphilus* NS21	type IIb	48.5 (T_m)	A0A1W6L588	135
PE-H (*Pa*PETase)	*Pseudomonas aestusnigri* VGX014	type IIa	50.8 (T_m)	A0A1H6AD45	136
Lip1 (Mors1)	*Moraxella* sp. TA144	type IIa	52.0 (T_m)	P19833	137
	Bacteroidota				
PET27	*Aequorivita* sp. CIP111184	type I*	nd	A0A330MQ60	138
PET30	*Kaistella* (*Chryseobacterium*) *jeonii*	type I*	nd	A0A0C1F4U8	138
	Unknown				
PET2 (lipIAF5-2)	metagenome derived	type IIa	69.0 (T_m)	C3RYL0	114,140
PHL-7	metagenome derived	type I	79.1 (T_m)	A0A165B1I1	139

[a]Classification within bacterial PET hydrolase types is provided (e.g., types I, IIa, IIb) and adapted from previous work.[134] Exceptions to this classification are mentioned (type I*). Indication of protein thermostability is provided when available, with assessments of melting temperature (T_m) or optimal temperature (T_{opt}). [b]na, not applicable, and nd, not determined.

unfavorable for an efficient degradation of amorphous PET.[87] In addition, the highly frequent presence of a N-terminal lid domain[121] prevents the accessibility of the active site of these enzymes to the polymeric substrate. Nevertheless, the commercialized HiC cutinase from the thermophilic fungus *Thermomyces insolens* (formerly *Humicola insolens*), which shows a high optimal temperature of 75−80 °C and can efficiently hydrolyze amorphous PET at 70 °C,[122,123] could be considered as a PET hydrolase.[87] Others add the FsC cutinase from *Fusarium solani pisi*[124] as another effective PET hydrolase,[72,74] while the PAZy database[57] also considers CalB, a lipase from *Pseudozyma (Candida) antarctica*,[122] as efficient for enzyme-based depolymerization of PET. CalB was indeed described to enhance PET depolymerization yield when used in combination with HiC enzyme. This is probably due to its esterase activity on soluble products (e.g., MHET, BHET) released during the depolymerization[123] and should thus not be considered as an effective PET hydrolase. Alternatively, the *Fo*Cut5a cutinase from *Fusarium oxysporum*[125] as well as *Tl*Lip from *Thermomyces lanuginosus*[126] have been reported as PET hydrolases in a dedicated review article.[88] Nevertheless, without minimizing the efforts devoted to characterize these enzymes, as well as to develop high throughput screening assays for fungal polyester hydrolyzing enzymes discovery using a synthetic copolyester such as poly(butylene adipate-*co*-terephthalate (PBAT),[127] we will focus our review only on bacterial PET hydrolases used as biocatalysts for PET depolymerization.

2.1.2.3. Other Bacterial PET Hydrolases. Several reports described PET depolymerization activities for carboxylesterases from *Bacillota*, one *p*-nitrobenzyl esterase (BsEstB) from *Bacillus subtilis*[128] and an esterase (Cbotu_EstA) from *Clostridium botulinum*.[129] These enzymes, larger than cutinases, share a temperature optimum of 40 °C and show a marginal level of PET hydrolysis. Therefore, they are considered as PET surface-modifying enzymes rather than PET hydrolases.[87,91] The most promising group of PET hydrolases, in addition to the previously described from *Actinomycetota*, consists of various enzymes characterized from different bacteria origins or metagenomic approaches. For instance, two highly thermostable and closely related PET hydrolases have been isolated from metagenomic approaches. The corresponding leaf-branch compost cutinase, abbreviated as LCC,[130] and a closely related protein from bacterium HR29, BhrPETase, share 93.8% sequence identity with the mature LCC.[131,132] Even if their precise organisms of origin are not known, bacterial *Chloroflexota* phylum appears to contain both protein sequences reported under GenBank accession number HEM19059.1 for LCC[133] and under GenBank accession number GBD22443.1 for BhrPETase[131] (Table 3). Their respective melting temperatures indicate their high level of thermostabilty, up to 86 °C for LCC[130] and above 100 °C for BhrPETase.[132] A growing set of enzymes from *Pseudomonadota* phylum have also been reported over the years. For instance, in 2016, the bacterium *Ideonella sakaiensis* was shown growth on amorphous PET as a sole carbon source, and the bacterial PET hydrolase named *Is*PETase was consecutively characterized as an efficient mesophilic catalyst for PET degradation.[90] Later, and using a Hidden Markov Model (HMM) profile constructed using PET hydrolases sequences previously characterized (e.g., PET hydrolases from *Actinomycetota*, LCC and *Is*PETase), the research performed on marine and terrestrial genomes led to the identification of hundreds of putative PET hydrolases. Among them, PET5 (OaCut) from *Oleispira antarctica*, PET6 from *Vibrio gazogenes*, and PET12 from [*Polyangium*] *brachysporum* were selected for deeper characterization and functionally verified as novel PET hydrolases, giving clearance on PET nanoparticle plates.[114] Therefore, their respective abilities to efficiently degrade other PET objects or powders remain to be elucidated. Another

https://doi.org/10.1021/acs.chemrev.2c00644
Chem. Rev. XXXX, XXX, XXX−XXX

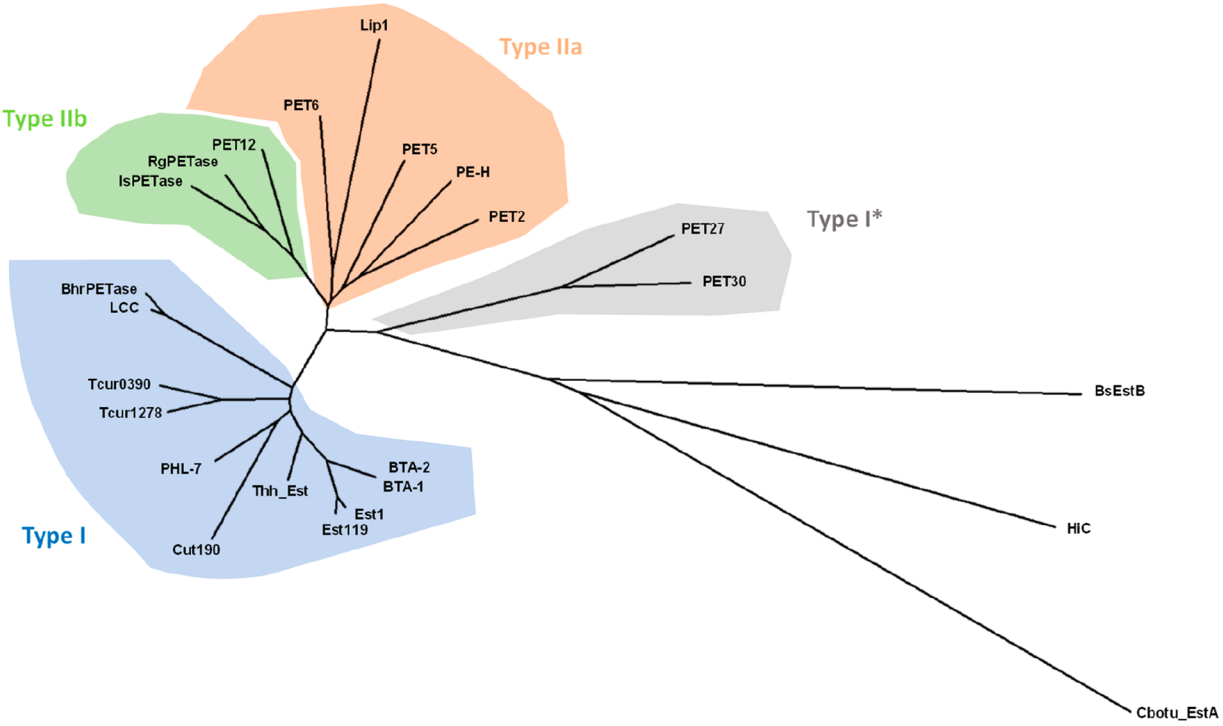

Figure 6. Unrooted phylogenetic tree of 24 PET hydrolases selected from bacterial PET hydrolases (enzymes highlighted in Table 2 and Table 3 without the 11 enzymes too closely related to BTA-1 and BTA-2) in addition with the fungal HiC cutinase. Clusters of enzyme types determined from specific primary protein sequence features are specified. Multiple amino acid sequences were aligned using ClustalW, and the guide tree was obtained based on the neighbor-joining method using the p-distance model. Scale bar: 0.25 amino acid substitution per single site. Analysis was performed using MEGA X.[146]

approach consisted in the classification of 69 cutinase-like sequences[134] that further led to the characterization of *Rg*PETase from *Rhizobacter gummiphilus*, another mesophilic enzyme able to depolymerize PET.[135] Similarly, PE-H from the marine bacterium *Pseudomonas aestusnigri*[136] and Lip1 (Mors1) from Antarctic bacterium *Moraxella* sp.[137] were also considered as PET hydrolases. None of these organisms appeared to be thermophilic. Moreover, melting temperatures (T_m) of these listed PET hydrolases confirmed their low level of tolerance to the envisioned reactional temperature, close to the T_g of PET,[87] to efficiently depolymerize PET. Indeed, assessed T_m of 46 °C for *Is*PETase,[90] 40 °C for PET5,[137] 49 °C for *Rg*PETase,[135] 51 °C for PE-H,[136] and 52 °C for Lip1[137] are far below the level of thermostability envisioned for an efficient enzymatic depolymerization catalyst for PET, requiring thermostability higher than 65 °C (preferably above 70 °C).[87] A similar approach, using identical HMM depicted previously,[114] has been performed to search for new PET hydrolase homologues in the *Bacteroidota* phylum[138] and two novel enzymes, PET27 from *Aequorivita* sp. and PET30 from *Kaistella (Chryseobacterium) jeonii* have been reported. Both enzymes display a C-terminal extension (Por secretion signal) that might be detrimental to their respective PET depolymerization efficiencies. Moreover, the Antarctic origin of both genomic samples could suggest low thermal stability of the enzymes, which thus requires further functional characterization. Finally, several metagenome derived PET hydrolases were reported from unknown bacterial origins. The PET2 (lipIAF5−2) enzyme[114] as well as the PHL-7 protein and its quadruple variant, PLH-7$^{A2E/L210F/D233N/S255A}$, named PHL-3,[139] appear to be promising PET hydrolases, notably because of their respective high thermal stabilities of 69 °C for PET2[140] and 79 °C for PHL-7[139] (Table 3). Lastly, PHL-7 has been renamed PES-H1, while PLH-7$^{A2E/L210F/D233N/S255A}$ has been called PES-H2.[141]

2.1.2.4. Sequence-Based Classification of Bacterial PET Hydrolases. To anticipate PET depolymerization properties of bacterial PET hydrolases and other bacterial PETase-like enzymes, it has been proposed to classify them into two types, namely type I and type II (Figure 6). Such classification has been proposed by comparison with *Is*PETase primary sequence features, *Is*PETase being assigned to type IIb PET hydrolases.[134] Type I PET degrading enzymes do not contain additional disulfide bond nor the extended loop found in *Is*PETase (Figure 7). Indeed, type I PET hydrolases have a unique C-terminal disulfide bridge, whereas type II enzymes show a second one, which is adjacent to the active site and connecting the β7-α5 and β8-α6 loops that harbor the catalytic aspartate and histidine residues, respectively. The second feature, specific of the type II enzymes, is the presence of a three amino acids extension in the β8-α6 loop. Additionally, it has been suggested that type I enzymes should possess His and Phe/Tyr residues at the corresponding positions of Trp159 and Ser238 found in *Is*PETase, respectively. Surprisingly, the recently characterized PET27 and PET30[138] do not contain any additional disulfide bond like type I enzymes. However, they do include an extended loop as well as Trp and Ser residues at specified corresponding *Is*PETase positions, turning them into an exception of the type I enzymes. In parallel, type II enzymes were separated into two subtypes, where type IIa enzymes have a Phe or Tyr residue at the corresponding position of Ser238 in *Is*PETase. To adequately define the PET2 enzyme as a type IIa PET hydrolase, Trp residue, another aromatic amino acid, should be considered for this

https://doi.org/10.1021/acs.chemrev.2c00644
Chem. Rev. XXXX, XXX, XXX−XXX

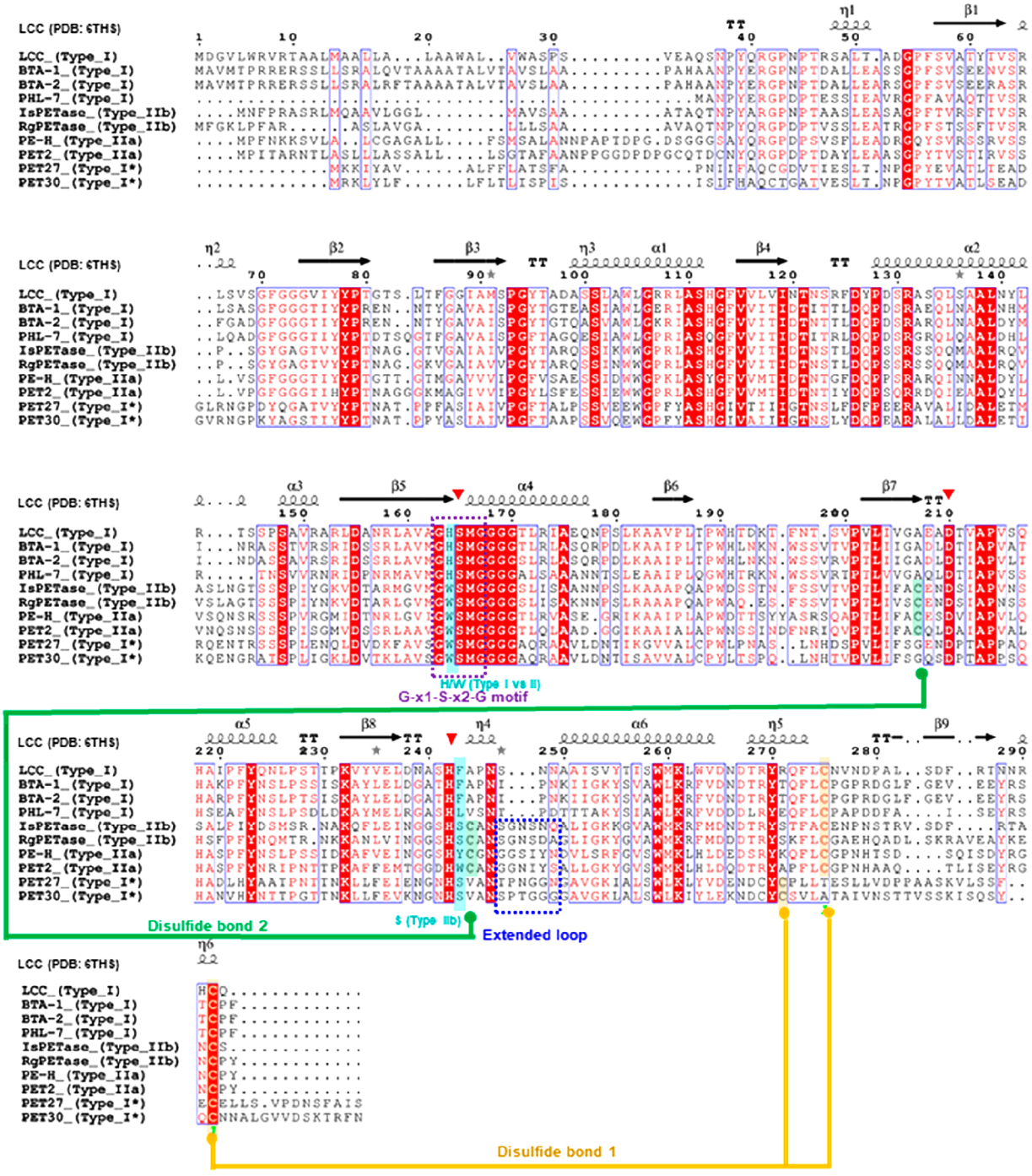

Figure 7. Multiple sequence alignment of selected bacterial PET hydrolases. Amino acid sequences of 10 selected PET-degrading enzymes of each type (e.g., type I, type IIa, type IIb, and type I*) are compared. Secondary structure elements are shown based on the LCC X-ray structure (PDB 6THS). Multiple amino acid sequences were aligned using ClustalW. Representation was done using ESPript.[147] Catalytic residues are indicated by red triangles, disulfide bridges are marked in yellow and in green for that defining the type II PET hydrolases. The extended loop defining type II and I* is highlighted in navy blue. The G-x1-S-x2-G motif is indicated in purple, with x1 = W for type IIa, IIb, and I* and x1 = H for type I. The S defining type IIb is highlighted in cyan color.

position (Figure 6, Table 3). While thermostable PET hydrolases, having a T_m higher than 70 °C, appear to belong to type I group, the type IIa and type IIb enzymes regroup mesophilic enzymes, with T_m lower than 55 °C, with the sole exception of PET2 PET hydrolase (Figure 6, Table 3). Consequently, the additional disulfide bond found for these type II enzymes does not seem relevant for their overall thermostability,[142] even if it is correlated to a gain of T_m of 13 °C in *Is*PETase.[134] This additional disulfide bond within the active site was effectively characterized as maintaining the integrity of the catalytic triad of *Is*PETase, having additionally the three amino acids extension of the $\beta 8$-$\alpha 6$ loop, while allowing higher flexibility at low temperature than their thermophilic counterparts (e.g., type I PET hydrolases).[143] Attempts to classify bacterial hydrolases according to their primary sequence features might be of interest but might need

https://doi.org/10.1021/acs.chemrev.2c00644
Chem. Rev. XXXX, XXX, XXX−XXX

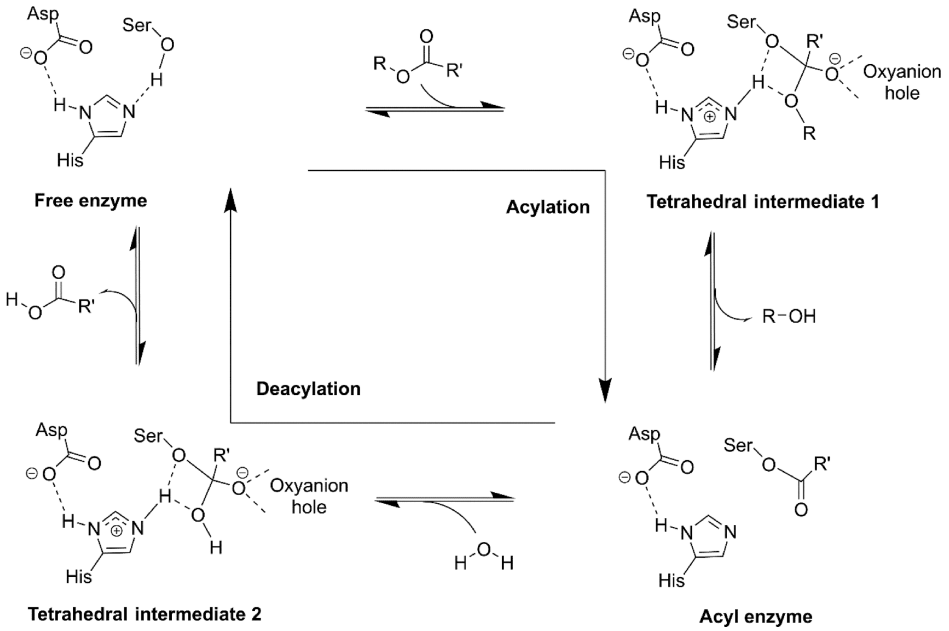

Figure 8. General hydrolytic mechanism of serine hydrolases. R-O-(CO)-R′ is the acyl donor, R-OH is the leaving group in the first step of the reaction (acylation), and H-O-H is the acyl acceptor in the second step (deacylation).

to be taken very carefully when trying to extend to general rules. Nevertheless, despite their types, bacterial PET hydrolases share common features, notably the catalytic triad (Ser-His-Asp), as well as the two residues, an aromatic amino acid (Phe or Tyr) located between the β3-strand and the α1-helix, and a Met residue in the α4-helix, next to the catalytic Ser, forming the oxyanion hole involved in the transition state stabilization (Figure 7). Moreover, bacterial PET-hydrolases have a highly conserved Gly-x1-Ser-x2-Gly motif surrounding the catalytic Ser in which x1 is an His for type I PET hydrolases, like LCC enzyme, or a Trp for the other types[144] and x2 is a Met residue, strictly conserved within all the bacterial PET hydrolases protein sequences.[134] Additionally, the C-terminal disulfide bond is conserved due to its importance on the overall stability by connecting the terminal α6-helix with β9-strand.[145] It is noteworthy that PET27 and PET30, two type I* PET hydrolases, revealed a subtle displacement of one of the cysteines forming the disulfide bridge in their primary sequence alignment (Figure 6), which was further confirmed in the crystallographic structure of PET30 (PDB 7PZJ).[138]

2.1.2.5. Catalytic Mechanism of the Bacterial PET Hydrolases. The hydrolytic process of PET degradation takes place in a flat, superficial, hydrophobic cleft found in PET hydrolases,[145] and no surface activation is required. Due to this architecture, these enzymes can hydrolyze high molecular weight polymer structures.[74,148] The hydrolytic mechanism exerted by the catalytic triad (Ser-His-Asp) of PET hydrolases has been described as a ping-pong reaction or an acylation/deacylation process, involving the formation of an acyl-serine intermediate occurring via a first tetrahedral intermediate and released via a second tetrahedral intermediate.[149−151] Enzymes involved in PET degradation belong to esterases subclass and possess a catalytic triad (Ser-His-Asp) which is characteristic of α/β-hydrolases. Ester bond hydrolysis is performed by the nucleophilic attack of the catalytic serine oxygen to the carbonyl carbon atom present in the scissile ester bond. Importantly, negatively charged aspartate stabilizes the positively charged histidine residue establishing a charge transfer network, which enables the proton shuttle required for serine activation and consecutive nucleophilic attack.[145,152] During this first (acylation) step, the nucleophilic serine attacks the ester scissile bond forming the first tetrahedral intermediate stabilized by the oxyanion hole,[153] thus leading to the formation of a covalent acyl-enzyme. In the subsequent deacylation step, nucleophilic attack by a water molecule takes place on the covalent acyl-enzyme to complete the cleavage of the ester bond, leading to a second tetrahedral intermediate. This is followed by the release of the reaction product, thereby regenerating the free enzyme (Figure 8).

Despite this canonical two-step serine hydrolase reaction mechanism employed by PET hydrolases, many questions remain.[11] For instance, the detailed interaction between the solid synthetic PET substrate and the PET hydrolases has not yet been reported.[96] Nonetheless, it is globally accepted that PET hydrolases catalyze endotype hydrolysis activity by cleaving internal ester bonds of PET, resulting in an increase of PET chain ends and the formation of oligomers.[85] However, both endo- and exotype hydrolysis activities have been demonstrated by NMR spectroscopy toward the mobile amorphous fraction (X_{MAF}) of crystalline PET when using thermophilic *Tf*Cut2 PET hydrolase. Consequently, the amorphous region of the polymer was rapidly hydrolyzed, whereas the remaining crystalline structure was only attacked through endotype chain scission activity and slowly hydrolyzed without any detectable weight loss.[154] Similar observation was reported when using $LCC^{Y127G/D238C/F243I/S283C}$ quadruple variant where an initial endotype scission activity of the PET hydrolase was followed by an exotype scission of the neighboring ester bond in the X_{MAF} of the PET substrate as the reaction proceeded.[155]

The hydrolytic mechanism of these enzymes on PET chains remains disputed at the molecular level.[145] Several modes of action for PET degradation by *Is*PETase have been proposed based on X-ray data, molecular docking, and site-directed mutagenesis experiments.[134] The proposed catalytic mecha-

https://doi.org/10.1021/acs.chemrev.2c00644
Chem. Rev. XXXX, XXX, XXX−XXX

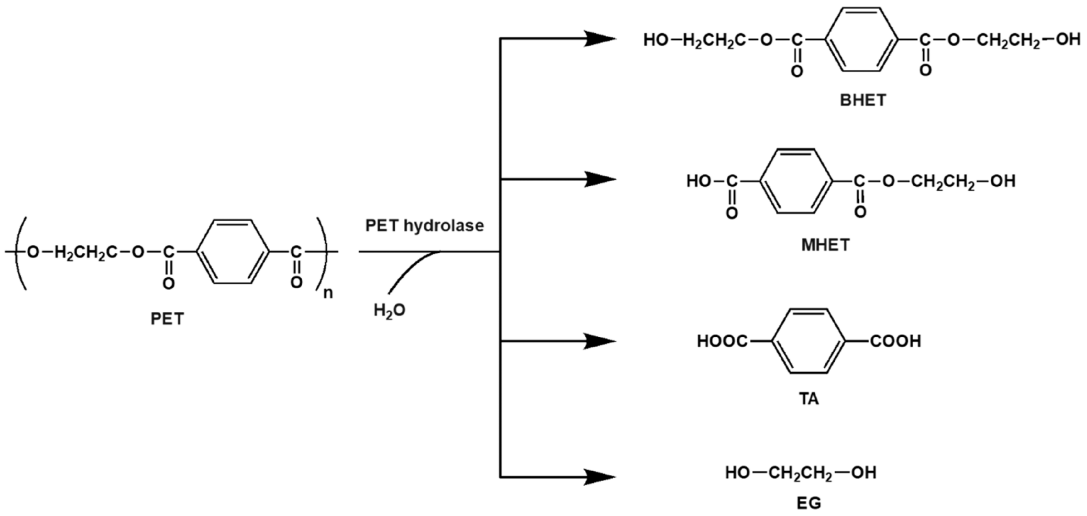

Figure 9. Chemical structures of PET and hydrolyzed products.

nism based on a docked 2-HE(MHET)$_4$ as substrate model and suggesting a *trans* conformation of the EG in PET[134] was later questioned.[156] Using solid-state NMR, Wei et al. showed that the conformation and the mobility of the PET oligomer chain could play a role on the PET degradation performance of the enzymes.[156] In particular, the ratio between *trans* and *gauche* conformations (*t*/*g* ratio) of EG, which coexist to different extents in amorphous (enriched in *gauche* conformation) and (semi-) crystalline (enriched in *trans* extended conformation) PET, was shown to depend on the temperature (9:91 at 30 °C vs 56:44 at 70 °C). A more-ordered state of PET was also observed at higher temperature. More recently, Guo et al. combined MD simulations, molecular docking, enzyme engineering, together with high-resolution microscopy and solid-state NMR, to investigate the PET conformation most susceptible to be degraded by PET hydrolases.[157] Their study not only revealed the ability of PETases to accommodate both *gauche* and *trans* conformations of the polymer chain but also the importance of PET conformational selection on the degradation performance of the enzyme. Interestingly, the authors also demonstrated how single amino acid mutations could alter conformational preference between *trans* and *gauche* and efficient binding in catalytically productive conformation, supporting a conformational selection mechanism rather than an induced fit one. This was illustrated by the engineering of *Is*PETase mutant S238A that displayed a totally reverse preference of the enzyme toward the *trans* conformation of PET (75.4% *trans* selectivity for S238A vs 10.1% for the wild type). This was assumed to be due to mechanistic differences in terms of *Re*- and *Si*-face nucleophilic attacks, the latter being facilitated in *trans* conformation.

Most of the PET hydrolases through enzyme-catalyzed PET depolymerization produce terephthalic acid (TA) and ethylene glycol (EG) with, to some extent, other degradation intermediates, including mono(2-hydroxyethyl) terephthalate (MHET) and bis(2-hydroxyethyl) terephthalate (BHET)[88] (Figure 9). These products are usually separated and quantified using reverse-phase HPLC.[158] More recently, longer soluble oligomers were also detected after small protocol adjustments when performing a PET depolymerization assay using Thc_Cut1 and Thc_Cut2 enzymes.[159] This study raised again the question of the enzyme processivity and PET depolymerization mechanisms. Nevertheless, there are exceptions to these observations and two PET hydrolases are unable to further cleave the ester linkage of MHET (*Is*PETase and PE-H). Consequently, the MHET is accumulating in solution during PET depolymerization, without major release of TA and EG.[88] Indeed, with the discovery of *Ideonella sakaiensis* 201-F6 able to grow on PET as a sole carbon source,[90] two enzymes were pointed out. The *Is*PETase responsible of PET depolymerization produces MHET, while a second enzyme named *Is*MHETase was immediately affiliated to a newly created class (EC 3.1.1.102). Activity of the *Is*MHETase enzyme (UniProtKD A0A0K8P8E7) is specific to MHET degradation in TA and EG, as it was previously described that this enzyme had no activity toward PET, BHET, or pNP-aliphatic esters.[90] Reminiscent of feruloyl esterases, *Is*MHETase possesses both a classical α/β-hydrolase domain and a lid domain conferring substrate specificity.[160] Numerous crystallographic structures have been reported regarding native *Is*MHETase, either without ligand (PDBs 6QGC, 6QG9;[160] 6JTU;[161] 6QZ1, 6QZ2, 6QZ4[162]), or with benzoic acid (PDB 6QGB[160]), or in complex with a nonhydrolyzable MHET analogue (PDB 6QGA[160]), or in complex with BHET (PDB 6JTT[161]) as well as a multiple variant of *Is*MHETase without ligand (PDB 6QZ3[162]). Consecutively, from a homology search against the 6671 tannases family sequences retrieved from the National Center for Biotechnology Information (NCBI), two close homologues of *Is*MHETase were identified. Indeed, an enzyme from *Comamonas thiooxydans* and another from *Hydrogenophaga* sp. PML113 sharing 81% and 73% sequence identity to *Is*MHETase, respectively. Both were shown to be active against MHET, with estimated k_{cat}/K_m 10–20-fold lower than the 2.17 μM^{-1} s^{-1} measured for *Is*MHETase.[162] Parallelly, from a metagenomic study using the biodegradation of an aromatic–aliphatic copolyester blend (PBAT) by a marine microbial enrichment culture, several MHETase-like enzyme candidates have been identified.[163] A marine mesophilic MHETase-like hydrolase (Mle), named Mle046, able to hydrolyze MHET, under broad temperature and pH conditions, has been further characterized.[164] Mostly because of a poor affinity with the MHET, Mle046 has a catalytic efficiency 40 times lower than that of *Is*MHETase but in the same order of magnitude as the *Comamonas thiooxydans* and *Hydrogenophaga* sp. PML113 MHETases. A second exception to MHET degradation by bacterial PET hydrolases

https://doi.org/10.1021/acs.chemrev.2c00644
Chem. Rev. XXXX, XXX, XXX−XXX

Table 4. Crystallographic Structures of Bacterial PET Hydrolases and Variants with Associated Resolution[a].[134]

bacterial PET hydrolase	enzyme type	PDB ID (resolution) of wild-type enzyme	PDB ID (resolution) of variant
Actinomycetota			
BTA-1 (TfH)	type I	5ZOA (1.54 Å)[184]	
*Tf*Cut2 (BTA-1$^{S58R/T176S}$)	type I	4CG1 (1.40 Å), 4CG2 (1.44 Å), 4CG3 (1.55 Å)[179]	
Thc_Cut1 (BTA-1)	type I	5LUI (1.50 Å)[185]	
Thc_Cut2 (BTA-2$^{K112E/S176T}$)	type I	5LUJ (2.20 Å)[185]	5LUK (1.45 Å), 5LUL (1.90 Å)[185]
Est119 (Est2)	type I	3VIS (1.76 Å), 3WYN (1.68 Å)[186]	
		6AID (1.30 Å)[187]	
Cut190	type I		4WFI (1.45 Å), 4WFJ (1.75 Å), 4WFK (2.35 Å)[188]
			5ZNO (1.60 Å), 5ZRQ (1.12 Å), 5ZRR (1.34 Å), 5ZRS (1.40 Å)[189]
			7CEF (1.60 Å), 7CEH (1.09 Å)[190]
			7CTR (1.20 Å), 7CTS (1.10 Å)[191]
Chloroflexota			
LCC	type I	4EB0 (1.50 Å)[192]	6THS (1.10 Å), 6THT (1.14 Å)[78]
		7VVE (1.98 Å)[178]	7VVC (1.82 Å), 7W45 (1.94 Å), 7W44 (1.85 Å), 7W1N (1.88 Å)[178]
BhrPETase	type I	7EOA (1.24 Å)[b]	
Pseudomonadota			
*Is*PETase	type IIb	5XG0 (1.58 Å)[152]	5XFY (1.40 Å), 5XFZ (1.55 Å), 5XH2 (1.20 Å), 5XH3 (1.30 Å)[152]
		5XJH (1.54 Å)[134]	5YNS (1.36 Å)[134]
		6ANE (2.02 Å)[143]	5YFE (1.39 Å)[193]
		6EQD (1.70 Å), 6EQE (0.92 Å), 6EQF (1.70 Å)[144]	6IJ3 (1.40 Å), 6IJ4 (1.86 Å), 6IJ5 (1.72 Å), 6IJ6 (1.95 Å)[194]
		6EQG (1.80 Å), 6EQH (1.58 Å)[144]	6ILX (1.45 Å)[195]
		6ILW (1.57 Å)[195]	6KUO (1.90 Å), 6KUQ (1.91 Å), 6KUS (1.80 Å)[b]
		6QGC (2.00 Å)[160]	6KY5 (1.63 Å)[196]
			7CQB (1.86 Å)[b]
			7CY0 (1.32 Å)[197]
			7OSB (1.45 Å)[198]
			7SH6 (1.44 Å)[199]
			7QVH (2.24 Å)[200]
*Rg*PETase	type IIb	7DZT (2.35 Å)[135]	7DZU (2.40 Å), 7DZV (1.60 Å)[135]
PE-H	type IIa	6SBN (1.09 Å)[136]	6SCD (1.35 Å)[136]
Bacteroidota			
PET30	type I*	7PZJ (2.10 Å)[138]	
Unknown			
PET2 (lipIAF5-2)	type IIa		7EC8 (1.35 Å), 7ECB (1.83 Å)[140]
PHL-7	type I	7NEI (1.30 Å)[139]	
		7CUV (1.45 Å), 7E30 (1.56 Å)[141]	7W69 (1.56 Å), 7E31 (1.38 Å)[141]

[a]Enzyme type definition is adapted from previous work. [b]Unpublished crystallographic structure released in PDB.

has been reported, and PE-H (*Pa*PETase) from *Pseudomonas aestusnigri*, a type IIa bacterial PET hydrolase, able to degrade amorphous PET film or BHET by producing MHET with no production of TA, has been characterized.[88,136] Nevertheless, no MHETase has been reported from this organism yet.

As emphasized above, acidic products (e.g., TA and MHET) accumulate in the reaction media when performing an enzyme-based PET depolymerization. This monoacid (MHET) and/or diacid production (TA) results in the acidification of the reaction media. The PET hydrolases, which prove highly active at alkaline pH because of their reaction mechanism, thus lose their catalytic efficiency, most likely by the protonation of the catalytic His. Increasing buffer strength and/or concentration has been proposed as an alternative to lower this enzyme inhibition induced by the acidification of the reaction media.[165,166] This could represent an efficient solution when performing a small-scale PET depolymerization for research studies but sounds odd when considering a potential industrial deployment using very high PET concentration and monomer recovery. Another alternative could be the use of acid-tolerant PET hydrolases exhibiting a broad pH optimum range. Several acid-tolerant cutinases have been identified to this end,[167−169] in particular an enzyme from the fungus *Thielavia terrestris* exhibiting detectable PET hydrolysis activity at pH 4 and 50 °C.[167] No further developments have been released since. Consequently, pH regulation using a strong base appears mandatory when performing a scaled-up enzyme-based PET depolymerization at high polymer concentration (e.g., 20% w/w).[78]

Modeling enzymatic reactions using high-level hybrid quantum mechanics/molecular mechanics (QM/MM) methods, although computing is time-consuming, can provide outstanding information to understand in detail the molecular mechanisms of PET degradation.[162,170,171] Reaction mecha-

https://doi.org/10.1021/acs.chemrev.2c00644
Chem. Rev. XXXX, XXX, XXX−XXX

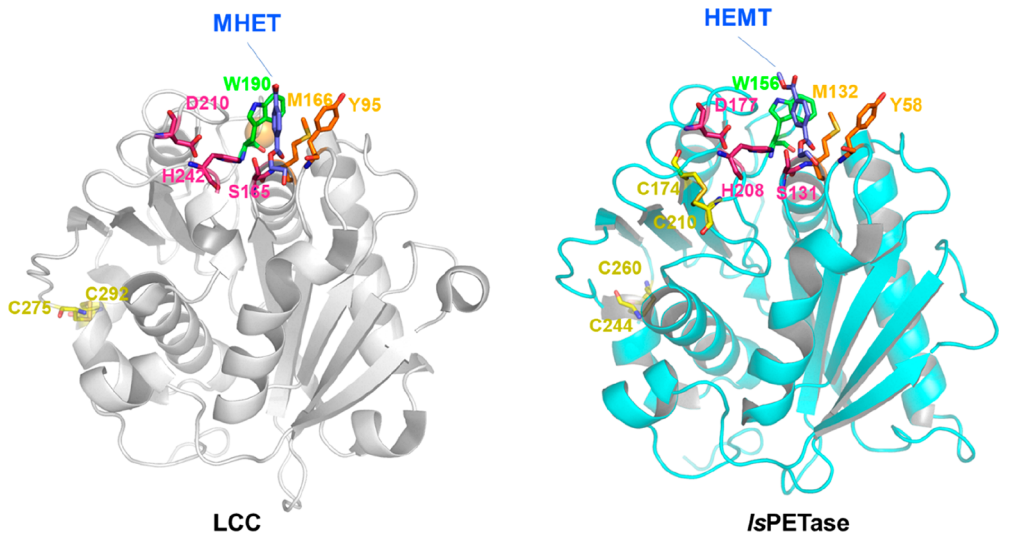

Figure 10. Three-dimensional structures of LCC (in complex with MHET, PDB 7VVE) and *Is*PETase (mutant R103G/S131A in complex with HEMT, PDB 5XH3). Catalytic triad is shown in magenta, residues forming oxyanion hole in orange, and disulfide bridges in yellow. The wobbling Trp is shown in green. Co-crystallized ligands are displayed in purple.

nism of *Is*MHETase, an enzyme acting in synergy with *Is*PETase to degrade PET, was the first investigated at atomic level using QM/MM method.[162,172] Starting from a modeled Michaelis complex with MHET,[162] a two-step mechanism to degrade MHET and BHET[161] into EG and TA was proposed for *Is*MHETase. These two steps include the acylation and deacylation via the formation of an acyl-enzyme intermediate. Although Knott et al. suggested that no metastable tetrahedral intermediates were formed during these steps,[162] Pinto et al. later revisited the mechanism and found evidence that transient tetrahedral intermediates were formed although short-lived.[172] In both studies, deacylation was predicted to be the rate-limiting step, as reported more generally for serine α/β-hydrolases. Recently, the reaction mechanisms catalyzed by *Is*PETase, LCC, and improved LCC$^{Y127G/D238C/F243I/S283C}$ quadruple variant[78] were also investigated using QM/MM methods starting from distinct docked substrates in distinct orientations, $(MHET)_2$, $(MHET)_3$,[170] or 2-HE$(MHET)_2$.[171] The most likely orientation of the polymer chain binding in the active site of these enzymes was debated based on the reported energetics.[170] Noteworthy, these studies rely on the modeling of substrate fragments, only partially representative of the real polymer substrate. The actual mechanism of the enzyme (endo- or exoactivity) is not fully established, and the impact of the temperature on the crystallinity grade of the polymer, the polymer substrate accessibility, and the enzyme conformation and stability are not considered in these calculations. These QM/MM studies suggested the occurrence of four concerted steps to complete the whole catalytic cycle. However, Zheng et al. suggested that the last concerted step of deacylation was the rate-limiting step of the reaction,[171] whereas Boneta et al.[170] identified the acylation as the limiting step. This latter study also concluded that subtle differences observed in the mechanisms of these PET degrading enzymes could not explain all differences experimentally observed regarding the performances of these enzymes. Hence, our comprehensive understanding on the mechanism of these enzymes still suffers from the lack of data and that many questions are still left to answer. More recently, Jerves et al.[173] proposed an alternative mechanism to the one by Boneta et al.[170] that comprises two steps of acylation and deacylation, the acylation being the rate-limiting step of the overall reaction mechanism.

2.1.2.6. Structural Characterization of Bacterial PET Hydrolases. The number of experimentally determined crystal structures of enzymes reported to degrade polymer chains has boomed over the recent years. Although many of these enzymes, including cutinases, lipases, and esterases, were already known for their activities on cognate substrates, they have recently regained interest when their promiscuous hydrolytic activity on polymers was revealed. Focusing on bacterial PET hydrolases, numerous high-resolution structures have been elucidated[87] (Table 4), evidencing that they exhibit conserved structural properties, which has allowed classifying them into a single subclass of the α/β-hydrolase fold enzyme superfamily. Wei et al. first solved *Streptomyces exfoliates* lipase structure (PDB 1JFR),[174] harboring nine β-strands within the protein, two of them being antiparallel.[175] This fold is effectively composed of a central β-sheet surrounded by seven to eight α-helices and shares a common catalytic machinery with a highly conserved catalytic triad (Ser-His-Asp), as emphasized previously.[176] Fungal PET hydrolases involving shorter polypeptides as the already mentioned HiC cutinase (PDB 4OYY), belong to a separated subclass, distinctive by the presence of only five parallel β-strands,[177] as well as the existence of a lid covering the active site shielding catalytic site from the solvent. Numerous crystallographic structures of PET hydrolases have been released, covering all enzyme types previously described (Table 4). Interestingly, even though *Is*PETase was isolated from a phylogenetically distant mesophilic bacterium, the structure of this type IIb enzyme (PDB 5XG0) showed a high structural similarity (Cα RMSD of 0.78 Å) compared to the structure of the highly thermostable LCC, a type I bacterial PET hydrolase (PDB 4EB0),[152] illustrating the conserved structural folding among bacterial PET hydrolases (Figure 10). Nevertheless, despite the conserved fold of bacterial PET hydrolases, important macroscopic differences have been pointed out regarding surface properties and characteristics of the catalytic pocket.[87,134,145] Notably, when comparing type I *Tf*Cut 2

https://doi.org/10.1021/acs.chemrev.2c00644
Chem. Rev. XXXX, XXX, XXX−XXX

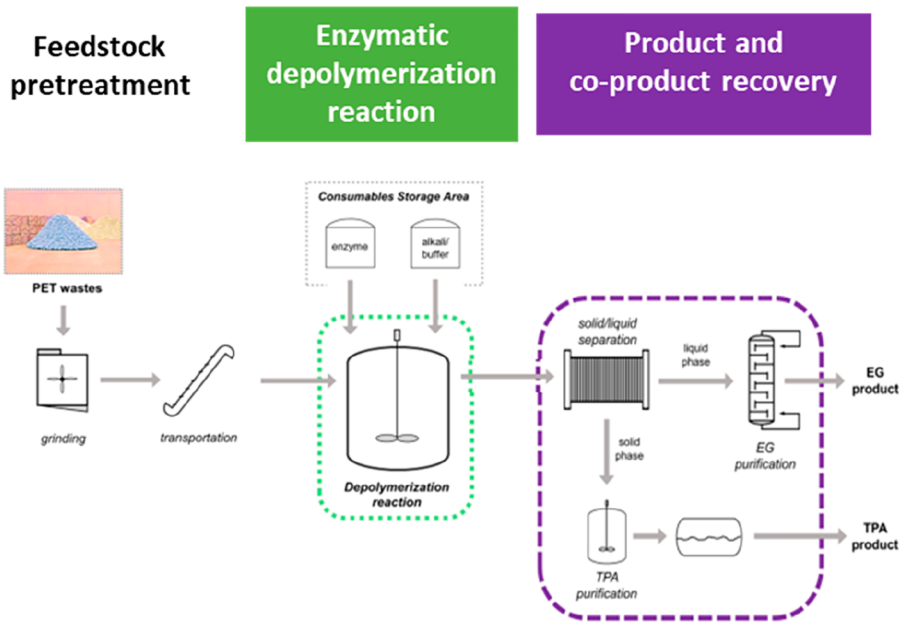

Figure 11. Enzymatic PET depolymerization process decomposed in three main sections (feedstock pretreatment, enzymatic depolymerization reaction, and product and coproduct recovery). Adapted with permission from ref 72. Copyright 2021 Elsevier.

with type IIb *Is*PETase enzymes, several features have been highlighted such as the highly polarized surface charge of *Is*PETase, its wider active-site cleft, potentially more suitable to accommodate large substrates as well as an enhanced hydrophobicity of the catalytic triad environment.[144] Another study of the effect of the structural differences on the active site dynamics of bacterial PET hydrolases revealed that the *Is*PETase active site displays enhanced flexibility at room temperature compared to the thermophilic type I enzymes like *Tf*Cut2 and LCC.[143]

Although many structures of native or variants of PET-hydrolases have been determined by X-ray crystallography, most of them are obtained in free form with no bound PET nor soluble products of PET depolymerization (Table 4). Nevertheless, a few structures of enzyme/ligand complexes have been released. Interestingly, structures of inactive catalytic serine variant of *Is*PETase complexed with a PET product analogue, the *p*-nitrophenol (PDB 5XH2), and with the 1-(2-hydroxyethyl)- 4-methyl terephthalate, a methyl ester of MHET, named HEMT (PDB 5XH3), were simultaneously released.[152] These structures provided some insight into the substrate-binding mode and supported the mechanism of action of action of *Is*PETase.[86,134,152] More recently, a structure of the inactive catalytic serine LCC^{ICCG} variant in complex with the mono(2-hydroxyethyl) terephthalic acid (MHET) (PDB 7VVE) has been released.[178] The enzyme−substrate interactions of LCC^{ICCG} appeared highly identical to those evidenced for *Is*PETase, the most notable variation being the deviation by 30° of the aromatic moieties of the two bound ligands. This angle deviation appeared to be determined by a conserved Trp residue (W190 in LCC^{ICCG} and W185 in *Is*PETase). Effectively, this residue adopts a wobbling conformation and is pushed down to a B-type conformation upon substrate binding in *Is*PETase[152] when this B-type conformation of the corresponding W190 in LCC^{ICCG} is not occurring because of the presence of other H218 and F222 residues. From this perspective, LCC^{ICCG} appears to display a more rigid substrate-binding groove than *Is*PETase, which may demand PET to bend a bit to fit in.[178] Additionally, three structures of the PHL-7 enzyme (renamed PES-H1) in complex with a PET product analogue, the 4-(2-hydroxyethylcarbamoyl) benzoic acid (MHETA) (PDB 7W6C, 7W6O, and 7W6Q) have been advertised but remain to be released by the PDB.[141] Similarly, a structure of the $PLH\text{-}7^{A2E/L210F/D233N/S255A}$ quadruple variant (renamed PES-H2) in complex with the bis(2-hydroxyethyl) terephthalate (BHET) (PDB 7W66) remains to be released in the PDB.[141] Finally, as most of the X-ray structures of PET hydrolases have mainly been determined in free form or in complex with small ligands, the binding mode of the polymers or their constitutive fragments (e.g., monomer, dimer, trimer, tetramer, etc.) has mostly been inferred by computational methods, usually derived from molecular docking.[78,96,134,135,143,144,179−181] This has led to the identification of amino acid residues that could play a key role in polymer binding or substrate accessibility. This also provided mutagenesis targets to improve catalytic performances of enzymes for polymer degradation.[182]

Complementarily to structural characterization of PET hydrolases, an in-depth solution NMR study of the native LCC, as well as the sequential variants leading to the LCC^{ICCG} quadruple mutant, has been recently carried out.[183] Using various NMR probes, such as backbone amide, methyl group, and histidine side chain resonances, elements of a potential interacting surface between the enzymes and MHET, used as a surrogate of a PET chain, were identified. Moreover, MHET induced chemical shift perturbations (CSP) in the spectra of the different LCC variants correlated well with the previously determined enzymatic activities of the latter. This NMR study, by the identification of many markers, demonstrated new possibilities to investigate further the molecular interaction between a PET hydrolase and a PET polymer surface.

2.1.3. Considerations for Industrial Development of Enzyme-Catalyzed PET Depolymerization. While the previous section emphasized the tremendous work carried out to discover and characterize efficient PET hydrolases, the main challenge remains the development of an enzyme

https://doi.org/10.1021/acs.chemrev.2c00644
Chem. Rev. XXXX, XXX, XXX−XXX

catalyzing PET depolymerization as a viable industrial process assorted with full recovery of the monomers produced. Such an industrial deployment would mean the depolymerization of tens of thousands of tons of PET plastic waste per year, and the production of the final monomers, preferably TA (under its acidic from) and EG. Those recovered monomers, following their respective purification scheme, will then be reintroduced into a process of PET production by a conventional existing plant. An ideal enzymatic PET depolymerization process can be decomposed into three main sections (Figure 11):[72,201] (i) feedstock pretreatment, (ii) enzyme-catalyzed PET depolymerization, and (iii) product and coproduct recovery.

Enzyme-based PET depolymerization is a heterogeneous reaction occurring at the solid/liquid interface (Figure 12) as

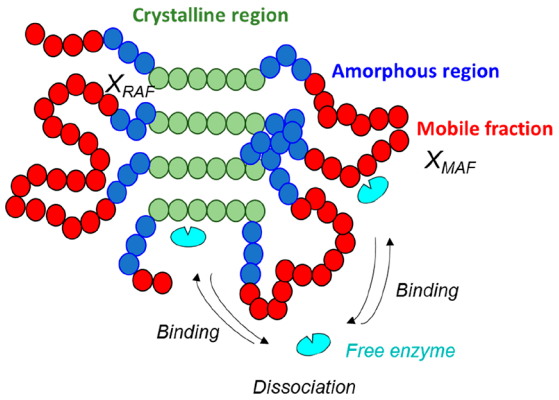

Figure 12. Schematic representation of PET hydrolysis by PET hydrolase. PET hydrolase binds to the surface of PET and acts on the mobile fraction of amorphous regions (X_{MAF}) when the rigid amorphous fraction (X_{RAF}) of amorphous regions as well as the crystalline regions of PET remain recalcitrant to depolymerization. Each sphere represents a monomer of MHET.

PET is a water-insoluble synthetic polymer. A key parameter affecting enzyme PET depolymerization efficiency is the crystallinity (X_c) of the polymer. As a semicrystalline polymer, the morphology of PET consists of both amorphous and crystalline domains with strong effect on its degradability.[75] The amorphous regions of PET consist of a mobile amorphous fraction at a temperature above the T_g (X_{MAF}) and a rigid amorphous fraction (X_{RAF}), the latter forming the interface between the crystalline regions and the X_{MAF}.[202] PET hydrolases are expected to preferentially hydrolyze the amorphous region of PET, especially in the X_{MAF}.[78,81,82,85,154] It thus appears crucial to perform a feedstock pretreatment to transform semicrystalline PET into an amorphous state. If not, the enzyme will degrade solely the accessible X_{MAF} of the polymer and only low yield of depolymerization will be reached. When considering the high price of PET waste and the cost of postreactional waste treatment, a minimum yield of 90% (ideally 95%) can meet expectations of an economically viable industrial recycling process.

Another key parameter to maximize the reaction kinetics is the exchange surface between the solid phase constituting the plastic and the enzyme, which is contained in the liquid phase. This exchange surface must be improved, the finer the particle size of the plastic powder, the faster the depolymerization kinetics will be. Several studies have emphasized this statement when performing PET depolymerization assays either by using a fungal cutinase, HiC from *Humicola insolens*,[203] or by using bacterial PET-hydrolases, Thc_Cut1[204] or LCC$^{Y127G/D238C/F243I/S283C}$ quadruple variant.[205]

Capital Expenditures (CAPEX) dedicated to the enzymatic PET depolymerization section depends mostly on the productivity of the reactor, expressed in grams of monomers produced per liter and per hour.[206] This productivity is influenced by two parameters, (i) the concentration of PET waste introduced in the reactor and (ii) by the kinetics of the reaction.

As emphasized above, an efficient enzyme-based PET depolymerization will generate TPA as a diacid and EG as a diol, accumulating in the reaction media. Such acidification is detrimental to the catalytic efficiencies of PET hydrolases. To both maximize the overall productivity and favor a complete PET depolymerization, a pH regulation using a strong base, rapidly appeared necessary. Upon complete neutralization, terephthalate salt instead of TPA is eventually produced. Consequently, the saturating concentration of this terephthalate salt in the medium at the completion of PET depolymerization reaction might dictate the optimum conditions to improve the productivity of the process by increasing the PET waste quantity. Indeed, it is crucial to keep the released monomers in the liquid phase to separate them from any potential residual solid waste. The solubility of disodium terephthalate in water is around 13% in weight and is not dependent on the temperature between 25 and 70 °C.[206] Consequently, the initial concentration of PET waste must be around 20% w/w. On the other hand, it has been shown that the accumulation of EG during PET depolymerization tends to reduce further this disodium terephthalate solubility[206] but with a very limited impact when considering a complete depolymerization of a 20% w/w PET concentration (e.g., around 5% of disodium terephthalate solubility reduction).

The reaction temperature is the main parameter enabling tuning of the reaction kinetics. Beyond the effect of a temperature increase on the enhanced enzyme-based PET depolymerization kinetics, via Arrhenius' law, there might have an additional favorable improvement related to the increased mobility of the polymer chains during its degradation. At temperatures below T_g, indeed, the chains within the amorphous phase are rigid, while an increased mobility of these latter is observed at temperatures close or above T_g, providing better substrate accessibility to the PET hydrolases.[91,122,144,155,207] Additionally, water has a plasticizing effect on PET, and the adsorption of water molecules into PET amorphous regions results in a decrease of T_g by approximately 10 °C.[110,208−210] This allowed slightly lowering of the temperature to perform an enzyme-catalyzed PET depolymerization. Effectively, the PET polymer is not a substrate like any other, as it might evolve depending on the conditions in which it is placed. Close to T_g, PET chains tend to crystallize, and this thermally induced crystallization is even more efficient as the temperature approaches T_g.[211] This thermally induced crystallization appears consecutively to PET incubation at a temperature above T_g. Those induced physical changes of PET chains (e.g., increase of X_c and increase of X_{RAF}) are known to impede the enzymatic attack.[155] In practice, when an amorphous PET powder does not crystallize after 24 h of incubation at 65 °C in an aqueous solution, a 40% degree of crystallinity (X_c) is obtained after 24, 15, and 5 h at 70, 72, and 75 °C, respectively.[78] Moreover, this crystallization kinetics proves as fast as the PET molecular weight is low. As a result, PET from textile waste crystallizes faster than PET arising from

https://doi.org/10.1021/acs.chemrev.2c00644
Chem. Rev. XXXX, XXX, XXX−XXX

bottle waste. As discussed above, the presence of comonomers in the PET chains (e.g., IPA in bottle grade PET) can help reducing the polymer regularity and thus slowing down the crystallization kinetics. Conversely, thermally induced crystallization is very limited (if occurring) below T_g, because of the restricted chain mobility of the amorphous regions.[212]

In summary, two competitive events take place during an enzyme-based PET depolymerization assay performed at a temperature close to T_g, namely, polymer chain depolymerization and recrystallization of the polymer. To thus maximize PET depolymerization yields, two conditions must be fulfilled. First, the enzyme must be sufficiently thermostable to work at a temperature close to the T_g of PET. Second, the PET hydrolase must have sufficient catalytic efficiency to act faster than the recrystallization.

2.1.4. Strategies to Improve the Reaction Performances. To enhance the catalytic performances of the PET hydrolases during a heterogeneous reaction of an enzyme-based PET depolymerization, both entities of this binary system have been studied for optimization. First, PET pretreatments to increase its amorphous state as well as to increase its surface of exchange with the enzyme. Second, various strategies of enzyme engineering: (i) improvement of substrate/enzyme interaction, (ii) increase of enzyme thermostability, (iii) optimization of the catalytic efficiency of the enzyme, and (iv) minimization of the enzyme inhibition. Those different approaches targeting specifically the PET hydrolases will be detailed further in the manuscript.

2.1.4.1. Substrate Properties Influencing Enzyme Based Depolymerization. It could be postulated that the ester bonds of PET could be easily hydrolyzed by many hydrolases. However, whereas diethylene glycol terephthalate was demonstrated to be biodegradable,[213] PET proves particularly stable. On the other hand, poly(ethylene succinate-*co*-terephthalate), a copolymer of lower crystallinity than PET, was shown to be easily hydrolyzed.[214] This confirms that high X_c limits chain mobility and consequently decreases the availability of chain ends for enzyme degradation.[77] Nevertheless, *Is*PETase from *Ideonella sakaiensis* was claimed as being able to degrade semicrystalline PET polymer.[90,148,196] However, no convincing evidence has supported this claim, in the sense that only a very small proportion of the crystalline PET polymer used was degraded (e.g., around 0.2% conversion for Coca-Cola, Nestlé, and Pepsi-Cola commercial bottles).[148] Effectively, an enzyme producing monomers from a crystalline PET object with a high crystallinity rate is not a convincing proof by itself, the PET hydrolase being able to attack specifically the sole amorphous regions of these objects. Moreover, the strain *Ideonella sakaiensis* has been found able to grow on amorphous PET but not on highly crystalline PET.[215] Finally, Lu et al. provided definitive proof that this enzyme did not degrade the highly crystalline PET of bottles.[199] Even if sooner or later the possibility that an enzyme will be capable to depolymerize crystalline PET cannot be ruled out, no such enzyme has been described yet. Consequently, different types of PET pretreatments have been investigated to promote an amorphogenesis of the substrate. A first approach consisted in soaking PET flakes with EG. To evaluate the impact of this pretreatment, a 22 h incubation at 37 °C has been performed prior to enzyme-based depolymerization, and no change in X_c of the pretreated PET have been observed. A positive but unconvincing increase of TA accumulation by 17% have finally been reported after its depolymerization.[123] Another approach aimed at reducing the crystallinity of PET consists in its solubilization by an organic solvent, such as 1,1,1,3,3,3-hexafluoro-2-propanol (HFIP) or trifluoroacetic acid 90%(v/v) (TFA), followed by its precipitation by addition of cold water under intense stirring.[216−218] However, these methods utilizing toxic solvents do not appear viable for an industrial deployment. Nevertheless, these solvent-based methods of production of PET nanoparticles have the positive advantage to generate particles of nanometric size (100−200 nm in diameter) increasing the exchange surface of the polymer, and consequently accelerating the enzyme-based depolymerization rates[217] and they are of interest to develop high throughput screenings. This beneficial effect has also been observed when PET objects are transformed into a powder, the enzymatic activity exhibiting a higher activity as the size of the particles is smaller.[204,205,219] Alternatively, PET pretreatment by UV irradiation inducing intramolecular breaks of amorphous PET films have been investigated.[220] Unexpectedly, no improvement was observed after enzyme-based depolymerization, most likely because such UV irradiation promoted increased rigidity of the polymer chain as well as an increased PET crystallinity, both factors preventing catalytic efficiency. Only a few reviews emphasized these important aspects of PET pretreatments useful to envision an industrial deployment using an efficient enzyme-based PET depolymerization process.[72,91,221] Alternatively, they also mentioned strategies to improve the reaction conditions as well as the use of potential additives, these aspects will not be developed further in this manuscript mostly because use of additives must be considered in technoeconomic feasibility. Indeed, their potential benefits must compensate a more complex portfolio of consumables and downstream requirements to meet the required purity of PET monomers produced. In this sense, the simpler the technology, the better.[72,221] Finally, Tournier et al. proposed an industrial-scale process both reducing the crystallinity of postconsumer washed colored flakes and maximizing the PET particles sizes for optimal activity.[78] Indeed, a twin-screw extruder was thus used to melt the PET at 265 °C to yield a molten polymer, which was subsequently pelletized in a die plate with water at 80 °C before rapidly cooling down the PET and fixing it into its amorphous state. Pellets of two to three millimeters in diameter were then micronized at room temperature to achieve a powder showing a granulometry between 200 and 250 μm.[78,222]

2.1.4.2. Improvement of Substrate/Enzyme Interaction. The interaction between an enzyme and the substrate surface has a dramatic effect on the enzymatic activity,[223] even more so if considering the heterogeneity of the enzymatic catalysis process of PET hydrolysis. Within such aqueous systems, free soluble enzymes encounter highly insoluble hydrophobic PET chains, potentially interfering with the adsorption of high amounts of biocatalysts to their surface.[109] No substrate-binding modules have been found in PETases' structures to promote substrate adsorption, in contrast to some enzymes that target hydrophobic polymers found in nature (e.g., carbohydrate-active enzymes). Consequently, the binding process is essentially dictated by electrostatic and hydrophobic interactions between substrate molecules and amino acid residues on the enzyme surface.[96,185] Therefore, the improvement of the enzyme−substrate interaction, with the aim at improving the biocatalytic efficiency, has been significantly explored over the last years, which has been specifically emphasized in several review articles.[72,182,224,225] As described

https://doi.org/10.1021/acs.chemrev.2c00644
Chem. Rev. XXXX, XXX, XXX−XXX

Table 5. Selected PET Hydrolases Engineering Studies in the Presence of Accessory Binding Domains (Carbohydrate-Binding Modules, CBM; PHA Binding Domain, PBM; Hydrophobin, HFB; Chitin Binding Domain, CBD; Anchor Peptides; Synthetic Zwitterionic Polypeptide, EK)[a]

binding domain type	binding domain name (origin)	binding domain fusion localization	PET hydrolase name	PET depolymerization (fold improvement)	PET substrate	pH	temp (°C)	incubation time (h)	ref
CBM	CMB_{CenA}^{W68L} of cellulase CenA (*Cellulomonas fimi*)	C-terminus	BTA-1	1.4	PET fiber	8	50	24	234
CBM	CMB_{CenA}^{W68Y} of cellulase CenA (*Cellulomonas fimi*)	C-terminus	BTA-1	1.5	PET fiber	8	50	24	234
CBM	TrCBH of cellobiohydrolase I (*Hypocrea jecorina*)	C-terminus	Thc_Cut1	1.4	amoPET film	7	50	72	235
PBM	PhaZAfa of PHA depolymerase (*Alcaligenes faecalis*)	C-terminus	Thc_Cut1	3.8	amoPET film	7	50	52	235
class II HFB	HFB4 (*Hypocrea jecorina*)	C-terminus	Thc_Cut1	>16	amoPET film	7	50	24	240
class II HFB	HFB7 (*Trichoderma harzianum*)	C-terminus	Thc_Cut1	>16	amoPET film	7	50	24	240
CBM	TrCBH of cellobiohydrolase I (*Hypocrea jecorina*)	C-terminus	IsPETase$^{S121E/D186H/R280A}$(ThermoPETase)	1.4	PET granules	9	40	18	236
CBM	ChBD, chitin binding domain from *Cm*Chi1 chitinase (*Chitinolyticbacter meiyuanensis* SYBC-H1)	C-terminus	$LCC^{Y127G/D238C/F243I/S283C}$	1.3	amoPET film, PcW-PET (X_c 16%), Hc-PET (X_c 40%)	8	65	12	238
CBM	TrCBH of cellobiohydrolase I (*Hypocrea jecorina*)	C-terminus	$LCC^{Y127G/D238C/F243I/S283C}$	1.1	amoPET film, PcW-PET (X_c 16%), Hc-PET (X_c 40%)	8	65	12	238
anchor peptide	DSI of dermaseptin SI (*Phyllomedusa sauvagii*)	N-terminus	TfCut2$^{D204C/E253C}$	22.7	amoPET film	8	70	96	249
synthetic	Zwitterionic polypeptide (EK) (na[b])	C-terminus	IsPETase	11	amoPET film, Hc-PET (X_c 45%)	9	40	96	197

[a]All studies were performed through the expression of a chimeric protein fusion formed between a PET hydrolase and a N-terminus or a C-terminus addition of a specific accessory binding domain, the orientation of this addition is specified. amoPET film, amorphous Goodfellow PET film; PcW-PET, amorphized postconsumer waste PET; Hc-PET, crystalline PET. [b]na, not applicable.

https://doi.org/10.1021/acs.chemrev.2c00644
Chem. Rev. XXXX, XXX, XXX−XXX

in the following sections, two main approaches have been developed, namely, the tailoring of the surface properties of plastic-degrading enzymes and the use of additives for polymer surface treatment.

2.1.4.2.1. Tailoring Surface Properties of Plastic-Degrading Enzymes. **Tailoring Surface Electrostatics.** Modification of hydrophobic surface and/or electrostatic properties are common strategies. Indeed, electrostatic repulsion between the PET substrate and the enzyme surface might be reduced by targeting charged, solvent exposed, protein amino acid residues, thus enhancing binding and PET degradation efficiency. For example, two closely related cutinases from *T. cellulosilytica* DSM44535 (Thc_Cut1 and Thc_Cut2), differing by only 18 amino acids, exhibited drastically different PET hydrolysis properties.[96] The contribution of protein surface charged amino acid residues was extensively analyzed and the R29N mutation of Thc_Cut2, generating a more neutral enzyme surface in a structural area located far away from the active site, was found to facilitate PET hydrolysis.[226] Similar catalytic enhancement of Cut190 was induced by the R228S substitution, which was thought to generate a neutral electrostatic surface area near the mutated site.[188] Another approach consisted in considering the PET surface negative charge increase during its enzymatic degradation, yielding anionic carboxyl, which attracted PET hydrolases through their positive charge surface.[166,227] Consequently, positive charge enhancement of the PET2 (lipIAF5-2) surface by the introduction of F105R and E110K mutations led to a 1.8-fold improvement of PET hydrolysis yield because of the 2.7-fold enhancement of the binding rate constant with PET.[140] Alternatively, a protein EKylation strategy was developed, inspired from zwitterionic polymers properties that were shown to provide a more stable environment to proteins and to reduce nonspecific adsorption.[228,229] EKylation consisted of a C-terminus addition to a PET hydrolase of a poly(EK) polypeptide, containing repetitively alternating negatively charged glutamate or positively charged lysine residues. Such an EKylation of the *Is*PETase successfully induced an 11-fold increase of PET hydrolysis efficiency (Table 5).[197]

Tuning Surface Hydrophobicity. Enzyme−substrate interaction could also be enhanced by tuning enzyme surface hydrophobicity. This was exemplified by the deletion of a lid structure formed by a 71 amino acids length N-terminal domain of Cbotu_EstA, a cutinase from *Clostridium botulinum*. Such a deletion exposed a hydrophobic surface area accessible for PET substrate adsorption, which resulted in higher enzymatic hydrolysis.[230] Upon increase of protein surface hydrophobic residues, however, enzymatic aggregation or structure disruption occurred due to unwanted additional intermolecular hydrophobic interactions, resulting in impaired catalytic activity.

Attachment of Accessory Binding Domains. An alternative to enhance enzyme−substrate interaction is inspired from carbohydrate-binding modules (CBMs). CBMs are auxiliary domains found in carbohydrate-active enzymes involved in natural biopolymer degradation and responsible of the enzyme−polymer adhesion mechanism.[231] CBMs have promiscuous abilities to bind various natural polymers and synthetic plastics.[231,232] Yet, no substrate-binding domains have been reported for PET degrading enzymes. Numerous approaches have thus emerged to enhance enzyme−substrate interaction through a protein fusion using heterologous polymer binding modules.

First reported in 2010,[233] a heterologous C-terminus protein fusion between a cutinase (UniProt ID Q47RJ6) isolated for *Thermobifida fusca* and the CBM of cellulase CenA from the bacterium *Cellulomonas fimi* (CBM_{CenA}) was generated, which further improved efficient hydrolysis of PET fibers.[234] Therefore, and owing to different properties existing between PET and cellulose fibers, single tryptophan mutations were introduced into CBM_{CenA} to seek for improvements. Finally, adhesion to PET fibers was enhanced, as well as the number of released products from an enzymatic PET degradation, 1.4-fold to 1.5-fold with W68L or W68Y, respectively (Table 5). The same year, the improvement of an enzymatic degradation of amorphous commercial PET film was described by adding a CBM to an already known cutinase. Indeed, a C-terminus fusion of Thc_Cut1 cutinase from *Thermobifida cellulosilytica* with trCBH, the CBM of 1,4-β-cellobiohydrolase I from *Hypocrea jecorina* (anamorph of *Trichoderma reesei*) achieved higher binding affinity to the PET surface and significantly increased enzymatic PET hydrolysis efficiency.[235] Lately, a C-terminus fusion of ThermoPETase, a triple mutant (S121E/D186H/R280A) of *Is*PETase, from *Ideonella sakaiensis* with TrCBH, significantly improved PET hydrolysis efficiency using commercial PET granules.[236] Finally, a chitin-binding domain (ChBD) was characterized in the *Cm*Chi1 chitinase from *Chitinolyticbacter meiyuanensis* SYBC-H1.[237] In the latter case, a 1.3-fold enzymatic PET hydrolysis efficiency improvement was observed through its C-terminus fusion with the $LCC^{Y127G/D238C/F243I/S283C}$ variant.[238] Moreover, the chimera protein was shown to accelerate similarly the degradation of PET samples regardless of its sourcing (e.g., commercial amorphous PET, amorphized postconsumer waste PET or crystalline PET). As CBMs exhibit a broad range of hydrophobic binding affinities with many natural biopolymer substrates, including cellulose, chitin, xylan, and starch,[239] this potential was explored with synthetic PET. In consequence, effort has been devoted to the development of a fast and reliable PET surface affinity assay to screen CBMs for PET film binding.[232] From the evaluation of eight CBMs belonging to distinct CBM families, BaCBM2 of chitinase B from *Bacillus anthracis* was identified as the most efficient PET-binding module when using biaxially oriented PET (boPET) film. Moreover, MD simulations unraveled that the mechanisms of such binding involved a combination of a protein planar surface harboring a tryptophan residues triad, in interaction with phenyl rings of the polyester chains, and formation of hydrogen bonds between other amino acid residues near the tryptophan triad and the ester linkage of PET.

In the past decade, chimera proteins built by associating PET hydrolases and CBMs were shown to improve initial PET hydrolase efficiency by enhancing their substrate binding affinity. Such improvements were demonstrated regardless of the PET sourcing (fiber, amorphous, crystalline, amorphized waste, and boPET), as shown in Table 5. Protein engineering studies using CBMs revealed that these domains could effectively promote adhesion of chimera proteins to PET surface. Similarly, research works were extended to other domains, such as polyhydroxylalkanoates domains,[235] hydrophobic domains,[240] and anchor peptides.[241] For example, a C-terminus fusion of Thc_Cut1 cutinase from *Thermobifida cellulosilytica*, with the polyhydroxylalkanoate-binding module (PBM) of the PHA depolymerase from the bacterium *Alcaligenes faecalis*, achieved higher performances (binding affinity and enzymatic PET hydrolysis efficiency) than its

https://doi.org/10.1021/acs.chemrev.2c00644
Chem. Rev. XXXX, XXX, XXX−XXX

counterpart using a CBM.[235] Hydrophobins are small amphiphilic proteins (<20 kDa) with surfactant-like behavior[242] produced by filamentous fungi. Mechanistically, hydrophobins can self-assemble into amphipathic layers at hydrophobic−hydrophilic interfaces.[243] Hydrophobins were shown to improve the enzymatic binding affinity to the PET surface when introduced as free molecules or used for material pretreatment (see the next section). The highest improvement of PET hydrolysis efficiency was described when hydrophobins were fused to a PET hydrolase. For example, class II hydrophobins (HFBs) from the fungal genus *hypocrea*, which are small secreted hydrophobic proteins, were described to stimulate enzymatic PET hydrolysis when expressed as fusion proteins.[244] Indeed, a C-terminus fusion of HFB4 or HFB7 to Thc_Cut1 cutinase from *Thermobifida cellulosilytica* could enhance the effective adsorption as well as the degradation activity of the PET film by more than 16-fold.[240] In contrast, protein fusion between HFB9b, an hydrophobin from pseudoclass I, and Thc_Cut1, showed very poor performances toward PET hydrolysis efficiency, even if HFB9b only was previously shown to have very good PET pretreatment properties. This observation corroborates the fact that different classes of hydrophobins affect enzymatic PET hydrolysis differently. This also suggests that, for each new PET hydrolase to improve through this approach, an extensive evaluation of each individual type of hydrophobin is necessary.[240] Moreover, any beneficial impact on PET hydrolysis efficiency using a PET hydrolase fusion protein with either CBM, PBM, hydrophobins, or anchor peptides needs to be specifically evaluated for every PET hydrolase. A variant of *Is*PETase showed impaired PET degradation yields when produced as a fusion protein with the hydrophobin HFB7 or a PBM of the PHB depolymerase from *Ralstonia pickettii*.[236] Similarly, no specific PET depolymerization improvement was detected when using a variant of LCC harboring a C-terminal extension composed by either the PBM of the PHA depolymerase from *Alcaligenes faecalis* or the hydrophobin HFB4.[238]

Amphiphilic properties of some bioactive polypeptides are involved in their strong adherence to the surface of various synthetic polymers.[247,248] This feature could be leveraged to improve enzyme polymer hydrolysis. For instance, a chimeric fusion was constructed by genetically linking Tachystatin A2 (TA2) anchor peptide to the C-terminus of a *Thermomonospora curvata* cutinase, which allowed achieving a 6.6 times higher polyester-PU nanoparticles hydrolysis efficiency.[241] Another anchor peptide, namely, the dermaseptin SI (DSI), could immobilize phenolic acid decarboxylase (PAD) to PET surface.[248] Lately, a comparative study was performed to improve PET hydrolysis efficiency of *Tf*Cut2, a cutinase from *Thermobifida fusca*.[249] The authors generated fusion proteins by adding a domain type from each previously described. PET binding abilities comparisons were performed using either BaCBM2 CBM,[232] HFB4 or HFB7 hydrophobins,[240] DSI[248] or TA2 anchor peptides.[241] Finally, the N-terminus fusion protein between DSI and *Tf*Cut2 achieved a 22.7-fold higher PET depolymerization hydrolysis efficiency (Table 5).

The lack of surface substrate-binding domain for PET degrading enzymes can be efficiently compensated by the addition of a PET substrate-binding domain, through the expression of a chimera protein. Even if numerous domains have already been described, directed evolution has been applied to these peptides to improve their polymer binding affinities, and the ultrahigh throughput screening systems developed concomitantly could potentially be used to engineer more efficient enzyme fusion for plastic degradation.[250] Nevertheless, high ligand-binding affinity may come at the cost of turnover speed.[251] This trade-off, depicted by the Sabatier principle, is well-known within heterogeneous catalysis[252] and a recent study claimed that both *Tf*Cut2 and LCC PET-hydrolases have too strong intrinsic interaction with PET polymer for an optimal turnover.[253] Effectively, a 20-fold improvement of k_{cat} for *Tf*Cut2 as well as a 5-fold improvement for LCC by weakening substrate binding using the surfactant cetyltrimethylammonium bromide (CTAB) is demonstrated. These results need to be put in perspective with depicted strategies of enzyme−substrate interaction enhancement using accessory binding domains. They are also pointing out the lack of a general framework to rationalize the kinetics of these interfacial enzymes hampering fundamental and comparative descriptions of PET-hydrolases.[253]

2.1.4.2.2. Additives for Polymer Surface Treatment. Hydrophobins can improve the enzymatic binding affinity to the PET surface when introduced to the enzymatic PET depolymerization assay as free molecules or used for material pretreatment.[244−246] For instance, addition of the lytic polysaccharide monooxygenase (LPMO) from the white-rot fungus *Pycnoporus coccineus*, named *Pc*AA14A, even under its enzymatically inactive form, improved the PET degradation efficiency when added to *Is*PETase by 30%.[254] The detailed mechanism of PET substrate recognition by *Pc*AA14A is still misunderstood because no auxiliary domain has been identified yet;[255] this LPMO might act itself as a CBM or a hydrophobin. Differently, a 3 h PET pretreatment by class I hydrophobins RolA from *Aspergillus oryzae* or HGFI from *Grifola frondosa* was necessary to significantly decrease the water contact angle at the polymer surface. In consequence, the self-assembly of the hydrophobins on the PET surfaces exposed their hydrophilic portions. The consecutively added *Is*PETase would then accumulate better at this modified substrate interface, enabling increase of PET hydrolysis efficiency by 1.5−1.6-fold[245,246] (Table 6).

Another alternative to enhance enzyme adsorption to the polymer surface could be through a PET substrate functionalization. Indeed, electrically charged amphiphilic molecules like surfactants can cover the PET surface through their hydrophobic portion, while the charged hydrophilic portion, exposed to the aqueous solution, can attract a specific PET depolymerase. Notably, a preincubated amorphous PET film with sodium tetradecyl sulfate (C_{14}-OSO_3^-) was 128-fold more prompt for depolymerization by the *Is*PETase enzyme than without treatment by this anionic long-chain alkyl surfactant.[227] The rationale behind this major improvement was that three positively charged amino acid residues (R53, R90, and K95), determining a large cationic region localized near the substrate binding site pocket of the enzyme, were driving ionic interaction with the anionic portion of the surfactant. In this way, the enzyme showed higher accessibility to the PET surface. Alternatively, rhamnolipids were also shown to improve by 4.5-fold the PET depolymerization mediated by the *Is*PETase enzyme when added in solution.[256] Later, and in an opposite manner, a preincubated amorphous PET film with dodecyl trimethylammonium (C_{12}-$N(CH_3)_3^+$) as cationic surfactant was 12.7-fold more susceptible for depolymerization by a *Tf*Cut2 variant of the enzyme from *Thermobifida fusca* than without PET surfactant pretreatment.[166] Finally, it is important to consider that promoting

https://doi.org/10.1021/acs.chemrev.2c00644
Chem. Rev. XXXX, XXX, XXX−XXX

Table 6. Selected Surface Treatments of PET Substrate Studies and Associated Polymer Depolymerizations by PET Hydrolases in the Presence of Accessory Proteins, like the Lytic Polysaccharide Monooxygenase (*Pc*AA14A) Used in Combination during Catalysis or Hydrophobins (HFB) Used for PET Substrate Pretreatment

binding domain type contained	protein name (origin)	utilization	PET hydrolase name	PET depolymerization (fold improvement)	PET substrate	pH	temp (°C)	incubation time (h)	ref
unknown	*Pc*AA14A (*Pycnoporus coccineus*)	Co incubation	*Is*PETase$^{S121E/D186H/R280A}$(ThermoPETase)	1.3	PET granules	9	40	120	254
class I HFB	RolA (*Aspergillus oryzae*)	3 h preincubation	*Is*PETase	1.5	PET fiber, crystalline PET (X_c 45%)	8	30	120	245
class I HFB	HGFI (*Grifola frondosa*)	3 h preincubation	*Is*PETase	1.6	PET fiber, crystalline PET (X_c 45%)	8	30	120	245

PET depolymerization through enzyme−surfactant interactions does not follow a straightforward development, because it relies notably on enzyme surface properties. For instance, such protein−surfactant interactions were shown to be deleterious by promoting structural changes, protein denaturation or aggregation, when applied to HiC enzyme.[257−259]

2.1.4.3. Improvement of Enzymatic Thermostability. As emphasized previously, thermostability of PET hydrolases is highly desired for an industrial PET depolymerization, especially for PET polymer exhibiting high T_g. However, the overall low thermostability of naturally occurring PET depolymerases is one major bottleneck for practical applications. Inspired by the unique structural features of thermophilic proteins, effective strategies have been successfully developed to improve the thermostability of PET hydrolases.[225] Numerous studies reported thermostability improvements of PET hydrolases over the years and were compiled in recent reviews.[74,87,88,91,221,224,225,260−262] Several distinct approaches that have been successfully applied to PET hydrolases to increase their PET depolymerization efficiencies at elevated temperatures are discussed below.

2.1.4.3.1. Decrease of Aggregation Phenomena. Glycosylation of proteins expressed in eukaryotic microbial cells can enhance enzyme thermostability by strengthening the protein thermodynamic stabilization and by preventing thermal protein aggregations. It has been demonstrated that the LCC, one of the most thermostable PET hydrolases, with a T_m of 86 °C, was susceptible to thermal-induced aggregation.[263] This may explain why despite its high T_m value, the protein half-life observed at high temperatures were relatively low (40 and 7 min at 70 and 80 °C, respectively).[192] The expression of the LCC PET hydrolase in the eukaryotic *Pichia pastoris*, leading to a glycosylated form of the enzyme via post-translational modification, enabled increase of the temperature at which the aggregation phenomenon is delayed by 10 °C, slowing down the aggregation kinetics for temperatures above 70 °C and increasing PET depolymerization efficiency at elevated temperature. However, the correct positioning of a glycan moiety at the surface of a protein is not well controlled and might interfere with the positioning of the PET chain in the active site of the enzyme.[204,264,265] Moreover, the nature of the glycan moiety, in terms of length and composition, will be dependent on the expression host. Consequently, this strategy must be implemented directly in the final host for enzyme production, provided that this latter has the machinery to make such post-translational modification.

2.1.4.3.2. Thermal Stability Improvement by Addition of Disulfide Bridges. Most PET hydrolases have divalent metal sites in their three-dimensional structure. The number of such sites can be up to three. For instance, three Ca^{2+} binding sites were identified in the Cut190 crystal structure (PDB 5ZNO).[111] The addition of divalent ions such as Ca^{2+} or Mg^{2+} has been shown to increase both thermostability and optimum temperature.[111,188] For instance, the stabilizing effect of calcium (Ca^{2+}) on LCC was assessed by circular dichroism (CD) demonstrating a 12 °C increase of T_m when supplemented by 20 mM Ca^{2+} (T_m = 98 °C),[192] while differential scanning fluorimetry (DSF) gave a value of 9.3 °C increase when using saturating concentrations of Ca^{2+}.[78] X-ray structures combined to MD simulations of substrate-bound states also suggested that Ca^{2+} binding in Cut190 could trigger conformational transitions between the open and closed states and drive the catalytic cycle.[262] Nevertheless, this observation

https://doi.org/10.1021/acs.chemrev.2c00644
Chem. Rev. XXXX, XXX, XXX−XXX

might be specific to Cut190, because until now the Ca^{2+} binding site involved has not been identified in other PET hydrolases.[183,262]

Disulfide bonds contribute to the thermal stability of enzymes. For instance, LCC contains a disulfide bond between Cys275 and Cys292, well conserved among thermophilic bacterial PET hydrolases, and its removal leads to a 15.6 °C loss of T_m.[192] Introduction of disulfide bridges to mimic the beneficial effects of these Ca^{2+} binding sites, and to remove the metal dependence, potentially detrimental for downstream processing of the PET depolymerization assay, were explored. Indeed, this strategy successfully led to the improvement of the thermal stability of various cutinases such as *Tf*Cut2 (variant D204C/E253C; T_m 92.8 °C; +21.6 °C),[266] Cut190 (variant D250C/E296C; T_m 79 °C; +20.0 °C),[111] and LCC (variant D238C/S283C; T_m 94 °C; +7.8 °C)[78] (Table 7). Despite a T_m of 86.2 °C, the LCC is not thermostable enough to carry out a reaction at 65 °C for 3 days. Although the D238C/S283C variant showed a 28% decrease in activity, it contributed to reach one of the most impressive depolymerization results obtained at 72 °C, a temperature close to the T_g of the PET polymer.[78] However, those results were only made possible because the depolymerization kinetics were faster than the crystallization kinetics and has implied a concomitant increased of the specific activity of the LCC PET hydrolase on top of its thermostability improvement, leading to the LCC^{ICCG} quadruple variant. This variant was able to depolymerize 90% of a 200 $g{\cdot}L^{-1}$ solution of PET in 10 h, which is an appropriate time frame avoiding recrystallization of PET.[78] Nevertheless, LCC^{ICCG} variant could not reach a conversion yield higher than 55% when the PET depolymerization was performed at 75 °C. Indeed, at this temperature, the kinetics of recrystallization prevailed over the kinetics of depolymerization. Effectively, a crystallinity higher than 40% was reached in only 6 h, and the reaction stopped before a high conversion was reached.[78] Additionally, the same approach of disulfide bridge introduction, targeting the same Ca^{2+} binding sites as previously described for type I PET hydrolases, has been performed in the type IIb $IsPETase^{S121E/D186H/R280A}$ triple variant, named ThermoPETase, and showed a T_m increase of 11.6 °C (Table 7).[267] Lastly, a disulfide bridge introduction has been introduced in the similar calcium binding site of the type I PHL7 PET hydrolase (renamed PES-H1). When this introduction showed no T_m improvement at low concentration of potassium phosphate buffer (e.g., 77.1 °C to 76.8 °C), the increased of buffer strength improved the wild-type enzyme T_m to 84.9 °C and the disulfide bridge addition leaded to an additional gain of 6.4 °C of T_m (Table 7).[141] However, use of high concentration of potassium phosphate buffer will be an economic brake on the industrial deployment of this solution.

Table 7. Stabilizing Effect of Ca^{2+} Divalent Cations Addition and Disulfide Bridge Introduction through the Estimated T_m Comparison of Selected PET Hydrolases[a]

PET hydrolase name	T_m (°C), no Ca^{2+}	T_m (°C), with Ca^{2+}	ref
LCC	86.2	98.0	130,192
$LCC^{D238C/S283C}$	94.0	97.6	78
*Tf*Cut2	71.2	84.6	93,266
$TfCut2^{D204C/E253C}$	92.8	92.8	266
Cut190	59.0	75.0	188
$Cut190^{D250C/E296C}$	79.0	78.9	111
ThermoPETase	56.6	nd[b]	194,267
$ThermoPETase^{N233C/S282C}$	68.2	nd	267
PHL7	84.9	nd	141
$PHL7^{R204C/S250C}$	91.3	nd	141

[a]ThermoPETase is the given name of the triple variant $IsPETase^{S121E/D186H/R280A}$ showing a 10.6 °C increase in T_m compared to the *Is*PETase's T_m of 46 °C.[194] [b]nd, not determined.

2.1.4.3.3. Thermal Stability Improvement by Other Approaches. Formation of hydrogen bonds and hydrophobic interaction between a proline and neighboring residues can stabilize the tertiary structure of a protein. Furthermore, the proline side chain's cyclic structure may contribute to higher structural rigidity. The introduction of proline residues has been successfully exemplified to increase the thermostability of PET hydrolases. Effectively, as early as in 2012, the beneficial impact on protein thermostability by the substitution of the S219 by a proline in the Est119 bacterial PET hydrolase from *Thermobifida alba* AHK119 has been reported.[101] The corresponding mutation was further transferred in the Cut190 bacterial PET hydrolase of *Saccharomonospora viridis* AHK190. Indeed, the $Cut190^{S226P}$ variant showed a T_m increased by 3.7 °C assorted by a PET depolymerization efficiency improvement.[110] Alternatively, the comparison of protein sequences of the PET hydrolases from the *Thermobifida* genus highlighted a proline to threonine evolution regarding the amino acid at position 253 for both tandem PET hydrolases originating from *Thermobifida alba* AHK119 (e.g., Est1 and Est119). A thermostabilizing effect of this proline was consecutively demonstrated by generating the $Est1^{T253P}$ variant, which showed a 5 °C increase of T_m.[107] Recently, the thermostability of the LCC^{ICCG} quadruple variant has also been improved by introducing a proline at the position N248.[178] This position, identical to the previously described T253 residue from Est1, has been targeted based on similar approach, a comparison of protein sequences with the most thermostable PET hydrolases from the *Thermobifida* genus. The introduction of this N248P mutation in the LCC^{ICCG} quadruple variant led to 3.6 °C increase of T_m. Alternatively, the thermostabilizing effect of this N248P monovariant in LCC has previously been described in a Carbios' patent, where a 4.4 °C increased of T_m was claimed.[268] Beyond the fact that the introduction of this N248P mutation to the LCC^{ICCG} quadruple variant illustrates the potential additivity of the mutations properties (e.g., increase of T_m), authors claimed that this variant exhibited higher PET depolymerization activity at 80 and 85 °C than LCC^{ICCG} based on initial rate determinations.[178] This statement might be biased and subjected to discussion. Effectively, as emphasized previously, performing an enzyme-based PET depolymerization at a temperature higher than the T_g of the polymer is detrimental to enzyme performances, principally because of the too-fast PET recrystallization kinetics and the inability of the PET hydrolases to depolymerize crystalline region of the PET (Figure 12).[75,78,155] Effectively, with only 3% conversion, achieved after 7 days of enzymatic treatment using a low PET concentration (e.g., 8 $g{\cdot}L^{-1}$), it can be postulated that the extremely high recrystallization rates, anticipated for assays performed at 80 and 85 °C, were responsible for the very low yields of the PET depolymerizations reported and were interfering with an unbiased comparison of the performances of the PET hydrolases involved.

https://doi.org/10.1021/acs.chemrev.2c00644
Chem. Rev. XXXX, XXX, XXX−XXX

Hydrogen bonding network improvement can maintain protein higher-order structures, which can promote structural stability and improve resistance to high temperature.[225] Engineering the formation of hydrogen bonds at the flexible regions to generate a more stable enzyme structure is another method to improve thermostability.[269] When the *Is*PETase derived from the bacterium *Ideonella sakaiensis* discovery has been released in 2016, the Science's research article received an incredible media attention and scientific success,[90] mostly because of the ability of the organism to grow on PET as the sole carbon source. The *Is*PETase showed higher degradation activities when performing an enzyme-based PET depolymerization at moderate temperature (e.g., 30−40 °C) than other thermostable PETases already described (e.g., BTA-1, BTA-2, LCC). Nevertheless, the *Is*PETase, with a T_m as low as 46 °C, suffered from very low thermostability, and once the specific activities of different PETases were compared at their optimum temperatures, the *Is*PETase was shown to be from 2 to 4 orders of magnitude less efficient than BTA-1 or BTA-2 from *Thermobifida fusca* DSM43793 and LCC, respectively.[78] Consequently, numerous strategies have been conducted to increase the thermostability of this promising enzyme, notably by the introduction of hydrogen bonds. For instance, using the structural information on *Is*PETase, and more particularly the *B*-factor values as a descriptor of the flexibility of the protein, a rational protein engineering strategy was applied to search for variants of improved thermal stability and PET degradation activity. Indeed, a rational protein engineering approach coupled with an evolutionary comparison between the *Is*PETase and the *Tf*Cut2 thermostable PET hydrolase (T_m = 69.8 °C) has been performed. Focusing on the $\beta6-\beta7$ connecting loop, it has been identified a His-Asp pairing in *Tf*Cut2 facilitating H-bond formation. Therefore, the *Is*PETase$^{S121E/D186H}$ double variant was generated to match the *Tf*Cut2, which indeed improved the T_m by 6 °C.[194] Drawing on previous work, showing enhanced catalytic activity with a R280A mutant,[134] authors further generated the *Is*PETase$^{S121E/D186H/R280A}$ triple variant (called ThermoPETase), revealing a T_m value increased by 8.8 °C (T_m = 57.7 °C). The PET degradation activity was enhanced by 13.9-fold at 40 °C in comparison to parental wild-type enzyme.[194] However, this positive result must be put into perspective because when using this improved variant with an enzyme loading of approximately 1.5 mg·g^{-1} of PET, less than 0.1% of the PET introduced (10 g·L^{-1}) was depolymerized in 72 h after an objective but approximate calculation of the yield reported. Effectively, this research article, as too many other ones, is performing PET depolymerization using a 6 mm diameter sample of PET film, without quantitation of exact mass introduced, additionally authors are comparing their enzyme improvements based on the quantity of released monomers (e.g., TA, MHET, and BHET), avoiding *de facto* any comparison and pertinence evaluation with other studies releasing objective yields.

Another approach consisted in a computational strategy called GRAPE was recently devised. The GRAPE strategy combined a systematic clustering analysis with greedy accumulation of beneficial mutations in a computationally derived library. When applied to *Is*PETase, this approach led to the redesign of a variant of *Is*PETase containing 10 mutations, called DuraPETase, that exhibited a T_m drastically increased by 31 °C (T_m = 71 °C).[196] Moreover, an enhanced degradation by 300-fold toward semicrystalline PET films (crystallinity: 30%) at 37 °C was obtained, corresponding to a maximum of 15% degradation at 37 °C of a 4g·L^{-1} PET solution in 10 days.

A neutral, deep learning-based approach has been used to improve catalytic activity and thermostability of the *Is*PETase.[199] The most thermostable variant described has an additional N233K mutation with respect to DuraPETase and has a T_m of 83.5 °C, leading to a first significant enzyme-based PET depolymerization efficiency reported when using an *Is*PETase variant at 60 °C (unlike the ThermoPETase and DuraPETase). The N233K mutation is establishing an intramolecular salt bridge between residues at position K233 and E204. Additionally, it can be postulated that dependency to Ca^{2+} has been removed because these two residues were part of the three residues that were involved in Ca^{2+} coordination in *Is*PETase (e.g., E204, N233, and S282). Moreover, when a disulfide bridge addition in ThermoPETase, leading to the ThermoPETase$^{N233C/S282C}$ variant, was showing a 11.6 °C increase of T_m,[267] the ThermoPETase^{N233K} variant, targeting and stabilizing the same N233 residue, exhibited a similar range of T_m enhancement with an 8.6 °C of improvement.[199] Similar mechanism of T_m enhancement in the reported DuraPETase^{N233K} variant could be reasonably hypothesized. Finally, the best compromise between thermostability and activity has been reported for the variant called FAST-PETase obtained through the addition of N233K and R224Q to the ThermoPETase variant.[199] The thermostability of the FAST-PETase being only of 67 °C, the PET depolymerization was carried at 50 °C. At this relatively low temperature, a PET depolymerization yield of 90% was achieved after 14 days of enzymatic treatment of a 45 g_{PET}·L^{-1} solution (e.g., amorphized PET bottle flakes) and using a total enzyme load of 1.8 mg·g^{-1} of PET. Indeed, fresh enzyme loading was performed every day during the 14 days of the PET depolymerization because of a fast FAST-PETase inactivation. Consequently, such a PET depolymerization process did not seem economically relevant because of the time length necessary for a complete depolymerization but also because of the very high dilution of the monomers generated that are collected at each step of the fresh enzyme loadings, jeopardizing their efficient purification under economic constraint.

Recently, computational approaches based on statistical methods and machine learning (ML) have been used to rationalize how structural characteristics derived from MD simulations were related to protein thermal stability.[270] These ML models were established based on a data set extracted from the ProTherm database (Thermodynamics Database for Proteins and Mutants)[271−273] and then used to predict thermal stability changes induced by sequence variations. Indeed, from a set of 177 predicted single-point variants of *Tf*Cut2 PET hydrolase, nine variants were selected for experimental evaluation, and among them, seven revealed an enhanced thermal stability compared to parental wild-type enzyme.[270] Then, following a semirandom recombination of the mutations, the *Tf*Cut2$^{S121P/D174S/D204P}$ triple variant showed an enhancement of the T_m value by 9.3 °C assorted by a 46-fold PET depolymerization efficiency improvement, when performed at 70 °C. The enzyme efficiency improvement appeared impressive, however, even if the PET depolymerization was performed by introducing crystalline PET (e.g., crystallinity 35.5%) the low substrate loading of 10 g·L^{-1} combined with the high amount of enzyme used (e.g., 5 mg·g_{PET}^{-1}) might biased the claimed PET depolymerization

https://doi.org/10.1021/acs.chemrev.2c00644
Chem. Rev. XXXX, XXX, XXX−XXX

efficiency improvement. Indeed, authors emphasized that there was no residual activity of the wild-type enzyme after 30 min, while the *Tf*Cut2$^{S121P/D174S/D204P}$ triple variant showed some residual activity up to 5 h when used at 70 °C.

Finally, with the development of an automated, high throughput directed evolution platform for engineering PET deconstructing enzymes, a new highly thermostable variant of *Is*PETase, namely HotPETase, with a T_m of 82.5 °C, has been reported.[200] Effort was made to overcome the limitations of structure-guided design using computational methods by increasing the whole throughput of their enzyme variants evaluation process and performing directed evolution of *Is*PETase. After multiple rounds of evolution, each targeting a specific set of residues identified either by the literature as potentially important for stability and catalysis for the improvement of *Is*PETase and LCC or by the protein flexibility properties or by their structural localization (e.g., end of α-helices and β-sheets) or by other consideration, the authors were able to evaluate >13 000 *Is*PETase variants and to identify the HotPETase variant, containing 21 mutations, and able to operate near or above the T_g of the PET polymer. When performing a PET depolymerization, using a low concentration of crystalline PET powder (e.g., 4 g·L^{-1}, crystallinity 36.4%, 300 μm) and around 0.3 mg of HotPETase per gram of substrate, approximatively 14% PET conversion was obtained after 50 h of treatment at 40 °C. The ability of this evolved enzyme to work closer to the T_g of PET was proven by performing a similar PET depolymerization at 60 °C, but it appeared that the thermostability improvement of the HotPETase was not sufficient. Indeed, after 5 h, only 8% conversion was reached, and the enzyme was already inactivated.[200]

Overall, considerable efforts have been devoted over the years to improve the thermostability of these catalysts used for enzyme-based PET depolymerization. The main objective being the development of a whole process of depolymerization operating at a temperature as close as possible to the T_g of PET (Figure 13).

2.1.4.4. Improvement of Enzyme Catalytic Activity. As emphasized previously, a lot of efforts have been made to improved PET hydrolases properties (e.g., substrate/enzyme interaction, enzyme thermostability), and the optimization of the PET hydrolases catalytic efficiency is probably one of the most challenging. Numerous studies have reported catalytic activity improvements of PET hydrolases over the years and were compiled in recent reviews.[88,145,224,225,261]

The interaction between the PET hydrolase active site and the PET substrate is a critical factor over the efficiency of the PET depolymerization. Indeed, strategies of PET hydrolases engineering for catalytic activity improvement are mainly focused on this active site region.[143,274] A common approach was to increase the polymer substrate accessibility by wider opening of the enzyme active site. Indeed, the L182A variant of *Fusarium solani* cutinase generating an enlarged active site cleft showed increased hydrolytic activity toward PET.[275] Since then, similar approaches were successfully implemented in engineering numerous PET hydrolases such as Cut190, *Is*PETase, LCC, or PE-H, enhancing their degradation activity toward the PET or the model substrate poly(butylene succinate-*co*-adipate) (PBSA).[136,193,276,277] Effectively, a substrate-bound 3D structure modeling strategy have been developed to determine the putative binding pocket on the crystal structures of the Cut190$^{S226P/R228S}$ thermostable

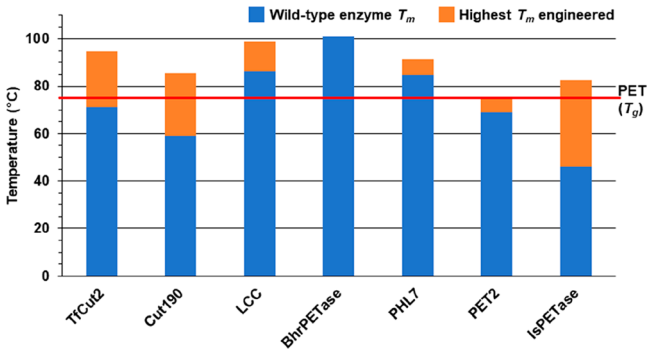

Figure 13. Melting temperature values of selected PET hydrolases and the highest T_m reported through various engineering efforts in comparison with the T_g of PET (no addition of calcium considered). Reported T_m of improved PET hydrolases also had improved or unchanged plastic degradation efficiency. Type I PET hydrolases: *Tf*Cut2[93] and *Tf*Cut2$^{D204C/E253C/D174R/G205D}$,[266] Cut190[188] and Cut190$^{S226P/R228S/Q138A/D250C/E296C/Q123H/N202H}$,[111] LCC[130] and LCC$^{F243I/D238C/S283C/Y127G/AS9K/V63I/N248P}$,[178] BhrPETase,[132] PHL7[141] and PHL7$^{R204C/S250C}$.[141] Type IIa PET hydrolases: PET2[140] and PET2$^{R47C/G69C/F105R/E110\ K/S156P/G180A/T297P}$.[140] Type IIb PET hydrolases: *Is*PETase[90] and HotPETase.[200] Adapted with permission from ref 88. Copyright 2021 MDPI.

variant.[276] The identified residues were then divided in several groups related to the enzyme catalysis (e.g., vicinity of oxyanion hole or catalytic triad, stabilization of the negative charge of the tetrahedral intermediate formed) and further targeted for amino acid mutagenesis. Many evaluated protein mutants were negatively impacting enzyme properties, but the I224A and Q138A variants as well as the I224A/Q138A double variant were dramatically increasing the K_{cat} toward PBSA even if the larger substrate binding surface area in the active site generated led to a loss of affinity for the polymer substrate. Similarly, a single amino acid substitution, namely Y250S, have been generated in the PE-H PET hydrolase, resulting in a rearrangement of the active site conformation having then twice the volume than in wild-type PE-H.[136] This rearrangement was potentially favored by the prevention of a polar contact between the Y250 residue located next to the catalytic active histidine (H249) and a loop region of the active site cleft. This active site structural modification led to a 30% increased of PET depolymerization yield. Structure-guided mutagenesis has also been applied to *Is*PETase to perform rational modification of certain residues, either located in the identified substrate binding pocket and/or located in a hydrophobic cave above the catalytic triad.[193] Amino acid substitutions that induced a wider opening of the binding center (e.g., Y58A, W130A, W130H, and A180I) or that enhanced aromaticity on the edge of the binding pocket (S185H) generated higher activity than that of the wild-type *Is*PETase. Another structural analysis combined with molecular docking of the tetrahedral intermediate from 2-HE(MHET)$_4$ suggested that the substrate binding site of *Is*PETase formed a long, shallow L-shaped cleft on a flat surface, the surface of the substrate binding cleft being mainly hydrophobic with the length of the cleft of ~40 Å. Additionally, based on the scissile ester bond of 2-HE(MHET)$_4$, the substrate binding site could be divided into two subsites, subsite I and subsite II, being able to bind one and three MHET moieties, respectively. The polar R280 residue located at the end of subsite IIc showed a protruding shape, and authors hypothesized that it was

https://doi.org/10.1021/acs.chemrev.2c00644
Chem. Rev. XXXX, XXX, XXX−XXX

hindering stable binding of PET substrate.[134] As expected, the *Is*PETase^{R280A} variant showed no change in BHET hydrolysis efficiency compared to the wild-type enzyme. Indeed, because of its distal localization from the catalytic site, the R280 residue was not expected to directly participate in the substrate binding when BHET was used. Conversely, PET depolymerization efficiency was increased by 22% to 32% after 18 h and 36 h of enzymatic treatment, respectively. Authors proposed that the R280A amino acid substitution was modifying the conformation of the substrate binding site (subsite IIc) of *Is*PETase, providing a hydrophobic and a nonprotruding cleft and allowing longer substrate binding even if located distal from the catalytic site with 22.8 Å.

However, a wide active site might also have weaker substrate affinity due to reduced binding ability.[276] Consequently, when developing a PET hydrolase engineering approach, there is no guarantee that an improved catalytic performance will arise according to an increase of the size of the PET substrate binding space. Indeed, the *Is*PETase$^{S238F/W159H}$ double variant where the amino acid substitutions were narrowing the active site showed an increased PET depolymerization efficiency. This catalytic activity improvement might be explained by a positive combination of π-stacking interaction induced by the S238F mutation and of deeper sitting of the PET substate in the active site cleft enabled by the W159H amino acid substitution.[144]

Alternatively, beyond the size of the PET hydrolase active site, the hydrophobicity of the substrate binding groove has also been successfully tuned. Indeed, an increase of hydrophobicity could be advantageous for PET binding due to higher affinity.[278] Indeed, through a molecular docking of a PET2 molecule (e.g., dimer of MHET) in the active site of an *Is*PETase crystallographic structure (PDB 5XG0), the authors found six key residues surrounding the substrate-binding groove. The enzymatic activities of the R61A, L88F, and I179F mutants exhibited 1.4-fold, 2.1-fold, and 2.5-fold increases, respectively, in comparison with the wild-type *Is*PETase. When it was previously reported that the I179A mutation was deleterious to the enzymatic activity because of a decreased interaction with PET substrate,[152] the I179F amino acid substitution, with a more hydrophobic phenylalanine residue and larger branch chains, showed the highest PET depolymerization efficiency.[278] Such an amino acid might function like the two inherent substrate phenyl ring binding residues previously reported (e.g., W156 and W130)[134,152] and involved in the immobilization of the phenyl ring of PET.

Furthermore, the combination of strategies aiming at opening the size of the active site and at increasing its hydrophobicity could synergistically improve the PET hydrolases catalytic performances. Indeed, the BTA-1$^{Q132A/T101A}$ double variant, creating more space and increasing the hydrophobicity in the active site, exhibited significantly higher PET depolymerization efficiency than the wild-type enzyme.[279]

Interestingly, the type IIb *Is*PETase shares high sequence identity to other type I thermostable PET hydrolases but has higher PET depolymerization efficiency at ambient temperature.[90] Structural analysis suggested that *Is*PETase harbored a substrate-binding residue, W185, with a wobbling conformation (e.g., conformation A, B, and C types) assorted with a highly flexible W185-locating $\beta6-\beta7$ loop, when in other homologous enzymes, the W185 conserved residue, strictly adopted a C-type conformation.[152] It was further hypothesized that this structural variation should be attributed to the S214 residue whose equivalent was a histidine in all others homologous enzymes.[280] The small side chain of S214 could leave W185 free to wobble, when in the other enzymes, the S214 equiv His residue packed against and restricted the Trp side chain from rotating. Additionally, the I218 residue from *Is*PETase whose equivalent was a phenylalanine in all others homologous enzymes was also identified as involved in the W185 wobbling conformation. Introduction of the mutations His/Phe to Ser/Ile to increase substrate-binding site flexibility in the thermostable LCC and *Tf*Cut2 PET hydrolases were proved to enhance PET depolymerization efficiencies[280] when performed at low temperatures. Effectively, even if the LCC$^{H218S/F222I}$ double variant PET depolymerization efficiency was improved when enzymatic treatment was performed from 40 to 60 °C, an important loss of efficiency was shown when performed at higher temperatures.

Recently, more systematic approaches using the knowledge accumulated over the last years have been developed to improve PET hydrolases catalytic activity. Effectively, structural analyses and computational modeling using molecular dynamics simulations have provided better understanding of how product inhibition and multiple substrate binding modes influenced key mechanistic steps of the enzymatic PET depolymerization by PET hydrolases. For instance, the key residues involved in substrate-binding as well as those identified as mutational hotspots in homologous PET hydrolases were subjected to mutagenesis in the type I thermophilic PHL7 PET hydrolase.[141] These approaches compensated the lack of rationalization by a high throughput development of screening methodologies. Nevertheless, the PHL7$^{L92F/Q94Y}$ double variant, incidentally, was introducing the equivalent amino acid residues of LCC (e.g., F125 and Y127) and showed a low increase of T_m of 1.8 °C but an impressive PET depolymerization efficiency improvement of 2.3-fold and 3.4-fold against amorphous PET films and pretreated real-world PET waste, respectively, when enzymatic treatment was performed at 72 °C.[141] As emphasized previously, since the first release of *Is*PETase properties in 2016,[90] numerous studies have developed intensive efforts to successfully improve its thermostability as well as its catalytic activity. Indeed, with the release of DuraPETase, a variant of *Is*PETase containing 10 mutations, obtained after greedy accumulation of beneficial mutations, a high number of single variant properties (e.g., T_m and catalytic activity) were also released. Some of these variants showed improved catalytic efficiency without T_m improvement and might not have been considered when constructing the DuraPETase variant.[196] Similarly, the release of the FAST-PETase variant, adding N233K and R224Q amino acid substitutions to the ThermoPETase variant of *Is*PETase, emphasized the implementation of a neutral, structure-based, deep learning neural network-based approach to determine the set of variants to evaluate.[199] This very innovative approach, still successful, might suffer from a lack of rationalization and reproducibility if applied to other PET hydrolases. Nevertheless, a few single amino acid substitutions (e.g., S121E, T140D, R224Q, and N233K), either in *Is*PETase, ThermoPETase, or DuraPETase, were shown to improve enzyme activity and were not subjected to any extensive discussion regarding their individual contribution to enzyme/substrate complex interaction. Conversely, computational design of an improved *Tf*Cut2 PET hydrolase by mining molecular dynamics simulations trajectories tried to rationalize how structural characteristics derived from MD simulations

https://doi.org/10.1021/acs.chemrev.2c00644
Chem. Rev. XXXX, XXX, XXX−XXX

were related to protein thermal stability through computational approaches based on statistical methods and machine learning (ML).[270] Numerous predicted single-point variants have been evaluated regarding their T_m and specific activities and further combined. Several combinations showed improved catalytic activity and might still need to be better characterized to avoid misinterpretation of the mechanisms involved mostly because of the concomitant T_m increase and the high temperature of the PET depolymerization performed (e.g., 65 °C). Finally, the automated, high throughput directed evolution platform approach applied to introduce 21 mutations in *Is*PETase, generating the Hot-PETase. The authors have well documented the T_m increase at each round of evolution following the addition of several amino acid substitutions, but we can deplore that they did not emphasize the temperature of the PET depolymerization performed to evaluate the specific activity of the best variant obtained at each round of evolution. Nevertheless, the specific activity improvement of the FAST-PETase was unambiguous when compared to the *Is*PETase$^{S121E/D186H/R280A}$ triple variant efficiency when a PET depolymerization was performed at low temperature (40 °C), alleviating bias of additional thermostability improvement.[200]

Overall, various strategies have successfully been developed to improve catalytic activity of PET hydrolases over the insoluble PET substrate in a heterogeneous system. Nevertheless, there is still a lack of a general framework to rationalize the kinetics of these interfacial enzymes hampering fundamental and comparative descriptions of PET hydrolases.[253] Indeed, unbiased comparison of PET hydrolases properties is not an easy task, moreover when considering separated studies. Effectively, no standardized PET depolymerization assay have been unanimously chosen by the scientific community. Such a standardization is made difficult by the heterogeneous nature of the catalysis which depends on the type of PET used, its molar mass, its crystallinity, and the presence of comonomers such as IPA as well as the shape of the degraded PET object (e.g., film, powder with a given particle size). An amorphous commercial Goodfellow film powder, either amorphous or crystalline, could appear as an appropriate sourcing accessible to everyone as we can deplore the extensive use of 6 mm punch hole samples from Goodfellow film in numerous research article introduced without consideration of mass in the enzyme-based PET depolymerization. Moreover, a PET powder, with known particle size distribution, could be a more representative sample when considering an industrial deployment. Additionally, most of published research articles presented PET hydrolases performances by giving the concentration of equivalent TA released in the reaction medium (e.g., μM or mM of TA equivalent), and even if this might be appropriate when comparing PET hydrolases in a single study, it jeopardizes greatly a fair evaluation of the depicted performances regarding other existing studies. Moreover, more rigorous description of the experimental conditions would be of benefit to all. Indeed, beyond the mass of PET substrate introduced, the enzyme/substrate ratio (e.g., mg of enzyme per g of PET), the final PET conversion obtained after a given time of enzyme treatment as well as the productivity (e.g., $g_{TA}{\cdot}L^{-1}{.}h^{-1}$) and the specific productivity (e.g., $g_{TA}{\cdot}L^{-1}{\cdot}h^{-1}{\cdot}g_{enzyme}{}^{-1}$) should be mandatory, as it was already pointed out in Kawai's excellent review.[87] Overall, such a standardization of the PET depolymerization accompanied by these amendments should benefit to the whole scientific community by enabling putting into perspective the enzyme engineering works presenting very significant improvements of PET hydrolases performances toward PET depolymerization but with modest performances when considering the effective PET conversion into monomers. Through this review article, we take the opportunity to propose the standardization of an enzyme-based PET depolymerization assay, and it could further be considered as a reference test to allow a fairly comparison of the performances of the new PET hydrolases released (e.g., new or engineered PET hydrolases) with other referenced PET hydrolases. Indeed, a 100 mg Goodfellow PET powder sample (sieved between 200 and 500 μm) must be introduced in an aqueous buffered solution at pH 8 (e.g., 50 mL of potassium phosphate buffer >100 mM). Thus, the initial PET concentration is known (e.g., 2 $g{\cdot}L^{-1}$) and the pH remains unchanged up to complete PET conversion where 10.4 mM of TA are formed. For instance, Tournier et al. used this test to fairly evaluate the PET depolymerization performances of five PET hydrolases, BTA-1, BTA-2, FsC, *Is*PETase, and LCC. Indeed, authors used each PET hydrolase under its optimal condition of pH and temperature to perform an enzyme-based PET depolymerization. Accordingly, *Is*PETase was proven to be a very inefficient enzyme, being approximately 10, 100, and 10 000 times less efficient than Fsc, BTA-1 and BTA2, and LCC, respectively.[78] These results agreed with comparisons made between *Is*PETase and Cut190[85] as well as *Is*PETase and LCC.[156] In 2019, Zimmermann et al. were the first to report a PET depolymerization, introducing plastic waste under reasonable waste and enzyme concentration conditions.[154] The authors used the enzyme *Tf*Cut2, purified from a *Bacillus subtilis* overexpression and presenting a T_m 4.1 °C higher than when purified from *E. coli*, and the PET concentration introduced, in a 1.8 mL reactor, was around 20 $g{\cdot}L^{-1}$. The enzymatic treatment was maintained at a temperature of 70 °C and pH 8, and up to 97% of an amorphous Goodfellow film (e.g., 2% crystallinity) was depolymerized in 120 h, leading to an average productivity of 0,17 $g_{TA}{\cdot}L^{-1}{\cdot}h^{-1}$. When considering postconsumer PET packaging containers for fruits and vegetables (e.g., 5% crystallinity), only 50% of depolymerization could be reached with an average productivity of 0.097 $g_{TA}{\cdot}L^{-1}{\cdot}h^{-1}$. The authors further demonstrated by DSC studies that the arrest of the enzyme's PET depolymerization was due to a rapid recrystallization of PET at 70 °C. Indeed, as it was emphasized previously, the crystallinity of the polymer, when incubated at 70 °C, increased from 5 to 17% regardless the presence of the enzyme. Alternatively, the HiC cutinase have been used to depolymerize a postconsumer PET of high crystallinity (e.g., 41.1%)[281] using an optimum PET concentration of 220 $g{\cdot}L^{-1}$ and a ratio of 4.5 $mg_{enzyme}{\cdot}g_{PET}{}^{-1}$. The PET depolymerization was arrested at 13% of conversion after 96 h, mostly because of the high degree of crystallinity of the introduced PET polymer. These data corresponded to an average productivity of 0.26 $g_{TA}{\cdot}L^{-1}{\cdot}h^{-1}$, with a maximum initial productivity being 1.15 $g_{TA}{\cdot}L^{-1}{\cdot}h^{-1}$. Finally, the most significant result was obtained using the optimized LCC^{ICCG} quadruple variant to depolymerize postconsumer-colored washed flakes. Indeed, the PET sample went through pretreatment steps of amorphization (e.g., 16% crystallinity) followed by micronization into fine powder (e.g., granulometry D50 between 200 and 250 μm). Up to 90% of a 200 $g{\cdot}L^{-1}$ PET solution was depolymerized in 10 h when introducing an enzyme concentration of 2 mg·

https://doi.org/10.1021/acs.chemrev.2c00644
Chem. Rev. XXXX, XXX, XXX−XXX

g_{PET}^{-1}, providing an average productivity of 15.5 $g_{TA}{\cdot}L^{-1}{\cdot}h^{-1}$ and a maximum initial productivity of 29 $g_{TA}{\cdot}L^{-1}{\cdot}h^{-1}$.[78]

2.1.4.5. Relieving Product Inhibition of PET Hydrolases. Efforts in optimizing the PET hydrolases have also been made to reduce product inhibition effects. Indeed, PET degradation intermediates or products (e.g., BHET, MHET, TA, EG) can inhibit enzyme activity,[282−284] and such inhibition can be alleviated by modifying the PET hydrolase's active site architecture. Only a few studies have reported enzyme inhibition relief of PET hydrolases over the years and were compiled in recent reviews.[225,261] When it was demonstrated that the *Tf*Cut2 PET hydrolase could be inhibited by MHET and BHET,[283] with MHET being the major competitive inhibitor limiting the enzyme-based PET depolymerization efficiency, several strategies have been proposed. For instance, it was suggested to use an ultrafiltration membrane reactor to perform an enzyme-based PET depolymerization introducing *Tf*Cut2, which could ultrafilter the soluble hydrolytic products released during the PET conversion to minimize the product inhibition of the enzyme and improve the efficiency of PET depolymerization by 70%.[285] Such an implementation might solve inhibitory effects but might be a very expensive and inefficient approach when considering industrial deployment. Alternatively, it was shown that MHET had a high affinity to PET hydrolases' substrate binding pockets, whose size and hydrophobicity were known to influence the enzyme depolymerization of PET substrate. Thus, to minimize the interactions between PET hydrolases and the hydrolytic products, such as the MHET, enzyme engineering approaches provided successful results. Indeed, the introduction of a G62A amino acid substitution, in *Tf*Cut2, to modify the substrate binding groove due to lower steric hindrance of Ala than that of Gly, resulted in a 5.5 times decrease in the binding constant for the inhibitory hydrolysis product, MHET, thus leading to improved PET degradation.[286] It is noteworthy that Cut190 having an Ala at this position was not inhibited by accumulation of the MHET. Another strategy to alleviate product inhibition was through the establishment of a two-enzyme system, including a PET hydrolase and a MHETase. Indeed, HiC cutinase and *Candida antarctica* lipase B (CalB) were combined to improve product inhibition, and these two enzymes revealed synergy for complete PET depolymerization to TA with an 7.7-fold increase of yield.[123] Alternatively, addition of an auxiliary enzyme capable of decomposing the intermediate compounds has been shown to be effective in reducing product inhibition.[287] Finally, since the characterization of the *Is*MHETase, this enzyme has been used to alleviate MHET inhibitory effect. Indeed, a chimera protein formed by *Is*PETase and *Is*MHETase showed increased PET depolymerization efficiency than the single *Is*PETase, which could be attributed to the role of the *Is*MHETase in degrading the intermediate MHET that inhibited the PET hydrolase.[162]

2.1.5. Outlook. As emphasized in this section dedicated to poly(ethylene terephthalate), enzyme-based depolymerization is a very promising alternative to either mechanical or chemical recycling of PET polymer. Scientific reports are booming over the last years, and numerous efforts are being made in multiple directions. Indeed, many high quality studies have thus been conducted using a few benchmark enzymes, such as thermostable cutinase(-like) enzymes from the *Actinomycetota* phylum, the plant compost-derived LCC cutinase, and *Is*PETase[224] to better assess the critical enzymatic parameters, to improve their promiscuous activity over PET, as well as to increase their enzymatic efficiency in a complex heterogeneous system in the perspective of an industrial development. Similarly, tremendous efforts are still made in the quest of new PET hydrolases from the existing diversity,[44,116,117] and future releases are expected. Other teams are focusing on the need of organizing this existing and upcoming diversity by developing and maintaining databases dedicated to plastic-active enzymes containing PET hydrolases (e.g., PAZy[57] and PlasticDB[56]). A next step might be the integration of amino acid substitution effects evaluated through enzyme engineering approaches applied to PET hydrolases, as recently reviewed.[88] On other hand, the recent multiplicity of structural characterization of PET hydrolases accompanied by model substrate or soluble products (e.g., HEMT, MHET, MHETA, BHET), as well as the development of NMR probes, will help for a better understanding of the interacting surface between the enzymes and the polymer. Strategies of enzyme engineering using rational approaches will directly benefit from these characterizations to better improve enzyme kinetics parameters. Undoubtedly, implementation of machine learning, as well as many sequence-based approaches to help enzyme engineering, will be fruitful,[199,270] as the development of directed or random evolution strategies.[200] The latter approaches compensated the potential lack of understanding by the development of automated and high throughput platforms able to screen very large numbers of enzyme variants. As emphasized, many parameters are influencing the PET hydrolase efficiency during a PET depolymerization. Tremendous efforts have been made to increase thermostability and enzyme efficiency, to tailor the enzyme affinity over the PET still considering the potential inhibitory products, to elucidate the fine mechanisms governing the exo- or endotype scission of the polymer. Enzyme-based depolymerization of crystalline PET and more precisely the crystalline region of PET remains a challenge. Until further improvements either through enzyme discovery or enzyme engineering, PET pretreatment and rigorous PET depolymerization temperature control are required. Even more, if considering the depolymerization of PET wastes, composed by an uncontrolled amount of PET objects of various crystallinities. Additionally, further characterization of such enzyme-based PET depolymerization efficiency about the additives found in PET objects (e.g., IPA, dyes) would be of interest. Indeed, further industrial deployment introducing textiles, either in PET or as blends, will benefit from the accumulated knowledge. Facing the remaining challenges to overcome, the scientific community would benefit to better rationalize their claimed enzyme-based PET depolymerization efficiencies and to contribute to a fair comparative evaluation between research articles. Interestingly, a techno-economic, life cycle, and socioeconomic impact analysis of enzymatic recycling of PET predicted that enzyme-based PET depolymerization could achieve cost parity with TA manufacturing as well as substantial reductions relative to virgin polyester manufacturing.[201] Finally, an industrial deployment of an enzyme-based PET depolymerization should soon be done. Indeed, it has been reported that up to 90% of a 200 $g{\cdot}L^{-1}$ PET solution was depolymerized in 10 h by using the LCC^{ICCG} variant at an enzyme concentration of 2 $mg{\cdot}g_{PET}^{-1}$ and providing an average productivity of 15.5 $g_{TA}{\cdot}L^{-1}{\cdot}h^{-1}$.[78] It was estimated that such enzyme efficiency improvement, accompanied by a demonstration of PET polymerization from the purified monomers, reached a technology readiness level (TRL) of five.[288] It was additionally claimed that Carbios'

https://doi.org/10.1021/acs.chemrev.2c00644
Chem. Rev. XXXX, XXX, XXX−XXX

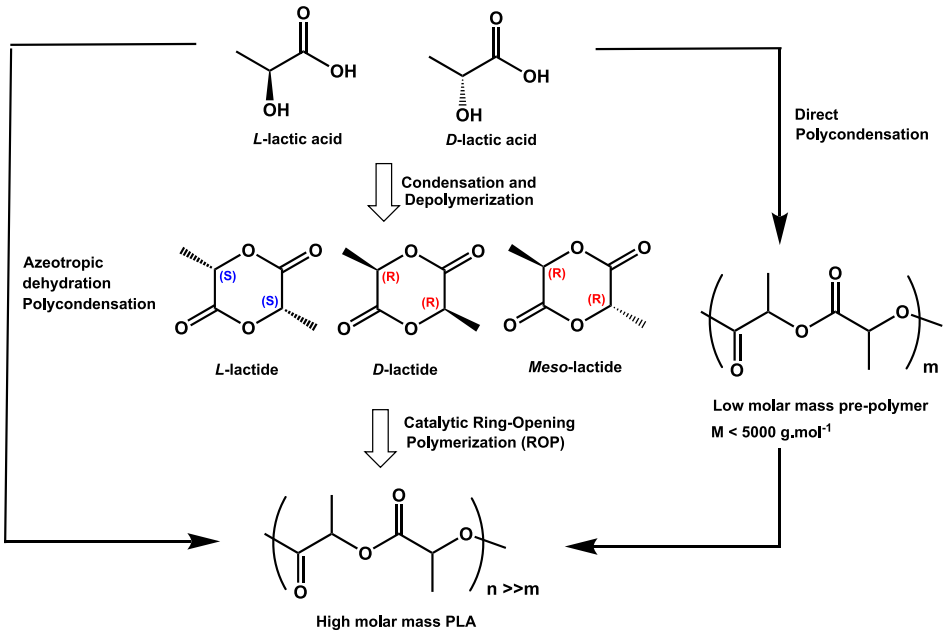

Figure 14. Synthetic routes to PLA either by direct polycondensation of lactic acid or ring-opening polymerization (ROP) of lactide.

promising technology was the closest to a system proven in an operational environment (TRL 9).[288] Since then, a demonstration plant has been built using this technology,[289] and Carbios announced the deployment in France of an industrial unit that should be operational in 2025.[290] We can therefore legitimately consider that the rise of a circular economy around the PET through the development of such a biological catalyst has now begun.

2.2. Poly(lactide) (PLA)

2.2.1. About PLA. PLA is a thermoplastic aliphatic polyester exhibiting a biodegradable feature in industrial composting conditions. Moreover, it is a biobased polymer, manufactured from biorenewable sources, such as corn starch, potato, or sugar cane instead of petrol in contrast to the many other currently produced polymers. The monomer, lactic acid, is produced by (homofermentative) lactic acid bacteria with impressive yields of 1.8 mol of lactic acid per mol of glucose, which is very close to the maximal theoretical yield of 2 mol of lactic acid per mol of glucose and titers exceeding 160 $g{\cdot}L^{-1}$.[291]

Processing methods used for PLA mass production include injection molding, sheet, and film extrusion, blow molding, foaming, fiber spinning, and thermoforming. PLA can eventually provide comparable optical, mechanical, thermal, and barrier properties when compared with commodity polymers, such as PP, PET, and PS. PLA is considered as a "Generally Recognized As Safe" (GRAS) material by the U.S. Food and Drug Administration (FDA). In the medical field, PLA is extensively used because of its biocompatibility with the human body, including for applications such as medical implants, surgical sutures, and medical devices.[292−294]

Despite a still low market (460 kt/year),[295] PLA is particularly attractive for its intrinsic degradation, which can be triggered by different means depending on the environment PLA is exposed to. Extensive research efforts have been directed toward the study of the degradation of PLA in human, processing, and composting environments. All of these features make PLA suitable for several applications, for instance, in the pharmaceutical and microelectronics fields, 3D-printing, or as a biodegradable plastic in packaging, bags, and mulching films. As it is compostable, PLA offers a promising alternative to reduce the municipal solid waste disposal issue by providing distinctive end-of-life scenarios, in comparison to more conventional plastics. For all of these reasons, the research on PLA has exponentially increased over the last 30 years, which is also explained by the development of industrial methodologies, such as polycondensation of lactic acid (LA) and ring-opening polymerization (ROP) of lactide, the lactic acid cyclic dimer, allowing the production of high molecular weight PLA to reach the market. PLA thus holds great promise to become a major commercialized biosourced and biodegradable polymer.[296−298] Nonetheless, PLA still shows some limitations in its applications. For instance, PLA is brittle, it exhibits poor elasticity, low thermal stability, low heat-distortion temperature, low rate of crystallization, and modest permeability to drugs, limiting its further commercial developments. Therefore, substantial research has focused on obtaining PLA products with desired properties. For instance, blending PLA with other synthetic or biobased polymers and/or processing PLA with plasticizers and/or fillers, such as fibers or micro- and nanoparticles, enable PLA properties to be tuned.[299] Typical plasticizers of PLA include LA itself,[300] glycerol,[301] citrate ester,[302] and poly(ethylene glycol) (PEG).[303] Instead of plasticizers, and in order to maintain the ductility of PLA, impact modifiers can be employed, e.g., ethylene-based copolymers. Although improving the impact strength, many of these additives also cause a decrease in transparency for PLA-based materials, which is a major drawback for packaging application. Finally, nucleating agents or crystallization-manipulating agents can be added (e.g., talc and montmorillonite or amides or hydrazides) to optimize the crystallization behavior during the industrial processing of PLA.[299] All of these new variations of PLA-based materials target enhanced performance of PLA while sometimes at the expense of losing the biodegradability of the polymer matrix and reducing its industrial commercial recovery. Moreover, there are still limitations due to the lack of suitable

https://doi.org/10.1021/acs.chemrev.2c00644
Chem. Rev. XXXX, XXX, XXX−XXX

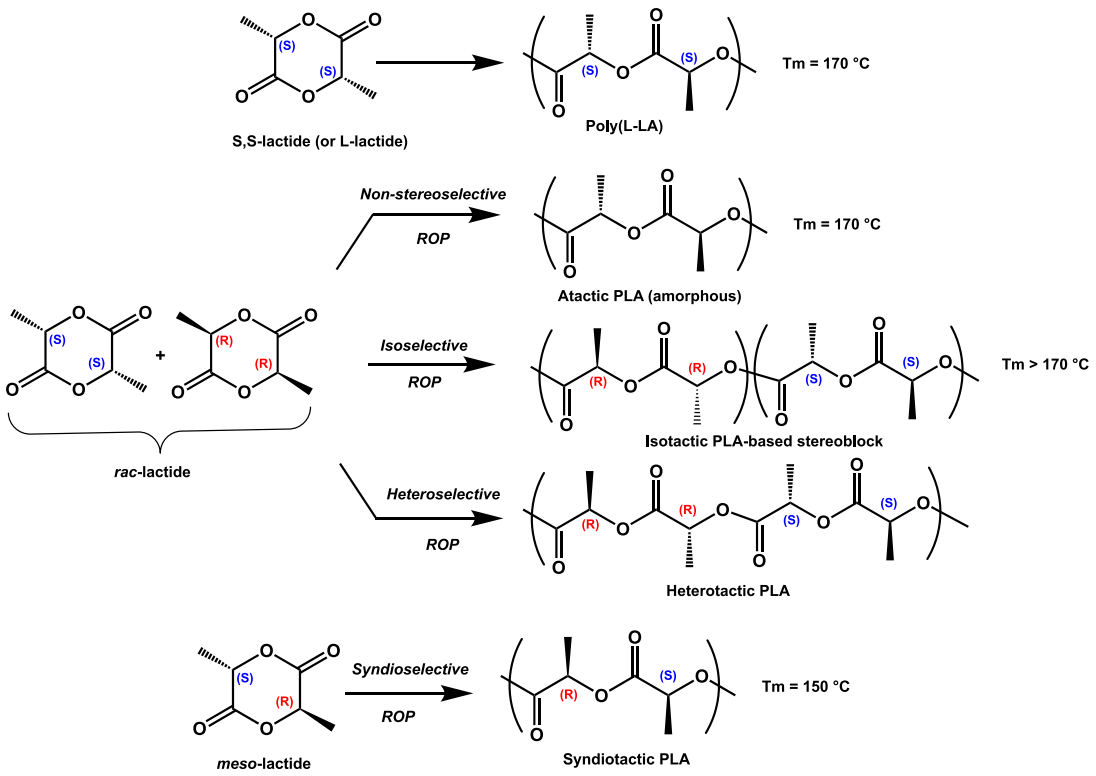

Figure 15. Different PLA microstructures from the stereocontrolled ROP of lactide.

infrastructure for sorting, recycling, and/or composting PLA products at their end of life.

The monomeric repeating unit of PLA is lactic acid (or 2-hydroxypropionic acid), which contains an asymmetric carbon atom (Figure 14). Hence, lactic acid exists as L(+) and D(−) stereoisomers. Lactic acid can be industrially produced by converting carbohydrates obtained from vegetable sources (e.g., corn, wheat, rice) by bacterial fermentation, forming almost exclusively lactic acid in the L-form. As for petrochemical synthesis, it yields a racemic mixture of the D- and L-forms. Commercial PLA grades are usually constituted of a mixture of L-LA (>95%) and D-LA (<5%). This little proportion of D-LA allows improving the processability of PLA using conventional melt-processing techniques. At high temperatures, however (>200 °C), thermal degradation of PLA takes place, which can involve different pathways, including hydrolysis, unzipping depolymerization reactions, oxidative degradation, and transesterification reactions.[304] Therefore, processing conditions often require suitable stabilizers (e.g., tris(nonylphenyl)phosphite) to minimize these side reactions.[305]

While some microorganisms have been engineered to produce PLA,[306−308] the main synthetic route to PLA remains the chemical polymerization (Figure 14). High molecular weight PLA can thus be achieved by direct polycondensation or by azeotropic dehydrative polycondensation. In the former case, removal of water as byproduct and long reaction times are required, producing PLA of rather low molecular weight (<30 kg·mol^{-1}).[309] Solid-state polymerization (SSP) can be conducted by heating PLA oligomers below T_m and by continuously removing water under reduced pressure. In this way, high molecular weight PLAs up to 500 kg·mol^{-1} can be obtained. Alternatively, the azeotropic dehydrative polycondensation of lactic acid leads to PLA of molecular weight up to 300 kg·mol^{-1}. In this case, tin-based catalysts are used as well as azeotropic solvents such as diphenylether. However, removal of water is still needed, and this process is typically conducted at 130 °C and requires long reaction times (∼40 h).[310] In the above polycondensation methods, only rather poor control over molecular weight and dispersity of PLA chains can be achieved. Much better control over macromolecular parameters, and consequently of PLA properties, is provided by ROP of lactide.[305,311] First PLA synthesis by ROP was reported by Carothers et al. in 1932.[312] Yet, the first industrial example was patented by NatureWorks (ex- Cargill Inc.) in 1992. This Cargill process involves the continuous synthesis of L-LA by fermentation of corn dextrose, followed by condensation forming oligomers, which are subsequently depolymerized under reduced pressure in the presence of a catalyst to give L-LA. The ROP step is then carried out in bulk in the presence of tin octoate as catalyst, leading to high-molecular-weight PLLA.[293] NatureWorks LLC and Total-Corbion are the two major producers of PLA, mostly PLLA (>90% L-LA).

As it contains two chiral centers, lactide eventually exists in three distinct diastereoisomers, namely, DD-, LL- (commonly used as a racemic mixture, *rac*-LA) and DL- (*meso*-LA). With appropriate catalysts/initiators, stereospecific ROP enables a controlled insertion of monomers into the polymer backbone based on their stereochemistry.[313−316] While ROP of either enantiomer yields isotactic PLA, stereocontrolled ROP of *rac*- and *meso*-LA forms different microstructures (Figure 15) with different properties. While both poly(D-LA) (PDLA) and poly(L-LA) (PLLA) are semicrystalline, atactic PLA is fully amorphous and brittle. PLLA exhibits a T_m around 160−180 °C. Both atactic PLA and PLLA exhibit a T_g value around 56−57 °C. Of particular interest, the T_m value can be dramatically increased up to 230−240 °C when mixing equimolar amounts

https://doi.org/10.1021/acs.chemrev.2c00644
Chem. Rev. XXXX, XXX, XXX−XXX

of PLLA and PDLA, owing to the formation of a stereocomplex.

The degradation rate of PLLA is actually very slow in vivo. It takes decades indeed to degrade in seawater, soil, landfills, and at home composting conditions (<37 °C), while it decomposes within 180 days in industrial composting facilities (>60 °C).[317] This is due to the hydrophobic nature and high degree of crystallinity (X_c) of PLLA. Copolymers consisting of L-LA and D,L-LA have been designed as a means to increase the degradation rate of PLLA. Likewise, copolymers incorporating glycolide (GA), trimethylene carbonate, and 1,4dioxan-2-one (PDX) as comonomer units with LLA have been conceived.

From the 50 000 tons of PLA waste generated in 2013 (mostly plates and cups, packaging, and other nondurable goods), only a negligible amount (less than 5000 tons, 10%) was recovered through recycling and/or composting.[293,318] According to Rossi et al., landfill is the less preferable option, given its high environmental impact.[319] Plasticulture applications also raise the question of contamination by pesticide residues. Studies on incineration with energy recovery were conducted by Natureworks LLC on their grade PLA Ingeo resin. A heat content of 19.5 MJ/kg was reported, which is like cellulosic-based materials, without production of additional toxicologically critical substances. Because PLA packages, such as blisters and bottles, show low contamination, recycling is a feasible route to recover these materials, reducing the demand for raw PLA. PLA sheets produced with 100% recycled PLA flakes (arising from thermomechanical recycling of cleaned postconsumer PLLA 500 mL water bottles from Primo Water Corporation) showed a 5% reduction in M_n, compared to the initial PLA, this reduction not affecting the production of PLA containers.[320] Since 2004, NatureWorks LLC recycles off-grade PLA Ingeo by using chemical recycling. Nevertheless, recycling is limited due to the lack of collection and suitable infrastructure for sorting out PLA at its end of life, concomitant with an insufficient critical mass to retreat. Moreover, the National Association for PET Container Resources (NAPCOR) and the Association of Postconsumer Plastic Recyclers (APR) have refuted the idea of mixing biobased polymers like PLA into the existing stream of recycled containers, expressing concerns regarding among others the cost of separation and processing.[293] Nevertheless, this process might not actually compete with the price of biological monomer production through fermentation, and an alternative would be upcycling. LA is easily catabolized and could fuel the central carbon metabolism of engineered microbes to produce single high added value products of choice. The production of various compounds found PLA yield in $Cmol_{product}/Cmol_{substrate}$ similar to those calculated with glucose as carbon source with *Pseudomonas putida* as the transforming cell factory.[321]

As LA is a nontoxic monomer[322,323] and the bioaugmentation with PLA-degraders does not influence the intrinsic soil microbial population and global health,[324] a solution of choice remains biodegradation. This can be achieved by composting, which is related to the propensity of an object to biodegrade. Biodegradability is defined as the capacity of a material to be metabolized in a given period of time, i.e., utilized by environmental ecosystems to produce biomass, H_2O, and CO_2/CH_4, thus displaying the great advantage of replenishing the carbon cycle. Biodegradation is thus viewed as a key strategy of circular economy. It is characterized by different steps, including fragmentation, which causes a reduction of the polymeric particle size without any change in molecular weight, degradation reducing molecular weight by coupled abiotic and biotic phenomena, and assimilation leading to final H_2O, biomass, and mineral carbon CO_2/CH_4. These steps largely depend on environmental factors such as temperature, pH, and oxygen availability. PLA is considered as biodegradable only at elevated temperature and under relative humidity (RH) conditions corresponding to those of industrial composting, namely at 58 °C and 50% RH, as defined by norms.[325] Only a few composting facilities accept biodegradable plastic materials, as it is not easy to distinguish biodegradable plastics from conventional ones. Thus, to conduct this material to its real potential of use in many applications, new methods for promoting its biodegradation in domestic compost conditions need to emerge. This is particularly important for applications where emissions or leakage is intended or inevitable, such as in agriculture with films used for greenhouses, mulching, and silage (mulching is among the largest applications of plastics in agriculture, with 2×10^6 tonnes/year produced, but nonrenewable inert PE is the default choice in the plasticulture industry[326]), geotextile, coated seeds, or fertilizers.

PLA biodegradation relies on three types of factors,[327,328] including: (i) chemical structure (molecular weight, crystallinity, purity, and configuration of the substrate), (ii) environment (UV, physical erosion, and mechanical/thermal stress that will mainly promote abiotic degradation, as well as temperature, pH, oxygen, and moisture), and (iii) microorganisms (metabolic pathways and enzymes). Here, we intend to compile the numerous studies aiming at the discovery of sources of enzymes degrading PLA and the understanding of underlying catalytic mechanisms to develop eco-friendly methods that could help its faster degradation in natural environment. This could make PLA transcend from a minor player in the market of commercial fossil-based polymers to a new solution for a bio-based economy.

2.2.2. Sources of Enzymes Degrading PLA. Recently, databases gathering plastic depolymerases, mostly through automated literature and database (NCBI and UniProt) searches, have emerged. The Plastics Microbial Biodegradation Database (PMBD) from Gan et al.[118] was the first to propose such a depository for degradation of 19 natural and synthetic polymers. When created in 2019, PMBD gathered 949 microorganisms−plastics relationships and 79 genes involved in the biodegradation of plastics. At this date, 24 microorganisms were reported to degrade PLA, and 7 PLA-depolymerases were reported with an accession number. Unfortunately, this database does not seem to be regularly incremented. Buchholz et al.[57] summarized 2500 publications addressing plastic degradation and less than 60 describing the isolation of plastic degrading enzymes. However, the authors excluded PHA and PLA from their searches. Zaaba et al. reported 2335 and 3586 articles related to microbial and enzymatic degradation of PLA, respectively.[329] Interestingly, Gambarini et al.[44,56] recently focused literature search on a large range of synthetic and natural plastics, resulting in a more complete database, which is regularly updated and allows searches and data visualization, namely the Plastic Degradation Database, PlasticDB[330] When first published, this latter included data from 421 publications, representing 562 microbial species and 111 isolated proteins. At this date, according to PlasticDB data on 66 synthetic and natural plastics,[44] 31 fungal and 63 bacterial species among the 436

https://doi.org/10.1021/acs.chemrev.2c00644
Chem. Rev. XXXX, XXX, XXX−XXX

Table 8. Microorganisms Evidenced as Producing PLA-Degrading Enzymes

Kingdom	Division	Class	Order	Family	Genus	Species	References
Bacteria	Actinobacteria	Actinobacteria (Actinomycetes)	Pseudonocardiales	Pseudonocardiaceae	Amycolatopsis	*Amycolatopsis* HT-32	336
						Amycolatopsis 3118	337
						Amycolatopsis sp. KT-s-9	338
						Amycolatopsis sp. strain 41	339
						Amycolatopsis mediterranei ATCC 27643	333
						Amycolatopsis K104-1	340
						Amycolatopsis orientalis subsp. *orientalis* IFO 12362	341
						Amycolatopsis orientalis ssp. *orientalis*	342
						Amycolatopsis tolypophorus IFO 14664T	343
						Amycolatopsis mediterranei IFO 14843	
						Amycolatopsis azurea IFO 14573T	
						Amycolatopsis thailandensis CMU-PLA07	344
						Amycolatopsis sp. strain SO1.1	345
						Amycolatopsis sp. strain SO1.2	
						Amycolatopsis sp. strain SNC	
						Amycolatopsis sp. strain SST	
						Amycolatopsis sp. SCM_MK3-3	334
						Amycolatopsis oliviviridis sp. SCM_MK2-4	
					Lentzea	*Lentzea albidocapillata*	343
					Saccharothrix	*Saccharothrix espanaensis* JCM 9112T	
						S. mutabilis subsp. *mutabilis* JCM 3380	
						S. waywayandensis JCM 9114T	
						Saccharothrix australiensis	
						Saccharothrix waywayandensis	346
					Kibdelosporangium	*Kibdelosporangium aridum*	343
						Kibdelosporangium sp.	343
					Saccharomonospora	*Saccharomonospora viridis*	110
					Pseudonocardia	*Pseudonocardia alni* AS4.1531T	347
						Pseudonocardia sp. RM423	348
					Streptoalloteichus	*Streptoalloteichus* sp.	343
			Streptosporangiales	Thermomonosporaceae	Thermomonospora	*Thermomonospora* sp.	349
						Thermobifida cellulosilytica	185
						Thermobifida alba AHK119	101,107
					Actinomadura	*Actinomadura keratinilytica* T16-1	350
						Actinomadura sp. TF1	351
				Streptosporangiaceae	Thermopolyspora	*Thermopolyspora* sp.	349
						Thermopolyspora flexuosa FTPLA	352
					Nonomuraea	*Nonomuraea terrinata* L44-1	350
						Nonomuraea fastidiosa T9-1	350
			Micromonosporales	Micromonosporaceae	Micromonospora	*Micromonospora* sp. GMKU 353, GMKU358, GMKU 362	45
						Micromonospora echinospora B12-1	350
						Micromonospora viridifaciens B7-3	350
			Streptomycetales	Streptomycetaceae	Streptomyces	*Streptomyces* sp. APL3	351
						Streptomyces sp. KKU215	353
	Proteobacteria	Alphaproteobacteria	Hyphomicrobiales	Phyllobacteriaceae	Mesorhizobium	*Mesorhizobium* sp.	335
			Rhizobiales	Bradyrhizobiaceae	Rhodopseudomonas	*Rhodopseudomonas palustris*	354
			Caulobacterales	Caulobacteraceae	Brevundimonas	*Brevundimonas* sp. MRL-AN1	355
		Gammaproteobacteria	Enterobacterales	Yersiniaceae	Serratia	*Serratia marcescens*	356
			Oceanospirillales	Alcanivoraceae	Alcalinovorax	*Alcalinovorax borkumensis*	357
			Pseudomonadales	Pseudomonadaceae	Pseudomonas	*Pseudomonas frederiksbergensis*	358
						Pseudomonas sp. strain DS04-T	359
						Pseudomonas tamsuii TKU015	360
						Pseudomonas sp. MYK1	361
						Pseudomonas aeruginosa S3	322
						Pseudomonas aeruginosa S4	
						Pseudomonas geniculata WS3	362
			Xanthomonadales	Xanthomonadaceae	Unclassified	*Xanthomonadaceae* bacterium	335
					Stenotrophonas	*Stenotrophomonas pavanii* CH1	362
						Stenotrophomonas maltophilia LB 2-3	48
		Betaproteopbacteria	Burkholderiales	Burkholderiaceae	Ralstonia	*Ralstonia* sp. strain MRL-TL	363
				Alcaligenaceae	Bordetella	*Bordetella petrii* PLA-3	364
	Firmicutes	Bacilli	Bacillales	Bacillaceae	Bacillus	*Bacillus amyloliquefaciens* MS2	365
						Bacillus smithii PL21	366
						Bacillus licheniformis	367
							368
							369
						Bacillus stearothermophilus	370
						Bacillus sp. MYK2	361
						Bacillus lentus	371
						Bacillus pumilus	358
					Geobacillus	*Geobacillus thermoleovorans*	372
						Geobacillus thermocatenulatus	373
				Paenibacillaceae	Aneurinibacillus	*Aneurinibacillus aneurinilyticus*	374
					Brevibacillus	*Brevibacillus* sp.	375
					Paenibacillus	*Paenibacillus amylotyticus* TB-13	376
				Thermoactinomycetaceae	Laceyella	*Laceyella sacchari LP175*	377
					Laceyella	*Laceyella sacchari* T11-7	350
					Thermoactinomyces	*Thermoactinomyces vulgaris*	350
	Bacteroidetes	Flavobacteriia	Flavobacteriales	Flavobacteriaceae	Chryseobacterium	*Chryseobacterium* sp. S1	322
		Sphingobacteriia	Sphingobacteriales	Sphingobacteriaceae	Sphingobacterium	*Sphingobacterium* sp. S2	

https://doi.org/10.1021/acs.chemrev.2c00644
Chem. Rev. XXXX, XXX, XXX−XXX

Table 8. continued

Kingdom	Division	Class	Order	Family	Genus	Species	References
Fungi	Basidiomycota	Tremellomycetes	Tremellales	Tremellaceae	Cryptococcus	*Cryptococcus* sp. strain S-2	378
						Cryptococcus flavus GB-1	379
						Cryptococcus magnus	380
		Microbotryomycetes	Sporidiobolales	Sporidiobolaceae	Rhodotorula	*Rhodotorula mucilaginosa*	356
		Ustilaginomycetes	Ustilaginales	Ustilaginaceae	Pseudozyma	*Pseudozyma antarctica*	381
	Ascomycota	Eurotiomycetes	Eurotiales	Aspergillaceae	Aspergillus	*Aspergillus calidoustus* VKM F-2909	382
						Aspergillus oryzae	383
						Aspergillus fumigatus	384
						Aspergillus awamori	385
						Aspergillus foetidus	
						Aspergillus nidulans	
						Aspergillus niger	
				Trichocomaceae	Penicillium	*Penicillium roqueforti*	356
						Penicillium sp.	
						Penicillium chrysogenum	356
						Penicillium aurantiogriseum VKM F-329	382
						Penicillium chrysogenum VKM F-227	
					Paecilomyces	*Paecilomyces* sp.	349
					Thermomyces	*Thermomyces lanuginosus*	384
		Sordariomycetes	Sordariales	Chaetomiaceae	Humicola	*Humicola insolens*	386
			Hypocreales	Nectriaceae	Fusarium	*Fusarium moniliforme*	385
				Cordycipitaceae	Engyodontium	*Tritirachium album*	387
				Hypocreaceae	Trichoderma	*Trichoderma harzianum*	385
						Trichoderma viride	388
		Dothideomycetes	Capnodiales	Davidiellaceae	Cladosporium	*Cladosporium sphaerospermum*	356
			Pleosporales	Phaeosphaeriaceae	Paraphoma	*Paraphoma* sp. B47-9	389
	Mucoromycota	Zygomycetes	Mucorales	Mucoraceae	Rhizopus	*Rhizopus oligosporus*	385
Archaea	Euryarchaeota	Methanobacteria	Methanobacteriales	Methanobacteriaceae	Methanosaeta	*Methanosaeta concilii*	335
		Methanomicrobia	Methanosarcinales	Methanosaetaceae	Methanobacterium	*Methanobacterium petrolearium*	

plastic degraders could degrade PLA (second polymer most degraded after PHAs). In September 2022, this number increased to 151 strains with the ability to degrade PLA, blends of PLA, or copolymers of LA (1 strain degrading poly(butylene succinate/terephthalate/isophthalate)-*co*-(lactate), PBSTIL), 6 uncultured bacteria, and 27 PLA-depolymerases. Gambarini et al.[44] used a statistic "*D*" binary test (presence or absence of reported degradation for each taxon) to measure the relationship between phylogeny and degradation of each type of plastic on a data set composed of all reported degraders and 7000 bacterial and fungal species randomly sampled from the full NCBI taxonomy database. The strongest signal was obtained for PLA degradation (D = 0.54), indicating a phylogenetic conservation in the tree. Indeed, PLA degraders are mostly found in Actinobacteria, whereas it corresponds to the second most frequently observed bacterial phylum of plastic degraders according to Gambarini et al.,[44] Proteobacteria being the first one (30%).

Table 8 intends to list all microorganisms isolated with a PLA-degrading activity. Most PLA-degraders from Actinobacteria[331,332] are members of the Pseudonocardiaceae family, gathering more than 25 degrading species from 7 different genera. Amycolatopsis contains the largest number of PLA degraders reported for a single genus. Pranamuda et al.[333] screened 25 strains of Amycolatopsis, demonstrating that 15 are able to form clear zones on PLA plates and suggested that PLA degraders are largely distributed within this genus. Less frequent, PLA-degrading microorganisms belonging to Proteobacteria and Firmicutes were also reported. Less abundant, studies also described the degradation of PLA by fungi. A study on degradation of PCL, PBS, and PLA led to the isolation of 79 PLA degraders, among which 5 isolates were fungi while 74 were actinobacteria.[334] Finally, only two representatives of Archaea were reported as plastic-degraders,[335] also probably related to these groups containing fewer documented taxa overall. These PLA degraders come from various environmental sources, such as compost, sludge, garbage, soil, or waste dumping sites.

The potential of PLA degradation by microorganisms was mined in available genomes of microbial taxa, with reported plastic-degrading capabilities to identify potential plastic-degrading genes.[44] A number of 2236 orthologues of the PLA-depolymerase from *Paenibacillus amylolyticus* (BAC67195) was found, of which 532 from Firmicutes, the phylum from which the enzyme was isolated.[376] However, no analysis of redundancy was provided. Zrimec et al.[390] mined ocean and soil metagenomes to assess the global potential of microorganisms to degrade plastics. A set of 10 experimentally evidenced PLA-depolymerases[340,376,378,391,392] and *E*-value < $1e^{-10}$ homologuous sequences from UniProt TrEMBL database enabled the identification of 31 potential PLA-degrading enzymes, with only one found in ocean metadata while remaining ones were from soil. Emadian et al.[393] also reported the higher abundancy of plastic microbial degraders in soil and compost than is fresh water and marine environment. Even if no experimental evidence of PLA degradation by such candidates was reported, the great potential of natural diversity exploration was highlighted.

Several studies have reported the increased rate of PLA degradation in the presence of submerged culture or single organism/consortia enriched soil and compost environments. Pranamuda et al.[336] was the first to report that *Amycolatopsis* HT-32 isolated from soil by applying the halo methods could degrade 60% of a 100 mg PLA film in 14 days. Many other examples of PLA degradation using submerged cultures was then reported. Yottakot et al.[353] described a weight loss of 84% of PLA-packaging (obtained from Dairy Home Co., not characterized) by *Streptomyces* sp. KKU215 after 4 weeks of incubation at 37 °C. Weight loss of a PLA film (home casted from Natureworks PLA 2002D, not characterized) was 71% after 4 weeks of incubation with *Pseudonocardia* sp. RM423 at 30 °C.[348] Approximately 37% of a PLLA film (50 μm home blown from Natureworks 4043D, 130 kg·mol^{-1}) was degraded by *Amycolatopsis* sp. *SCM_MK2-4* after 7 days of cultivation at 30 °C and 58% after 14 days.[334] Another strain of *Amycolatopsis* extensively eroded the PLA polymer (PLLA casted film from 4032D Natureworks, M_w 190−230 kg·mol^{-1}), leading to a weight loss of 36% in one month in mesophilic conditions (30 °C).[345] *Pseudonocardia alni* AS4.1531T could reduce a PLA film (home casted from Natureworks PLA

https://doi.org/10.1021/acs.chemrev.2c00644
Chem. Rev. XXXX, XXX, XXX−XXX

Table 9. Commercial PLA-Depolymerases

enzyme name	supplier	enzyme class	origin	PLA substrate used for activity assay	methods of evaluation	ref
Lipase	Sigma	EC 3.1	*Rhizopus delemar*	PLA stereocopolymer, M_n = 2 kDa	weight loss	403
Proteinase K	nd[a]	EC 3.4	*Tritirachium album*	PLLA from ICI Ltd.; fibrous particules	product detection, pH monitoring, weight loss	387
Bromelain	nd	EC 3.4	pineapple	PLLA from ICI Ltd.; fibrous particules	product detection, pH monitoring, weight loss	
Pronase	nd	EC 3.4	*Streptomyces griseus*	PLLA from ICI Ltd.; fibrous particules	product detection, pH monitoring, weight loss	
Proteinase K	Sigma	EC 3.4	*Tritirachium album*	home-polymerized P(L/D)LA; M_n = 155−245 kDa; cast film	pH monitoring, weight loss	404
Proteinase K	Nakalai Tesque Co.	EC 3.4	*Tritirachium album*	PLA from Shimadzu; M_w = 233 kDa; cast films	product quantification	371
Savinase 16.0L	Novo Nordisk Bioind. Co.	EC 3.4	*Bacillus lentus*			
Protin A	Daiwa Kasei Co.	EC 3.4	*Bacillus subtilis*			
Purafect 4000L	Kyowa Enzymes Co.	EC 3.4	*Bacillus lentus*			
Orientase Y	Hankyu Bioind. Co.	EC 3.4	*Bacillus subtilis*			
Proleather	Amano Pharm. Co.	EC 3.4	*Bacillus subtilis*			
Orientase 5BL	Hankyu Bioind. Co.	EC 3.4	*Bacillus subtilis*			
Bioprase AL-15FG	Nagase Biochem. Ind. Co.	EC 3.4	unknown			
Alkaline EC3.4 GL-440	Kyowa Enzymes Co.	EC 3.4	*Bacillus licheniformis*			
Alcalase 2.5L DX	Kyowa Enzymes Co.	EC 3.4	*Bacillus licheniformis*			
Orientase 22BF	Hankyu Bioind. Co.	EC 3.4	*Bacillus subtilis*			
Pancreatin F	Amano Pharm. Co.	EC 3.4	animal pancreas			
Esperase 8.0L	Novo Nordisk Bioind. Co.	EC 3.4	*Bacillus lentus*			
Protease A	Amano Pharm. Co.	EC 3.4	*Aspergillus oryzae*			
Lipase-PL	Meito	EC 3.1	*Alcaligenes* sp.	LACTY 1012 from Shimadzu; M_w = 187 Kda; film	weight loss, SEC, product quantification	405
Proteinase K	Sigma	EC 3.4	*Tritirachium album*	LACTY 1012 from Shimadzu; M_n = 130 kDa; compression molding film	product quantification	406
Subtilisin Carlsberg	Sigma	EC 3.4	*Bacillus licheniformis*			
Subtilisin BPN	Fluka	EC 3.4	*Bacillus amyloliquefaciens*			
α-Chymotrypsin	various for comparison	EC 3.4	bovine pancreas	LACTY 1012 from Shimadzu; M_n = 190 kDa; coated paper	TOC	402
Trypsin	Sigma	EC 3.4	bovine pancreas			
Elastase	Wako Pure Chemical Industries Ltd.	EC 3.4	porcine pancreas			

https://doi.org/10.1021/acs.chemrev.2c00644
Chem. Rev. XXXX, XXX, XXX−XXX

Table 9. continued

enzyme name	supplier	enzyme class	origin	PLA substrate used for activity assay	methods of evaluation	ref
Subtilisin	Sigma	EC 3.4	*Bacillus licheniformis*			
Proteinase K	ICN Biomedicals Inc.	EC 3.4	*Tritirachium album*			
Novozym 42044	Novozymes	EC 3.1	nd	PLLA and PDLA home synthesized by ROP (M_w = 165 kDa) and stereocomplex of 50/50 (not characterized); emulsion and cast films	turbidity decrease, SEC, SEM, ESI-TOF-MS	407
Savinase 16L	Novozymes	EC 3.4	*Bacillus lentus*			
Savinase CLEA	Shigematsu	EC 3.4	*Bacillus clausii*			
Lipases PS	Amano	EC 3.1	*Burkholderia cepacia*			
Proleather FG-F	Amano	EC 3.4	*Bacillus subtilis*			
Proteinase K	nd	EC 3.4	*Tritirachium album*			
Proteinase K	Qiagen	EC 3.4	*Tritirachium album*	PLLA from Sigma; M_n = 10 kDa; emulsion	NaOH consumption	408
Subtilisin A	Sigma-Aldrich ref P4860	EC 3.4	*Bacillus licheniformis*			
HiC	Novozyme	EC 3.1	*Humicola insolens*	PLLA from Goodfellow; films of 50 μm thickness	product quantification, WCA, AFM	386

[a]nd, not defined.

https://doi.org/10.1021/acs.chemrev.2c00644
Chem. Rev. XXXX, XXX, XXX−XXX

Table 10. PLA-Depolymerases Purified and Characterized, Still Lacking Sequence Identification

enzyme class	origin	PLA substrate used for activity assay	methods of evaluation	pH opt	T opt (°C)	ref
nd[a]	*Geobacillus thermocatenulatus*	PLA from Shimadzu; M_n = 47 kDa; films of 50 μm thickness	SEC, weight loss	nd	nd	373
EC 3.1	*Bacillus smithii* PL21	PLLA from Nacalai Tesque; M_w = 10 kDa	SEC	5.5	60	366
EC 3.4	*Amycolatopsis* sp. strain 41	LACTY 1012 from Shimadzu; M_w = 140 kDa; powder	TOC, product quantification	6	37−45	339
EC 3.4	*Amycolatopsis orientalis* ssp. orientalis IFO 12362	LACTY 1012 from Shimadzu; M_n = 340 kDa; powder	product quantification	nd	nd	341
EC 3.1	*Pseudomonas tamsuii* TKU015	PLA 2002D from Cargill Dow; M_n = 12.5 kDa; emulsion	halo, product quantification	10	60	360
EC 3.4	*Actinomadura keratinilytica* T16-1	LACEA; emulsion	turbidity decrease	10	70	350
EC 3.1	*Pseudomonas* sp. strain DS04-T	PLA from Zhejiang Hisun Biomaterial; M_n = 400 kDa; hot pressed film	product quantification	8.5	50	359
EC 3.1	*Ralstonia* sp. strain MRL-TL	PLLA from Sigma; M_n = 50 kDa; emulsion	turbidity decrease	7	50	363
EC 3.1	*Brevundimonas* sp. MRL-AN1	PLLA from Sigma; M_n = 50 kDa; emulsion	turbidity decrease	30	6	355
EC 3.1	*Pseudomonas aeruginosa* strain S3	PLA from NatureWorks; M_w = 200 kDa; extruded films	product quantification, LC-MS, SEM, FTIR, weight loss	7	30	409
nd	*Micromonospora* sp. GMKU 353	PLA vyloecol BE-400 from TOYOBO; M_w = 43 kDa; cast film	SPR	nd	nd	45
	Micromonospora sp. GMKU 358			nd	nd	
	Micromonospora sp. GMKU 362			10	nd	
EC 3.4	*Bacillus amyloliquefaciens* MS2	PLA bags from Nature-tech Ltd.; film	GC-MS, FTIR, DSC	nd	nd	365
EC 3.1	*Bacillus licheniformis*	PLA from Purac Biomaterials; emulsion	turbidity decrease	6−7	50−60	368

[a]nd: not defined.

4042D, 74 kg·mol^{-1}) by more than 70% weight in 8 days in liquid culture at 30 °C.[347] *Pseudomonas* sp. *MYK1* and *Bacillus* sp. *MYK2* incubated at 30 °C for 4 days produced 10 times increased amounts of CO_2 from PLLA granules (Natureworks 4042D, 95.8% L-lactide, 4.2% D-lactide, M_n 183 kg·mol^{-1}) compared with the initial sludge inoculum.[361] Culture medium of *Amycolatopsis* could degrade 60% of a PLA film (Heat pressed, PLLA from shimadzu, M_n 188 kg·mol^{-1}, 100 μm thickness) after 14 days at 30 °C.[336] After 14 days of cultivation at 30 °C, *Tritirachium album* ATCC 22563 degraded about 76% of a PLA film (commercial blown from Shimadzu, not characterized).[394] Satti et al.[322] determined a PLA degradation rate constant (Mn/Mno vs time) of −0.0263 g/mol/day for isolated strains of of *Sphingobacterium* sp. and *P. aeruginosa* at 30 °C (casted film from PLA 2003D NatureWorks, M_w 210 kg·mol^{-1}, M_n 110 kg·mol^{-1}).

Karamanlioglu et al.[384] showed that coupons of food containers formulated from PLA Ingeo PLLA (NatureWorks grade 2003D, M_w 160 kg·mol^{-1}, 35% crystallinity) could be degraded after 4−5 weeks by sterile wheat inoculated with *Thermomyces lanuginosus* PLA18 or *Aspergillus fumigatus* at 50 °C. The usefulness of soil bioaugmentation with specific PLA degraders to accelerate PLA degradation in soil microcosm was also demonstrated.

Pattanasuttichonlakul et al.[395] reported on the synergistic action of a microbial consortium in the soil mixture and *Pseudomonas geniculata* WS3 on accelerating PLA biodegradability. A consortium of *Penicillium chrysogenum, Cladosporium sphaerospermum, Serratia marcescens,* and *Rhodotorula mucilaginosa* degraded 26% of a 100 mg PLA solvent-casted film prepared from Sigma commercial grade PLA (M_w 85−160 kg·mol^{-1}) in 15 days in a sterilized compost pile made of soil (70%) and kitchen waste (30%) under regulated moisture, pH, and temperature conditions (45−50%, 6 and 40−60 °C, respectively).[356] PLA degradation after 60 days in nonsterilized soil enriched with *Pseudonocardia* sp. was found to be 1.2−3-fold higher than without enrichment at 58 and 30 °C, respectively.[348] Saadi et al.[396] showed a consortium of fungal strains (*Aspergillus niger* (DSM 1957), *Chaetomium globosum* (DSM 1962), *Paecilomyces variotti* (DSM 1961), *Penicillium pinophilium* (DSM 1064), and *Trichoderma viridens* (DSM 1963)) could degrade 84% of a PLA film (heat-pressed from PLLA Materianova pellets, M_n 116 kg·mol^{-1}, T_g 60.8 °C) in 75 days at 58 °C. These cocultured simulated systems could be reminiscent of multienzymatic cocktails used for biomass deconstruction, as evidenced by the synergy between bacteria and fungi observed in real compost.[396]

Other factors have been shown to contribute to PLA degradation. Among them, UV irradiation can not only create C═C double bonds within the PLA structure through a Norish II mechanism, but also chain cleavage with a decrease in molecular weight through bulk erosion. Jeon et al.[48] thus showed that UV treated PLA was degraded more rapidly by microorganisms, with a decrease in such degradation if UV treatment was carried out for too long. Pattanasuttichonlakul et al.[395] also evidenced that UV irradiation of PLA followed by burying in a soil mixture of dairy wastewater sludge with *P. geniculata* WS3 inoculation efficiently accelerated degradation of PLA waste.

Copinet et al.[397] previously reported that an increase in temperature and relative humidity (RH) could also fasten the degradation of high M_w PLA films (quasi total degradation in 30 weeks if RH was 100% and temperature above 45 °C), without any enzymatic action due to ester bond cleavage in the presence of water. Temperature was also found to be an important parameter for biodegradation: PLA degraded in compost at 50 °C, but not at 20 °C,[384] PLA degradation was 2.7-fold higher at 58 °C than at 30 °C,[348] and PLA degradation

https://doi.org/10.1021/acs.chemrev.2c00644
Chem. Rev. XXXX, XXX, XXX−XXX

Table 11. PLA-Depolymerases with a Characterized Sequence

enzyme name	UniProtKB accession number	PDB ID	enzyme class	origin	PLA substrate used for activity assay	methods of evaluation	pH opt	T opt (°C)	ref
CLEcs	Q874E9	2CZQ[410]	EC 3.1	*Cryptococcus* sp. strain S-2	LACEA HT-100 from Mitsui Chemicals; M_w = 140 kDa; emulsion	turbidity decrease	7	37	378
PLD	Q75UA4		EC 3.4	*Amycolatopsis* sp. strain K104-1	PLA from Shimadzu; M_w = 220 kDa; emulsion and cast film of 5 μm thickness	halo, turbidity decrease, TLC	9.5	55−60	340
PLD	Q75UA4		EC 3.4	*Amycolatopsis* sp. strain K104-1	PLA from Shimadzu; M_n = 220 kDa; emulsion	TLC, product quantification, turbidity decrease, NMR	nd[a]	nd	392
PlaA	Q83VD0		EC 3.1	*Paenibacillus amylolyticus* TB-13	PDLLA from Wako; M_w = 5/10/20 kDa; emulsion	halo, turbidity decrease, TOC, product quantification	10	50	376
CutL1	P52956		EC 3.1	*Aspergillus oryzae*	PLA Plasema L110 from DaiIchi Kogyo Seiyaku; emulsion	turbidity decrease	8	35−55	383
PLAase I	only N-terminus available		EC 3.4	*Amycolatopsis orientalis* ssp. *orientalis*	PLA from Sigma; M_w = 85−160 kDa; emulsion	product quantification	9.5	60	342
PLAase II	B0FLR6		EC 3.4	*Amycolatopsis orientalis* ssp. *orientalis*	PLA from Sigma; M_w = 85−160 kDa; emulsion	product quantification	10.5	50	342
PLAase III	B0FY08		EC 3.4	*Amycolatopsis orientalis* ssp. *orientalis*	PLA from Sigma; M_w = 85−160 kDa; emulsion	product quantification	9.5	60	
PlaM9	A4UZ14		EC 3.1	metagenomic library	PDLLA from Wako; M_w = 5 kDa; powder	turbidity decrease, TOC	nd	nd	391
PlaM8	A4UZ13		EC 3.1	metagenomic library	PDLLA from Wako; M_w = 5 kDa; powder	turbidity decrease, TOC	nd	nd	391
PlaM7	A4UZ12		EC 3.1	metagenomic library	PDLLA from Wako; M_w = 5 kDa; powder	turbidity decrease, TOC	nd	nd	391
PlaM5	A4UZ11		EC 3.1	metagenomic library	PDLLA from Wako; M_w = 5 kDa; powder	turbidity decrease, TOC	nd	nd	391
PlaM4	A4UZ10		EC 3.1	metagenomic library	PDLLA from Wako; M_w = 5 kDa; powder	turbidity decrease, TOC	7	70	391
pla	from article, not deposited		EC 3.4	*Actinomadura keratinilytica* T16-1	LACEA, Japan; emulsion	turbidity decrease	nd	nd	401
Est1	D4Q9N1		EC 3.1	*Thermobifida alba* AHK119	nd	halo	6	50	107
Ta_cut/Est119	F7IX06	3VIS for wild-type enzyme[186] and 6AID for inactive variant S169A[187]	EC 3.1	*Thermobifida alba* AHK119	home-synthesized PLLA M_w = 169 kDa and PDLA M_w = 163 kDa; emulsion	halo	6	45−50	101
PaE	S6BC01		EC 3.1	*Pseudozyma antarctica*	PLLA from Toyota Motor; M_w = 186 kDa and M_n = 113 kDa; cast film	SPR and AFM	nd	nd	411
PaE	S6BC01		EC 3.1	*Pseudozyma antarctica*	PDLLA-0020 from Wako Chemicals; M_w = 20 kDa; cast films	TOC, SEM, product quantification	9.5	40	381
CmCut1	A0A060N5H2		EC 3.1	*Cryptococcus magnus*	PLLA from Polyscience; M_w = 100 kDa and PDLLA from Wako Pure Chemical Industries; M_w = 20 kDa; cast films	TOC	7.6	40	381
LP175	A0A291HVH1		EC 3.4	*Laceyella sacchari* LP175	PLLA objects from Natureplast, milled to 500 μm particles; M_w = 71 kDa	turbidity decrease, product quantification	9	60	412
PCLE	A0A060N399		EC 3.1	*Paraphoma*-related fungal strain B47-9	PDLLA from Wako Pure Chemicals; M_w = 20 kDa; cast films	TOC, SPR	7.2	45	389
CLEcf	A0A0P0ZE81		EC 3.1	*Cryptococcus flavus* GB-1	PLLA from Polyscience Inc.; Mw 100 kDa and PDLLA from Wako Pure Chemicals M_w = 20 kDa; Cast films	TOC	7.8	45	379
MGS0010	W0M2H4		EC 3.1	metagenomic library	PDLLA from PolySciTech; M_w = 2 kDa; emulsion	halo	8−10	30	357
MGS0109	T1W006		EC 3.1	metagenomic library	PDLLA from PolySciTech; M_w = 2 kDa; emulsion	halo	8−10	30	357
ABO_1197	Q0VQA3		EC 3.1	*Alcalinovorax borkumensis*	PDLLA from PolySciTech; M_w = 2 kDa; emulsion	halo	8−10	30	357
MGS0105	T1W153		EC 3.1	metagenomic library	PDLLA from PolySciTech; M_w = 2 kDa; emulsion	halo	8−10	15	357
ABO_1251	Q0VQ49		EC 3.1	*Alcalinovorax borkumensis*	PDLLA from PolySciTech; M_w = 2 kDa; emulsion	halo	8−10	35	

https://doi.org/10.1021/acs.chemrev.2c00644
Chem. Rev. XXXX, XXX, XXX−XXX

Table 11. continued

enzyme name	UniProtKB accession number	PDB ID	enzyme class	origin	PLA substrate used for activity assay	methods of evaluation	pH opt	*T* opt (° C)	ref
ABO_2449	Q0VLQ1		EC 3.1	*Alcanivorax borkumensis*	PLA10 from Sigma; M_w = 10−18 kDa; powder	halo, turbidity decrease, product quantification	9.5−10	30−37	354
RPA1511	Q6N9M9	4PSU	EC 3.1	*Rhodopseudomonas palustris*	PLA10 from Sigma; M_w = 10−18 kDa; powder	halo, turbidity decrease, product quantification	9.5−10	55−60	
MGS0084	A0A0G3FL20		EC 3.1	metagenomic library	PDLA M_w = 2 kDa; emulsion	halo	nd	25	413
MGS0156	A0A0G3FEJ8	5D8M	EC 3.1	metagenomic library	PDLA M_w = 2 kDa; emulsion	halo	nd	nd	
MGS0156	A0A0G3FEJ8	5D8M	EC 3.1	metagenomic library	PLA10 Resomer R 202 H from Sigma; M_w = 10−18 kDa; powder	halo, turbidity decrease, product quantification	10	40	414
GEN0105	A0A0G3FJ39		EC 3.1	metagenomic library	PLA10 Resomer R 202 H from Sigma; M_w = 10−18 kDa; powder	halo, turbidity decrease, product quantification	5−10	35	414
Thc_cut1	E9LVH8	5LUI	EC 3.1	*Thermobifida cellulosilytica*	PLLA from Goodfellow; film of 50 μm thickness	product quantification, TOC	nd	nd	185
Thc_cut2	E9LVH9	5LUJ	EC 3.1	*Thermobifida cellulosilytica*	PLLA from Goodfellow; film of 50 μm thickness	product quantification, TOC	nd	nd	185
Thc_cut2 R29N/A30V		5LUK	EC 3.1	*Thermobifida cellulosilytica*	PLLA from Goodfellow; film of 50 μm thickness	product quantification, TOC	nd	nd	185
Thc_cut2 R19S/R29N/A30V		5LUL	EC 3.1	*Thermobifida cellulosilytica*	PLLA from Goodfellow; film of 50 μm thickness	product quantification, TOC	nd	nd	
Cut190; variant S226P/R228S	W0TJ64 (wild-type protein)	7CEF[190]	EC 3.1	*Saccharomonospora viridis*	home-synthesized PDLA M_w = 163 kDa; cast films	halo, weight loss	6.5−7	65	110
polyesterase	from patent, not deposited		EC 3.4	*Actinumadura keratinilytica* T16.1	PLLA powder from Natureplast (100 μm to 2 mm), PLA films from Goodfellow (50 μm thickness) or PLA objects	product quantification	8.5	50	415,416
extracellular serine proteinase	P80146		EC 3.4	*Thermus* sp. strain Rt41A	PLLA powder from Natureplast (500 μm)	product quantification	8	90	417

[a]nd: not defined.

https://doi.org/10.1021/acs.chemrev.2c00644
Chem. Rev. XXXX, XXX, XXX−XXX

drastically higher at 58 °C than at 30 °C.[396] Nevertheless, mineralization of PLA by soil bioaugmented with *Sphingobacterium* sp. S2 was demonstrated at ambient temperature.[322]

Results on PLA biodegradation are promising, although they are difficult to compare due to plethora of operating conditions and substrates used. Interestingly, Gambarini et al.,[44] reported that approximately 24.5% of the plastics used for discovery and characterization of PLA-degrading activity were of analytical grade, 17.7% were not of analytical grade, and 57.8% could not be assigned. As described in the following section, this entails a bias, given that various physicochemical properties of particular relevance for enzymatic depolymerization depend on the substrate initially used and its subsequent treatment.

Finally, despite numerous studies describing the degradation of PLA by microorganisms, most experiments were conducted at laboratory scale with regard to both substrate treatment and quantity to degrade, and only very few were patented for the production of such activity and their further application in bioremediation (*Alcaligenes*.[398] *Pseudomonas* sp. strain LXM88,[399] *Tritirachium*, *Amycolatopsis*, *Saccharothrix*, *Streptomyces*, *Bacillus*, *Streptoalloteichus*, *Kibdelosporangium*, *Lentzea*, *Saccharomonospora*, *Staphylococcus*, or *Saccharopoly*[400]).

As the use of super PLA-degraders GMO for bioremediation, even in restricted areas, is questionable, and no study relate on the potential of microorganisms described above in real conditions (amount of PLA waste, treatment needed, and cost), a promising opportunity relies on the identification of enzymes responsible for PLA-degradation for the development of processes and materials.

2.2.3. PLA-Depolymerases. *2.2.3.1. Reported Protein Sequences.* Compared to the numerous PLA-degrading microorganisms, only a limited number of PLA-depolymerizing enzymes have been isolated and characterized. Williams et al.[387] was the first to report the enzymatic hydrolysis of PLA using commercial enzymes, including proteinase K from *Tritirachium album* (PRK, P06873). Purification of a PLA-degrading enzyme from *Amycolatopsis* sp. strain 41 was reported in 2001.[339] Since then, many other PLA-depolymerases were purified and characterized for a PLA-depolymerization activity, but their sequences were only partially or not identified at all.[342,401] These enzymes were mostly isolated from bacteria and fungi, but few were also found produced by mammals[402] or plants.[387] Only 7 PLA-degrading enzymes and 19 enzymes with activity but with no assigned sequence can be found in the PMBD database. Ten PLA-degrading enzyme sequences are listed in PlasticDB.[44,56] Tables 9, 10, and 11 gather all PLA-depolymerases reported to date, either from commercial sources (Table 9), purified to be characterized, but without an associated sequence (Table 10), or having an identified sequence (Table 11).

PLA-depolymerases were shown to belong to EC 3 hydrolase enzymes, particularly serine hydrolases, half from EC 3.1 (esterases, lipases, cutinases) and half from EC 3.4 (proteases) (Tables 9 to 11). Still, an enzyme isolated from *Geobacillus* hardly showed any esterase or protease activities, which could represent a novel PLA-depolymerase acting on the ester bond between lactate units but not on the common lipase and protease substrates.[373] Due to multiple families of PLA-hydrolyzing enzymes, the Brenda database does not list PLA-depolymerases as a unique family, according to EC numbers, contrarily to PET degrading enzymes.

Proteases depolymerizing PLA were identified from both chymotrypsin (which include chymotrypsin, trypsin, and elastase-like enzymes) and subtilase (including subtilisin and homologues) families, respectively, S1 and S8 families from the MEROPS protease database classification.[418,419] These two families belong to serine proteases (EC 3.4.21), which use a nucleophile serine in the canonical triad composed of an aspartic acid, a histidine, and a serine. The order in sequence of these residues differs in these two families, His/Asp/Ser and Asp/His/Ser in S1 and S8, respectively. Despite different structural folds, the active sites of subtilisin and chymotrypsin are superimposable. Nevertheless, a divergence in subtilisins with respect to PLA-depolymerizing activity exists, as evidenced by Oda et al.,[371] who showed that subtilisin from Boehringer Mannheim was not active, whereas other subtilisins, Savinase and Alcalase, were active.

Lipases, cutinases, and esterases were also found to depolymerize PLA. The difference between lipases, cutinases, and esterases lies, in one hand, in the presence of a lid covering the active site of lipases, with a related interfacial activation corresponding to the opening of the lid that exposes the active site of the enzyme in the presence of a biphasic medium (insoluble lipidic substrate). This does not occur in the case of esterases and cutinases. On the other hand, the chain length of the preferred substrate is different, i.e., short and long chain fatty acids for esterases and lipases/cutinases, respectively. They make use of the same catalytic triad as serine proteases despite the topology of their active site being mirror images. Differences were observed among EC 3.1 within the pentapeptide containing the catalytic serine.[376,378]

Kawai et al.[407] proposed to distinguish type I (proteases) and type II (cutinases/esterases/lipases) PLA degrading enzymes. Type II polyester hydrolyzing enzymes (lipases/cutinase-type), which include PLA-depolymerases, are distributed across esterase families I, III, IV, V, VI, and new esterase families, and they exhibit a significant phylogenetic diversity.[354,414]

Most PLA-depolymerases are characterized by the presence of a signal peptide enabling their secretion to the culture medium, where the insoluble substrate stands. This criterion was used as a critical piece of information for assessing whether or not an enzyme could be a potential plastic degrader when using the PlasticDB search tool.[56] For both enzyme classes, it was hypothesized that the insoluble substrate was first partly hydrolyzed in the extracellular medium by the enzyme constitutively produced in small amounts. The soluble low molecular weight products would then enter the cell and induce the production of larger amounts of enzyme. As for other plastic degrading enzymes (for instance, cutinase Thc[420]), the production of proteins able to depolymerize PLA was shown to be inducible by distinct molecules, and not only plastics and related. PLA-depolymerizing proteases production could be induced by PLA,[360,421,422] but also silk fibroin,[339] gelatin,[346,348,394,421,422] soybean,[423] elastin, or keratin.[47] Jarerat et al.[346] studied the effect of various inducers on *Tritirachium album*, *Lentzea waywayandensis*, and *Amycolatopsis orientalis*. While the best inducer was different for these organisms, the supplement of only 0.1% silk fibroin could increase the level of PLA-degrading activity in the culture medium of *A. orientalis* from 0 to 450 $U \cdot mL^{-1}$. Silk is a natural polymer which was reported to contain a crystalline domain with large amounts of L-alanine and glycine. Most other protease inducers also contain L-alanine, which shows a chemical structure like that of (L)LA and therefore suggested that silk fibroin can be considered as a PLLA analogues.

https://doi.org/10.1021/acs.chemrev.2c00644
Chem. Rev. XXXX, XXX, XXX−XXX

Lipases, esterases, and cutinases with PLA-degrading activity were also shown to be inducible by biodegradable plastics (PBS and PBSA)[383,424] or PLA.[365]

In addition to a signal peptide enabling their secretion, PLA-depolymerases are mostly produced as precursor proteins with a N-terminal prodomain. This was evidenced by discrepancy between N-terminal sequencing of purified protein and gene sequencing.[342] The N-terminal prodomain of lipase, esterase, and cutinase PLA-depolymerases serves as an intramolecular chaperone promoting the correct folding of the mature domain and is cleaved by an extra protein from the producing host, whereas the prodomain of protease PLA-depolymerase not only promotes the folding but could also prevent from toxicity to the producing host through a ligand-like binding in the catalytic domain of the protein. Moreover, the processing of the prosequence might sometimes be autocatalytic,[392] like for family S8 proteases (subtilase), or not such as in the case of family S1 proteases (chymotrypsin).

The three amino acid residues of the catalytic triad are known to be essential for peptide/ester bond cleavage for natural activity of EC 3.1 and EC 3.4 members. This catalytic triad could also be evidenced both for EC 3.1[354,414] and EC 3.4[392] as being essential for PLA-depolymerizing activity, as mutation of catalytic residues entailed their inactivation. Tchigvintsev et al.[357] isolated an esterase belonging to the esterase family VIII, including β-lactamase-like enzymes. MSG0105 indeed displays a catalytic triad consisting of a catalytic Ser nucleophile, as well as conserved Lys and Tyr residues acting as a general base and a proton acceptor, respectively. The functional significance of the β-lactamase-like active site residues of MGS0105 was confirmed using site-directed mutagenesis.

2.2.3.2. Structure and Engineering. Apart from the catalytic triad, amino acid residues involved in the substrate binding could not be experimentally evidenced, due to the lack of X-ray structures of the enzymes in complex with bound polymeric ligands. This is primarily due, such as for other synthetic polymers, to the insoluble nature of the substrate. This has fairly limited the comprehension of the molecular determinants involved in activity of PLA-depolymerases, as well as their molecular engineering to enhance their performances. Nevertheless, some X-ray structures of PLA-depolymerases have been determined in their free form or in complex with either their cognate substrate or inhibitors. For instance, the 3D-structure of commercial savinase (PDB 1SVN[425]) and other subtilisins (subtilisin BPN, PDB 1SBT,[426] Subtilisin Carlsberg, PDB 1CSE[427]), as well as PRK (PDB 2PRK[428]), have been solved in various conditions. Several structures of cutinases have also been determined but with structurally distinct substrates mainly related to other enzymatic activities (CLE, PDB 2CZQ[410]), (Hic, PDB 4OYL[429]), (Est119, PDBs 3VIS and 3WYN[186]), (Cut190, PDB 4WFI[188]).

Protein properties, i.e., surface charge, hydrophobicity, and size of the substrate binding site, or thermostability, have been shown to influence enzyme activity. For instance, Thumarat et al.[107] compared Est1 and Est119 sharing 95% of sequence identity and possessing similar 3D structures. Est1 displayed the same degradation pattern as Est119 toward various polymers.[101] However, activity ratio of Est1 to Est119 was approximately 2-fold on PLA agar plates, possibly due to the several amino acid residues in the substrate-docking loops that differ from each other, but no mutational experiment was carried out to confirm the role of these residues in PLA-depolymerase activity.

Hajighasemi et al. determined the crystallographic structure of RPA1511 (PDB 4PSU) at 2.2 Å resolution.[354] The structure corresponds to a classical α/β-hydrolase fold, with a wide-open active site containing a molecule of poly(ethylene glycol) bound near the catalytic triad. One extremity of the PEG 3350 ligand is buried in the RPA1511 active site with the terminal OH-group positioned close to the side chain of W218 residue. The authors thus suggest that W218, exhibiting a homologous Trp in the active site of PHB depolymerases, might represent a structural motif for the potential hydrolytic activity against polyester substrates. The main part of the bound ligand is in the alcohol binding site with the other extremity spreading to solvent. The ligand binding mode in the active site cavity of RPA1511 suggests that this enzyme is likely to perform both exo- and endoesterase cleavage of PLA. Moreover, by means of alanine replacement, the authors identified several residues in RPA1511, which were not essential for activity against soluble monoesters (α-naphthyl propionate) but critical for the hydrolysis of PLA (T48, Q172, R181, L212, M215, W218, L220, and K252), while some other residues were found to be important for the hydrolysis of both substrates (H113, L182, and Y198), suggesting distinct binding interactions. As residues are not all found in direct contact or close to the bound poly(ethylene glycol) ligand, they might potentially contribute to the binding of different chain-length PLA molecules. In 2018, the same group determined the structure of MGS0156 at 1.95 Å resolution and revealed a modified α/β hydrolase fold, with a lid domain and a highly hydrophobic active site.[414] Such structure revealed two conformations for the catalytic Ser232 side chain, suggesting resting and acting states of the active site. Here again, mutational studies of MGS0156 identified residues critical for hydrolytic activity against both PLA polyester and monoester substrates (L299G, L335A, and M378G), while others (E330, L335, F338, and V353) are only involved in polyesterase activity. In both studies, a mutant with increased PLA-depolymerase activity (e.g., RPA1511^{V202A} and MGS0156^{L169A}) was disclosed. Unfortunately, MGS0156 was not associated with any known hydrolase families, while RPA1511 was predicted to belong to the esterase family V. As their primary sequence and 3D structure are quite different from other PLA-degrading cutinases, this prevents from extrapolating active site features to other PLA-degrading enzymes.

Kitadokoro et al.[187] were successful in obtaining crystals of Est119, a cutinase from *Thermobifida alba* AHK119 previously shown to form clear halo on PLA agar plates,[101] in complex with ethyl lactate (EL) (PDB 6AID). From this structure, one lactate (LAC) could be evidenced, as well as one EL occupying different positions in the active site cleft. The binding mode of EL is assumed to represent the state prior to reaction while LAC is an after-reaction product. Only the D-type configuration of EL was observed, consistent with the enzyme hydrolyzing PDLLA more easily than PLLA,[101] as well as the inhibition by D-EL slightly higher than that of L-EL. The active site of Est119 resembles a mouth-like cleft, divided by two jaw-shaped regions. One front-tooth side is constructed by Y99 and T100, and the other by I217 and F248. S105 and W194 are placed at each terminal edge of the cleft, while H168, M170, and H247 are located at the bottom of the cleft, near the catalytic center (made of S169, H247, and D215).

https://doi.org/10.1021/acs.chemrev.2c00644
Chem. Rev. XXXX, XXX, XXX−XXX

The side chains of Y99, M170, W194, and I217 form a sandwich with LAC.

Mutations on residues F106, T107, and W201 of Cut190 from *Saccharomonospora viridis* (corresponding to Y99, T100, and W194 in Est119) were indeed found important for activity toward PBSA,[276] suggesting that the indole ring and the phenyl group were important for substrate binding. In this study, Q138A showed significantly increased affinity toward PBSA, probably because of the additional space for the polymer substrate generated by the mutation. This residue is conserved in both Est119 (e.g., Q131) and Thc_Cut2 (e.g., Q93).

An alternative to the cocrystallization of an enzyme with a ligand is the use of molecular docking techniques to gain insight on the binding mode. Ribitsch et al. compared Thc_Cut1, Thc_Cut2 (97.3% identity), and two variants of Thc_Cut2.[185] The Thc_Cut2$^{R29N/A30V}$ double variant showed an increased activity toward PLLA. Effectively, after 6 h of incubation, Thc_Cut2$^{R29N/A30V}$ released 4.5 times more lactic acid from PLLA when compared to the native Thc_Cut2. When studying the docking mode of PLLA into Thc_Cut2$^{R29N/A30V}$, it was evidenced that the lowest energy docking modes generally had fewer PLLA subunits (often only one) located on the "alcohol side", which can be explained by the binding site cavity in this area being significantly narrower than the one on the opposite "acid side." In these models, residues R29 and A30, located on the surface of the protein, do not seem directly involved in interactions with the substrate. However, when considering PLLA subunits extension from the "alcohol side", it appears conceivable that longer oligomers and the polymer may interact with residues in this surface region. Unfortunately, the crystallographic structures of Thc_Cut2 and variants were determined in unliganded forms.

Two studies of particular interest are presented in patents. The first one describes the identification of a proteinase from *Actinomadura keratinilytica* T16.1 that possesses a high PLA-depolymerizing activity. It can depolymerize micronized objects made of PLLA, with 98% conversion of PLA cup powdered to 250−500 μm after 48 h reaction at 45 °C.[415] This enzyme was further optimized by engineering.[416] Indeed, 5 positions were found crucial for activity and a combination of 3 mutations could give a 14.2-fold improvement in PLA-depolymerizing activity compared to wild type. Moreover, this triple variant S101F/S103L/T106I was shown to be more thermostable (2.1 °C increase in T_m). The second study has discovered that a formerly characterized serine protease from *Thermus* sp. strain Rt41A[430,431] also exhibited a PLA-degrading activity. Authors engineered the active site of this poorly PLA-depolymerizing protease and obtained a sextuple variant more active than the optimized variant of the protease from *A. keratinilytica* T16.1 and with a higher thermostability of 79 °C against only 58 °C.[417] These two PLA-depolymerases and variants were shown particularly useful in the design of processes for degrading PLA and new material (see section 2.2.4).

2.2.3.3. Catalytic Mechanism and Factors of Influence. It was proposed that serine hydrolases identified to have PLA-degrading activity could act through similar mechanism as for peptide bond cleavage (see mechanism of serine hydrolases in Figure 8): (1) substrate binding in the catalytic site, (2) nucleophilic attack by the γ-oxygen of the catalytic serine on the substrate ester bond, (3) release of the C-terminal part of the substrate and subsequent formation of a covalent acyl enzyme intermediate, (4) hydrolysis of the covalent intermediate in the deacylation step (by incoming water molecule), to release the carboxyl group of the second product and regenerate active enzyme for another catalytic cycle to begin. The apparent energy of activation (EA) of the hydrolysis of PLA by *B. licheniformis* protease was estimated to be 112.7 kJ mol^{-1},[408] that is distinctly higher than the EA for the enzymatic degradation of natural polymers such as cellulose. Various factors were found important for the PLA-depolymerization reaction and will be discussed below.

2.2.3.3.1. Adsorption. Panyachanakul et al. showed that increasing the agitation speed of a PLA-depolymerization carried out by the PLA-depolymerase from *Actinomadura keratinilytica* strain T16-1 in a 5 L stirred tank reactor from 50 to 100 rpm decreased the conversion yield by approximately 1.7-fold.[432] This could be due to the denaturation of the enzyme by the shear force of the disc turbine, or to lower adsorption of the enzyme. Qualitative adsorption of PLD[392] and PlaM4[391] on PLA was evidenced by SDS-PAGE analysis. By means of surface plasmon resonance (SPR), Susuki et al.[389] showed that PCLE from *Paraphoma*-related fungus B47-9 was able to bind PLLA with an association rate constants (k_a) of 3.2×10^6 M^{-1} s^{-1}. Moreover, they showed that Ca^{2+} ions enhanced k_a by 2-fold, while no change in dissociation rate was observed. Nevertheless, experiments were carried out using an unreactive substrate and therefore could not be correlated to the catalytic activity. Shinozaki et al.[411] also investigated the adsorption of PaE cutinase-like by SPR and found that the amount of PaE adsorption on amorphous PLLA film was 1.14 ng·mm^{-2}, corresponding to an apparent 30 nm^2 cross-area per one molecule of bound PaE. Using crystalline nondegraded PLLA, the authors determined a k_a of 8.4×10^5 M^{-1} s^{-1}. Yamashita et al.[51] studied the adsorption of PRK from *Tritirachium album* (PRK) and the subsequent depolymerization of an amorphous PLLA film by atomic force microscopy (AFM) and quartz crystal microbalance (QCM). They reported that buffer exchange or water washing could not desorb the enzyme, contrarily to EtOH 40%. The protein covered the entire surface of the film at 50 μg/mL (25 molecules/100 × 100 nm^2), but the number of enzyme molecules on the film continued to increase with enzyme concentrations up to 100 μg/mL (32 molecules/100 × 100 nm^2), despite the absence of space on the film, correlated with a decrease in cross-area per one enzyme molecule. From these experiments, it was concluded that the enzyme could undergo conformational changes upon adsorption, leading to a high density packing on the surface of the film. According to Yamashita et al.,[51] as the width measured for adsorbed PRK was lower than for PLA degradation hollow, the enzyme could degrade the film by moving around, which was accompanied by conformational changes in order to enable catalytic residues to attack the film. Finally, Yamashita et al.[51] also showed a correlation between the adsorbed concentration of the enzyme and the degradation rate. It was thus suggested that the enzymatic erosion rate could be simply determined by the concentration of the enzyme on the film surface. When Numata et al.[52] used PLA monolayer for AFM and weight loss study, they reported lower degradation rate (21×10^{-7} mg/(min·cm^2) at 20 °C with 10 μg/mL of enzyme compared to 1.1×10^{-4} mg/(min·cm^2) at 25 °C with 10 μg/mL in Yamashita et al.[51]). The authors attributed this difference to the enzyme molecules easily detaching from the surface of the monolayer because of the loss of polymer layer as an anchoring scaffold through the enzymatic degradation, leading to a

https://doi.org/10.1021/acs.chemrev.2c00644
Chem. Rev. XXXX, XXX, XXX−XXX

restricted amount of enzyme molecules participating in the hydrolysis reaction of PLLA monolayer compared with a film surface. It was suggested that *A. oryzae* uses several types of proteins to recruit lytic enzymes to the surface of hydrophobic solid materials and promotes their degradation.[433] The depolymerization of PBSA by the PLA-degrading enzyme CutL1 from *A. Oryzae*[383] was promoted by HsbA[433] and RolA.[434] At that time, no such recruitment was reported to enhance PLA adsorption or depolymerization.

2.2.3.3.2. Endogenous or Exogenous Scission Catalytic Mechanism. Hypothesis on the mode of action of PLA degrading enzymes started from Williams et al.[387] While three enzymes were detected with an activity on PLLA, two of them (pronase and bromelain) caused a physical breakdown in the polymer, yielding a much finer dispersion, while one of them (PRK) did not substantially alter the physical form of the powder. Since then, several studies were conducted to elucidate the endogenous or exogenous scission mechanism of PLA-degrading enzymes. Most of them, regarding either EC 3.1 or EC 3.4, seemed to evidence mostly an endogenous scission mechanism, in addition to minor exomode hydrolysis from the hydroxyl chain end. This would be consistent with all of the characterized peptidases of the chymotrypsin and subtilisin family being endopeptidases. Indeed, Matsuda et al.[392] demonstrated that the protease PLD can degrade PLA with an average molecular mass of 220 kDa into lactic acid dimers through lactic acid oligomers and finally into lactic acid. Thus, it was proposed that the enzyme attacked within the polymer. The finding that dimers are formed suggested that subsite S2 occupancy might be important for PLA-depolymerization. Based on their experiments on D/L distribution in PLA films, McDonald et al.[435] also discussed the importance of available (L)-(L) dyads for enzymatic activity.

Other studies demonstrated the evolution of M_w and M_n values when PLA was incubated with enzymes, as analyzed by SEC on residual PLA.[366,373,407,436] TOC measurements were also reported, which could not account only for LA but also revealed the presence of water-soluble oligomers as degradation products.[376,381] This enabled to conclude that deesterification might occur at any region of the polymer chain through a random endogenous scission mechanism. Concomitant with a decrease in M_w and M_n values, oligomers (DPn from 2 to 24) were confirmed by ESI-TOF-MS after degradation of PLA with CLE.[407] In the same manner, Noor et al.[409] reported the detection of lactic acid oligomers of intermediate chain lengths (DPn from 6 to 13), as well as oligomers of cyclic- PLA consisting of 9 to 11 monomer units, during degradation of PLA with an esterase from *Pseudomonas aeruginosa* strain S3. Hajighasemi et al.[354] also reported that both ABO2449 and RPA1511 could catalyze complete or extensive hydrolysis of solid PLA with the production of lactic acid monomers, dimers, and larger oligomers as products (DPn from 2 to 13). Another way to access endogenous or exogenous scission mechanism would be to provide the enzyme with a global amount of substrate of different M_w, therefore providing PLA chains with various chain extremities. Few studies report on the influence of PLA initial molecular weight on the degradation. Akutsu-Shigeno et al.[376] showed that the shorter the PLA, the higher the rate of hydrolysis by lipase from *Paenibacillus amylotyticus* TB-13. Nevertheless, all three substrates used in their study were somehow low molecular weight PLA (M_w 5/10/20000) and could be depolymerized in 1 h to 1 h 30 min, as evidenced by total turbidity decrease. PRK could degrade PLA of identical stereocomposition and crystallinity over a wide range of M_n (30−200 kg·mol^{-1}), with no significant effect from chain length,[435] as evidenced by normalized weight loss rates showing little deviation (average 4 μg/mm^{-2}/h^{-1}), respectively. The authors concluded that the effects of PLA chain length on PRK catalyzed degradation rates were not significant. This was supported by Reeve et al.,[404] who showed that PRK hydrolyzed PLA-70 and PLA-75 to a lesser extend relative to PLA-80 and PLA-85, despite their lower M_w, the % of L-LA units being the predominant factor (see paragraph below). In another study from Numata et al.,[52] the hydrolysis rate for linear PLLA samples by PRK increased with a decrease in the molecular weight, but as the rate constant of enzymatic hydrolysis of PLLA samples was not proportional to the number of chain ends of the initial state, they concluded for a dual endo- and exoscission mode.

Studies on PLA-depolymerization by PRK led to divergent conclusions. Indeed, in a study by Reeve et al.,[404] the residual film after PRK degradation showed no change in M_w, which was attributed to surface degradation. In contrast, Kawai et al.[407] found that PRK degraded a PLLA emulsion with a reduction of M_w, from initial 169 kg·mol^{-1} to 44.6 kg·mol^{-1}, after only 2 h. This might be explained by the difference in the substrate used for the depolymerization assays, as the former used a film and the latter particles emulsion, thus providing different surfaces for degradation. The available surface area was therefore evidenced as being a key parameter during enzymatic PLLA degradation. Vichaibun et al.[406] reported a linear increase in the rate of PLA degradation by PRK with available surface area of PLA (single or multiple film pieces), as previously reported for soil biodegradation of polybutylene sebacate fragments.[437] Numata et al.[52] also found that the rate of PRK hydrolysis, followed by AFM and weight loss, was proportional to the exposed surface. This is consistent with the enzymatic hydrolysis following a surface erosion mechanism, contrarily to the nonenzymatic hydrolysis of the PLLA, which proceeds mostly through surface and bulk erosion mechanisms depending on the pH.[438]

2.2.3.3.3. Inhibition and Activation. The inhibition of PLA-depolymerizing activity by di-isopropyl fluorophosphates (DFP), aprotinin, and phenylmethanesulphonylfluoride (PMSF) further confirmed the belonging of some PLA-depolymerizing enzymes to the family of serine proteases.[340,342,350,412] Some of these PLA-depolymerizing proteases were also inhibited when the surfactant Plysurf A210G was added to the reaction mixture.[377,402] Similar results were reported upon using other surfactants such as SDS, Tween 20, Tween 80, CTAB, and Triton X-10.[377,412] Depending on the surfactant, however, distinct effects were observed, i.e., either an inhibition or an activation of the PLA-depolymerization, or sometimes both, depending on the concentration used.[406] As this effect was not found on protease activity assayed on azo-albumin, the authors suggested that surfactants probably interfered with the binding of the enzyme to the solid PLA substrate. In the same manner, when using soluble substrate pNPB, a PLA-depolymerizing esterase purified from *Ralstonia* sp. strain MRL-TL was not inhibited by SDS or Triton X-100[363] or even enhanced by Tween 80 and Triton X-100.[409] Unfortunately, no effect was reported on PLA-depolymerizing activity. In absence of surfactant, ABO2449 produced little lactic acid, but in the presence of 0.1% Plysurf A210G, it quickly degraded solid PLA10 (90% conversion) into lactic

https://doi.org/10.1021/acs.chemrev.2c00644
Chem. Rev. XXXX, XXX, XXX−XXX

acid.[354] It was thus suggested that Plysurf A210G could facilitate the binding of ABO2449 to solid PLA because the surfactant showed no stimulating effect on the enzyme activity against the monoester substrate α-naphthyl propionate.

The presence of two calcium sites, with high and low affinity, was reported for various subtilases with PLA-depolymerizing activity. Calcium ions were also shown to be important for PLA-depolymerization activity by proteases. Indeed, their activity might be inhibited by ethylenediamine tetraacetic acid disodium salt (EDTA), a divalent ion chelator,[350,377,402,412] or 1,2-bis(*o*-aminophenoxy)ethane-*N*,*N*,*N*′,*N*′-tetraacetic acid (EGTA).[377] This effect was attributed to enzyme denaturation rather than inhibition of the enzyme molecules by removing Ca^{2+} ions from the enzyme. Indeed, whereas little effect of Ca^{2+} was observed on the proteolytic activity of PRK, removal of Ca^{2+} opens the structure of the protein[439] and might account for a higher susceptibility to proteolysis, as already observed for other proteases. In addition, Ca^{2+} were shown to stabilize PRK (increase of average 10 °C of T_m) by bridging different parts of its tertiary structure.[439] Metallic cations such as Cu^{2+}, Na^{+}, Mn^{2+}, Fe^{2+} Mg^{2+}, and Zn^{2+} were found to inhibit the PLA-depolymerase from *Laceyella sacchari*, while Co^{2+}, Ca^{2+}, and K^{+} stimulated its activity. The latter cationic species affected the thermostability of the enzyme at 60 °C, as evidenced by an increased residual activity from 84 to 100% after 2 h at 60 °C, upon addition of 1 mM of Ca^{2+} during incubation.

The influence of ions on PLA-depolymerizing activity was also studied for EC 3.1. It also showed to be inhibited by EDTA,[365] that is also coherent with the finding of Ca^{2+} binding sites in various structures.[187] A study from Wang et al.[359] showed that PLA-degradation by the lipase from *Pseudomonas* was activated by 5 mM Na^{+} and K^{+} while decreased by all other ions added (Zn^{2+}, Mg^{2+}, Cu^{2+}, and Fe^{2+}). Thumarat et al.[101] showed that Mg^{2+}, Mn^{2+}, and Ca^{2+} at concentrations of 0.25 and 0.5 mM enhanced the pNPB activity of PLA-depolymerase Est119, while trivalent ions (Al^{3+} and Fe^{3+}) and monovalent ions (Li^{+} and Rb^{+}) inhibited this activity. In the presence of Ca^{2+}, the activity and thermostability of Est119 were intensified both on pNPB hydrolysis and PBSA degradation to a greater extent than with Mg^{2+} and Mn^{2+}. The PBSA degradation activity of PLA-depolymerase CmCut1 was also enhanced in the presence of up to 2.5 mM Ca^{2+} and Mg^{2+},[380] while Ca^{2+} and Mg^{2+} showed contrasting effects on emulsified PBSA-degrading activity of PCLE PLA-depolymerase: it was enhanced in the presence of 1−2.5 mM Ca^{2+} but inhibited by Mg^{2+} at the same concentrations.[389] The authors suggested that the alteration of affinity between PCLE and its substrates by these metal ions could greatly affect enzyme activity. The PBSA-degrading activity of CfCLE was inhibited by Ca^{2+} and Mg^{2+} at concentrations higher than 0.5 and 0.2 mM,[379] but no data were provided on their influence on PLA degradation.

The inhibition by lactic acid (2−8 g/L) was also evidenced for *A. keratinilytica* T16.1 PLA-degrading enzyme.[432] Nevertheless, authors did not relate this inhibition to either LA concentration or decrease in pH (9 to 3.8). Kawai et al.[407] also mentioned substrate inhibition caused by both PLLA and PDLA if higher than 1.6 and 1.8 mg/mL, respectively. L-LA displayed inhibition on cutinase CutL1 pNPB activity,[383] and ethyl lactate was also reported as being the most suitable for inhibition among the various alkyl lactates tested by Kitadokoro et al.[187] during hydrolysis of pNPB by cutinase Est119.

Several other factors discussed hereafter were shown to affect the enzymatic degradation of PLA. They are either associated with the first-order structure (chemical structure, i.e., stereochemistry and distribution of LA units, and molecular weight) or with the higher-order structure (PLA crystallinity) or to the surface conditions (surface area).

2.2.3.3.4. Influence of the Substrate Stereochemistry on PLA Depolymerization. Lipases, esterases, and cutinases use the same catalytic triad as serine proteases despite the topology of their active site being the mirror image of the latter's one, which might explain their respective preference for either PLLA or PDLA. Kawai et al.[407] compared 8 proteases and 10 lipases from different sources (purified, recombinant, commercial) and showed that lipases preferentially hydrolyzed PDLA substrate, although with a more flexible enantioselectivity. This might be explained by both the (*S*)- or (*R*)-enantioselectivity toward their native substrates. Notably, upon increasing the concentration of CLE, both PDLA and PLLA were completely hydrolyzed in less than 1 h and difference in hydrolysis rates toward PDLA and PLLA could not be measured. This flexible enantioselectivity was also reported for instance for esterase from *Paenibacillus amylotyticus* TB-13[376] and PlaA lipase from *Aspergillus niger* MTCC 2594,[440] that are active on PDLLA, and for an esterase isolated from *Bacillus smithii* active on PLLA.[366] In the same manner, Shinozaki et al.[411] showed that PaE esterase from *Pseudozyma Antarctica* could degrade PDLLA to a higher extent, compared to amorphous PLLA (with a notable low plateau for PLLA hydrolysis), as does the cutinase-like CfCLE from *Cryptococcus flavus*,[379] Est119 from *Thermobifida alba* AHK119,[101] and the cutinase CmCut1 from *Cryptococcus magnus*-related strain BPD1A.[380] In the structure of esterase Est119 obtained by Kitadokoro et al.,[187] only the D-type conformation of ethyl lactate could be observed in cocrystallization studies, in agreement with the halo-degrading experiments which revealed that PDLA was somewhat easier to hydrolyze than PLLA. Finally, stricter enantioselective EC3.1 members were also reported: PCLE from *Paraphoma*-related fungus B47-9 was able to degrade PDLLA but not PLLA, which could also be related to differences in molecular weight (M_w 20 kg·mol^{-1} PDLLA and 130 kg·mol^{-1} PLLA) or crystallinity (not explicated).[389]

Proteases, known as naturally hydrolyzing proteins which are polymers of L-amino acids, hydrolyze PLLA almost exclusively.[407] Nevertheless, few studies compare PLA-depolymerizing proteases toward their activity on PDLA/PLLA, most of them focusing on PRK. In their SPR experiments, PRK could not degrade PDLLA,[411] as previously reported.[404,407] By means of homemade high molecular weight amorphous films containing various ratio of D/L-lactide, Li et al.[441] confirmed that PRK highly degrades L-lactyl units, as opposed to D-lactyl ones, while no degradation occurred with pure PDLA. This finding was in agreement with a previous hypothesis from the same group that PRK was capable of cleaving L−L, D−L, and L−D bonds, but not D−D bonds.[442] Reeve et al.[404] studied the influence of D/L enantiomer ratio on the degradation of PLA solvent casted films by PRK. Degradation was found to increase with the % L-LA introduced, until a dramatic increase in crystallinity due to the introduction of less than 8% D-LA lowered the enzymatic activity. The degradation rate of a PLLA containing 92% of L-LA, X_c = 32%, and PLLA containing 94% of L-LA, X_c = 44%, were found equal to 1.75 and 0.99 mg/

https://doi.org/10.1021/acs.chemrev.2c00644
Chem. Rev. XXXX, XXX, XXX−XXX

mm^2/h, respectively. Using homemade controlled copolymers of PLA, McDonald et al.[435] studied the influence on enzymatic depolymerization of PLA with PRK of PLA film of varied stereochemical composition and isomer distribution as independent variables (equivalent chain enantiopurity and crystallinity). For amorphous films containing 80−95% L-LA, the rate of weight loss was almost constant, showing an unexpected tolerance for D-LA units. The rate of weight loss dramatically decreased when the %(D) exceeded 20−25%. The authors claimed that this might be due to the availability of (L)−(L) dyads necessary for enzymatic activity, which would saturate PRK cleavage sites, so that a maximum enzyme−substrate conversion rates was eventually observed. Nevertheless, a 43% decrease in weight loss rate was noted for films produced by copolymerization of (L,L)/(L,D) lactides, compared to copolymerization of (L,L)/(D,D) lactides. These results thus evidenced that enzyme interaction were dependent on the distribution of (L) and (D) units of LA, with a possible inhibition by (L)−(D)−(L) triad sequences present in (L,L)/(L,D) but not in (L,L)/(D,D) copolymers.

The different preference toward PLLA and PDLA of EC3.1 α/β-hydrolase fold enzymes and EC3.4 serine proteases might be explained by the topology of their catalytic triad being mirror images[407] (Figure 16). The former will accommodate either PDLA or PLLA in the active site, while the latter do not hydrolyze PDLA, probably because PDLA cannot be accommodated in the active site or PDLA cannot form an acyl-enzyme intermediate. The study from Kawai et al.[407] is among the rare to determine kinetic parameters for 2 PLA-depolymerizing enzymes, thus enabling an accurate comparison of activities in terms of substrate characteristics, quantification of degradation and reaction conditions. Data confirmed the preference toward PDLA hydrolysis for CLE (V_{max} 0.09 mg/min, corresponding to twice the V_{max} for PLLA, and a K_m of 8 mg/mL), and its superior activity compared to hydrolysis by PRK (V_{max} of 0.03 mg/min for PLLA hydrolysis), as already observed by Masaki et al.[378]

2.2.3.3.5. Crystallinity Degree Also Influencing Depolymerization. As highlighted for PET, substrate crystallinity is a key parameter influencing enzymatic depolymerization of PLA. Yet, it turns out that most of the enzymes are assayed on amorphous substrate, i.e., solvent casted films or emulsions, and therefore disregard this parameter. Oda et al.[371] tested commercial proteases on solvent casted films and found that 10 enzymes showed specific activities superior to 5 μg of liberated LA·min^{-1}·mg^{-1} enzyme, whereas none of the enzymes produced lactic acid from a polylactide film industrially manufactured by Shimadzu. The authors thus hypothesized that the surface structure of their film was highly amorphous, so that certain enzymes were readily capable to trigger its hydrolysis.

As described for PE,[443] owing to the high-ordered structure of PLA, which relates to its temperature treatments, one can distinguish three regions, namely, the crystalline region, the restricted amorphous regions inside PLLA spherulites, and the free amorphous region outside the spherulites as in a completely amorphous film. The surface of crystalline regions is connected with three types of amorphous chains, i.e., tie chains, folding chains, and chains with a free end. The thermal history of the polymer directs this high-ordered structure, the free volume and mobility of the polymer chains,[444] and thus the accessibility of the depolymerizing enzyme.

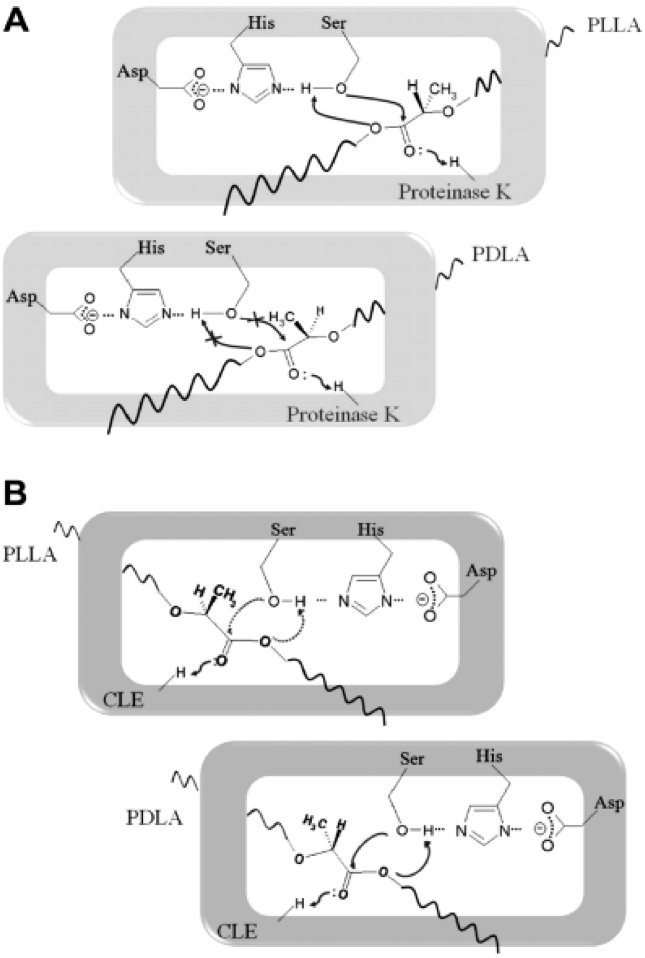

Figure 16. Illustration of the differences in enantioselectivity observed for proteinase K (A) and CLE (B) toward PLLA and PDLA, respectively. The topology of a catalytic triad in α/β-hydrolase fold enzymes is the mirror image of that in serine proteases, which probably causes the different preference toward PLLA and PDLA. Reproduced with permission from ref 407. Copyright 2011 Elsevier.

Several studies accurately deepened the effects of PLLA highly ordered structures on its enzymatic hydrolysis by PRK. On the basis of a weight loss analysis, the enzymatic hydrolysis rate by PRK was found to decrease, while at the same time X_c of the polymer increased. McDonald et al.[435] evidenced the dramatic negative effect of X_c: even a low 10% of X_c value entailed a 38% decrease in weight loss rate, compared to amorphous film, whereas a X_c value of 50% caused almost complete inhibition of PRK activity. Reeve et al.[404] evidenced that this parameter was even dominating over PLLA stereochemistry. Indeed, the structural effects caused by changes in PLA stereochemistry dominate the observed degradation rate, only once a critical degree of disruption of the crystalline phase was reached, i.e., at around 30%. When Shinozaki et al.[411] analyzed the hydrolysis of crystalline c-PLLA by *Pseudozyma antarctica* esterase, they attributed the decrease in the SPR signal on the first injection of PaE to the degradation of amorphous regions existing interspherulite and interlamellae. Upon analyzing the PDLA and PLLA resulting from incubation for 4 days with CLE and PRK by WAXS and DSC, Kawai et al.[407] showed that the crystallite size increased. The authors explained these results by a preferential hydrolysis of interfacial amorphous edge between crystallites in

https://doi.org/10.1021/acs.chemrev.2c00644
Chem. Rev. XXXX, XXX, XXX−XXX

spherulites, the average size of the remaining crystals becoming bigger, concomitant with an increase in X_c, from 40 to 60% after 1 day.

By means of AFM, Kikkawa et al.[445] showed that PRK preferentially eroded PLLA films in the free amorphous region around the crystal, whereas the restricted amorphous region between the crystal and the glass substrate was degraded at slower rate. Iwata et al.[446] studied the enzymatic hydrolysis of PLLA single crystals using PRK by AFM, soluble products release, and SEC of residual PLLA. The authors concluded that PRK hydrolyzed preferentially at the disordered chain-packing regions of crystal edges rather than the chain-folding surfaces of single crystals, when both the molecular weights of PLLA chains in crystals and the thickness of monolamellar parts remained unchanged during the enzymatic degradation. Tsuji et al.[438] observed a decrease in the high M_w species upon a 20 h incubation of PLA, concomitant with the increasingly appearance of a lower M_w polymeric species. These peaks were ascribed to the chains of one-, two-, and 3-fold in the crystalline region, which strongly suggested that the enzymatic hydrolysis of PLLA films took place predominantly at the free and tie chains in the restricted amorphous region rather than at those in the folding surface of the PLLA lamellae. As previously shown by the same group the areas of these peaks became higher with hydrolysis time, without any change in M_w, revealing that the folding chains in the restricted amorphous region were much more hydrolysis-resistant than the tie chains and the chains with free ends.[447]

Fukusaki et al.[403] correlated the depolymerization of amorphous regions of low molecular weight PDLA (M_n 2200) by the commercial lipase from *Rhizopus delemar* to water adsorption. The latter was found 10 times lower in crystalline copolymers, rendering difficult the accessibility of these regions by the enzyme. By in situ AFM monitoring, Kikkawa et al.[53] showed that, within 15 min, the free amorphous region of a PLA film was completely eroded by PRK, whereas that of the crystalline region remained unchanged. Friction force measurements and AFM observations also suggested that the adsorption of water molecules on the PLA film surface enhanced the surface molecular mobility of the glassy amorphous region of PLA, favoring enzymatic hydrolysis by PRK. Finally, Kawai et al.[407] presumed that despite a low X_c value of 29%, a 50/50 stereocomplex of PDLA and PLLA could not be degraded by CLE because of strong interaction between chains, preventing penetration of water or enzyme.

If crystallinity is for sure a crucial limiting factor, the limit is still not well established. A study by Cai et al.[448] showed that the degradation rate of PLA96 (96% of L-LA unit) by PRK decreased with the increase in X_c, with a sudden drop observed in the weight loss values beyond the heat of fusion of 20 J/g. This indicated that, above a critical X_c value, degradation was inhibited, which was in accordance with weight loss data from PRK enzymatic hydrolysis of PLA. Indeed, as reported by Li et al.,[449] above a crystallinity around 26%, the degradation rate drastically dropped because the vast majority of material is no more amorphous and accessible for enzymatic attack. The same frontier was observed previously:[447] PRK depolymerization activity was compared with PLLA films of X_c varying from 0 to 57%. Different behaviors were thus observed at a frontier of X_c 33%, where either the free (below X_c 33%, outside spherulites) and restricted (above X_c 33%, between crystalline regions inside spherulites) amorphous regions were predominant. The X_c value had high and small effects on the rate of enzymatic hydrolysis below and above this 33% frontier, respectively, showing higher hydrolysis resistance of the PLLA chains in the restricted amorphous region of the film.

It should therefore be highlighted that the discrepancy in the results for PLA-depolymerizing activity could result from the use of substrate with different characteristics. For instance, both Masaki et al.[378] and Kawai et al.[407] tested lipase PS from *Burkholderia cepacia* (commercial from Amano). The latter showed no activity on PLA LACEA from Mitsui chemicals (no characterization provided), whereas the former proved active on an emulsion of homemade high molecular weight PDLA. Out of 18 commercially available lipases, only CLE was found able to degrade a high M_w PLA (LACTY no. 1012 from Shimadzu). Vichaibun et al.[406] used the same LACTY no. 1012 PLA from Shimadzu and that only proteases were active, but not lipases. As several proteases could be isolated for their activity on this substrate, this might be a bias caused by the low percentage of D-LA unit in the tested polymer. In the same vein, the commercial substrate PLA ref 765112 obtained from Sigma (pure PLLA) was hydrolyzed by proteolytic enzymes but not by lipases.[408] Again, a PLA-depolymerizing enzyme from *Actinomadura keratinilytica* could hydrolyze 99% of a PLA powder (80% L-LA and 20% D-LA, M_w 43 kg/mol from Toyobo), whereas only 32% hydrolysis was achieved after 48 h at 60 °C when this enzyme was used on commercial trays (90% polylactic acid, size of 0.3 cm × 1 cm and thickness of 0.1 mm).[432] As discussed above, the high crystallinity of substrate might also be responsible for low activity as well as insufficient available surface area.

Therefore, rigorous reporting of polymer chemical composition and preprocessing before experience that could potentially affect the structure of the material, physical properties, as well as reaction conditions, is a paramount requirement to ensure accurate comparison and reproducibility. Unfortunately, almost no study was conducted with the same substrate or reaction conditions, rendering difficult the comparison of enzyme performances, except when comparing with PRK, which remains a reference enzyme for PLA hydrolysis.

2.2.3.3.6. Blends and Additives Influencing Enzymatic Degradation of PLA. As mentioned, in order to overcome PLA disadvantages, such as mechanical brittleness, low heat resistance, or slow crystallization, PLA can be used in blends in the presence of either a reinforcing phase, e.g., cellulose, corn, starch, chitosan, or plasticizers/compatibilizers, or fillers (organic, mineral, or glass based) and other additives (heat and light stabilizers, antioxidants, and flame retardants).

The use of blends intends not only to modulate polymer properties but also to reduce the cost of the materials.[450] These blends might also be seen as alternative materials, with increased biodegradability compared to pure PLA, as some of the used additives might increase the enzymatic hydrolysis of the polymer.[393]

Starch, PHAs (polyhydroxy alkanoates), natural fibers, or soy protein can improve biodegradability while lowering the cost of PLA-based materials. However, the use of these more hydrophilic materials often requires the use of compatibilizers to promote interfacial bonding and blend quality (cyclic anhydres or glycerol for example). The biodegradability values of PLA/starch blends (90/10 to 50/50), obtained in a controlled environment, could thus be enhanced by increasing starch content.[451] In spite of a higher crystallinity, maleic

https://doi.org/10.1021/acs.chemrev.2c00644
Chem. Rev. XXXX, XXX, XXX−XXX

anhydride compatibilized blends showed higher biodegradability than PLA/starch blends at the same PLA ratio.[451] The percentage of mineralization of PLA/starch blends in various composting conditions proved superior to the required 60% value for the definition of a biodegradable material (at 58 °C). Moreover, the presence of starch was found to facilitate biodegradation of PLA.[452] This might be caused by a superior water absorption capacity of blends containing starch, whose abundance of hydroxyl groups confers on it a hydrophilic nature. Plasticizers are suggested to introduce free volume in the matrix, promoting the diffusion of water and accelerating biodegradation through bulk erosion. It was suggested that maleic anhydre might form an acid group due to water in the compost, and this acid accelerated the chain scission of PLA, resulting in high biodegradability.[451] The incorporation of soy protein in PLA (50/50 and 33/67, with adipic anhydride as plasticizer) was shown to significantly accelerate the biodegradation rate of this binary blend, compared with pure PLA in soil medium at 21 °C.[453] In the same manner, blends of PLA with green coconut fibers (5 to 20 w% with MA as plasticizer) were more easily degraded than pure PLA in a *Burkholderia cepacia* compost at 35 °C and 50% RH, exceeding 68% after 21 days.[454]

Adding poly(hydroxy butyrate) (PHB) to PLA allowed improving its mechanical properties due to the finely dispersed PHB crystals acting as a fillers and nucleating agents in PLA. Weng et al.[455] reported higher biodegradation under real soil conditions (20 °C at 20 cm depth) with higher poly(3-hydroxybutyrate-*co*-4-hydroxybutyrate) content. Indeed, only fragments from pure PLA sample remained in the soil after 5 months burial. Zhang et al.[456] also reported biodegradability of PHB/PLA blends after burial in moist compost at room temperature improved upon increasing PHB content. Kikkawa et al.[457] observed that miscibility of PLLA/atactic PHB blends, which is dependent on the ratio, the M_w of both polymers and the processing method influenced the enzymatic degradation by PRK of the PLLA content: degradation in the miscible blends proceeded faster than in immiscible and partially miscible ones. Several fungal bacterial genera able to degrade PLA/PHB blend mulching foils could also be isolated.[458] The presence of PEG also accelerated the biodegradation of PDLLA/PHBV(polyhydroxybutyrate-*co*-valerate)/PEG blends in the soil at room temperature, and the mass loss reached 80% after 30 days for a 70/30/20 blend.[459] This was attributed again to the hydrophilic character of PEG that could help absorb and keep the water. In the same manner, the addition of PEG and ATBC (acetyl-tri-*n*-butyl citrate) as plasticizers accelerated the biodegradation at 58 °C of PHB/PLA blends.[460] PRK enzymatic depolymerization at 37 °C was found to be faster in blends of PDLLA/PEG blends than in the neat PLA, with enhanced degradation when increasing the PEG content.[461] Possible explanations were that dissolution of PEG increased either porosity, thus the available surface area for enzyme to access, hydrophilicity, or chain mobility. Biodegradation using *Lentzea waywayandensis* was performed to study various PLA blends and their degradation capacity (in the form of cast film, 1:1 in weight with either gum arabic starch, microcrystalline cellulose, PEG, or PHB, with glycerol as compatibilizer) and reported weight loss superior to 85% within 4 days at 30 °C for all blends.[462]

PLA/PCL blends could improve the ductility and toughness of PLA while raising the tensile strength of PCL. These blends were designed mainly for biomedical applications. Enzymatic degradation of PLLA/PCL blends (75/25, 50/50, 25/75) was studied using PRK or *Pseudomonas* lipase; PRK was able to degrade the amorphous domain of PLLA, but not the crystalline part of PLLA or PCL, while *Pseudomonas* lipase could degrade both amorphous and crystalline PCL, but could not degrade PLLA.[463] When investigating enzymatic degradation in toluene at 60 °C of PDLLA, PCL and their blends by Novozym 435, both polymers were found to degrade independently of each other, while the copolymer showed enhanced degradation.[464] Addition of EVA (ethylene-vinyl acetate with 18 wt % VA content) allowed improving strain at break and elasticity compared to PLA. Moreover, the microbial degradation of PLA/EVA was shown to increase upon addition of EVA (20 and 40 wt %), with a maximum of 32% weight loss observed after 15 months burial under Vietnamese agricultural soil (temperature 26 °C and 40% moisture) for the PLA/PVA (60/40) blend, and degrading-strain of *Nitrospirae*, *Rhizobium*, and *Alpha proteobacterium* could be isolated.[465]

Poly(vinyl acetate) (PVAc) could improve elongation at break of PLA. Nevertheless, enzymatic degradation rate of the blends by PRK dramatically decreased upon addition of PVAc in PLA, even at a content as low as 5%.[466] The same trend was observed during enzymatic depolymerization of PDLLA/PVAc blends by lipasesin organic solvent.[467]

As a means to increase the degradation rate of PLLA, copolymers consisting of L-LA and D,L-LA, as well as copolymers deriving from glycolide (GA), trimethylene carbonate, and 1,4dioxan-2-one (PDX) and LLA, have been specifically designed.[468]

Addition of nanoclays (inorganic layered silicate minerals) at low levels of loading (<5 wt %) was shown to enhance the mechanical, physical, and barrier properties of polymers. Castro-Aguirre et al.[469] used nanofillers, such as organo-modified montmorillonite, halloysite nanotubes, and Laponite to produce bionanocomposite (BNC) of PLA and studied their degradation under controlled composting conditions (at 58 °C): BNCs showed a higher mineralization of the films containing nanoclay in comparison to the pristine PLA during the first 3−4 weeks of testing. Nevertheless, the enzymatic degradation rate of PLA blends could be accelerated or decelerated depending on the chosen additional clay: the incorporation of Cloisite 20A into the PLA/PBSA (7/3) blends accelerated the degradation rate by PRK at 37 °C, whereas Cloisite 30B decelerated the degradation rate.[470]

PBS and PLA can be blended with the aim at obtaining plastic formulations with mechanical properties in the range of polypropylene (PP). Tolga et al.[471] used chalk and talc as fillers in such PLA/PBS (7/3) blends and studied their disintegration in industrial compost at 60 °C and 70% RH. Interestingly, talc led to lower and chalk to higher disintegration rates.

2.2.4. Application of PLA-Depolymerases for PLA Biorecycling. *2.2.4.1. Use of Free Enzymes for Recycling Purposes.* Among the studies of enzymatic depolymerization of PLA, the work from Lomthong et al.[412] is of note, as these authors showed that the PLLA-degrading enzyme from *Laceyella sacchari* LP175 could depolymerize real objects made of PLLA at a high concentration of 100 $g{\cdot}L^{-1}$ and small enzyme loading (0.13%). The percentage conversion to lactic acid of the PLLA objects (milled to fine powder) were 64, 39, and 68% for cup, spoon, and tray obtained from NaturePlast, respectively, after incubation at 50 °C for 24 h.

Some methods were also patented[472−475] claiming the use of enzymes, either lipases, proteases, or esterases, to promote the

https://doi.org/10.1021/acs.chemrev.2c00644
Chem. Rev. XXXX, XXX, XXX−XXX

biodegradation in liquid composition of PLA-containing materials. The inventors took advantage of commercially available CLE, Savinase, Esperase, or PRK, previously demonstrated as being PLA-depolymerizing enzymes, to show degradation of 120 mg[472,473] to 1 g[474] of PLA 100 μm thickness films homemade from NatureWorks PLA. In CA02924964,[473] 46% degradation could be demonstrated by weight loss measurements, using the Savinase 16L from Novozymes after 16 h at 45 °C. In JP2011157483,[474] methanization of the decomposition solution could be obtained by mL of a plant liquid collected from the methane fermentation tank equipment as an inoculum. In WO2004013217,[475] Novozym 435 was used at 100 °C for 1 day to depolymerize 90% of PLLA (150 mg) and Lipozym at 60 °C for 1 day to depolymerize 82% of PDLLA (10 mg). Carbios, in collaboration with TBI patented PLA hydrolysis of a 50 mg PLA film (Goodfellow, 50 μm thickness, 2% D-lactic acid) using 90 μg of a PLA-depolymerase from *Actinomadura* sp..[415] Up to 55% and 82% conversion could be reached after 24 and 72 h of reaction, respectively, at 45 °C. The inventors highlighted two parameters, including: (1) the importance of granulometry, as discussed above, i.e., the thinnest the powders were, the more efficient the hydrolysis rate was (a reaction carried on particles of 100−250 μm lead to 68% conversion in 24 h), and (2) PLA crystallinity in the range of 5−24% had little influence on hydrolysis performances. Moreover, it was shown that the higher the concentration was, the higher was the productivity of lactic acid formation tending to a 10 h productivity of 0.2 g lactic acid/mg of enzyme/h with a concentration of 300 g/L of PLLA (1 g/3 mL). Finally, their protease could readily depolymerize commercial objects (PLA cups, trays, film, and cutlery powdered to 250−500 μm by micronization), with up to 98% of conversion for PLA cup after 48 h and 93% and 84% of conversion of film and trays, respectively, after 72 h. A study from Youngpreda et al.[421] also showed that the repolymerization of LA, issued from an enzymatic depolymerization process, to oligomers of PLA was possible. LA obtained after depolymerization with the crude enzyme produced by *A. keratinilytica* strain T16-1 was thus purified and used to generate a low M_w PLA (378 Da).

Despite these last few studies and patents, there is still a need to bridge the gap by shifting research trends from merely isolating the microbial species or even enzymes with lab-scale biodegradation potential, to developing large scale protocols to biodegrade such polymers. Moreover, and as discussed, these methods still lack infrastructures and collections specific to PLA, as does industrial composting. Thus, other methods are being developed to directly create materials with increased biodegradability, such as blending PLA with biodegradable polymers. Embedding enzymes in the polymer matrix also emerged over a decade ago as a promising strategy to control plastic end-of-life.

2.2.4.2. Embedded Enzymes for Biodegradable PLA. Reminiscent of previous studies,[476,477] DelRe et al.[478] discussed the production of PCL with nanodispersed lipase from *Burkholderia cepacia* by mixing dissolved polymer and stabilized enzyme solution at room temperature. It was shown that (1) lipase was uniformly dispersed throughout semi-crystalline spherulites, (2) up to 2 wt % enzyme PCL mechanical properties only changed by 10% (stress−strain curve), and (3) PCL containing 0.02 wt % BC−lipase degraded internally once immersed in a 40 °C buffer solution until 98% conversion in 24 h. Moreover, no change in crystallinity was observed up to 80% degradation, nor any decrease in M_w despite substantial weight loss, contrarily to depolymerization by external enzyme (acting by random scission mechanism). Authors claimed that nanodispersed enzyme should proceed via consecutive reactions without releasing its substrate, through processive depolymerization. In the same manner, Greene et al.[479] recently created 3D-printed enzyme-embedded plastics. To this end, cryogrounded PCL (T_m = 60 °C, processing 90 °C) was mixed with the thermostable Amano lipase under powder form to minimize the surrounding water and therefore increase its stability. The mixture was used to feed the printing reservoir. The resulting printed enzymated film (400 μm thickness, enzyme loading 1 wt %) was degraded within 7 days, with a total weight loss of 92.9%, compared to addition of 1 wt % external enzyme to the PCL film (15.7% weight loss).

DelRe et al.[478] also showed that 1.5 wt % PRK nanodispersed in PLA could promote 80% PLA-depolymerization in 1 week at 37 °C. This dispersion was also found to accelerate depolymerization in industrial soil composts, as shown by films disintegration in 6 days at 50 °C for PLA. Nevertheless, this latter method required mixing the enzyme in the dissolved polymer and thus an extended use of volatile organic solvent (dichloromethane for PLA), prior to drying the casted films, a process which is not suitable for industrial plastic processing facilities. Melting PLA via an extrusion process required significantly higher temperature (around 170 °C), thus, Huang et al.[480] immobilized PRK on polyacrylamide to thermostabilize the enzyme before the production of enzymated films. The PLLA solution-cast film with embedded PRK (0.5%) showed weight loss of 78% after 96 h incubation, i.e., twice the yield obtained with externally added PRK. The extruded film with embedded PRK (0.5%) showed weight loss of 6% after 21 days incubation at 37 °C, and the extruded film with embedded thermostabilized immobilized-PRK (0.015%) showed weight loss of 15% after 21 days incubation. Experiments were not conducted to reach higher depolymerization yield, neither to evidence composting capacities of such films in compost standard conditions. A further limitation relies in the use of an all-carbon backbone, inherently nondegradable, polyacrylamide immobilization support.

Carbios, in collaboration with TBI, embedded a PLA-depolymerase from *Actinomadura* sp. and variants[415,416] to create a self-degrading plastic. Biodegradable PLA compounds were prepared by mixing PLA PLE 003 from Natureplast in granulated form (96% by weight) and a solid formulation containing the wild-type enzyme (4% by weight) thanks to a corotating twin-screw extruder. Biodegradation tests performed in liquid medium at 28, 37, or 45 °C on 1 g of such enzymated PLAs showed average 6% conversion into lactic acid and dimers at 37 and 45 °C after 70 days. The engineering work carried out in patent WO2019/122308, and described in section 2.2.3.2, led to a triple variant of this protease from *A. keratinilytica* highly improved, which gave 75 and 77% depolymerization of enzymated PLA (90% PLA + 10% enzymatic formulation) in liquid medium in 24 h at 45 °C and 10 days at 28 °C, respectively. Carbios and TBI also used the optimized quadruple variant N102F/S104L/S106T/N107I of a protease from *Thermus* sp. strain Rt41A (described in section 2.2.3.2) to create self-degrading enzymated-PLA:[417] 84 and 87% of the material (90% PLA and 10% of enzyme formulation) degraded in liquid medium in 24 h at 45 °C and 10 days at 28 °C, respectively. Carbiolice developed Evanesto,

https://doi.org/10.1021/acs.chemrev.2c00644
Chem. Rev. XXXX, XXX, XXX−XXX

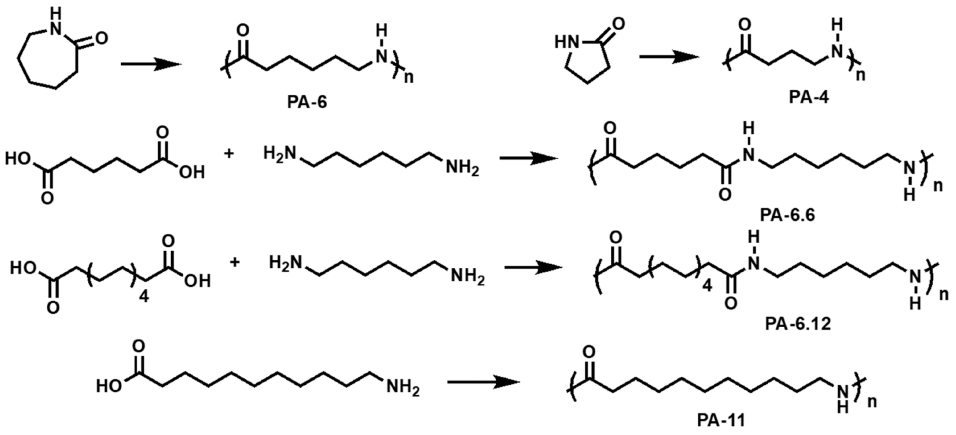

Figure 17. Chemical structures of some PAs.

an enzyme-based additive that makes products containing PLA compostable under home conditions. Evanesto presents the great advantage that it can be added to composite plastics containing 35% to more than 70% PLA on conventional industrial plastics tools.

2.2.5. Outlook. As emphasized in this section, PLA represents a promising alternative to replace conventional plastics. Not only it is a biobased polymer, but its properties can be tuned to respond industrial properties requirements. Nevertheless, PLA is currently only compostable in industrial composting conditions, which means at a temperature higher than 60 °C. If there is no further progress in market size, collecting, and sorting of PLA, recycling will not be considered, thus emphasizing the need to design innovative methods to rethink its end-of-life. PLA-degraders and the enzymes responsible for PLA-depolymerization have thus attracted a growing interest as they offer novel opportunities. Programmable decomposition under home compost, industrial, or methanization conditions, by embedding PLA-depolymerases, would be an efficient solution, overcoming the need to separate PLA products from municipal organic waste. Concepts are being demonstrated, still, methods must be implemented at larger scale to bring PLA to be a major plastic of the market.

3. BIODEGRADATION OF OTHER MAIN POLYMERS

3.1. Polyamides (PA)

3.1.1. About PA. The success of polyamides (PA) is primarily due to the regular distribution of amide functions (−CONH−) in their structure, forming hydrogen bonding interactions. These are at the origin of the cohesion and the mechanical strength of PA-based materials (Figure 17). There are several families of PA, which can be aliphatic, semiaromatic, or aromatic, depending on the nature of the linkers separating amide functions. Aliphatic and semiaromatic PA are identified by the two numbers designating, respectively, the number of carbon atoms present in the diamine and the diacid they are derived from. A single number is used if an amino acid or a lactam is employed as monomeric precursor with both amine and acid functions (Figure 17).

Due to the wide range of available monomers, PA can exhibit a broad range of properties. Semicrystalline for the most part, PA display high mechanical properties (tensile modulus, strength, impact resistance including at low temperature, abrasion resistance, resilience), heat resistance, resistance to chemical aging, electrical insulation properties, and good biocompatibility.

First appearing in the 1930s, PA, also referred to as Nylons, represent high-performance materials of choice, with a market of 8 Mt, which is expected to grow at the rate of 2.2%, reaching up to 10.4 Mtby 2027.[481−483] The 96% of PA are composed of short-chain with half of polycaprolactam (PA-6) and half of polyhexamethylene adipamide (PA-6.6 obtained from two monomers, adipic acid, and hexamethylenediamine (HMD)), and 4% of specialty PA (long-chain PA and polyphthalamides), with 60% used as fibers and 40% as engineered polymers (Figure 17).[484] The world demand for PA is increasing every year because of their wide use in various applications for automotive, electrical, electronic, construction, packaging, carpets, and sportswear. Differences between PA-6 and P-A6.6 include, for instance, temperature resistance that is lower for PA-6, while PA-6.6 has higher modulus and better wear resistance. Cost production is lower for PA-6. Other PA have been developed but remain minor, such as the polybutyrolactam (PA-4, T_m = 260−268 °C) obtained from biobased butyrolactam (derived from glutamate obtained from glucose), polyhexamethylene dodecanediamide (PA-6.12) obtained from hexamethylenediamine and 1.12-dodecanedioic acid, polyundecanamide (PA-11) obtained from biobased 11-aminoundecanoic acid (amino acid from castor oil), and polylauroamide (PA-12) obtained from lauryllactam. Interestingly, PA-4 has been shown to be biodegradable in different environments, including in seawater.[485]

As most of PA are nonbiodegradable, the issue of recycling and disposal of a growing volume of PA waste has therefore attracted an increasing attention. Part of PA waste is collected in Europe through extended responsibility of producers (ERP) in automotive, textile, fishing, and electric and electronic sectors. However, few PA wastes are treated today, mainly production waste through mechanical recycling.

Depolymerization of PA-6 back to its caprolactam monomer has been investigated for a long time. Chemical recycling to monomer (CRM) of PA-6 has seen some commercial developments, as operated by Shaw Industries, Aquafil, and DOMO Chemicals. The Aquafil group produces Econyl yarn made of 100% recycled PA-6, emanating from production waste, oligomers, and postconsumer waste (fishing nets, carpets, rigid textiles, etc/).[486] Their patent WO2013032408A1 protects the removal of Spandex from polyamide elastomeric fabrics composed of PA-6 and/or PA-6.6 fibers, by thermal treatment and washing of degraded

https://doi.org/10.1021/acs.chemrev.2c00644
Chem. Rev. XXXX, XXX, XXX−XXX

Spandex using solvent.[487] Another patent filed by Aquafil, WO2014072483A1 covers both a method and a device for treating polymers by continuous depolymerization and/or dissolution.[488] DOMO Chemicals (ex- Solvay) has focused on airbag fabrics, composed of 15% silicone coated PA-6.6 fabrics, with its move4earth continuous process consisting in micronization and chemical separation to deliver recycled PA-6.6. Construction of an industrial-scale facility in Poland was announced to become operational in 2016, but there has been no information about it since. Depolymerization of PA can be performed by hydrolysis or aminolysis, these processes requiring harsh reaction conditions, notably temperatures higher than 250−300 °C. Other methods based on glycolysis or aminoglycolysis have been described, but they do not result in efficient regeneration of PA monomers from the degraded polymers. Recycled PA-6 arising from a CRM process represents less than 2% of the 4.4 million tons of global PA-6 production per year. This low fraction can be explained by the challenge for removing contaminants (e.g., elastan fibers) from PA-6. If the contaminants remain in the material when, for example, pulling new fibers, this results in low melt strength and breakage. Such a chemical recycling of PA has been the topic of recent reviews. A recent example of successful catalytic CRM of PA-6 in closed loop, namely hydrogenative depolymerization using a designed ruthenium-based catalyst, has been reported by Milstein et al.[489]

Solvay also produces Amni Soul Eco, a PA-6.6 yarn with enhanced biodegradability. It is only biodegraded under landfill conditions in 3−5 years. Their patent WO2016079724A2[490] protects a fiber comprising PA having a hygroscopicity of at least 4%, and a biodegradation agent (0.5−5% by weight) with chemoattractant compound (sugar, coumarin, furanone), glutaric acid or its derivative, carboxylic acid (such as hexadecenoic acid), biodegradable polymer (PLA, PLGA, PCL, PHA, chitosan, etc.), and swelling agent (natural fiber, cyclodextrin PLA, etc.).[490] There is also an example showing 14% biodegradation after 300 days instead of 2% for PA-6.6 alone, hence 90% biodegradation in around 5 years, if the biodegradation rate stays constant, that remains to be demonstrated. From an environmental and industrial point of view, there is thus a need for identifying enzymes active on PA, and to use them either for improving biodegradability of PA, or for recycling a wide range of PA waste thanks to enzyme specificity.

Although the amide bond of PA is common to the amide bond between amino acids composing proteins, PA is far less sensitive to biodegradation than proteins. This can be explained by the fact that PA is not soluble in water, unlike proteins. Moreover, the presence of hydrogen bonds between PA chains was reported to increase its crystallinity,[491] that is known to be a bottleneck for biodegradation.

3.1.2. Methods to Identify PA-Active Enzymes and Microorganisms Involved in PA Biodegradation. Most protocols to identify PA depolymerization enzymes are fully described in Negoro et al.[492] The halo method can be used with 6-aminohexanoate (Ahx)-cyclic oligomers, obtained by fractionation of byproducts from PA-6 factories. Indeed, during the ring-opening polymerization of caprolactam, i.e., PA-6 synthesis, and because of thermodynamic equilibrium, free monomers remain, and the formation of cyclic oligomers formed by head-to-tail condensation are released into factory waste.[493] LB-tributyrin plate can also be used; 270 ± 140 μm powder of PA-6 can be used after limited hydrolysis by formic acid treatment and freezing disruption. A thin layer with average thickness of 260 nm can be obtained by spreading PA dissolved in 2,2,2-trifluoroethanol (TFE).

Degradation products released in aqueous medium, Ahx and Ahx linear dimer, can be detected on a TLC plate by ninhydrin reagents or quantitatively assayed using a C18 reversed phase HPLC column and a detection using absorbance at 210 nm. It is also possible to quantify the released amino groups by a colorimetric method using 2,4,6- trinitrobenzenesulfonic acid (TNBS). Adipic acid can also be assayed by HPLC.[494] Indirect methods consisting in measurement of hydrophilicity by drop test or rising height can also be used to detect surface modification of PA.[494]

Four bacterial strains, *Arthrobacter* sp. KI72, *Pseudomonas* sp. NK87, *Agromyces* sp. KY5R, and *Kocuria* sp. KY2, can grow on Ahx oligomers as sole carbon and nitrogen sources.[495] However, the biodegradability of PA-6 and PA-6.6 is very low. *Geobacillus thermocatenulatus* is responsible of PA-6.6 molecular weight (viscosity average molecular weight, M_v) decrease from 43 000 to 17 000 g/mol in 20 days at 60 °C and has no action on PA-6.[496]

Even if examples of enzymatic degradation of PA-based materials are scarcer than for polyesters, two types of enzymatic activities have been identified, as described hereafter: (i) hydrolases active on PA oligomers with an action limited to the PA surface and (ii) oxidases reducing molar mass of PA.

3.1.3. Surface Modification of PA Fabrics Using Hydrolases. Surface hydrolysis can be implemented to increase PA hydrophilicity, to produce for instance ultrafiltration membrane less clogged by proteins, to improve textile comfort allowing better evaporation of perspiration, or to better color fibers.[497] It can also be used to perform partial hydrolysis and remove oligomers to smoothen the fabric surface. Three types of enzymes can be used for this purpose, namely, proteases, cutinases, and amidases. There is no direct quantification of depolymerization activity but indirect evidence through hydrophilization measurement.

3.1.3.1. Proteases. A slight hydrolysis of PA-6.6 has been described with papain, trypsin, and α-chymotrypsin.[498] Aspartic protease, metalloprotease, and cysteine protease are also used for PA textile modification, in particular, papain, proteases from Genencor (bromelain, Purafect OX 4000 E, protease GC 106, Protex Multiplus L), protease M from Amano, Corolase N from AB Enzyme, and Flavourzyme 500L from Novozymes[499] Alcalase 2.4L from Novozymes was used to modify surface of PA-6.6 fibers.[500] Conditions of action were described in detail by Parvinzadeh et al. using commercial proteases from Genencor (Protex Gentle L and Protex 40L, which are subtilisins produced in *Bacillus subtilis* and covalently linked to propylene glycol; Protex multiplus L-serine alkaline protease; Protex 50FP endo/exo peptidase produced in *Aspergillus oryzae*).[501] PA-6.6 fabric was treated in 40 mM sodium acetate buffer pH 6.5 with 50 $g{\cdot}L^{-1}$ PA-6.6, 30 $mg_{enzyme}{\cdot}g_{PA\text{-}6.6}{}^{-1}$ for 80 min at 30 °C to improve coloration of PA-6.6 fibers. From an industrial point of view, if the reaction time is short and temperature is mild, the enzyme concentration is quite high. A protease from *Bacillus* sp. was demonstrated to be active on PA-6.6 model substrate (adipic acid bis hexyl-amide, Figure 18) and even a better enzyme than cutinases.[502] This highest activity is correlated with the highest adsorption of the enzyme.

https://doi.org/10.1021/acs.chemrev.2c00644
Chem. Rev. XXXX, XXX, XXX−XXX

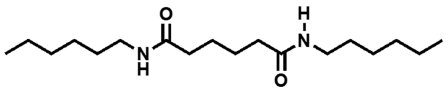

Figure 18. PA-6.6 model substrate (adipic acid bis-hexyl-amide).

3.1.3.2. Cutinases. Surface hydrolysis of PA-6.6 fibers was reported with different cutinases: Genencor's GCI 2002/1410 cutinase,[503] and the FsC cutinase from *Fusarium solani pisi*.[502,504] For instance, the FsC cutinase was active on adipic acid bis hexyl-amide but presents a 4-times lower activity than the protease from *Bacillus* sp, mostly because of its 3-times lower adsorption.[502] Molecular modeling studies combining both molecular dynamics and molecular mechanics (MD/MM) simulations have enabled identification of amino acid targets for mutagenesis to enlarge the active site of FsC and accommodate larger substrates, leading to the evaluation of single mutants L81A, N84A, L182A, V184A, and L189A.[275] The FsC^{L182A} variant showed 45% higher activity than the native enzyme and a 3-times higher adsorption when considering the adipic acid bis-hexyl-amide model substrate. Moreover, this FsC^{L182A} variant was 19% more active than the wild-type enzyme on PA-6.6 fabric. The substitution of leucine by a smaller amino acid, such as alanine, near the active site, could result in a more open structure, allowing a better fit of PA into the active site and a stabilization of the tetrahedral intermediate formed during the reaction. This study highlights that the exchange surface is a crucial parameter on enzyme activities toward polyamide. Unfortunately, there was no control to detect the effect of agitation solely in the absence of enzyme.

The Thc_Cut1 cutinase of *Thermobifida cellulosilytica* has been described to modify the surface of PA-6.6. Its X-ray structure (PDB 5LUI) was further analyzed to identify the amino acid residues composing the active site. Indeed, the I179 amino acid residue was proposed to be a key residue to establish a hydrogen bonding interaction with the NH group of the PA amide and could be necessary for the hydrolysis of the C−N bond.[505] This was confirmed through the obtention of variants with higher activity than wild-type enzyme toward the model substrate, *N*1,*N*6-dihexylhexanediamide (3PA-6.6), at 50 °C pH 7. The amidase activities of mutants I179Q, I179A, and I179N were found improved by 6-, 7-, and 15- fold, respectively. The amino acid mutations enabled creation of a reallocated water network to facilitate the nitrogen inversion mechanism by H-bonding and enhanced transition state stabilization. This stabilization was further confirmed by MD simulations. However, these variants remained poorly active on PA-6.6 film (Goodfellow, thickness 50 μm).

3.1.3.3. Amidases. Five enzymes able to catalyze hydrolysis of PA-6 were identified in *Arthrobacter* sp. KI72:[492,506−510]

- EI = NylA 6-aminohexanoate-cyclic-dimer (Acd) hydrolase (EC 3.5.2.12, 52 kDa, optimal pH and temperature 7.4 and 34 °C) hydrolyzes the amide bond, generating 6-aminohexanoate-linear-dimer (Ald).
- EII = NylB Ald hydrolase (EC 3.5.1.46, 42 kDa, optimal pH and temperature 9.0 and 40 °C, also active on trimer to icosamer), releases 6-aminohexanoate (Ahx) by an exotype mode of action.
- EII′= NylB′ (88% amino acid sequence identity with EII, e.g., 46 amino acids different, but 200 times less active, 42 kDa).
- EIII = NylC Ahx-oligomer endohydrolase (EC3.5.1.117, 37 kDa, optimal pH and temperature 7.0 and 42 °C) hydrolyzes cyclic and linear oligomers of more than 3 units until more than 100 units by an endotype mode.
- Amidehydrolase NylC-like.

EII is more active on 6-aminohexanoyl-8-aminooctanoate (Ahx-Aoc) and 6-aminohexanoyl-aniline (Ahx-Ani) than on Ald, but it is barely active on 4-aminobutyryl-6-aminohexanoate or 8-aminooctanoyl-6-aminohexanoate (Ahx-Aoc) (Figure 19).[511] EII has no detectable activity on Acd, nor on 6-

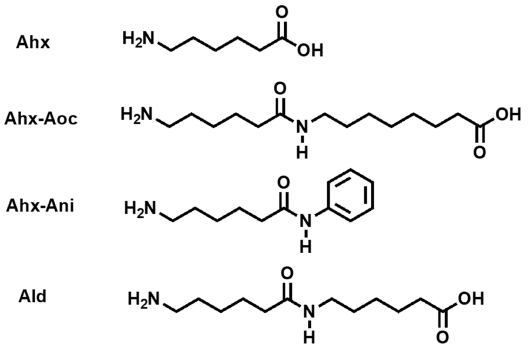

Figure 19. Chemical structures of various amide compounds. 6-Aminohexanoate (Ahx), 6-aminohexanoyl-8-aminooctanoate (Ahx-Aoc), 6-aminohexanoyl-aniline (Ahx-Ani), 6-aminohexanoate-linear-dimer (Ald).

aminohexanoate-cyclic-oligomers, nor on more than 60 kinds of various peptides. EII also possesses hydrolytic activity for carboxyl esters with short acyl chains: C2-ester and lower activity toward C4-ester. EII specifically recognizes amide compounds containing Ahx as the N-terminal residue in the substrate, but the recognition of the C-terminal residue in the substrate is not stringent. With Ald, Ahx is detected after only 15 min with 0.057 mol EII/mol Ald. EII releases 4.16 μmol Ahx/min/mg enzyme.

Two other enzymes have been identified in *Agromyces* sp. KY5R,[495] namely A-NylB (identical to EII) and A-NylC, the latter being more thermostable and more active at alkaline pH than EIII. In addition, homologues of EI have been found in several strains, including the *Pseudomonas* sp. NK87 and the alkaline strain *Kocuria* sp. KY2.[509] A homologue of EIII has also been identified in *Kocuria* sp. KY2 and named K-NylC.[495] Comparatively, EIII has a T_m of 52 °C, whereas A-NylC has a T_m of 60 °C and K-NylC has a T_m of 67 °C, with 5 and 15 differing amino acids from EIII, respectively.[512] Of note, two patents from Rhone-Poulenc (e.g., WO1997004083A1 and WO1997004084A1) protect an amidase from *Comamonas acidovorans* active on PA-6 and PA-6.6 as well as an enzyme-based hydrolysis process.[513,514] The strain was selected as growing on oligomers and a 50.5 $g{\cdot}L^{-1}$ of DP8 oligomers preparation showed 72% conversion into monomers and oligomers of DP < 4 after treatment by 6.2 g of cells for 18 h. Two enzymes were also identified from *Nocardia farcinica* isolated from soil: an aryl acylamidase of 190 kDa able to hydrolyze a PA-6.6 model substrate[515] and a polyamidase of 51 kDa, named NfpolyA.[516] The aryl acylamidase has an optimal pH between 8 and 11 (active at pH 6−11) and an optimal temperature of 50 °C (half-life 35 min). NfPolyA have been purified from an *E. coli* overexpression and was active on *n*-butylamine used as a model substrate and on a PA-6.6 fiber surface. Screening of 12 fungi showed that *Beauveria*

https://doi.org/10.1021/acs.chemrev.2c00644
Chem. Rev. XXXX, XXX, XXX−XXX

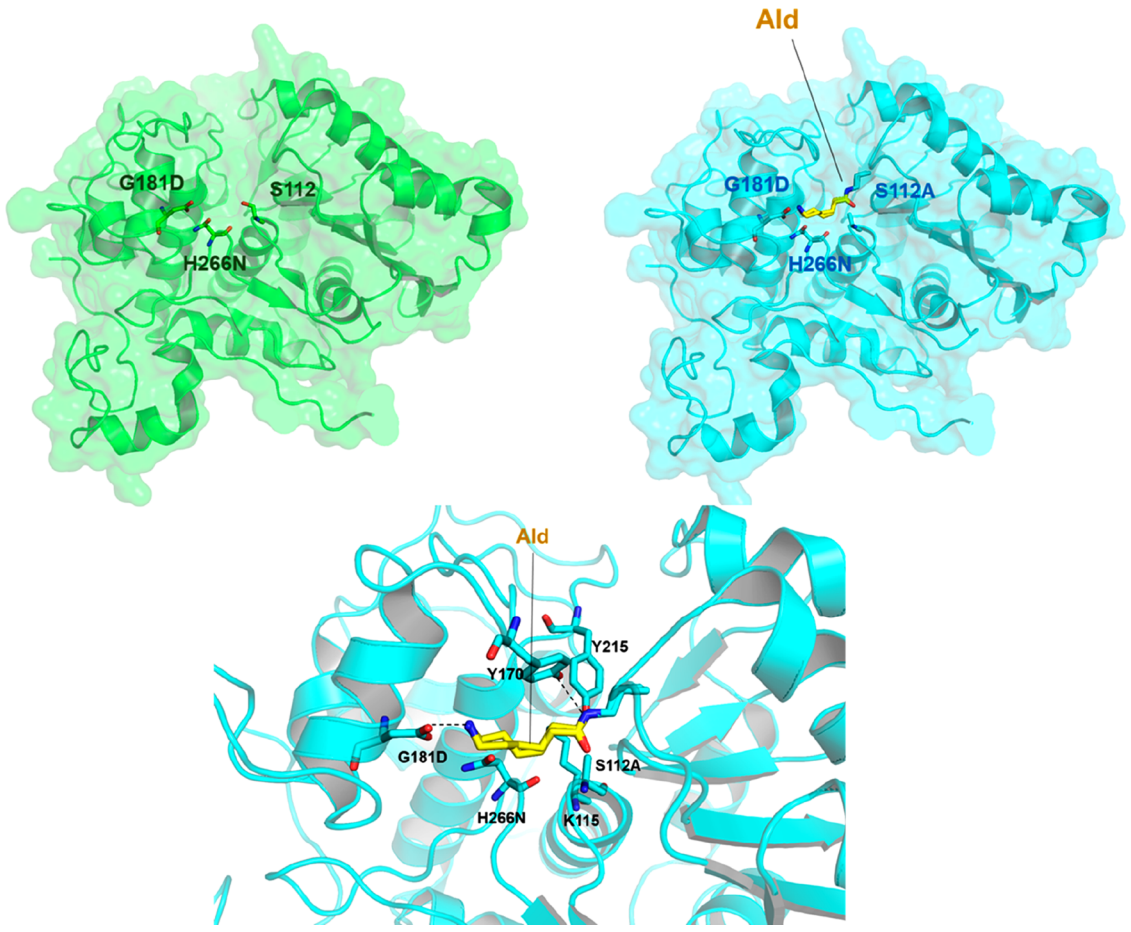

Figure 20. Three-dimensional structure of the Hyb-24$^{G181D/H266N}$ (PDB 1WYC) (green color) and the inactive Hyb-24$^{S112A/G181D/H266N}$ in complex with Ald (PDB 2DCF) (cyan color). An enlarged view of the amino acid residues involved in interaction with Ald is shown at the bottom.

brongniartii and *B. bassiana* were the most efficient to hydrophilize PA.[497] Indeed, a polyamidase of 55 kDa was identified from *B. brongniartii*, to be active on both PA-6 and PA-6.6. Additionally, and without precision of its origin, a ceramidase able to degrade amide and urethane links in polymeric material (PA, PU, polyester, PP, PVC, PS, starch) was patented by Tohoku University.[517]

The X-ray structure of EI has been determined in free form and in complex with Acd (PDB 3A2P and 3A2Q), revealing a catalytic center constituted by the S174/S150/K72 triad responsible for EI catalytic function.[509] Analysis of enzyme/substrate interactions in the complex structure with inactive EI revealed that A171 and A172 residues were involved in oxyanion stabilization and that C316 residue is responsible for Acd binding by forming a hydrogen bond with the nitrogen of Acd amide bond.

Crystallization of purified EII failed under tested conditions.[507] However, the 3D structure of a hybrid between EII and EII′, namely Hyb-24 (variant of EII′: T3A/P4R/T5S/S8Q/D15G), has been successfully determined. Hyb-24 presented only 0.55% activity compared to EII. A homology search based on the Hyb-24 structure was carried out in the Protein Data Bank. Although the sequence identity between Hyb-24 and the proteins in the penicillin-recognizing family of serine reactive hydrolases is low (10−19%), their overall structures were very similar, especially for DD-peptidase and carboxylesterase (EstB). DD-Peptidase has no corresponding residue at the position of G181 of Hyb-24. H266 is a residue constitutive of the catalytic site. Mutations at these two positions have thus been investigated. Interestingly, the combined G181D/H266N mutations in EII′ enabled activity to be restored, while in Hyb24, they led to 85% activity of EII. The X-ray structures of the Hyb-24$^{G181D/H266N}$ double variant (PDB 1WYC) and the catalytically inactive Hyb-24$^{S112A/G181D/H266N}$ counterpart in complex with Ald (PDB 2DCF) have been determined[508] (Figure 20). EII utilizes the S112/K115/Y215 triad as common active site, for both Ald-hydrolytic and esterolytic activity, but requires at least two additional specific amino acid residues (D181 and N266) for Ald-hydrolytic activity (Figure 20).

A catalytic mechanism has been proposed for EII (Figure 21)[508] that involves the following steps: (i) the catalytic center interacts with the N-ter of Ald, (ii) Ald induces then a conformational transition of the enzyme from open to closed form, (iii) a nucleophilic attack of Ald by S112 leads to the formation of a tetrahedral intermediate, (iv) the acyl-enzyme is then formed with the enzyme in open form, and (v) followed by the deacylation of the enzyme by a water molecule and the regeneration of the free enzyme, via the formation of a tetrahedral intermediate. The hydroxyl function of S112 is assumed to attack the ester-carbonyl and amide-carbonyl bonds of the substrate, leading to the formation of the acyl-enzyme. Residues K115 and Y215 are likely involved in maintaining the optimum electrostatic environment to ensure efficient catalytic activity in such a way that either one of these two residues can act as a general base or promote the

https://doi.org/10.1021/acs.chemrev.2c00644
Chem. Rev. XXXX, XXX, XXX−XXX

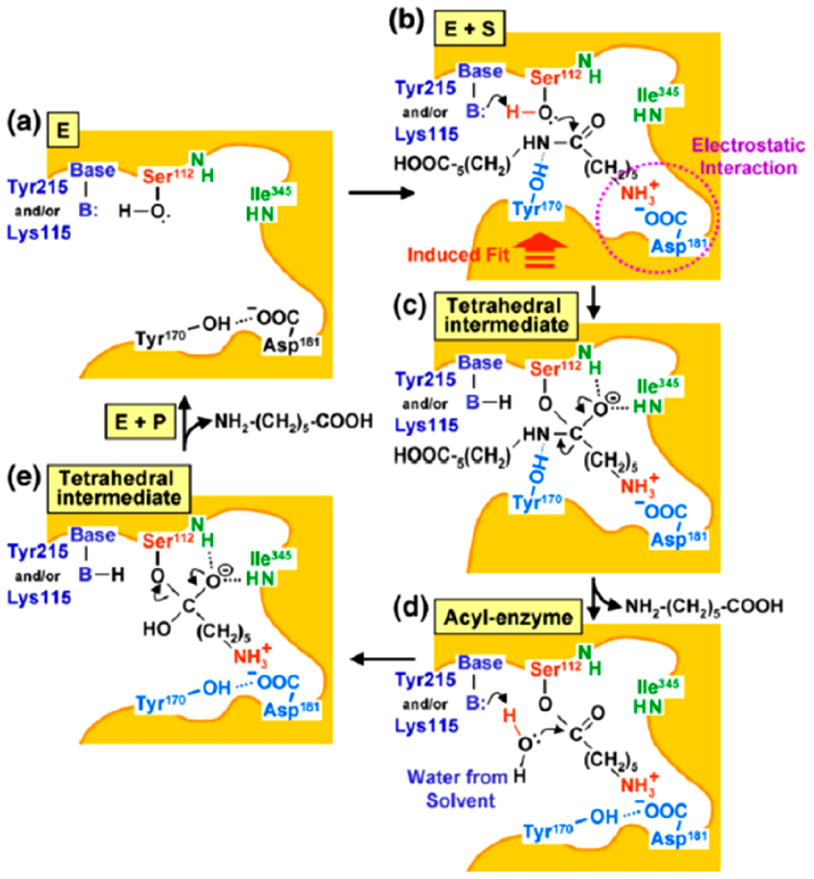

Figure 21. Proposed catalytic mechanism of EII along the following steps:[508] (a) free enzyme in open form, (b) enzyme + substrate, (c) tetrahedral intermediate in closed form (d) acyl-enzyme, and (e) tetrahedral intermediate in open form. Reproduced with permission from ref 508. Copyright 2007 Elsevier.

nucleophilic attack by S112. The subsequent deacylation step involves the attack of the acyl enzyme by a water molecule.

The amide bond cleavage mechanism of PA-6.6 and nonbiological amide bonds by EII was investigated using computational quantum mechanics/molecular mechanics approach coupled to metadynamics (QM/MM CPMD).[492,518,519] It follows the two-step mechanism of serine-reactive hydrolases involving a Ser/Lys/Tyr catalytic triad and an oxyanion hole. The acylation via a tetrahedral intermediate was shown to be the rate-limiting step. The work also revealed the dual role of a unique Y170 residue in the stabilization of the acyl-enzyme and the enhancement of the proton donation of the general acid to the amide substrate in the tetrahedral intermediate.

The 3D structure of A-NylC has also been determined (PDB 3AXG).[512] It is constituted of a dimer of 36 kDa, each dimer being composed of 2 subunits α and β of 27 and 9 kDa, respectively. A-NylC adopts a doughnut-shaped quaternary structure with putative catalytic residue T267 at the N-ter of the β-subunit that participates in a H-bonding network with N219, D306, and G307. The autoproteolysis of the precursor produces the active enzyme.

3.1.4. Enzymatic Oxidative Degradation. Enzymatic oxidative degradation has only been reported by a Japanese team who also studied amidases, but there has been no publication for 20 years. White rot fungi *Deuteromycotina* sp. FERM BP-1859, *Phanerochaete chrysosporium* ATCC 34541, and *Trametes versicolor* IFO 7043 were shown to degrade PA-6 and PA-6.6 under ligninolytic conditions thanks to a manganese peroxidase induced by $MnSO_4$ (MnP, 43 kDa).[520−522] This manganese peroxidase is active from pH 3.5 to pH 5 with an optimum at pH 4.5. After its degradation, PA displays various functions such as −CHO, −NHCOH, $-CH_3$, and $-CONH_2$. The methylene group adjacent to the N atom in the polymer chains is attacked by the peroxidase. The M_w and the M_n of a PA-6.6 membrane decreased by 57% and 75%, respectively, after 2 days of incubation at 30 °C with the purified enzyme. Alteration of a PA-6 fiber was also visible on SEM. Additionally, the laccase of *Trametes versicolor* with 1-hydroxybenzotriazole (HBT) degraded a PA-6.6 membrane, showing a decrease of the M_w and the M_n by 81% and 72%, respectively.[523] Alternatively, several patents were released. Indeed, a decomposition method of PA compound was reported using the culture of basidiomycetes such as *Phanerochaete chrysosporium* ATCC 34541 under N and C starvation. The M_w and the M_n were found to decrease by 86% and 90%, respectively, after 20 days at 20−28 °C.[524] A decomposition method of PA using MnP and Mn(II) and phosphate such as $MnSO_4$ et KH_2PO_4 was also described.[525] A degradation method of PA using MnP and additives such as acetic/succinic/phosphoric acid.[526] Finally, a decomposition method of PA using a laccase mediator system, preferably 1-HBT, was also reported.[527]

3.1.5. Outlook. Whereas partial hydrolysis of PA-6 and PA-6.6 has been reported, especially for textile applications, complete depolymerization of PA fibers by enzymes has not been established yet. It appears that a unique research group has reported the screening and the discovery of enzymes for

https://doi.org/10.1021/acs.chemrev.2c00644
Chem. Rev. XXXX, XXX, XXX−XXX

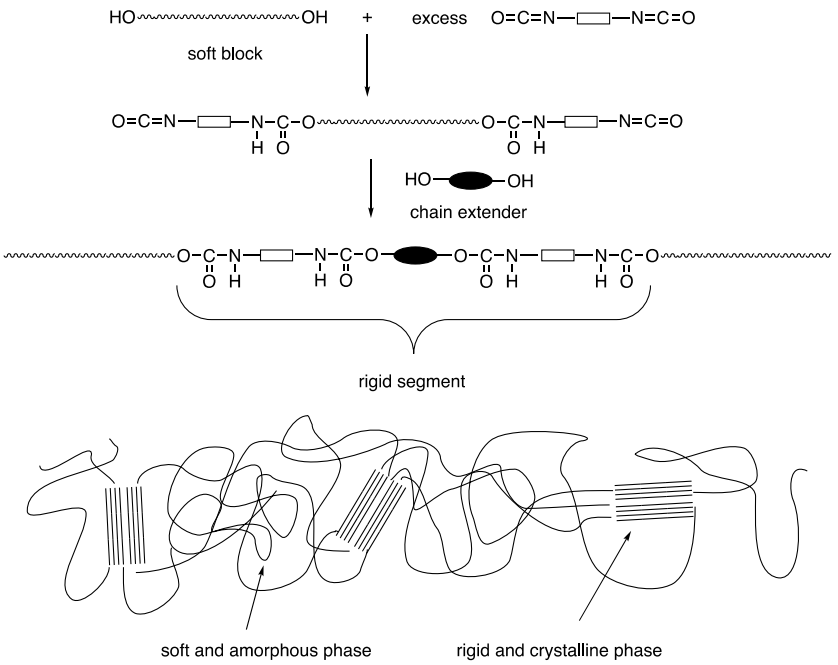

Figure 22. A two-step route to linear PU combining hard and soft segments and their representative nanostructuration in the bulk, with amorphous and crystalline phases.

PA degradation.[506] Currently, the Open plastic project supported by the Queen's University, Ontario, Canada,[528] and involving Carbios and DuPont among the partners is searching for new microbes and new enzymes that could depolymerize PA and could offer novel opportunities to develop efficient PA degradation processes. Except for the surface modification of fabrics, no industrial utilization of enzymes has been reported so far to degrade PA waste. When comparing with PET recycling, it appears certainly crucial to first develop a method of PA pretreatment, to decrease the crystallinity and to increase enzyme accessibility. Second, this would require optimization of the enzyme thermostability to work as close as possible to the glass transition temperature of PA ($T_g \sim 50$ °C). Of course, the improvement of the activity might also be mandatory as the enzymes reported to be active on PA have not been designed for this purpose by Nature. In addition, potential inhibition of the enzyme by released degradation products and adsorption of the enzyme on PA remain to be further investigated.

PA-6 and PA-6.6 monomers are biodegradable. It could thus be of interest to incorporate an enzyme inside the PA to release monomers for short-life applications. However, it is unlikely that an enzyme can be incorporated inside the PA to improve its biodegradability as PA is transformed at high temperature (>230 °C for PA-6 and >265 °C for PA-6.6). Effectively, enzymes will be denaturated at these high temperatures. An alternative could be to add the enzymes to the PA via surface coating avoiding such temperature of denaturation, as shown by Kuraray et al. in a released patent.[529] This approach presents however a risk of enzyme leakage, losing the ability to biodegrade PA. Another solution could be to use the enzyme to treat PA wastes in composting or methanization units, monomers of PA-6 and PA-6.6 being metabolizable.

Alternatively, the enzyme could be used in controlled reactors to recover monomers. Ahx can be reused after conversion to ε-caprolactam by intramolecular dehydration for the repolymerization of PA-6, leading to closed loop recycling. Adipic acid and HMD can also be recovered, purified, and directly used for new synthesis of PA-6.6. In many wastes, such as textiles and automotive parts, PA-6 and PA-6.6 are present in mixture. If the same enzyme is used to depolymerize PA-6 and PA-6.6, three monomers will need to be separated, which can be a more complex and tedious task. Another method would be to optimize two enzymes, a first one selective for PA-6 and a second one for PA-6.6, to treat wastes by successive use of these two enzymes. Combination of oxidases and hydrolases could be investigated, but it would require anticipating the recovery of degradation products. For instance, after PA degradation, Negoro et al. suggests performing biotransformation of recovered monomers to valorize them by conversion into other metabolites such as organic acids or alcohols.[492] The metabolic pathway for the conversion of Ahx to adipate has been reported in *Arthrobacter* sp. KI72.[510]

3.2. Polyurethanes (PU or PUR)

3.2.1. About PU. Polyurethanes, abbreviated as PU or PUR, represent a class of polymers constituted of carbamate (= urethane) linkages. PU are the sixth most used polymers in the world, with a consumption reaching more than 20 Mt per year.[530] Flexible foams are used for the cushioning of furniture, bedding, or automotive seats, while rigid foams are used as thermal insulators in the construction. PU are also used as coatings, adhesives, sealants, and elastomers (CASE). PU coatings provide a protection layer against weather, abrasion, and corrosion. Elastomers are both elastic and flexible and can be used in application, such as wheels for rollerblades. Certain types of PU are biocompatible and used in medical application, such as cardiovascular devices or orthopedic prosthesis. Elastan is a particular PU used in textile.[531]

Classically, PU result from the polyaddition of a diol (or polyol) onto a diisocyanate (or polyisocyanate). The latter is directly produced from the corresponding amine and phosgene, which is highly toxic. The hydroxylated oligomers

https://doi.org/10.1021/acs.chemrev.2c00644
Chem. Rev. XXXX, XXX, XXX−XXX

("polyols") have a varied structure. However, they are most often either based on polyether, especially in foams, which is the main application of PU, or on polyester, in particular in thermoplastic polyurethanes (TPU). Corresponding polymers are thus often coined as "polyetherurethane" and "polyesterurethane", respectively. The polyether chains are essentially constituted of poly(oxyethylene), (PEO, also referred as PEG for poly(ethylene glycol)), poly(oxypropylene), (PPO or PPG for poly(propylene glycol)), and poly(oxytetramethylene) (PTMO). Main aliphatic polyesters derive from polyadipate [butylene or ethylene/butylene] and poly(ϵ-caprolactone) (PCL). Aromatic oligomers are also used to produce PU or polyisocyanurate foams, improving their fire resistance. Hence, PU can show a rich chemical diversity as they can be produced from a wide range of at least two types of monomers, which enables to tune their physical properties.

PU synthesis usually requires a catalyst, e.g., 1,4-diazabicyclo{2.2.2}octane (DABCO) as a tertiary amine, or dibutyltin dilaurate (DBTDL), in order to accelerate the polymerization reaction, to balance the different reaction events that can take place during the formation of urethane linkages (e.g., trimerization of the isocyanate, reaction between water and the isocyanate, etc.).

To achieve high performance elastomers or thermoplastics, a third component like a diol (respectively diamine) or a triol, (respectively triamine) of low molar mass can be incorporated into the formulation. Difunctional reactants are often referred to as "chain extenders", while higher functionality compounds will be referred to as "cross-linkers". Their presence will lead to the formation of chain or network portions, where the isocyanate patterns will be very close together with a strong density of urethane bonds. For entirely linear TPU, the urethane moieties behave as rigid "hard" segments, as opposed to chains deriving from the macrodiol oligomer behaving as flexible "soft" segments. If there is a sufficiently significant thermodynamic incompatibility between the hard and the soft segments, this will result in the separation of the material into rigid and flexible nanodomains.

The phenomenon is accentuated when the polymer is synthesized in two steps via a prepolymer (Figure 22), which forces the chain extender molecules to come together in the chain to form a longer rigid segment (casting elastomers), whereas a one-step synthesis (particularly in the case of TPU synthesized by reactive extrusion) results in a more random distribution of the different patterns.

The main defects being the toxicity of some precursors and the difficulty in properly recycling PU waste, alternative synthetic pathways are currently assessed that could overcome those issues. In this concern, the most studied and promising routes to PU include (i) the transurethanization polycondensation between a bis-carbamate and a diol and (ii) the polyaddition between cyclic carbonates and (pluri)amines.

Recent works have been performed to design biodegradable PU for biomedical applications. On the opposite, current commercial PU designed for long-term application are recalcitrant to biodegradation. A review on PU biodegradation is somehow difficult, as it is a diverse family of polymers which differ considerably in their physical properties due to varied nature of the different building blocks used for their synthesis. Moreover, the exact composition of PU used in the different publications is often unknown. At best, there is a commercial name of PU, but PU producers do not provide information neither about their chemical formula, nor about their molecular weight. In some cases, however, PU were purposely synthesized by the authors and were thus rather well characterized.

To investigate the existence of biodegradation activity on urethane bond, low molecular weight urethane-based model molecules have been specifically designed. For instance, a fungal strain of *Exophiala jeanselmei* can hydrolyze toluene-2,4-carbamic acid diethyl ester into tolulene-2,4-diamine (TDA).[532] Likewise, 2,4-toluene diisocyanate (2,6-TDI)-based diethyl ester can be degraded by *E. jeanselmei*. A strain of *Rhodococcus equi* can hydrolyze toluene-2,4-carbamic acid dibutyl ester (TDCB) into TDA, but its growth was inhibited by TDA concentration higher than 1.0 mM.[533] The *R. equi* strain also showed hydrolytic activities on the urethane bonds in methylene bisphenyl carbamic acid dibutyl ester (MDCB) and hexamethylene carbamic acid dibutyl ester (HDCB), releasing 3,3′-methylendianiline (MDA) and hexamethylene diamine (HDA), respectively. There are thus enzymes able to hydrolyze urethane bond despite the fact that they have not been identified yet. However, theses enzymes may not necessarily be able to degrade commercial PU as urethane bonds are most often localized in the crystalline regions of the polymeric structure.

This diversity in PU makes difficult the design of an enzyme able to degrade a large variety of PU. It is obvious that a specific enzyme must be developed for each specific PU.

Polyester-PU particle dispersions are generally used for screening, then most promising strains are studied on bulk polymers, polyester-PU, or polyether-PU, in the form of thin films (coatings) or foams. Numerous microorganisms have thus been identified for PU biodegradation and reported in reviews.[534−536] Presence of characteristic enzymatic activity (esterase, protease, urease) has often been evaluated but without evidence on its involvement on PU biodegradation and without specific enzyme identification.

Impranil DLN from Bayer Corporation (now Covestro) is often used as a PU model substrate. It is obtained from polyhexane neopentyl adipate polyester and hexamethylene diisocyanate (HDI,[537] Diethylene glycol (DEG) is also a component of Impranil-DLN.[538] It is an aliphatic polyester-PU colloidal dispersion used for textile, leather, and aircraft fabric coatings.[539] It is a white milky suspension composed of 40% dry mass of ∼200 nm sized spheres and can remain suspended in water-based media for several days. It becomes translucent when hydrolyzed, enabling easy enzymatic activity detection.

Hydrolysis of urethane bond was confirmed with Impranil DLN. For instance, a fungus strain of *Cladosporium pseudocladosporioides* degraded up to 87% after 14 days with the loss of carbonyl groups and NOH bonds, a decrease in the ester compounds, and an increase in the alcohols and hexane diisocyanate, indicating the hydrolysis of the ester and the urethane bonds.[540] A strain of *C. tenuissimum* was isolated at the same time on Impranil DLN and was also able to degrade solid foam of polyether-PU (PolyLack from Sayer Lack Mexicana), leading to a 65% weight loss. Another fungal strain, *Aspergillus* sp. reduced the initial weight by 20% after 28 days of a polyester-PU film, obtained by solvent casting in tetrahydrofuran (THF) of methylene diphenyl diisocyanate (MDI) polyester PU {poly[4,4′-methylene-bis(phenyl isocyanate)-*alt*-1,4-butanediol/poly(butylene adipate)]} pellets.[541] Recently, microbial communities were selected by enrichment with PolyLack, from deteriorated PU foams collected in a municipal landfill.[542] There were already reported PU-

https://doi.org/10.1021/acs.chemrev.2c00644
Chem. Rev. XXXX, XXX, XXX−XXX

degrading genera (*Paracoccus, Acinetobacter*, and *Pseudomonas*), but also new genera (*Advenella, Bordetella, Microbacterium, Castellaniella*, and *Populibacterium*).

3.2.2. Enzymatic Hydrolysis of PU. Different classes of enzymes have been identified and characterized for their involvement in PU biodegradation: esterases, lipases, cutinases, proteases, amidases, ureases, and oxidases. They are discussed in the following paragraphs.

3.2.2.1. Esterases, Lipases, and Cutinases. Esterases represent the main class of enzymes (EC 3.1) involved in the degradation of polyester-PU. They are known to hydrolyze the ester bonds in the soft segments, leading to the release of carboxylic acid and alcohol end-groups.[543] Esterase activity has been detected in several strains degrading polyester-PU (for instance, military paint Unicoat;[544] coating Hydroform[545]). In some cases, the enzyme was identified and its key role in the PU biodegradation process was established.

Impranil DLN was degraded with lipases from *Candida rugosa* (Sigma) at pH 7 and 35 °C with 2.5 g/L PU and 28 mg lipase/g PU, generating diethylene glycol (DEG), adipic acid, and trimethylol propane (recoverable in paints and coatings).[538] It is unknown if the reaction goes on after 1 h and the total degradation of PU into DEG is not described. Biffinger et al. have also studied commercial esterases from Sigma on Impranil DLN: the recombinant esterase from *Pseudomonas fluorescens*, the triacylglycerol lipase from the *Pseudomonas* sp.[539] The lipase was applied at the lowest concentration (1.75 mg lipase/g PU with 4 mg/mL PU). It showed the highest esterase activity and was the only enzyme to completely "clear" 5.0 mg of Impranil after 24 h, generating the highest concentration of soluble hydrolysis products (3.9 mM of the soluble alcohol). The esterase activity was neither inhibited by Impranil DLN nor its hydrolysis products and remained stable after 24 h exposure to Impranil DLN.

Several extracellular serine-hydrolases (EC 3.1) with consensus sequence GXSXG were shown to be able to clear Impranil DLN. The PulA (48 kDa) arises from *Pseudomonas fluorescens* and is known to exhibit an esterase activity. Its PU degradation activity was confirmed after production in *E. coli*.[546] An approximately 21 kDa enzyme was purified from the cell-free filtrate of *Pestalotiopsis microspora*.[547] The secretion of active protein appeared to be induced under PU growth conditions. This enzyme is thermostable because a treatment at 98 °C for 20 min was required to inactivate the enzyme. An enzyme of 28 kDa was identified in *Curvularia senegalensis* with an esterase activity, stable 10 min at 100 °C.[548] An enzyme (~66 kDa) was identified in *Acinetobacter gerneri* and its activity was increased with 5 mM of $CaCl_2$.[537] *Aspergillus flavus* ITCC 6051 causes 61% mass loss of polyester-PU sheet of 1 mm thickness (from Instapark) after 30 days.[549] A strain of *Pseudomonas putida* degraded 92% of Impranil DLN within 4 days at 30 °C, with decrease of ester functional groups and emergence of amide groups.[550] Esterase activity was detected in the cell lysate and a 45 kDa protein able to degrade PU was detected by zymogram.

Two other enzymes were identified in *Pseudomonas chlororaphis* ATCC 55729 by zymogram.[546,551] One of 63 kDa (PueA) exhibited both esterase and protease activities with respective optimum pH of 8.5 and 7.0, whereas the other of 31 kDa showed esterase activity and an optimum pH of 8.5. The enzyme activities of both proteins proved stable after 10 min at 100 °C. Then, a third enzyme was identified in *P. chlororaphis* (PueB, 60 kDa[552]). Genes encoding PueA and PueB were cloned in *E. coli*.[552,553] According to sequence homology, PueA is a lipase and has 56% identity in amino acid sequence with PulA. PueA and PueB only share 42% identity of amino acid sequence. The recombinant PueB showed esterase activity when assayed with various *p*-nitrophenyl substrates and lipase activity when assayed with triolein. PueA and PueB are both part of an ABC transporter gene cluster[554] with an ATPase-binding protein (ABC), an integral membrane protein (MFP), and an outer membrane protein (OMP[534]). Both enzymes are stable up to 100 °C. Insertional mutations in the pueA and pueB genes generating knockout mutants suggest that PueA may play a more major role in PU degradation than PueB based on cell density and growth rates. Later, *P. chloroaphis* was also found to degrade an open-cell polyester-PU foam used in car seats, releasing DEG but without significant weight loss.[555] A method using this strain to remove PU coating was patented by the U.S. Ship.[556] Two lipases PueA and PueB were also found in *Pseudomonas protegens*.[557−559] Deletion of the pueA gene reduced PU-clearing activity, while pueB deletion exhibited little effect. Nevertheless, removal of both genes was necessary to stop degradation of PU.

PueB from *P. chlororaphis* was studied by 500 ns MD simulations either as a free enzyme or complexed with a PU monomer (formed by polybutylene adipate (PBA) and 4,4′-methylene diphenyl diisocyanate (MDI)).[560] Along the simulation of PU-MDI with the PueB, several residues (S31, T32, P33, Q60, R95, T97, Y104, A108, L111, H151, L153, P184, T201, W207, H250, P251, Q252, S253, A254, V255, L256, P259, and Q260) were found to establish van der Waals interactions, while T32, T62, R76, R98, S152, and L252 formed hydrogen bonds. These results indicated that the PU monomer (MDI) suffered only small rearrangements, as it maintained interactions with specific residues from the same region of PueB during the entire simulation.

Despite their quite old discovery, all of these enzymes remain to be characterized in deeper detail to quantify and compare their activity on different PU. Especially, the degradation products should be investigated to determine if they only hydrolyze the ester bonds in the soft segments. Indeed, the enzymes able to degrade PU are often, and irrelevantly, called polyurethaneases due to their activity on PU but without characterization of their abilities to hydrolyze urethane bonds.

A strain of *Comamonas acidovorans* completely degraded 10 $g{\cdot}L^{-1}$ of polyester-PU in cube shape with long chain polyester segments (homemade by reacting poly(diethylene glycol adipate) (M_n 2,5 $kg{\cdot}mol^{-1}$) with 2,4-tolylene diisocyanate) after 7 days into diethylene glycol (DEG) as well as few trimethylolpropane (TMP) with PU as sole carbon source.[561] The weight loss was 48% when PU was the sole carbon and nitrogen source and, in this case, adipic acid was additionally detected. In both cases, it was important to avoid acidification by maintaining neutral pH. No metabolite was detected that could be derived from diisocyanate segment. Moreover, *C. acidovorans* was not able to degrade either poly(propylene glycol) or polyether-PU (homemade by reacting poly-(propylene glycol) with 2,4-tolylene diisocyanate). *C. acidovorans* has a membrane-bound esterase PudA of 62 kDa,[562,563] and the PudA protein purified from an *E. coli* overexpression was able to degrade solid polyester-PU (DEGA, 2,4-tolylene diisocyanate). PudA contains the GXSXG motif characteristic of serine hydrolases. Close to a Glu residue

https://doi.org/10.1021/acs.chemrev.2c00644
Chem. Rev. XXXX, XXX, XXX−XXX

(E324) of the S199/H433/E324 catalytic domain of PudA, there are three hydrophobic domains, one of which forms a surface-binding domain, which is present in the C-terminus of most bacterial poly(hydroxyalkanoate) (PHA) depolymerases.

An esterase of *Cryptococcus* sp. MTCC 5455 capable of degrading different aliphatic polymers and copolymers was reported.[564] Between 35 and 55% degradation of PU film (no reference on the type of PU) was obtained by the freeze-dried enzyme in 12 h and complete degradation in 24 h. The enzyme, which was characterized by a molecular weight of 25−28 kDa, was stable at pH 4−10 up to 60 °C and proved active at pH 5−8 and 10−50 °C.

Bayer filed a patent on a process for the enzymatic decomposition of biodegradable adhesives (polyesteramides and polyesterurethanes containing urea groups) with a lipase (*Candida antarctica* lipase B, named CalB, *Mucor miehei* lipozyme, *Aspergillus niger* lipase) and/or a cutinase (HiC from *Humicola insolens*).[565] Examples included polyesters and urethane polyester (Desmocoll VPKA 8741 Bayer). Similarly, another Bayer's patent protected a process for decomposing molding bodies, tablecloth structures, coatings, bonding assemblies, or biodegradable polymer foams, with enzymes.[566] This process reported the enzymatic decomposition of polyesteramides and polyesterurethanes comprising urea groups, with a lipase or cutinase. In the examples, a film of polyester amide (60% caprolactam and 40% statistical copolymer of adipic acid and butanediol) was completely degraded using CalB lipase.

The degradation of Impranil DLN was shown with four polyester hydrolases: LCC, *Tf*Cut2 from *Thermobifida fusca* KW3, and Tcur0390 and Tcur1278 from *Thermomonospora curvata* DSM43183.[543] Tcur0390 and Tcur1278 appeared less thermostable than *Tf*Cut2. The highest initial kinetics and hydrolysis rates were obtained for *Tf*Cut2 and Tcur0390. A turbidity of 30−40% of Impranil remains after treatment with all the enzymes (plate), indicating only partial hydrolysis. *Tf*Cut2 showed the highest substrate affinity for Impranil DLN. The four enzymes were also able to generate weight losses of the solid thermoplastic polyester PU Elastollan B85A-10 and C85A-10 without additives (supplied by BASF). Indeed, up to 4.9% and 4.1% weight loss of Elastollan B85A-10 and C85A-10, respectively, with 0.6 $mg_{LCC}{\cdot}g_{PU}{}^{-1}$ and 80 $g_{PU}{\cdot}L^{-1}$ was observed after around 8 days at 70 °C. Size exclusion chromatography confirmed a preferential degradation of the larger polymer chains, with a decrease of up to 19% of M_w and no change of M_n. Degradation of long chain preferentially occurred at the polymer surface, and the urethane bonds were reported to resist to hydrolysis.

The bacterial cutinase Tcur1278 was fused with the anchor peptide Tachystatin A2 and produced in *Pichia pastoris*, which led to an increased hydrolytic activity by a factor of 6.6 on Impranil DLN compared to the wild-type enzyme.[241] Degradation half-lives of PU nanoparticles were reduced from 41.8 to 6.2 h (6.7-fold) in a diluted PU suspension (0.04% w/v).

A polyester-PU film (5 $g{\cdot}L^{-1}$, obtained by solvent casting in THF of PU1080 pellets from Bayer) has been incubated with commercial HiC cutinase (Novozym 51032, 100 $mg_{enzyme}{\cdot}g_{PU}{}^{-1}$, e.g., a high concentration) at 50 °C for 7days.[567] M_n decreased by 84% from 22 $kg{\cdot}mol^{-1}$ to 3.4 $kg{\cdot}mol^{-1}$, and M_w decreased by 42% from 108 $kg{\cdot}mol^{-1}$ to 63 $kg{\cdot}mol^{-1}$ after 3 days without any further change after 7 days. Thus, the molar mass dispersity increased from 4.89 to 17.89. Unfortunately, results for PU incubated in the same conditions at 50 °C without enzyme are not presented in the article. Scanning electron microscopy (SEM) showed cracks at the surface of the PU films because of enzymatic surface erosion. Liquid chromatography time-of-flight/mass spectrometry (LC-MS-Tof) analysis revealed the presence in the incubation supernatant of all the monomer constituents of the polymer (3,3′-methylendianiline (MDA), 1,4-butanediol and adipic acid), but there was no quantification of degradation products. Their concentration increased throughout incubation. The presence of MDA indicates that the enzyme was able to cleave not only the ester bond, but also, to a lesser extent, the urethane portion of the PU. Oligomers (dimers, trimers) concentrations first increased, then decreased. They were probably hydrolyzed to monomers. Four PU were synthesized, namely, 2 TPU with a PCL diol (M_n of 2 $kg{\cdot}mol^{-1}$) and either TDI or MDI, 2 thermoset closed-cell foams with PCL diol (M_n 0.53 $kg{\cdot}mol^{-1}$) and PCL triol (M_n 0.9 $kg{\cdot}mol^{-1}$), and either TDI or MDI.[568,569] Molar masses were 13 and 17 $kg{\cdot}mol^{-1}$ (M_n) and 76 and 110 $kg{\cdot}mol^{-1}$ (M_w) for the TDI- and the MDI-based TPU, respectively. Foams and coatings obtained by solvent casting were incubated with CalB lipase from Sigma. The highest weight loss (25%) was obtained with the TDI-based PU foam, indeed, 1 g of TDI-based PU foam (67 $g{\cdot}L^{-1}$) was degraded by CalB ($1061_{unit}{\cdot}g_{PU}{}^{-1}$) after 24 h at 37 °C when only 3% weight loss occurred for the negative control. Walls of the cells were fully degraded by the enzymes. These results represent the first report on a complete degradation of a whole PU compartment. 6-Hydroxycaproic acid (HCA) and a short acid-terminated diurethane were recovered. Finally, authors demonstrated recyclability of recovered monomers through organometallic-catalyzed synthesis. A polymer with a high M_w of 74 $kg{\cdot}mol^{-1}$ was obtained by mixing 50% of recycled building blocks and 50% of neat HCA without the use of toxic polyisocyanates. Synthesis with only recycled building blocks was not effective, as trimethylolpropane was present after the hydrolysis of PCL triol segments of the foam and induced cross-linking. Even with 50% neat HCA, polymerization yield was only 37% instead of 67% with 100% neat HCA.

Cholesterol esterase (CE) from Sigma, an enzyme located in the extracellular granules of liver cells, aortic intima, and leukocytes, was able to degrade both polyester PU and polyether PU at 37 °C for 3 weeks with regular replacement of enzymatic solution.[570] PUs were synthesized from 2,4-toluene diisocyanate (TDI), methylene di-*p*-phenyl diisocyanate (MDI), PCL (1.25 $kg{\cdot}mol^{-1}$), and poly(tetramethylene) oxide (PTMO, 1 $kg{\cdot}mol^{-1}$), polyethylene glycol (PEO, 1 $kg{\cdot}mol^{-1}$), ethylene diamine (ED), and butanediol (BD). PU were in the form of film obtained by solvent casting with dimethylacetamide (DMAC). Among TDI/PTMO/ED, TDI/PCL/ED, MDI/PTMO/ED, and MDI/PTMO/BD blends, the cholesterol esterase was only effective for TDI/PCL/ED blend in releasing degradation products that contained hard-segment components.

Metagenomics tools allowing screening of bovine rumen microbiome were developed to select carbamate degrading enzymes.[571] This led to the discovery of a novel carboxyl-ester hydrolase belonging to the lipolytic family IV, named CE_Ubrb, that was able to clear Impranil DLN.

3.2.2.2. Proteases. After 3 weeks at 30 °C, a strain of *Alternaria solani*, expressing a protease activity, caused 66% weight loss in the polyester-PU film (supplied by Nakajima-

https://doi.org/10.1021/acs.chemrev.2c00644
Chem. Rev. XXXX, XXX, XXX−XXX

Kambe homemade by reacting poly(diethylene glycol adipate), M_n 2.5 kg·mol^{-1}, with 2,4-tolylene diisocyanate). This was evidenced through (i) the reduction in the number of −CH− groups and increase in the number of −OH groups, (ii) detection of acid and amine fractions attributed to the hydrolysis of diisocyanate segment and adipic acid, diethylene glycol, and trimethylolpropane released from the polyester segment.[572]

The polyether PU elastomer film (Biomer, Ethicon), which is used in some blood-contacting devices, was treated with the plant papain (EC 3.4.22.2) for 1−6 months at 37 °C. Degradation occurred at the urethane bonds, shown by mechanical tests, SEC, and FTIR analyses.[573]

Human neutrophil elastase (HNE) and porcine pancreatic elastase (PPE) were able to degrade a poly(ester-urea-urethane) containing toluene diisocyanate (TDI), poly(caprolactone) (PCL), and ethylenediamine (ED), and a poly(ether-urea-urethane) containing TDI, poly(tetramethylene oxide) (PTMO), and ED, PPE being the most active.[574]

Bromelain (EC 3.4.4.24) and ficin (EC 3.4.22.3) were found to be more effective than other proteases in the cleavage of urethane bonds in PU.[575] Diisocyanates have often been used for chain extension of polyester oligomers. In the field of biomedical materials, the enzymes mainly used are chymotrypsin, papain, and cholesterol esterase to ensure the cleavage of urethane bonds. Lysine diisocyanate (LDI) based PU with M_w 10.8 kg·mol^{-1} to 44 kg·mol^{-1} were synthesized by polyaddition of LDI with various diols, such as ethylene glycol (EG), diethylene glycol (DEG), and 1,4-butanediol (BD). They are considered to give nontoxic degradation products and are suitable biomaterials for tissue engineering, such as scaffold materials. PUs prepared in this work were amorphous and had a softening point under 70 °C, although all showed a glassy state at room temperature. After coating of 10 μm thickness by solvent casting, 37%, 53%, and 54% hydrolysis of LDI/BD and LDI/EG LDI/DEG, respectively, were observed with 100 $mg_{ficin}{\cdot}g_{PU}^{-1}$ after 7 days at 37 °C and pH 7. Protease K and chymotrypsin also hydrolyzed the PUs. The degradation products of poly(LDI/BD) and model compounds by papain were studied by NMR and SEC analysis. The hydrolysis of pendant methyl ester in lysine moiety and the formation of low molecular weight of compounds by cleavage of urethane bonds in the backbone chain were confirmed.

Papain and α-chymotrypsin led to a decrease of M_w by more than 30% after 10 days on a new biodegradable PU synthesized from triethylene glycol (TEG) and 1,6-hexamethylene diisocyanate (HMDI).[576]

A protease from *Pseudomonas* sp. (PDB 1GA6), able to degrade PU.[577] was investigated by MD simulations[560] in free form and in complex with a PU monomer (formed by poly(butylene adipate) (PBA) and 4,4′-methylene diphenyl diisocyanate (MDI)). Eight hydrogen bonds were formed between the protease and the PU monomer units throughout the simulation time, of which 1 to 3 were stable. The residues K6, W81, L83, D170, R179, W220, E222, K229, W231, Q268, L273, Y275, L280, Q281, G284, and G285 were found to be involved in van der Waals interactions, while E171 and S287 formed hydrogen bonds with PU-MDI. Along the simulation, the PU monomer, although continuously interacting with the protease, suffered a rearrangement in the interaction pocket.

3.2.2.3. Amidases. Several enzymes were tested in Tris HCl buffer 100 mM pH 7 at 50 °C for 7 days on a model of polyester-PU soluble in water, namely, 1-methoxypropan-2-yl (4-nitrophenyl)carbamate carrying a *para*-nitroaniline group adjacent to the urethane bond via a linker of 1,4-β-cellobiohydrolase I of *Trichoderma reesei*.[578] Hydrolysis of the urethane bond released *p*-nitroaniline quantified at 405 nm. Only penicillin G amidase and mainly polyamidase showed activity on the model substrate. Native polyamidases (2.5 μM) were also active on 200 g·L^{-1} of commercial PU pellets (PU1080 and PU1050 from Bayer) previously washed. The monomer, 4,4′-diaminodiphenylmethane (MDA), and the oligomers, 4-hydroxybutyl (3-(3-aminobenzyl)phenyl)-carbamate, bis(4-hydroxybutyl)(methylene bis(3,1-phenylene))dicarbamate, bis(4-hydroxybutyl) (methylenebis-(3,1-phenylene)) dicarbamate, and 4-(((3-(3-(((4-hydroxybutoxy)carbonyl)amino)benzyl)phenyl)carbamoyl)-oxy)butyl (4-hydroxybutyl) adipate, were released. This was a clear indication that the enzyme was able to cleave both ester and urethane bonds. The polymer with a higher content of the rigid segment, MDA, was hydrolyzed to a lower extent. A fused polyamidase with a binding module from the PHB depolymerase of *Alcaligenes faecalis*, was up to 4 times more active on the polymer when compared to the native enzyme, confirming the relevance of enzyme adsorption for efficient hydrolysis. The 3D model of the fused polyamidase suggested that the active site residues and the binding site tunnel are not directly affected by the fusion as they are in opposite directions. The entrance of the active site could however be influenced by a nonconserved loop/helix region consisting of 26 amino acids, from P388 to W413.

3.2.2.4. Ureases. Ureases (EC 3.5.1.5) hydrolyze the urea bonds on poly(ether urea) PU, releasing two amines and carbon dioxide.[573]

Urease activity was induced in the culture supernatant of *Staphylococcus epidermidis* in the presence of polyether-PU composed of 4-4′-diisocyanato diphenylmethane and poly(tetramethylene glycol) from Goodrich.[579] The strain could modify the surface properties of two films of Tuftane (400 μm thickness) and Biomer from Ethicon (200 μm thickness, composed of same building blocks), as attested by the reduction of water angle, increase of C/N ratio at the surface. However, there was no evidence of correlation between urease activity and PU degradation.

3.2.2.5. Oxidases. A segmented polyester-PU elastomer made from poly(ethylene adipate) (PEA, M_n 2 kg·mol^{-1}), 4,4′-diphenylmethane diisocyanate (MDI), and a chain extender of ethylene glycol (EG) was synthesized[580] and further blended with small flax lignin concentrations (4.2 and 9.3 wt %). Thin cast films of PU and its lignin blends were incubated for 3 days at 30 °C with buffered solutions of peroxidase (EC 1.11.1.7) and laccase (E.C. 1.10.3.2) produced in *Aspergillus* sp. by Novozymes. According to ATR-FTIR analysis, peroxidase produced a high surface enrichment in methylene groups, carboxyl group formation, and secondary amine and unassociated carbonyl decrease. The oxidative attacks, although nonspecific, seemed to be oriented on the scission of ester groups in soft segments and in a lower extent on substitution of urethane hydrogen. In contrast, laccase generated increased PEA concentration and weaker associations formed by polyester segments. The urethane carbonyls and virtually all secondary amines proved more affected by laccase. Laccase was thus thought to degrade the urethane segments and might be involved in cross-linking and aromatic ring reactions. With lignin, PU was less enzymatically modified,

https://doi.org/10.1021/acs.chemrev.2c00644
Chem. Rev. XXXX, XXX, XXX−XXX

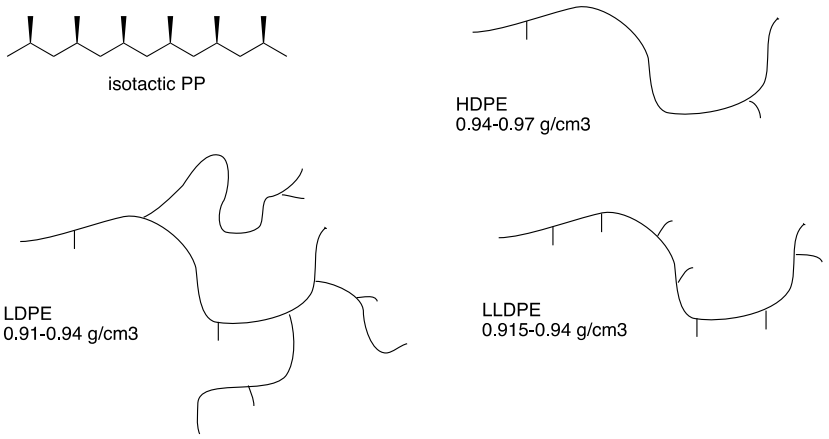

Figure 23. Representation of isotactic polypropylene (iPP) and of high density polyethylene (HDPE), low density polyethylene (LDPE), and linear low density polyethylene (LLDPE)

especially with 4.2% lignin. With 9.3% lignin, laccase had a different profile of PU degradation, as it was likely more prone to attack polyester than urethane segments. This could be explained by surface externalization of polyester segments when PU was blended with 9.3% lignin. Cross-linking reactions and physical interactions between partially degraded lignin and scissored polyester chains might also mask the ATR−FTIR spectral evidence of true degradation extent in the blend. Enzymatic degradation was also confirmed by SEM, which showed surface erosion, by tensile testing, reflecting a lowering of mechanical properties, and by TGA as well. Laccase appeared to generate more efficient degradation than peroxidase. Furthermore, horseradish peroxidase (HRP) from Sigma did not enable to detect any PU degradation at 37 °C among TDI/PTMO/ED, TDI/PCL/ED, MDI/PTMO/ED, and MDI/PTMO/BD.[570]

A laccase mediated system was tested on four representative PU models. The system was composed by LMS (laccase from *Trametes versicolor* from Sigma) and hydroxybenzotriazole (HBT) at pH 4.5, incubated at 37 °C for 18 days with a fresh enzyme addition every 2 or 3 days. Different structures and compositions were thus evaluated, including a thermoplastic coating and a foam by adding glycerol to the formulation (cross-linked structure), a polyester- and a polyether-based PU.[581] All of these PU precursors were synthesized from toluene diisocyanate (TDI), two of them being based on a polyester polyol (PCL, M_n of 2 kg·mol^{-1}) and two others on poly(tetrahydrofuran) (PTHF, M_n of 2 kg·mol^{-1}). The two thermoplastics PU (TPU) exhibited similar molar masses (M_w in the range of 70−80 kg·mol^{-1} and M_n of about 20 kg·mol^{-1}), comparable to those conventionally found on commercial TPU. The PCL-based PU foam was rigid, while the PTHF-based PU foam was much more flexible. Long building blocks based on flexible polyethers bring a high mobility to the corresponding macromolecular architectures. Weight losses were quite higher with LMS compared to the negative control (17 and 7%, respectively, for the PCL-based PU; for other PU, the difference was less important). Oligomers of around 0.3 kg·mol^{-1} appeared in both TPU coatings degraded with LMS. Both foams initially showed closed cells, desired for insulation foams, but probably limiting for the enzyme diffusion to the core of the foam. Through SEM observation of foams, formation of holes with LMS was evidenced for the PCL-based PU and more extensively for PTHF-based PU. The mean maximal stress was also reduced in both PU, more extensively with the softer PTHF-based foam (reduced to 87% of the initial value with LMS against 77% with the negative control). Slight changes in IR spectra are also shown after treatment with LMS. In conclusion, it should be noticed that degradation is very low despite the use of large amount of enzyme.

3.2.3. Outlook. PU represent a large family of different chemical structures based on various functional monomers and each type, used for a specific application, is produced at moderate or even low scale (foams, fibers, adhesives for instance). Thus, it is difficult to recover a waste stream with a unique PU as main component. To date, very few efficient enzymes have been reported for PU degradation. Of note, during the revision of this review, the first true urethanases isolated from a soil metagenome library were reported.[582] Three enzymes, UMG-SP-1, UMG-SP-2, and UMG-SP-3, with GenBank accession numbers of OP972509, OP972510, and OP972511, respectively, were found to hydrolyze low molecular weight dicarbamates resulting from chemical glycolysis of polyether-polyurethane foam. These enzymes showed from 60% to 83% of sequence identity with their closest homologues, amidases. This scientific release offers novel perspectives for the enzymatic depolymerization of PU. However, degradation of each PU might necessitate a specific hydrolyzing enzyme that could be either isolated in nature or engineered by mutagenesis. All of this leads to the conclusion that it is improbable that a universal enzymatic recycling process can be developed. An exception could be envisioned in the case of the development of a recycling process dedicated to a unique PU and in close relation with its producer, controlling all of the value chain. Ecoconception of PU seems to be preferable, using biodegradable monomers and including enzymes able to cleave urethane bonds. Such an enzyme must be optimized to be resistant to PU synthesis conditions as PU are often thermosets obtained in situ by reaction between a diol or polyol and a diisocyanate and to increase its activity at ambient conditions that will certainly require long-term efforts.

3.3. Vinylic Polymers

3.3.1. Polyolefins (PO). *3.3.1.1. About PO.* Polyolefins (PO) represent the major class of commodity plastics, combining low production costs and outstanding mechanical properties. The annual production of PO is around 170 Mt per year, and their annual growth of around 3−4% is remarkable.

https://doi.org/10.1021/acs.chemrev.2c00644
Chem. Rev. XXXX, XXX, XXX−XXX

This family alone represents more than 60% of the production of plastic material.[583] The success of PO lies on an innovative research activity both in chemistry and processes of polymerization. These researches have led to polymers with innovative properties and thus to new applications, where PO have replaced other materials.

PO are found everywhere in our daily life, covering a wide range of applications: (i) packaging by allowing safe and light packaging, which increases food conservation and reduces energy consumption for transport, (ii) automotive by replacing the metal, once again allowing a lightening and therefore a reduction of emissions, (iii) infrastructure for the safe transport of water, gas and electricity, and (iv) medicine by being used in prostheses or as a suture. There are four main classes of semicrystalline PO, namely, isotactic polypropylene (iPP), low density polyethylene (LDPE), linear low density polyethylene (LLDPE), and high density polyethylene (HDPE), differentiated by the presence of short and long branches which will impact their crystallinity and their usage properties (Figure 23).

PO are produced by radical polymerization or by polymerization catalysis. The radical polymerization of ethylene is an old process developed in the 1930s by the Imperial Chemical Industry in the UK. The polymerization conditions are extreme, involving both very high pressure (P > 1000 bar) and high temperature (T > 150 °C). Under these conditions, both intra- or intermolecular transfer reactions to the polymer are very frequent, giving rise to highly branched PE-based structures, i.e., LDPE, which is therefore less crystalline and less dense than HDPE. The latter materials are synthesized by polymerization catalysis, which was developed in the 1950s around Phillips and Ziegler−Natta catalysis, requiring much milder polymerization conditions. These so-called conventional catalysts are, in general, heterogeneous, and multisites Ziegler−Natta catalysis dominates the synthesis of PO. It is used to produce HDPE, LLDPE, as well as iPP. Modern catalysts are today based on titanium chloride activated by organometallic aluminum compounds, but several generations of Ziegler−Natta catalysts have been set up, to improve catalyst productivity (trace catalyst residues are no longer separated from the polymer), selectivity in particular isospecificity of propylene polymerization by active site selection processes, but also to improve the morphology of the catalytic solid, an essential parameter to guarantee the growth of polymer particles.

LDPE is mostly amorphous, with short branches (10−30 $-CH_3$ per 1000 carbon atoms). This branching system makes LDPE chains more accessible and the tertiary carbon atoms at the branch sites more susceptible to attack than HDPE. The HDPE can hold 1 to 2 short connections ($-CH_3$) per 1000 carbon atoms of the main chain. It typically has a crystallinity of 60−80% and a T_m of about 135 °C.[584] Further, the molar mass of HPDE is much higher. The iPP contains 333 $-CH_3$ per 1000 C, which can be organized in a crystal lattice (about 60% crystallinity), with a T_m of about 165 °C.[584] The iPP is less resistant to oxidation than PE due to its tertiary C sensitive to the attack of free radicals.

During processing and during their lifetime, PO are subjected to the action of temperature and light even if antioxidants are used to slow the abiotic breakdown of PO. That is why there is some difficulty to recycle PO waste coming from long-term applications. However, mechanical recycling is quite well developed, and efforts are made to improve quality of recycled PO. Currently, there is no food grade recycled PO. The Nextloop project led by Nextek envisions to produce food grade r-PP thanks to drastic sorting and waste cleaning prior to recycling. Reborn has developed a technology B.Clear to deink PE film. Chemical recycling has also been developed by solvolysis (PureCycle for PP). Pyrolysis is also extending (Thermal Anaerobic Conversion technology of Plastics Energy; RewindTM Mix of Repsol and Axens), including the treatment of complex waste such as the ones encountered in automotive parts (partnership between Audi and Karlsruhe Institute of Technology KIT).

When PO end up in landfill or worse, scattered in the oceans, they are hardly biodegradable. LDPE is the most abundant plastic waste discarded in landfills in the form of plastic bags (69%).[585] Microplastics are commonly found in the marine environment.[586] They are mainly PE, PP, and PS. Primary microplastics are microplastics that are manufactured for industrial or domestic applications to be of a microscopic size. They include plastic particles used in facial cleansers, shower/bath gels, deodorant, toothpaste, resin pellets, cosmetics (scrubs, peelings, eye shadow, blush powders, make up foundation, mascara, hair coloring, nail polish), shaving cream, baby products, insect repellents and sunscreen, synthetic clothing, abrasives found in cleaning products, drilling fluids, and air-blasting media, and vectors for drugs. Secondary microplastics are coming from large plastic debris fragmenting over time. Due to awareness of plastic pollution, numerous studies have been conducted on PO biodegradation, all around the world with the aim at identifying potential microorganisms in different environments (soil, compost, marine water, sewage water). Although some PO-eating enzymes have been recently reported, compelling evidence of efficient degradation can be questioned. For instance, some studies have been performed in the presence of other sources of carbon in addition to the plastic, or studies are lacking of evidence for monomer formation. Generally, prior functionalization under abiotic conditions involving a radical mechanism, for example, using UV irradiation and/or oxidation agents, is applied to insert carbonyl and/or hydroxyl groups or double bonds, to then expose the thus-treated polymer to enzymatic or microbial degradation. Furthermore, it is important to note that colonization of PO-based plastics by enzymes or microbes does not necessarily mean that enzymatic degradation has really taken place.[22,43] Indeed, some biodegradable additives used for formulation of these plastics are likely preferentially assimilated by the enzymes, rather than the polymer matrix itself. Thus, enzymatic degradation of petroleum-based polymers remains a challenge to be tackled. Besides these attempts to degrade PO by a biocatalytic approach, efforts have been made to produce biobased ethylene and propylene and to reduce environmental footprint of PE and PP. However, this does not improve the biodegradability of PE and PP. Numerous studies have also been carried out on PO formulation with biodegradable polymers such as starch. Despite biodegradation of overall material is generally high, no evidence of PO biodegradation has been brought.

3.3.1.2. Many Microorganisms Involved in PE and PP Biodegradation Represent Sources for Enzyme Identification. 3.3.1.2.1. Polyethylene (PE). Most publications deal with PE films or powders. A significant biodegradation of LDPE film with two *Aspergillus* strains in only 10 days was reported. Indeed, the formation of holes and cracking was observed by SEM and around 80% of biodegradation according to CO_2

https://doi.org/10.1021/acs.chemrev.2c00644
Chem. Rev. XXXX, XXX, XXX−XXX

assay.[587] However, this yield seems to be overestimated, as only a surface modification has been observed by SEM. Similar results were reported when a 46% weight loss of PE film was observed after 6 months pf treatment with a *Streptomyces* strain,[588] and when a 22% weight loss of LDPE and HDPE was quantified after 2 weeks of incubation with a consortium of *Bacillus cereus*, *Bacillus pumilus*, and *Arthrobacter* sp..[589] Some reviews have been published on this subject.[583,590]

More recently, LDPE pellets incubated with *Streptomyces* sp. presented a 47% weight loss after 6 months.[591] A fungi *Zalerion maritimum* was responsible for a 57% weight loss of PE pellets after 14 days.[592] *Aspergillus oryzae* allowed a 36% weight loss of a LDPE film after 3 months.[593] A consortium of *Aspergillus niger*, *A. flavus*, and *A. oryzae* was responsible for the 26% weight loss of an LDPE bag after 55 days.[594] This weight loss was found to be higher than those obtained by using a single species of fungus. The loss of weight obtained when the LDPE is the sole carbon source (15%) is less than that obtained when other carbon sources are provided.

Singh et al. reported a 43% weight loss of 40 μm PE film with *Bacillus* sp. in 40 days.[595] In another study, after 30 days at 55 °C with *Bacillus* sp. BCBT21, the weight losses of three plastics bags, namely HL (with nanoadditives), VHL (oxo-biodegradable with more than 70% LLDPE and less than 30% HDPE), and VN1 (plastic bags with additives claimed to be environmentally friendly) were respectively of 61%, 11%, and 4%.[596] The average molecular weight M_v determined based on the data from viscosity measurement of the polymer solution of bags was significantly reduced (43%) from 205 kg·mol^{-1} to 116.8 kg·mol^{-1}. Properties and morphology of treated plastic bags had also significantly changed.

HDPE film was colonized by *Achromobacter xylosoxidans*, which induced a 9% weight loss.[597] Surprisingly, two fungi were reported to better degrade HDPE than LDPE, but authors did not give any information on the films (thickness, molecular weight). Indeed, *Penicilium oxalicum* degraded HDPE and LDPE after incubation for 90 days with a weight loss of 55% and 37%, respectively, while *Penicillium chrysogenum* degraded 59% and 34%, respectively.[598]

Structural variations in PEs formed during polymerization and subsequent processing, such as unsaturated carbon−carbon double bonds, carbonyl groups, and hydroperoxide groups[584] have been shown to be consumed first by the bacteria resulting in rapid growth.[585]

Some old patents described microorganisms able to degrade PE to some extent. Indeed, the use of a consortium of *Microbacterium* sp., *Pseudomonas putida*, *P. aeruginosa*, and *Bacterium* sp.,[599] the use of *Saccharomyces cerevisiae*, *S. carlsbergensis*, *Hansenula subpelliculosa*, etc., cultivated in the presence of an alternating electric field to treat wastewater and decrease its PE and PP content of 15% to 19% after 48 h at 28 °C.[600] The patent US3909468 protects a biodegradable PO thanks to addition of a yeast.[601] More recently, a group from Northeast Forestry University (China) filed two patents, involving microbial degradation of PE by *Pichia guilliermondii* and *Serratia marcescens*, reaching after 60 days, a weight loss of 4% and 14%, respectively.[602,603] In another patent, they proposed the degradation of PE and simultaneous production of alkanes using *Pichia guilliermondii*, as a possibility to associate the mitigation of an environmental problem of pollution and energy generation.[602] Finally, a patent protects *Penicillium citrinum* for PE film degradation.[604]

Sullivan et al. have recently developed a process for converting mixed plastic waste into distinct chemicals.[605,606] Their method combines chemical recycling and engineered bacteria to upcycle mixtures of HDPE, PS, and PET into valuable chemicals. This is particularly attractive from the perspective of an industrial development, as this recycling approach could avoid the expensive sorting of mixed plastics. The polymer blends were first chemically oxidized under air conditions, in the presence of a cobalt−manganese−bromide catalytic system, which produces a mixture of carboxylic acids, namely, benzoic acid and dicarboxylic acids issued from HDPE and PS breakdown, respectively. Second, the resulting oxygenated compounds were fed to genetically modified soil bacteria, i.e., using *Pseudomonas putida* for further conversion. Genetic engineering was thus implemented to design two distinct bacteria strains to convert the carboxylic acid mixture. Namely, one bacterium strain selectively led to poly(hydroxyalkanoates) (PHAs), a useful biodegradable polymeric material for food packaging and for biomedical devices. The other strain allowed biocatalytic conversion of carboxylic acids into β-ketoadipate, which can serve as a synthon for performance-enhanced nylons. This combined recycling process by tandem chemical oxidation and biocatalytic conversion also appeared to be suitable for multilayer packaging and some textiles. Obviously, the economics of this two-step plastic recycling process still need to be analyzed.

3.3.1.2.2. Polypropylene (PP). Although PP is more sensitive to oxidation than PE, it is also more crystalline with a higher T_m and a few publications have focused on it. A slight weight loss of 6% was reported with *Rhodococcus* sp. and 4% by *Bacillus* sp. after 40 days of incubation on PP microplastics.[586]

Two publications reported a more significant biodegradation of PP. First, from a selective enrichment culture prepared with different soil samples on 85% LDPE-15% starch, Cacciari et al. isolated four microaerophilic microbial communities able to grow on this kind of plastic with no additional carbon source.[607] One consortium composed of *Pseudomonas* sp., *Vibrio* sp., and *Aspergillus niger* was able to degrade pure iPP strips in a mineral medium containing 0.05% glucose and 0.05% sodium lactate. After incubation and biofilm removal, iPP was extracted with dichloromethane, a suitable solvent for the extraction of apolar and slightly polar organic molecules. The weight of extracts increased with incubation time up to 40% after 5 months. The extracted materials were characterized by performing chromatographic and spectral analyses and revealed a mixture of hydrocarbons with some ketones and alcohols and a mixture of aromatic esters, probably due to the plasticizers usually added to polyolefinic structures. Second, a bacterial consortium of *Enterobacter* and *Pseudomonas* obtained from cow dung showed a 63% weight loss of PP after 160 days.[608] FTIR analysis revealed functional groups' formation and SEM analysis showed cracks at the polymer surface.

3.3.1.2.3. Genome Sequencing and Transcriptomic Studies for Enzyme Identification. Genome sequencing of some microorganisms (*Stenotrophomonas maltophilia* PE591 active on PE,[609] *Paenibacillus aquistagni* DK1 active on PE with AlkB-like protein[610]) could lead to the identification of enzymes that could then be expressed recombinantly, characterized, and further optimized. Alternatively, a few studies have performed transcriptomic studies to identify the upregulated genes, although there is no strong piece of evidence of enzymatic degradation. *Rhodococcus ruber* C208 (DSM 45332) was cultivated for 3 days with 0.6% of various

https://doi.org/10.1021/acs.chemrev.2c00644
Chem. Rev. XXXX, XXX, XXX−XXX

forms of PE described in Table 12 in culture medium.[611] The PE4K-OX, a commercial PE from Sigma-Aldrich, with low molecular weight and thermo-oxidized during 14 days at 120 °C, recapitulated quite nicely the size distribution of the PE fragments, which are obtained under natural photo-oxidation of a commercial PE film containing pro-oxidants. Carbonyl index was calculated with the ratio between the peak intensity for the ketone carbonyl at 1715 cm^{-1} and the peak intensity of the C−H stretching at 1465 cm^{-1}. An increase of the expression of 158 genes was observed after incubation with PE. Large PE fragments are not likely to be efficiently internalized by *R. ruber* and extracellular oxidases could be excreted to reduce the average molecular mass of external PE. Three highly homologous sequences were identified, related to laccases/multicopper oxidases (namely RRUB_S0078_04240, RRUB_S0078_03834, and RRUB_S0078_04261), but none of them appeared to be upregulated in the presence of PE. Short length PE fragments probably require dedicated transport systems. Within the 19 putative transporters identified in this study to be upregulated, in at least one condition of PE supplementation, nine of them belong to the major facilitator superfamily (MFS) and five belong to the ATP binding cassette (ABC) family. Finally, additional cytoplasmic oxidation steps could be involved to provide small PE fragments compatible with their entry in the alkane degradation process. Additionally, 34 different transcripts encoding putative cytoplasmic oxidases were identified. Interestingly, one of the most upregulated pathways is related to alkane degradation and β-oxidation of fatty acids. Upregulation of genes involved in fatty acid elongation was observed as well as those of a key enzyme of the glycolipid metabolism, namely a diacylglycerol kinase (EC 2.7.1.107; RRUB_S0078_05576), which catalyzes the conversion of diacylglycerol (DAG) into phosphatidic acid (PA), a central intermediate of the phospholipid (PL) biosynthesis pathway. These observations suggested that PE fragments might also be, at least in part, incorporated within PLs.

Table 12. Characterization of Different PE Samples Using Data from ref 611

	PE description	M_n (g mol^{-1})	M_w (g mol^{-1})	carbonyl index
PE4K	Sigma with $M_n \sim 1700$ g/mol according to provider	4900	7200	0.27
PE4K-OX	PE4K thermo-oxidized during 14 days at 120 °C	1200	2700	2.50
PEfi	80% LLDPE/20% LDPE 23 μm thickness	26 700	94 100	0.10
PEfi-OX	80% LLDPE/20% LDPE 23 μm thickness containing prooxidant (organometallic cobalt salt) and fragmented after storage at room temperature for 10 years	1600	3800	1.15

Rhodococcus opacus R7 grown on PE powder, prepared at 1.2% as only carbon and energy source was also analyzed by transcriptomics.[612] It confirmed the activation of genes encoding laccase-like enzymes. LMCO1 that was described as a laccase-like multicopper oxidase (LMCO) was upregulated by 19.5-fold. LMCO1 gene is located on the chromosome downstream a genome region comprising genes encoding a benzoate dioxygenase system and two-component monooxygenase, named PheA1 [(4-hydroxyphenylacetate 3-monooxygenase (EC 1.14.13.3), and nitrilotriacetate monooxygenase component B (EC 1.14.13.−)]. Two other LMCO were considered, although the RNA-seq analysis did not show any evidence of their induction. The amino acidic identity with laccase-like enzyme sequence identified in *R. ruber* C208 was 48% with respect to LMCO1, 53% with respect to LMCO2, and 23% with respect to LMCO3. LMCO1, and LMCO2 also shared more than 25% of sequence identity with respect to crystallographic structure of Lac15 from a marine microbial metagenome (PDB 4F7K). LMCO3 does not have a specific known laccase domain but shows 57% of sequence identity with respect to the crystallographic structure of a reference multicopper oxidase (PDB 3GDC). This study also allowed the identification of several candidate genes that might be important for the further steps to reduce alkane fragment length, leading to the β-oxidation pathway. Notably, the alkB gene encoding an alkane monooxygenase, the cyp450 gene encoding cytochrome P450 hydroxylase, and seven other genes encoding membrane transporters, alcohol dehydrogenase (alcdedh), aldehyde dehydrogenase (aldedh), acetaldehyde dehydrogenase (mhpF), and long-chain-fatty-acid-CoA ligase (fadD).

In a publication of 2021,[613] a fungus from *Alternaria* sp. was reported to display a prominent capability of colonizing PE of commercial PE bags or additive-free plastic films from Goodfellow (e.g., type ET311350 PE plastic of 250 μm of thickness and type ET311126 PE plastic of 25 μm of thickness). After removing the microbial layer, numerous holes were observed in the PE surface. The diameter of some holes could reach 0.5 μm, and some holes almost penetrated across the film. The M_w of PE film decreased by 95% after 4 months (12 kg·mol^{-1} instead of 230 kg·mol^{-1}, a 20-fold decrease), the M_n was also decreased 9-fold (3.2 kg·mol^{-1} instead of 29 kg·mol^{-1}). Its crystallinity decreases from 63% to 52%. It must be noticed that films were treated with H_2O_2 to remove biofilm, and no control is presented to certify that the observed degradation is not the consequence of the H_2O_2 treatment. Using GC-MS, the degradation products were found to have between 3 and 27 carbons, the four-carbon product, diglycolamine, accounted for 93% of all degradation products. It is still not clear how diglycolamine does derive from the PE and whether it will be degraded further or directly utilized by the fungus. Degradation products were also characterized after 60 days with a different profile: from 12 to 30 carbons. The product, 1-monolinoleoylglycerol trimethylsilyl ether, possessing 27 carbons, was predominant, accounting for 51% of all products. The rest predominant products were hexanedioic acid bis(2-ethylhexyl) ester (16%), squalene (14%), tributyl phosphate (7%), cycloheptasiloxane tetradecamethyl (3%), cyclohexanamine *N*-cyclohexyl (2%), and 13-docosenoic acid methyl ester (8%).

Transcriptome of this fungus cultured with or without PE for 45 days was analyzed, and 153 potential enzymes closely associated with biodegradation were significantly upregulated in the presence of PE. These enzymes include 3 peroxidases, 3 laccases, 26 hydroxylases (4 hydroxylases, 15 monooxygenases, 7 oxygenases), 49 dehydrogenases, 18 oxidoreductases, 10 oxidases, 22 reductases, 16 esterases, 4 lipases, and 2 cutinases. The transcription levels of laccase encoding gene (Gene id: evm.TU.contig_8.535), peroxidase encoding gene (Gene id: evm.TU.contig_5.872), and oxidoreductase encoding gene (Gene id:evm.TU.contig_5.292) were respectively increased by 23-, 44-, and 102 fold. Two putative PE degrading enzymes were purified from an *E. coli* overexpression, a glutathione

https://doi.org/10.1021/acs.chemrev.2c00644
Chem. Rev. XXXX, XXX, XXX−XXX

peroxidase (evm.model.contig_3.359) and a laccase (evm.model.contig_8.535). After 48 h with 0.1 $g_{enzyme}·L^{-1}$, cracks and signs of plastic film degradation were observed by SEM. Both glutathione peroxidase and laccase showed a clear synergetic degradation effect on the PE film. The M_n and M_w of the PE film treated by both glutathione peroxidase and laccase were respectively 20.9 kg·mol^{-1} and 109 kg·mol^{-1}, which showed about 18% and 7% decrease compared to those of control (M_n of 25.5 kg·mol^{-1} and M_w of 116 kg·mol^{-1}). The authors did not specify the amount of PE film treated in their study.

3.3.1.2.4. Biodegradation by Insects and Their Gut Microorganisms. Multiple recent reports showed biodegradation of PE by employing macroorganisms such as mealworms (larvae of *Tenebrio molitor*),[614] dark mealworm (*T. obscurus*),[615] waxworm (*Achroia grisella*)[616] on HDPE, or superworms (larvae of *Zophobas atratus*).[617] Naturally, these worms were eating beeswax composed of a highly diverse mixture of compounds, including alkanes, alkenes, fatty acids, and esters. This feeding could explain why these worms were also able to biodegrade PE similar to long chain alkanes. The PE biodegradation by worms has been recently reviewed.[618] Beworm is a German startup which works with bacteria isolated from waxworm and aims at identifying enzymes involved in PE biodegradation to use them in a reactor after abiotic pretreatment.

A 70% weight loss was observed on PE foam after 58 days with a dose of 5.2 mg of plastic per mealworm, but 40% plastic residues were present in frass, meaning that only 30% were really biodegraded.[619] After exposure to ∼100 larvae of the greater wax moth (*Galleria mellonella*) for 12 h, a PE plastic bag lost 92 mg (e.g., 13% of weight loss).[620] A crude wax worm extract was made by homogenizing fresh worms at low temperature (0−4 °C). The resulting paste was smeared on the surface of PE film and left in contact for 2 h, then gently removed and replaced with a fresh layer of wax worm homogenate. This routine was repeated 7 times for a total of 14 h. The estimated weight loss demonstrated that not the sole effect of mastication was involved. A 140% increase in surface roughness was observed. It was not clear whether the hydrocarbon-digesting activity of *G. mellonella* derived from the organism itself or from enzymatic activities of its intestinal flora. However, Billen et al. were skeptical about the use of insects. Indeed, a diet of LDPE is insufficient for growth; the consumption of PE serves for life subsistence, rather than for growth.[621] Moreover, 4−10 tons of larvae are needed to digest 1 ton of plastic. No significant weight loss was obtained when homogenated paste is brought, only once, in contact with LDPE films or paraffin.

Zhong et al. show that mealworms were capable of ingesting LDPE and PS but not LLDPE or PP, although the hardness and density of LLDPE were lower than those of LDPE.[622] Authors explain these observations by an influence of crystallinity, but the highest one is those of PP and is only 9%. M_n and M_w of LDPE increased 27% and 9%, respectively, after ingestion by mealworms, while dispersity decreased from 4.20 to 3.66, implying that mealworms tended to attack the lower molecular weight polymer chains. Transcriptome analysis and KEGG mapping revealed that fatty acid degradation pathways may play important roles in the digestion of plastic. A total of 413 sequences showed significant changes after feeding on LDPE. After annotation, 60 databases of essential gene (DEGs) were matched as uncharacterized proteins, while 77 DEGs showed no matches in the database, which may result from insufficient reference transcriptome data. After 3 weeks, 185 DEGs were downregulated and 86 upregulated. Hydrolases had the greatest changes in all classes of enzymes. Upregulations were observed in hydrolases acting on ester bonds (i.e., 2w, phosphatidylinositide phosphatase SAC2; 3w, esterase FE4, phospholipase D2; 4w, type I inositol 1,4,5- trisphosphate 5-phosphatase), sugars (i.e., 2w, myrosinase 1, glycoprotein endo-α-1,2-mannosidase; 3w, lysosomal α-mannosidase-like protein, β-galactosidase-1-like protein 2; 4w, β-galactosidase-1-like protein 2), and C−N bonds (3w, neutral ceramidase), probably producing long-chain alcohols, long-chain C−C or C−N linked carboxylates, or long-chain fatty acids from LDPE. According to the KEGG mapping results, the DEGs of the mealworms fed on LDPE were significantly enriched in 39 specific pathways.

In some studies, gut microbial communities were characterized. For instance, Yang et al. found that the larvae of *Plodia interpunctella* were capable of degrading PE films.[623] Two bacterial strains capable of degrading PE were isolated from this worm's gut, *Enterobacter asburiae* YT1 and *Bacillus* sp. YP1. They form biofilms and the PE films' hydrophobicity decreased. Modification of the surface was observed by SEM and AFM, as well as the formation of carbonyl groups, 6−11% weight loss was observed and ∼6−13% reduction of M_w and M_n after 60 days. The release of 12 water-soluble products was also detected, covering a m/z range from 100 to 600. In another study, a strain of *Enterobacter* sp. was isolated from the gut of *Galleria mellonella* and was responsible for roughness on the surface of PE films, formation of carbonyl functional groups and ether groups when evaluated after 14 days.[624] LC-MS also revealed formation of water-soluble products such as alcohols, esters, and acids, especially ethyldodecanoate, 6-methyl-5-hepten-2-ol, monobenzyl phthalate, and *N*-acetylglutamic acid. Additionally, three bacterial species (*Lysinibacillus fusiformis, Bacillus aryabhattai*, and *Microbacterium oxidans*) were isolated from whole body extracts of *Galleria mellonella*.[625] They were able to utilize LDPE powder from Sigma, with a M_n of 1.7 kg·mol^{-1} and a M_w 4 kg·mol^{-1}, as sole carbon source according to growth curves, cell biomass production, LDPE weight loss, and the presence of LDPE hydrolysis products in the media. Consortia of these bacteria with three other bacteria previously shown to degrade LDPE (*Cupriavidus necator* H16, *Pseudomonas putida* LS46, and *Pseudomonas putida* IRN22) were also tested. The bacterial consortia were better able to degrade LDPE than the individual species. The maximum percent of LDPE weight loss (14% after 18 days) was obtained with the consortium of *C. necator* H16, *P. putida* LS46, and *P. putida* IRN22. GC analyses revealed the presence of linear alkanes and other unknown putative LDPE hydrolysis products.

A strain of *Acinetobacter* sp. and a strain of *Bacillus* sp. were also isolated from *T. molitor*.[626] The cells of both strains did not grow on PE, but their coculture grew on LDPE and was responsible for a 18% weight loss over 30 days. This suggests that biodegradation of LDPE requires multiple microbes. Two commercial LDPE foams without plasticizer additives were biodegraded by *T. obscurus*.[615] Low molecular weight PE (<5 kg·mol^{-1}) was rapidly digested, while longer chain portions (>10 kg·mol^{-1}) were broken down. Mass balance analysis indicated that nearly 40% of ingested LDPE was digested to CO_2. Finally, the antibiotic suppression of gut microbes in *T. molitor* and *T. obscurus* larvae with gentamicin obviously reduced their gut microbes on day 15, but the M_n and M_w

https://doi.org/10.1021/acs.chemrev.2c00644
Chem. Rev. XXXX, XXX, XXX−XXX

decreased. This confirmed that LDPE biodegradation in *Tenebrio* was independent of gut microbes. According to authors, the low extent of broad depolymerization under antibiotic suggested the presence of digestive enzyme(s) to break down LDPE, but this could also be due only to mastication. Biodegradation of ingested LDPE was confirmed through the formation of oxidized intermediates and chemical/physical modifications, which was confirmed using FTIR, ^{1}H NMR, and TGA analyses. Gut community was changed significantly after the larvae received a diet of LDPE compared with those fed on bran and unfed. The predominant gut microbes associated with LDPE degradation included bacterial families of *Enterobacteriaceae*, *Enterococcaceae*, and *Streptococcaceae*. At the genus level, *Spiroplasma* sp. and *Enterococcus* sp. were strongly associated with LDPE biodegradation.[615] On the opposite, PE, PP, and PS biodegradation by *Zophobas atratus* was reported to be microbial-dependent. Significant relative abundance changes were observed after PE diet of *Z. atratus* larvae such as increased abundances of *Enterococcus* and *Citrobacter*.[627] An increase in protease activity was also observed. It is difficult to prove which microbial genera or families are responsible for enhanced biodegradation because only a few plastic-biodegrading microorganisms have been isolated. *Enterococcus* genus is strongly associated to PE biodegradation by distinct species of insect larvae: *G. mellonella*,[628] *T. molitor*,[627] *T. obscurus*,[615] and *Z. atratus*.[627] A patent protects the use of microorganisms isolated from the gut of the larva of *Tenebrio molitor* (*Klebsiella oxytoca*, *Escherichia fergusonii*, and *Bacillus toyonensis*) for the degradation of different polymers (PE, PP, PET, PVC, and PS).[629]

Even if research on polyolefins biodegradation continues to discover new microorganisms, efforts remain to be devoted to the identification of the enzymes responsible for the biodegradation in these microorganisms as well as to the description of their associated mechanisms. Briefly, the process of biodegradation can be divided into four stages: (i) colonization/corrosion, (ii) oxidation leading to polymer chain scission, (iii) assimilation, and (iv) mineralization. Once PO has been fragmented under abiotic action and achieve a minimal size enabling them to enter cells, numerous microorganisms can mineralize them. The border limit of transfer of molecules through the bacterial cell wall is around 500 g·mol^{-1} (35 carbons) (depending on the bacterial species and molecule shape). In the case of *n*-alkanes, it is reported that paraffin (44 carbons, 618 g·mol^{-1}) can be assimilated directly by some bacteria.[630] In experiments with PE with a M_w of less than 5000 g·mol^{-1}, a large proportion of the fragments in the range of 100−2000 g·mol^{-1} are rapidly metabolized by the bacteria.[631] Very recently, Sanluis-Verdes et al. have reported that the saliva of *Galleria mellonella* larvae would be capable of oxidizing and eventually depolymerizing PE films. Namely, the animal enzymes include arylphorin, renamed Demetra (NCBI accession number XP_026756396.1), and an hexamerin renamed Ceres (NCBI accession number XP_026756459.1), both belonging to the phenol oxidase family.[632] Using very high concentration of purified enzymes (∼10−15 g per g_{PE}), the M_w value was only very slightly decreased (from 207 to 199 kg·mol^{-1} for film and from 4.0 to 3.9 kg·mol^{-1} for PE4000), eventually questioning the efficacy of the enzymatic degradation despite the authors' claims. These were in fact based on the appearance of carbonyl groups after treatment, but carbonyl index proved rather low (at most 0.1). Some degradation products were also identified by GC-MS: small oxidized aliphatic chains, like 2-ketones from 10 to 22 carbons, as well as butane, 2,3-butanediol, and sebacic acid. A small aromatic compound, benzenepropanoic acid, a known antioxidant of plastic, was found, suggesting an "opening" in the polymeric structures with the release of additives. According to the authors, this aromatic compound could be the target of the phenol oxidase and would generate free radicals leading to the initiation of the autoxidative chain reaction. This preliminary stud is surely innovative but fails to provide convincing proof of an efficient enzymatic degradation of PE.

This field is still in the early stages of development with first transcriptomics studies. Furthermore, no study on thermophiles which could act in conditions where plastics are softened has been reported so far. At the opposite, study of insects is quite popular, even if little evidence on real biodegradation has been brought. The chewing action by larvae can lead to polymer fragmentation, which can greatly contribute to the increase in plastic surface area for biodegradation. More research needs to be carried out on replicating the intestinal processes and conditions to fully understand the synergic actions between larvae digestion and microbial metabolism and to better characterize the enzymatic systems involved in plastic biodegradation.[618]

3.3.1.3. Enzymes for Oxidative Degradation. As the border limit of material penetration through cell wall is constant, secretion of PE-degrading enzymes is important to increase biodegradation rate. Different oxidases have been described. A recent publication proposes hypothetical PE degradation pathways as well as the mode of interaction of PE with enzymes.[180] A model substrate of PE was used (dodecane $C_{12}H_{26}$) and modeled into the active site of four distinct enzymes: a laccase, a manganese peroxidase, a lignin peroxidase and an unspecific peroxidase.

3.3.1.3.1. Laccases. Laccases (EC 1.10.3.2) or phenol oxidases correspond to oxidoreductases acting on diphenols and using oxygen as an oxidant.[633] They are present in plants, in many fungi, as well as in some bacteria. The active site of laccases consists of four copper atoms. As a result, laccases are called multicopper blue enzymes. The organization of copper atoms is as follows: an isolated copper, place of oxidation of the substrate, and a trinuclear cluster, place of reduction of oxygen. The copper atoms of the laccases allow the transfer of electrons from the reducing substrate to oxygen without the release of toxic peroxide intermediates, thanks to four mono-oxidations of the substrate catalyzed by the isolated copper. The electrons are then transferred to the trinuclear cluster, where oxygen reduction and the release of water molecules take place. In addition, oxidation of substrates creates radicals that can cause nonenzymatic reactions without substrate specificity.

Laccases are involved in the degradation of natural polymers such as lignin or humic acids. Due to steric clashes, laccases do not act directly in contact with polymers. The reaction mechanism involves the oxidation of small organic compounds or metals (manganese, polyoxometalates), which then act as mediators of the oxidation reaction. The natural mediators of laccases are 3-hydroxy-anthranilic acid (3-HAA), 4-hydroxybenzoic acid, 4-hydroxybenzylic alcohol, "phenol red", and phenolic compounds close to the structure of lignin (acetosyringone, syringaldehyde, vanillin, acetovanillone, methyl vanillate, sinapic acid, ferulic acid, *p*-coumaric acid, etc.). Mediators have different redox potentials and generate

https://doi.org/10.1021/acs.chemrev.2c00644
Chem. Rev. XXXX, XXX, XXX−XXX

more or less stable radicals. Artificial mediators (2,2′-azino-bis (3-ethylbenzothiazoline-6-sulfonic acid (ABTS), 1-hydroxybenzotriazole (HBT), *N*-hydroxyphthalimide (HPI), violuric acid (VLA), *N*-hydroxyacetanilide (NHA), TEMPO, nitrosated compounds, triphenylamine or phenothiazine derivatives, phenylpyrazolones) may also be used in biotechnological processes to increase the oxidation potential of laccases.[634]

Only two publications report the use of laccases to oxidize PE, and they are quite old, with lack of details on PE substrate used. First, the *Trametes versicolor* laccase caused a 88% decrease in M_w in 3 days at 30 °C on a PE membrane in the presence of the mediator 1-hydroxybenzotriazole (HBT).[523] Second, the laccase of *Rhodococcus ruber* C208 (DSM45332) causes a 20% drop in M_w in 15 days at 37 °C on a preirradiated UV film for 60 h.[635] The supernatant was simply dialyzed against phosphate buffer and then freeze-dried. It was resuspended in phosphate buffer before use. The optimal conditions of the enzyme are 70 °C and pH 7. The dispersity does not vary, which would indicate that the enzyme acts at the extremities of polymer chains rather than inside the chains. The same PE film degradation test was performed with *T. versicolor* laccase, and no change in the FTIR-ATR spectrum was observed. This could be due to the absence of mediators, which, on the contrary, are present in the raw extract of *R. ruber*. A better specific activity of the laccase is obtained by daily addition of 20 μM of copper for 6 days. Copper plays a role in induction of enzyme production as shown by measuring the amount of mRNA encoding the laccase. The addition of copper in strain cultures with PE as the only source of carbon allowed an increase in the mass loss of PE films (2.5% instead of 1.5% in 30 days).

Zymergen has filed a patent[636] to protect compositions and methods for degrading PE, containing microbes from the genus *Pseudomonas* (*P. nitroreducens* or *P. citronellolis*) and/or various enzymes (laccase from *Trametes versicolor*), which when brought into contact with PE lead to a reduction in the molecular weight of the material. Different protein sequences of laccases are provided. One example shows a 2% weight loss of UV-treated PE after 30 days with *Pseudomonas* sp., with a 25% reduction of M_w and 33% of M_n. Laccase from *T. versicolor* from Sigma was also tested with HBT, and a 44% reduction of M_w (50 kg·mol^{-1} instead of 89 kg·mol^{-1}) and 56% of M_n (6.6 kg·mol^{-1} instead of 15 kg·mol^{-1}) was observed after 30 days. Oxidation of PE is shown in another example with 1 mg of laccase applied 5 times over 14 days on 250 mg of PE powder and 0.5 mM HBT and 0.05% Triton X100 in 100 mM citrate buffer: apparition of carbonyle at 1715 cm^{-1}. Laccase treatment is reported to have the same oxidation effect than 34 days UV irradiation. Growth of *Pseudomonas* on laccase pretreated PE is also shown.

Krueger et al. listed bond dissociation energies (BDE) for lignin subunits of 160 and 300 kJ mol^{-1} in the case of C−O ether bonds and 240−425 kJ mol^{-1} for C−C bonds.[637] In contrast, for plastics such as PE, PP, PS, and PVC, the BDEs are 330−370 kJ mol^{-1} in the C−C bonds of their backbones and 350−470 kJ mol^{-1} for C−H bonds. This presents a challenge for oxidases, with the highest redox potential falling short of what is required for plastic degradation. Some approaches have used the creation of mutant libraries in various directed evolution strategies, including classical adaptive evolution, consensus design, and chimera genesis, coupled with screening assays to identify thermostable high redox potential laccases (HRPL) at 70−80 °C.[638,639] These optimized enzymes have not yet been investigated for PO biodegradation but represent promising candidates considering the high redox potential of the C−C bonds found in the backbone polymer chain. In complement, the selectivity and stability of high redox mediators should be studied.

3.3.1.3.2. Peroxidases. Peroxidases are universal enzymes of the living world that catalyze redox reactions involving the reduction of a peroxide and the oxidation of a substrate, varying from one class of peroxidase to another. Nonanimal peroxidases are subdivided into three classes: class I containing catalase-peroxidases (CP), ascorbates peroxidases (APx), and cytochrome c peroxidases (CcP), classes II or lignin peroxidases only detected in fungi, which are capable of degrading lignin, and classes III present only in plants.

LiP and MnP appear to be of interest for the biodegradation of polyolefins. Pometto et al. concentrated culture supernatants of *Streptomyces viridosporus* T7A, *S. badius* 252, and *S. setonii* 75Vi2 with LiP activities.[640] They pretreated films of PE-6% starch-prooxidant 10 days at 70 °C and then treated them with enzyme for 3 weeks at 37 °C. The M_w decreases even with inactivated enzymes but more significantly with the active enzymes. High MM PE is also degraded by lignin-degrading fungi under nitrogen and carbon deficiency conditions and by partially purified manganese peroxidase (MnP) of a strain of *Phanerochaete chrysosporium*.[641] Such a manganese peroxidase (MnP) preparation degraded PE, as measured by decreases in elongation and tensile strength.[642]

The patent of Nishida et al.[526] protects the use of a MnP (from basidiomycete of white rot such as *Phanerochaete chrysosporium*) for the biodegradation of polyolefins and polyamides, in the presence of manganese and an additive selected from the group consisting of phosphoric, succinic, and acetic acids and salts of said acids. In the example, the reaction is carried out with 1.5 units of enzyme at pH 4−4.5 at 40 °C for 48 h with 0.1% w/w of Tween 80 on a PE membrane of M_w 125 kg·mol^{-1} and M_n 29 kg·mol^{-1} (2 g/L). The best enzyme reduces M_w to 46 kg·mol^{-1} and M_n to 13 kg·mol^{-1}. Hydrogen peroxide does not improve results, and β-hydroxy acids are inhibitors. Another patent from Mellizyme Biotechnology (WO2021205160A1)[643] concerns polyalkene polymers degradation such as PE by an "unspecific peroxygenases" (UPO), named KatG/EC 1.11.1.21 polyalkenase. This enzyme can be used together with a peroxide generating enzyme (such as formate oxidase, formate dehydrogenase, formaldehyde dismutase, methanol oxidase) and a plasticase enzyme (such as laccase, MnP and LiP) and a cofactor. KatG is used to produce biofuel or carboxylic acids or to obtain biodegradable plastic. The patent's examples describe the use of *Ralstonia picketti* ATCC 27511, achieving a significant weight loss of PE and PP powders (>20% in one month) or films. Supernatant allows fragmentation of films. The variant KatG$^{Y221F/R410N}$ used at 100 mg·L^{-1} enables release of degradation products with 5 g·L^{-1} polymer (ultra high molecular weight PE, PP, PS, PVC, PTFE).

Zhao et al. modified the film surface of HDPE (70 μm thickness) by enzymatic catalysis, with soybean peroxidase (SBP) and hydrogen peroxide as an oxidizing agent in a phosphate buffer in the presence of benzenediol.[644] The O/C ratio increases, and new functions such as −CO− appear. The surface becomes rougher. Hydrophilicity is improved. Unfortunately, no control to determine the effect of hydrogen peroxide alone is presented. Horseradish peroxidase (HRP) is another commercial plant enzyme. It is widely studied in

https://doi.org/10.1021/acs.chemrev.2c00644
Chem. Rev. XXXX, XXX, XXX−XXX

biotechnological applications and could therefore be tested for the biodegradation of polyolefins.

3.3.1.3.3. Latex Clearing Protein (Lcp). A recent publication describes the use of Lcp from *Streptomyces* sp. K30 to degrade UV-pretreated polyolefins.[645] This enzyme has been first identified for its activity on natural rubber and degradation products were characterized as oligomers, ending with either ketones or aldehydes. Here, the characteristics of the introduced films of PE, PP, and PS are not given, and they were additionnaly preoxidized by a UV treatment at 70 °C for 2−5 days. The reported dispersities are very high, leading to the estimation of very low M_n. Lcp was added repeatedly to a preoxidized PE film at 37 °C for 5 days, with an enormous final concentration of 1.38 $g_{Lcp} \cdot g_{PE}^{-1}$. The best result, using a 5 days UV pretreated film, observed a decrease of M_w by 42%. The same experiment has been performed on PP with less significant results, and no modification has been observed on PS.

3.3.2. Other Vinylic Polymers. *3.3.2.1. Polystyrene (PS).* Despite PS being the fifth most used polymer in the world after PET, PP, PE, and PVC, and being one of the few amorphous thermoplastics, limited work has been done so far on its biodegradation[646,647] and PS is considered as nonbiodegradable. Landfills are 30% filled with PS.[648] PS is also found in aqueous media in the form of microplastics accumulation and toxicity shown on fish.[649]

It was recently reported that the genome mining of PS degrading microorganisms for the presence of enzymes involved in alkane depolymerization or aromatic cleavage.[650] Cytochrome P450s, alkane hydroxylases, and monooxygenases ranked as the top potential enzyme classes that might degrade PS because they could break C−C bonds. Ring-hydroxylating dioxygenases could break the side chains of PS and oxidize the aromatics generated from the decomposition of PS. However, this genomic study was unable to predict if these enzymes were able to degrade insoluble substrate such as PS outside the cell.

Only one study reports experience with a purified enzyme, the hydroquinone peroxidase from *Azotobacter beijerinckii* HM121, a lignin decolorizing bacterium. The enzyme degraded PS (2 g/L, indicated molecular weight = 235 000 g/mol, 0.5 g enzyme/g PS, pH 7.0 at 30 °C), in a two-phase system (dichloromethane−water), in the presence of 10 mM hydrogen peroxide and 10 mM tetramethylhydroquinone.[651] PS dissolved in dichloromethane was completely transferred to the water phase in 10 min by the enzymatic reaction, leading to degradation products (M_r 350). This result is very promising, but it requires dissolution of PS in a solvent. Surprisingly, little work has been pursued in this domain.

Recently, PS biodegradation by insects is a growing field of research. Indeed, the larvae of *Tenebrio molitor* (mealworms) was able to ingest Styrofoam (containing PS > 98% with M_n of 40 $kg \cdot mol^{-1}$ and M_w of 124 $kg \cdot mol^{-1}$) and to convert the polymer into CO_2 (48% of the carbon ingested after 16 days) as well as to incorporate part of the carbon released into lipids.[652] A Chinese university has filed a patent[653] protecting a method of degradation of plastic foam by *Tenebrio* larvae. A bacteria *Pseudomonas* sp. DSM 50071 was isolated form the gut of superworm *Zophobas atratus* and was responsible for a 2.6% weight reduction of PS beads (diameter of 1500 μm, M_w of 371 $kg \cdot mol^{-1}$, M_n of 154 $kg \cdot mol^{-1}$, 99.5% purity, from Myung-IL FOAMTEC) after 15 days and apparition of carbonyles and hydroxyls.[654] Serine hydrolase (SH) and *S*-formylglutathione hydrolase (SGT) were upregulated, respectively, 7-fold and 2-fold. On the other hand, expression levels of the other four selected enzymes: α/β fold hydrolase (AB), arylesterase (AE), autotransport domain containing esterase (AT), and thioesterase (TE) were reduced by 90, 30, 80, and 80%, respectively. This decrease may be necessary to improve the energy efficiency during PS degradation. In the presence of 50 μM SH inhibitor-7 (*tert*-butyl 4-[{2-fluorophenyl}carbamoyl]-piperazine-1-carboxylate), the PS biodegradation was completely blocked.

Among mealworms, greater wax moth (*Galleria mellonella*), and superworm, the superworm had the strongest PS consumption capacity, the highest survival rate after 30 days and the highest ability to degrade PS into low molecular weight substances, while the yellow mealworm efficiently depolymerized PS by destroying the benzene ring.[655] It has been observed that there was a decrease of microbial diversity in superworm and yellow mealworm after ingestion of PS but an increase of microbial diversity in greater wax moth. A 34% decrease of M_n and a 26% decrease of M_w of the PS in frass was observed from the initial PS foam (styrofoam without additive from SINOPEC, M_n of 64 $kg \cdot mol^{-1}$ and M_w 144 $kg \cdot mol^{-1}$). This can be due to mastication action and does not give any evidence of enzyme involvement. Similarly, Song et al. showed a 31% mass loss of PS in feces of snail *Achatina fulica*, with a decrease of molecular weight.[656] A loss of microbial gut diversity and the presence of opportunistic pathogens with PS feeding of superworm (*Zophobas morio*) was also observed by Sun et al.[657]

3.3.2.2. Poly(vinyl chloride) (PVC). PVC is formulated with biocides to avoid its deterioration by microorganisms.[658] Only surface degradation of PVC is observed, and most of the biodegradation reported concerns PVC plasticizers[659−663] For instance, *Micrococcus luteus* enabled only 9% mineralization of PVC after 70 days.[664] Beyond 5 g/L, PVC inhibits microbial growth.[665] The unique significant report stated that the use of a microbial consortium led to a decrease in molecular weight of PVC from 70 $kg \cdot mol^{-1}$ to 16 $kg \cdot mol^{-1}$ after 9 months.[665] Alternatively, a study of biodegradation using an insect has also been reported. The egested frass of *Tenebrio molitor* contained about 35% of residual PVC with 33% M_n decrease and 33% M_w decrease and chlorinated organic compounds.[617]

4. CONCLUSIONS AND FUTURE PERSPECTIVES

Since their discovery almost a century ago, plastics have developed in a strictly linear economic mode, using fossil resources for the vast majority of their production, with far too little (<20%) truly being recycled. Almost 9 billion tons of polymer materials have been produced for the past 70 years, but, like for other materials, the management of their end-of-life has been taken into account in recent years only. More than 6 billion tons of plastic waste has accumulated in the environment, namely in landfills and, for a large part, as macro-, micro-, and nanoplastics polluting our subsoil, our rivers, our seas, and our oceans and certainly animal and human bodies. The awareness that end-of-life plastics are causing a major ecological crisis and pose a threat to the environment has sparked new initiatives to put plastics back at the center of a circular economy. Rethinking the plastics economy by developing more sustainable materials requires a paradigm shift to consider plastic waste as a real source of valuable and exploitable carbon in its own right. In this context, tertiary recycling, that is, (bio)chemical recycling and upcycling of polymers, is expected to provide superior

https://doi.org/10.1021/acs.chemrev.2c00644
Chem. Rev. XXXX, XXX, XXX−XXX

economic value while drastically reducing environmental impacts, in comparison to primary and secondary (mechanical) recycling (see Figure 3). In this regard, the development of highly selective and efficient biocatalytic systems that can be implemented under much milder processes and conditions and lesser energy-intensive, compared to more traditional chemical recycling, is taking place and should help tackling the daunting challenge of white pollution.

It is important to note that before recycling, it is crucial to efficiently collect plastic, not only in developed countries but everywhere on the planet. Regulations are becoming stricter, especially in Europe. For instance, the Directive "Single-Use Plastics" asked for an improvement in the collection of bottles, with the objective to reach 90% collection in Europe by 2029, whereas it was only 60% for bottles and 20% for food trays in 2018. Of the 1.8 Mt recycled, only 31% rebecome bottles. The remaining 69% goes into other products with lower quality or are nonrecyclable. A big proportion of PET bottles placed on the market are quickly lost for recycling and end up in incineration or lost to the environment. In addition, even for PET, collection is far from being efficient, as the fibers, representing two-thirds of its production, are marginally collected. Efforts also have to be made on the sorting by nature of plastics and on development of efficient technologies for automatic sorting and for the removal of hard points in the textiles. The EU directive also asked to extend circularity to the textile market (EU directive March 30, 2022).

This review has discussed recent advances in biocatalysis and in the design of related biocatalytic processes to recycle or upcycle commodity plastics. The work presented highlighted that this emerging field is interdisciplinary in essence, as being at the crossroads of several disciplines, including polymer chemistry and physical chemistry, synthetic processes and chemical engineering, biotechnology and enzyme engineering combined to structural and computational biology as well. This literature review also shows that biotechnological recycling is still in its infancy. It is obvious that, despite numerous research efforts over the last 20 years, the efficient enzymatic degradation of recalcitrant polymers such as PE, PP, PVC, PS, and even some polyamides and ether-based polyurethanes has met with very limited success. Although some polyolefin-eating enzymes have been reported recently, most of these studies indeed fall short for evidencing a true enzymatic degradation, for instance, through the compelling formation of polyolefin oligomers, so that it has not been clearly established yet that these recalcitrant polymers, i.e., constituted of stable C−C bonds in their backbone, can be biocatalytically converted into oligomers and/or small molecules. Therefore, an important issue, that enzymologists and polymer scientists are still facing, is to find polymer-active enzymes targeting the massively produced and fossil-fuel-based polymers, such as PE, PP, PS, or PVC.

PET, which is one of the most important plastics of our everyday life, is definitely an exception to the previous observations since enzymatic recycling of PET has now reached a high degree of maturity. Who would have imagined 10 years ago that an industrial plant could recycle thousands ton of plastics per year using an enzyme to depolymerize this plastic? This plant does not yet exist, but the French company Carbios announced its construction and a beginning of operation in 2025. Nevertheless, many efforts are needed to better recycle plastic waste following biobased routes, either using microorganisms or catalytic enzymes. There is plenty of room, not only to discover in Nature novel efficient plastic-degrading enzymes, but also to improve performances of task-specific enzymes, with the objective of improving their productivity to recycle plastic waste at large scale. Regarding the recycling of the PET, the number of publications is nowadays increasing very rapidly, more and more PETases are being discovered and characterized, more and more variants are proposed with improved thermostability and activities. Given the flow of data, it is important to encourage the scientific community to rationalize the presentation of the results to facilitate their analysis and comparisons. Taking the opportunity of this review, we propose that results should no more be only reported in μM of products without giving the conversion of the substrates. It is important to rather compare initial rates, conversions at the end of the reaction, proportions between the different products (TA, MHET, BHET, etc.) and volume and specific productivities ($g_{TA}{\cdot}L^{-1}{\cdot}h^{-1}$ and $g_{TA}{\cdot}L^{-1}{\cdot}h^{-1}{\cdot}mg_{enz}{}^{-1}$, respectively). For polymers other than PET, the way is even longer to reach this standard.

More efforts are also needed to better understand at fundamental level the underlying depolymerization reaction mechanisms operated by enzymes and to gain more insight into relationship between sequence, structure, dynamics, adsorption phenomena, activity, and stability of the enzymes. This will provide essential information to further guide rational engineering and improve the biocatalytic performances of these enzymes in terms of selectivity, activity, stability, and scalability. For this purpose, advanced characterization techniques allowing monitoring of the evolution of the reaction, the polymer being transformed and the reaction products, combined with theoretical calculations, are extremely valuable. In particular, more accurate multiscale modeling is needed to better model the polymer structure, the enzyme adsorption, and finally to model the activity of the enzyme on its true substrate (e.g., a pellet of PET). Indeed, most often, short oligomers are used in structural and molecular modeling studies to investigate enzyme−substrate interactions, but they are unable to fully represent the behavior of enzymes on polymer chains. All of these approaches, combining both experimental and computational methods, will provide a fine and precise analysis of the enzymatic reaction of depolymerization at different scales.

The engineering of performing enzymes will undoubtedly benefit from the tools and the methodologies developed in the domain of enzyme engineering and screening. In particular, the development of efficient and (ultra)high throughput screening strategies, such as droplets microfluidics, could be promising to isolate from large collections efficient enzymes able to degrade polymers. The amount of data anticipated from these approaches combined to statistical analyses and machine- or deep-learning algorithms should also open the way to the establishment of new rules relating enzyme structure and sequence to activity and accelerate the development of efficient enzymes.

For most industries, one material does not fit all the requirements in terms of properties and as Europe with other nations are developing policy decisions based on science and developing a hierarchy for both material circularity and carbon footprint, the EU ensures that we always use the simplest and most recyclable solutions and materials with the smallest carbon footprint at production and then being fully recycled. Exciting advances can be anticipated soon in this highly active field, which requires, more than ever, integrative multi-

https://doi.org/10.1021/acs.chemrev.2c00644
Chem. Rev. XXXX, XXX, XXX−XXX

disciplinary and multiscale approaches to address the various bottlenecks encountered to develop efficient enzymes performing in industrial process conditions and opening the road to a viable circular economy.

AUTHOR INFORMATION

Corresponding Authors

Isabelle André − *Toulouse Biotechnology Institute, TBI, Université de Toulouse, CNRS, INRAE, INSA, Toulouse, France, F-31077 Toulouse Cedex 04, France*; Email: isabelle.andre@insa-toulouse.fr

Daniel Taton − *Université Bordeaux, CNRS, Bordeaux INP, LCPO, 33600 Pessac, France*; orcid.org/0000-0002-8539-4963; Email: taton@enscbp.fr

Alain Marty − *Carbios, Parc Cataroux−Bâtiment B80, 63100 Clermont-Ferrand, France*; Email: alain.marty@carbios.com

Authors

Vincent Tournier − *Carbios, Parc Cataroux−Bâtiment B80, 63100 Clermont-Ferrand, France*

Sophie Duquesne − *Toulouse Biotechnology Institute, TBI, Université de Toulouse, CNRS, INRAE, INSA, Toulouse, France, F-31077 Toulouse Cedex 04, France*

Frédérique Guillamot − *Carbios, Parc Cataroux−Bâtiment B80, 63100 Clermont-Ferrand, France*

Henri Cramail − *Université Bordeaux, CNRS, Bordeaux INP, LCPO, 33600 Pessac, France*; orcid.org/0000-0001-9798-6352

Complete contact information is available at: https://pubs.acs.org/10.1021/acs.chemrev.2c00644

Author Contributions

[‖]V.T. and S.D. contributed equally. CRediT: **Vincent Tournier** writing-original draft, writing-review & editing; **Sophie Duquesne** writing-original draft, writing-review & editing; **Frédérique Guillamot** writing-original draft, writing-review & editing; **Henri Cramail** writing-original draft, writing-review & editing; **Daniel Taton** writing-original draft, writing-review & editing; **Alain Marty** writing-original draft, writing-review & editing; **Isabelle André** writing-original draft, writing-review & editing.

Notes

The authors declare the following competing financial interest(s): V.T., F.G. and A.M. are employees of Carbios. V.T., S.D., A.M. and I.A. have filed several patents reported in the review on enzyme-based degradation of plastics. All other authors declare no competing interests.

Biographies

Vincent Tournier studied Biology and Biotechnologies and obtained a M.Sc. from the University Paul Sabatier Toulouse III (France) in 2001. He developed methodologies in the field of molecular virology at the Institute Jacques Monod in Paris (France) before joining Rutgers University in Piscataway (NJ, USA), where he conducted his research to better characterize biological processes in vivo. He is dedicating, since 2016, his expertise to develop enzyme-based depolymerization of synthetic polymer approaches and is currently deputy Chief Scientific Officer of Carbios. He has published 13 research articles in peer-reviewed journals and filed 10 patents.

Sophie Duquesne graduated from ENSCP in 2002 (Paris' Technical Institute of Chemistry), and further received a Ph.D. in Biochemistry from the University of Paris 6 in 2007. She spent two years as an Associate Professor (2006−2008), conducting her research in metabolic enzymology at the French National Center of Sequencing (Génoscope), while giving her expertise in Biochemistry by teaching at the University of Evry (France). Sophie joined the INRAE in 2008 as a research Scientist. She is currently working at the Toulouse Biotechnology Institute in France, on the Catalysis and Molecular Enzyme Engineering department. Her research interests include enzyme discovery through the development of screening methodologies, fine characterization of the biochemical and catalytic properties of these enzymes, activity−structure relationship comprehension, and optimization through protein engineering for enzyme implementation in processes. Over the past 11 years, she has focused her research on plastic depolymerases through several ambitious projects (ADEME, BPI-France). She is the coauthor of 25 publications in peer-reviewed journals, three book chapters, and coinventor of 14 patents.

Frédérique Guillamot studied Biotechnology and Organic Chemistry. She received a Ph.D. in Environmental Biosciences from Marseille University (France) in 2010. Her Ph.D. work, funded by ADEME in close relation with Eiffage, focused on ground tire rubber (GTR) microbial treatment to stabilize GTR suspension in bitumen and obtain improved properties, leading to a patent filling. Then, F. Guillamot led a postdoc in Microbial Ecology, where she studied impact of soil contamination, especially antimony, on enzyme activity and microbial respiration. F. Guillamot joined Carbios in 2012 with different positions: microbiology researcher, R&D collaboration manager, and innovation manager. She contributed to one publication and five patent filings. As innovation manager, she was responsible for identifying and implementing innovative projects, such as identification of new enzyme/polymer couples to adapt Carbios's process to waste containing polyamides or polyolefins.

Henri Cramail is Professor of Polymer Chemistry at the University of Bordeaux. In 2004, he was awarded the position of Junior Member of the "Institut Universitaire de France". He was Director of the Laboratoire de Chimie des Polymères Organiques (LCPO), CNRS-University of Bordeaux, from 2007 to 2016. He is currently leading the team "Biopolymers and Biobased Polymers" within LCPO. His researches are focused on the development of green pathways to biobased polymers from renewable resources (vegetable oils, polysaccharides, terpenes, lignin, CO_2).

Daniel Taton obtained his Ph.D. in Polymer Chemistry in 1994 from the University Pierre & Marie Curie (Paris 6, now Sorbonne University). He holds a professorship position at the University of Bordeaux, France, and he develops his research activities at the Laboratory of Organic Polymer Chemistry (LCPO), of which he is the deputy director since 2018. These activities are focused on both "catalysis of polymerization" and "polymerization for catalysis". He is interested, primarily, but not exclusively, in *N*-heterocyclic carbenes (NHCs) for organic catalysis of polymerization in order to achieve both high catalytic activity and high (stereo)selectivity and to also access a variety of metal-free polymers. His team has also developed recyclable polymeric supports. The in situ generation of carbenes confined in custom-designed polymer supports provides unique catalytic activity in benchmark reactions of molecular chemistry, including in aqueous media.

Alain Marty holds a degree in engineering and a Doctorate in Biochemical Engineering from INSA in Toulouse (the French National Institute of Applied Sciences). He began his career in 1992 as a Senior Lecturer at the INSA in Toulouse. He became professor in 2007. For 25 years, he led a research group in the

https://doi.org/10.1021/acs.chemrev.2c00644
Chem. Rev. XXXX, XXX, XXX−XXX

Toulouse Biotechnology Institute. His areas of research include biotechnology, biocatalysis, enzymology, molecular engineering of enzymes, developing intensified enzymatic reactors, and metabolic engineering. Over the course of his career, he has brought together cutting-edge research with the challenge of implementing it in the industrial sphere through industrial collaborations. He has been involved from the beginning in the Carbios adventure, first as academic researcher and member of the Scientific Advisory Board of Carbios. Prof. Marty has been the Chief Scientific Officer of Carbios since April 2015. He has published >70 research papers and filed 26 patents. He is a member of the French Academy of Technology and obtained in 2022 one award from the 10th International Congress on Biocatalysis.

Isabelle André received a Ph.D. in Molecular Chemistry in 1995 from the University of Grenoble (France). She then held a postdoctoral position at the Instituto Rocasolano in Madrid, Spain. From 1997 to 2003, she worked for GLYCODesign Inc., a Canadian biopharmaceutical company. Upon her return to France, she joined the CNRS in 2005 as a Research Scientist. She completed her habilitation at the University of Toulouse, and she became Research Director at CNRS in 2011. She is currently working at the Toulouse Biotechnology Institute in France, in the Catalysis and Molecular Enzyme Engineering Department. She has published >90 research papers, five reviews, three book chapters, and filed 19 patents. Her research interests include understanding enzyme mechanisms and structure–dynamics–activity relationships, developing molecular modelling methodologies to assist protein design, and engineering of biocatalysts for biotechnologies.

ACKNOWLEDGMENTS

This work was partially supported by the LIFE programme of the European Union under the agreement no. LIFE20 ENV/FR/000596 (LIFE CYCLE OF PET) and the ADEME project Ce-PET under the contract no. 1882C0098. This work also received financial support from the French government in the framework of the University of Bordeaux's IdEx "Investments for the Future" program/GPR PPM. Authors are grateful to Nicolas Panel, Marc Guéroult, and Laurie-Anne Chabaud for their help in the conception of the TOC and cover art. V.T., S.D., A.M. and I.A. thank all members of PoPlaB (Polymers Plastics & Biotechnologies), a Carbios-TBI joint lab, for their help and usefull discussions during the writing of this review.

REFERENCES

(1) Staudinger, H. Über Polymerisation. *Ber. Dtsch. Chem. Ges. B* **1920**, *53*, 1073.
(2) Coates, G. W.; Winey, K. I. *Report of the Basic Energy Sciences Roundtable on Chemical Upcycling of Polymers, April 30–May 1, 2019, Bethesda, MD*, 2019.
(3) Kumar, S.; Singh, E.; Mishra, R.; Kumar, A.; Caucci, S. Utilization of Plastic Wastes for Sustainable Environmental Management: A Review. *Chem. Sus. Chem.* **2021**, *14*, 3985–4006.
(4) Billmeyer, F. W. *Textbook of Polymer Science*, 3rd ed.; John Wiley & Sons, 1984.
(5) Elias, H.-G. *An Introduction to Polymer Science*, 1st ed.; Wiley-VCH, 1997.
(6) Painter, P. C.; Coleman, M. M. *Fundamentals of Polymer Science*, 2nd ed.; CRC Press, 1997.
(7) Wypych, G. *Handbook of Polymers*, 3rd ed.; ChemTec Publishing, 2022.
(8) Geyer, R.; Jambeck, J. R.; Law, K. L. Production, Use, and Fate of All Plastics Ever Made. *Sci. Adv.* **2017**, *3*, No. e1700782.
(9) *Additives for Plastics Handbook*, 2nd ed.; Murphy, J., Ed.; Elsevier Science, 2001.
(10) Hahladakis, J. N.; Velis, C. A.; Weber, R.; Iacovidou, E.; Purnell, P. An Overview of Chemical Additives Present in Plastics: Migration, Release, Fate and Environmental Impact during Their Use, Disposal and Recycling. *J. Hazard. Mater.* **2018**, *344*, 179–199.
(11) Ellis, L. D.; Rorrer, N. A.; Sullivan, K. P.; Otto, M.; McGeehan, J. E.; Román-Leshkov, Y.; Wierckx, N.; Beckham, G. T. Chemical and Biological Catalysis for Plastics Recycling and Upcycling. *Nat. Catal.* **2021**, *4*, 539–556.
(12) Billiet, S.; Trenor, S. R. 100th Anniversary of Macromolecular Science Viewpoint: Needs for Plastics Packaging Circularity. *ACS Macro Lett.* **2020**, *9*, 1376–1390.
(13) Lange, J. P. Managing Plastic Waste-Sorting, Recycling, Disposal, and Product Redesign. *ACS Sustain. Chem. Eng.* **2021**, *9*, 15722–15738.
(14) Summers, J. W. The Melting Temperature (or Not Melting) of Poly(Vinyl Chloride). *J. Vinyl Addit. Technol.* **2008**, *14*, 105–109.
(15) MacArthur, D. E. Beyond Plastic Waste. *Science (80-.).* **2017**, *358*, 843.
(16) Garcia, J. M.; Robertson, M. L. The Future of Plastics Recycling. *Science (80-.).* **2017**, *358*, 870–872.
(17) Schneiderman, D. K.; Hillmyer, M. A. 50th Anniversary Perspective: There Is a Great Future in Sustainable Polymers. *Macromolecules* **2017**, *50*, 3733–3749.
(18) Vollmer, I.; Jenks, M. J. F.; Roelands, M. C. P.; White, R. J.; van Harmelen, T.; de Wild, P.; van der Laan, G. P.; Meirer, F.; Keurentjes, J. T. F.; Weckhuysen, B. M. Beyond Mechanical Recycling: Giving New Life to Plastic Waste. *Angew. Chemie - Int. Ed.* **2020**, *59*, 15402–15423.
(19) Sheldon, R. A.; Norton, M. Green Chemistry and the Plastic Pollution Challenge: Towards a Circular Economy. *Green Chem.* **2020**, *22*, 6310–6322.
(20) Schirmeister, C. G.; Mülhaupt, R. Closing the Carbon Loop in the Circular Plastics Economy. *Macromol. Rapid Commun.* **2022**, *43*, 12200247.
(21) *Plastics—The Facts 2021*; Plastics Europe: Brussels, 2023; https://plasticseurope.org/knowledge-hub/plastics-the-facts-2021/ (accessed 2022-07-01).
(22) Wei, R.; Tiso, T.; Bertling, J.; O'Connor, K.; Blank, L. M.; Bornscheuer, U. T. Possibilities and Limitations of Biotechnological Plastic Degradation and Recycling. *Nat. Catal.* **2020**, *3*, 867–871.
(23) Ignatyev, I. A.; Thielemans, W.; Vander Beke, B. Recycling of Polymers: A Review. *ChemSusChem* **2014**, *7*, 1579–1593.
(24) Schyns, Z. O.G.; Shaver, M. P. Mechanical Recycling of Packaging Plastics: A Review. *Macromol. Rapid Commun.* **2021**, *42*, 2000415.
(25) Achilias, D. S.; Giannoulis, A.; Papageorgiou, G. Z. Recycling of Polymers from Plastic Packaging Materials Using the Dissolution-Reprecipitation Technique. *Polym. Bull.* **2009**, *63*, 449–465.
(26) Ügdüler, S.; Van Geem, K. M.; Roosen, M.; Delbeke, E. I. P.; De Meester, S. Challenges and Opportunities of Solvent-Based Additive Extraction Methods for Plastic Recycling. *Waste Manag.* **2020**, *104*, 148–182.
(27) Triebert, D.; Hanel, H.; Bundt, M.; Wohnig, K. Solvent-Based Recycling. In *Circular Economy of Polymers: Topics in Recycling Technologies*; ACS Publications, 2021.
(28) Hong, M.; Chen, E. Y. X. Chemically Recyclable Polymers: A Circular Economy Approach to Sustainability. *Green Chem.* **2017**, *19*, 3692–3706.
(29) Worch, J. C.; Dove, A. P. 100th Anniversary of Macromolecular Science Viewpoint: Toward Catalytic Chemical Recycling of Waste (and Future) Plastics. *ACS Macro Lett.* **2020**, *9*, 1494–1506.
(30) Coates, G. W.; Getzler, Y. D. Y. L. Chemical Recycling to Monomer for an Ideal, Circular Polymer Economy. *Nat. Rev. Mater.* **2020**, *5*, 501–516.
(31) Wei, R.; Tiso, T.; Bertling, J.; O'Connor, K.; Blank, L. M.; Bornscheuer, U. T. Possibilities and Limitations of Biotechnological Plastic Degradation and Recycling. *Nat. Catal.* **2020**, *3*, 867–871.

https://doi.org/10.1021/acs.chemrev.2c00644
Chem. Rev. XXXX, XXX, XXX–XXX

(32) Veskova, J.; Sbordone, F.; Frisch, H. Trends in Polymer Degradation Across All Scales. *Macromol. Chem. Phys.* **2022**, *223*, 2100472.
(33) Chen, X.; Wang, Y.; Zhang, L. Recent Progress in the Chemical Upcycling of Plastic Wastes. *ChemSusChem* **2021**, *14*, 4137−4151.
(34) Roy, P. S.; Garnier, G.; Allais, F.; Saito, K. Strategic Approach Towards Plastic Waste Valorization: Challenges and Promising Chemical Upcycling Possibilities. *ChemSusChem* **2021**, *14*, 4007−4027.
(35) Jehanno, C.; Alty, J. W.; Roosen, M.; De Meester, S.; Dove, A. P.; Chen, E. Y. X.; Leibfarth, F. A.; Sardon, H. Critical Advances and Future Opportunities in Upcycling Commodity Polymers. *Nature* **2022**, *603*, 803−814.
(36) Mohanty, A.; Borah, R. K.; Fatrekar, A. P.; Krishnan, S.; Vernekar, A. A. Stepping towards Benign Alternatives: Sustainable Conversion of Plastic Waste into Valuable Products. *Chem. Commun.* **2021**, *57*, 10277−10291.
(37) Qin, Z.-H.; Mou, J.-H.; Chao, C. Y. H.; Singh Chopra, S.; Daoud, W.; Leu, S.-Y.; Ning, Z.; Tso, C. Y.; Chan, C. K.; Tang, S.; et al. Biotechnology of Plastic Waste Degradation, Recycling, and Valorization: Current Advances and Future Perspectives. *ChemSusChem* **2021**, *14*, 4103−4114.
(38) Jönsson, C.; Wei, R.; Biundo, A.; Landberg, J.; Schwarz Bour, L.; Pezzotti, F.; Toca, A.; Jacques, L. M.; Bornscheuer, U. T.; Syrén, P. O. Biocatalysis in the Recycling Landscape for Synthetic Polymers and Plastics towards Circular Textiles. *ChemSusChem* **2021**, *14*, 4028−4040.
(39) Rahimi, A.; García, J. M. Chemical Recycling of Waste Plastics for New Materials Production. *Nat. Rev. Chem.* **2017**, *1*, 0046.
(40) Kosloski-Oh, S. C.; Wood, Z. A.; Manjarrez, Y.; De Los Rios, J. P.; Fieser, M. E. Catalytic Methods for Chemical Recycling or Upcycling of Commercial Polymers. *Mater. Horizons* **2021**, *8*, 1084−1129.
(41) Roy, P. S.; Garnier, G.; Allais, F.; Saito, K. Strategic Approach Towards Plastic Waste Valorization: Challenges and Promising Chemical Upcycling Possibilities. *Chem. Sus. Chem.* **2021**, *14*, 4007−4027.
(42) Chu, M.; Liu, Y.; Lou, X.; Zhang, Q.; Chen, J. Rational Design of Chemical Catalysis for Plastic Recycling. *ACS Catal.* **2022**, *12*, 4659−4679.
(43) Chow, J.; Perez-Garcia, P.; Dierkes, R.; Streit, W. R. Microbial Enzymes Will Offer Limited Solutions to the Global Plastic Pollution Crisis. *Microb. Biotechnol.* **2023**, *16*, 195−217.
(44) Gambarini, V.; Pantos, O.; Kingsbury, J. M.; Weaver, L.; Handley, K. M.; Lear, G. Phylogenetic Distribution of Plastic-Degrading Microorganisms. *mSystems* **2021**, *6*, 1−13.
(45) Lohmaneeratana, K.; Champreda, V.; Srikhirin, T.; Thamchaipenet, A. Poly(L-lactic acid)-Degrading Activity from Endophytic Micromonospora Spp. and Catalytic Analysis Using Surface Plasmon Resonance. *Agric. Nat. Resour.* **2020**, *54*, 673−680.
(46) Malafatti-Picca, L.; de Barros Chaves, M. R.; de Castro, A. M.; Valoni, É.; de Oliveira, V. M.; Marsaioli, A. J.; de Franceschi de Angelis, D.; Attili-Angelis, D. Hydrocarbon-Associated Substrates Reveal Promising Fungi for Poly (Ethylene Terephthalate) (PET) Depolymerization. *Brazilian J. Microbiol.* **2019**, *50*, 633−648.
(47) Tokiwa, Y.; Calabia, B. P. Biodegradability and Biodegradation of Poly(Lactide). *Appl. Microbiol. Biotechnol.* **2006**, *72*, 244−251.
(48) Jeon, H. J.; Kim, M. N. Biodegradation of Poly(l-Lactide) (PLA) Exposed to UV Irradiation by a Mesophilic Bacterium. *Int. Biodeterior. Biodegrad.* **2013**, *85*, 289−293.
(49) Grabher, C.; Wittbrodt, J. Meganuclease and Transposon Mediated Transgenesis in Medaka. *Genome Biol.* **2007**, *8*, S10.
(50) Stoleru, E.; Hitruc, E. G.; Vasile, C.; Oprică, L. Biodegradation of Poly(Lactic Acid)/Chitosan Stratified Composites in Presence of the *Phanerochaete Chrysosporium* Fungus. *Polym. Degrad. Stab.* **2017**, *143*, 118−129.
(51) Yamashita, K.; Kikkawa, Y.; Kurokawa, K.; Doi, Y. Enzymatic Degradation of Poly(L-Lactide) Film by Proteinase K: Quartz Crystal Microbalance and Atomic Force Microscopy Study. *Biomacromolecules* **2005**, *6*, 850−857.
(52) Numata, K.; Finne-Wistrand, A.; Albertsson, A. C.; Doi, Y.; Abe, H. Enzymatic Degradation of Monolayer for Poly(Lactide) Revealed by Real-Time Atomic Force Microscopy: Effects of Stereochemical Structure, Molecular Weight, and Molecular Branches on Hydrolysis Rates. *Biomacromolecules* **2008**, *9*, 2180−2185.
(53) Kikkawa, Y.; Fujita, M.; Abe, H.; Doi, Y. Effect of Water on the Surface Molecular Mobility of Poly(Lactide) Thin Film: An Atomic Force Microscopy Study. *Biomacromolecules* **2004**, *5*, 1187−1193.
(54) *Global Markets for Enzymes in Industrial Applications*; BCC Research, 2021; https://www.bccresearch.com/market-research/biotechnology/global-markets-for-enzymes-in-industrial-applications.html (accessed 2022-07-15).
(55) Fields, R. D.; Rodriguez, F.; Finn, R. K. Microbial Degradation of Polyesters: Polycaprolactone Degraded by P. Pullulans. *J. Appl. Polym. Sci.* **1974**, *18*, 3571−3579.
(56) Gambarini, V.; Pantos, O.; Kingsbury, J. M.; Weaver, L.; Handley, K. M.; Lear, G. PlasticDB : A Database of Microorganisms and Proteins Linked to Plastic Biodegradation. *Database: J. Biol. Databases and Curation* **2022**, *2022*, baac008.
(57) Buchholz, P. C. F.; Feuerriegel, G.; Zhang, H.; Perez-Garcia, P.; Nover, L.; Chow, J.; Streit, W. R.; Pleiss, J. Plastics Degradation by Hydrolytic Enzymes: The Plastics-active Enzymes Database— PAZy. *Proteins: Struct. Funct. Bioinformatics* **2022**, *90*, 1443−1456.
(58) Lepoittevin, B.; Roger, P. Poly(ethylene terephthalate). In *Handbook of Engineering and Speciality Thermoplastics: Polyethers and Polyesters*; Sabu Thomas, V. P. M., Ed.; Scrivener Publishing, 2011; Vol. 3, pp 97−126.
(59) MacDonald, W. A. New Advances in Poly(Ethylene Terephthalate) Polymerization and Degradation. *Polym. Int.* **2002**, *51*, 923−930.
(60) Pang, K.; Kotek, R.; Tonelli, A. Review of Conventional and Novel Polymerization Processes for Polyesters. *Prog. Polym. Sci.* **2006**, *31*, 1009−1037.
(61) Gantillon, B.; Spitz, R.; McKenna, T. F. The Solid State Postcondensation of PET, 1: A Review of the Physical and Chemical Processes Taking Place in the Solid State. *Macromolecular Materials and Engineering.* **2004**, *289*, 88−105.
(62) Ciolacu, F. C. L.; Choudhury, N. R.; Dutta, N.; Kosior, E. Molecular Level Stabilization of Poly(Ethylene Terephthalate) with Nanostructured Open Cage Trisilanolisobutyl-POSS. *Macromolecules* **2007**, *40*, 265−272.
(63) *Handbook of Plastics Recycling*; La Mantia, F., Ed.; Rapra Technology: Shrewsbury, UK, 2002.
(64) García, J. M. Catalyst: Design Challenges for the Future of Plastics Recycling. *Chem.* **2016**, *1*, 813−815.
(65) Barnard, E.; Rubio Arias, J. J.; Thielemans, W. Chemolytic Depolymerisation of PET: A Review. *Green Chem.* **2021**, *23*, 3765−3789.
(66) Karayannidis, G. P.; Chatziavgoustis, A. P.; Achilias, D. S. Poly(Ethylene Terephthalate) Recycling and Recovery of Pure Terephthalic Acid by Alkaline Hydrolysis. *Adv. Polym. Technol.* **2002**, *21*, 250−259.
(67) Nikles, D. E.; Farahat, M. S. New Motivation for the Depolymerization Products Derived from Poly(Ethylene Terephthalate) (PET) Waste: A Review. *Macromol. Mater. Eng.* **2005**, *290* (1), 13−30.
(68) Siddiqui, M. N.; Redhwi, H. H.; Al-Arfaj, A. A.; Achilias, D. S. Chemical Recycling of Pet in the Presence of the Bio-Based Polymers, Pla, Phb and Pef: A Review. *Sustain.* **2021**, *13*, 10528.
(69) Tricker, A. W.; Osibo, A. A.; Chang, Y.; Kang, J. X.; Ganesan, A.; Anglou, E.; Boukouvala, F.; Nair, S.; Jones, C. W.; Sievers, C. Stages and Kinetics of Mechanochemical Depolymerization of Poly(Ethylene Terephthalate) with Sodium Hydroxide. *ACS Sustain. Chem. Eng.* **2022**, *10*, 11338−11347.
(70) Wei, R.; Zimmermann, W. Microbial Enzymes for the Recycling of Recalcitrant Petroleum-Based Plastics: How Far Are We? *Microbial Biotechnology.* **2017**, *10*, 1308−1322.

https://doi.org/10.1021/acs.chemrev.2c00644
Chem. Rev. XXXX, XXX, XXX−XXX

(71) Koshti, R.; Mehta, L.; Samarth, N. Biological Recycling of Polyethylene Terephthalate: A Mini-Review. *J. Polym. Environ.* **2018**, *26* (8), 3520−3529.
(72) Carniel, A.; Waldow, V. de A.; Castro, A. M. de. A Comprehensive and Critical Review on Key Elements to Implement Enzymatic PET Depolymerization for Recycling Purposes. *Biotechnol. Adv.* **2021**, *52* (July), 107811.
(73) Zimmermann, W. Biocatalytic Recycling of Polyethylene Terephthalate Plastic: Biocatalytic Plastic Recycling. *Philos. Trans. R. Soc. A* **2020**, *378* (2176), 20190273.
(74) Carr, C. M.; Clarke, D. J.; Dobson, A. D. W. Microbial Polyethylene Terephthalate Hydrolases: Current and Future Perspectives. *Front. Microbiol.* **2020**, *11*, 571265.
(75) Soong, Y. H. V.; Sobkowicz, M. J.; Xie, D. Recent Advances in Biological Recycling of Polyethylene Terephthalate (PET) Plastic Wastes. *Bioengineering* **2022**, *9*, 98.
(76) Awaja, F.; Pavel, D. Recycling of PET. *Eur. Polym. J.* **2005**, *41*, 1453−1477.
(77) Webb, H. K.; Arnott, J.; Crawford, R. J.; Ivanova, E. P. Plastic Degradation and Its Environmental Implications with Special Reference to Poly(Ethylene Terephthalate). *Polymers (Basel).* **2013**, *5*, 1−18.
(78) Tournier, V.; Topham, C. M.; Gilles, A.; David, B.; Folgoas, C.; Moya-Leclair, E.; Kamionka, E.; Desrousseaux, M. L.; Texier, H.; Gavalda, S.; et al. An Engineered PET Depolymerase to Break down and Recycle Plastic Bottles. *Nature* **2020**, *580*, 216−219.
(79) Wei, R.; Zimmermann, W. Biocatalysis as a Green Route for Recycling the Recalcitrant Plastic Polyethylene Terephthalate. *Microb. Biotechnol.* **2017**, *10*, 1302−1307.
(80) Tokiwa, Y.; Suzuki, T. Hydrolysis of Polyesters by Lipases. *Nature* **1977**, *270*, 76−78.
(81) Marten, E.; Müller, R. J.; Deckwer, W. D. Studies on the Enzymatic Hydrolysis of Polyesters - I. Low Molecular Mass Model Esters and Aliphatic Polyesters. *Polym. Degrad. Stab.* **2003**, *80*, 485−501.
(82) Marten, E.; Müller, R. J.; Deckwer, W. D. Studies on the Enzymatic Hydrolysis of Polyesters. II. Aliphatic-Aromatic Copolyesters. *Polym. Degrad. Stab.* **2005**, *88*, 371−381.
(83) Kleeberg, I.; Hetz, C.; Kroppenstedt, R. M.; Müller, R. J.; Deckwer, W. D. Biodegradation of Aliphatic-Aromatic Copolyesters by *Thermomonospora Fusca* and Other Thermophilic Compost Isolates. *Appl. Environ. Microbiol.* **1998**, *64*, 1731−1735.
(84) Müller, R. J.; Schrader, H.; Profe, J.; Dresler, K.; Deckwer, W. D. Enzymatic Degradation of Poly(Ethylene Terephthalate): Rapid Hydrolyse Using a Hydrolase from *T. Fusca*. *Macromol. Rapid Commun.* **2005**, *26*, 1400−1405.
(85) Kawai, F.; Kawabata, T.; Oda, M. Current Knowledge on Enzymatic PET Degradation and Its Possible Application to Waste Stream Management and Other Fields. *Appl. Microbiol. Biotechnol.* **2019**, *103*, 4253−4268.
(86) Taniguchi, I.; Yoshida, S.; Hiraga, K.; Miyamoto, K.; Kimura, Y.; Oda, K. Biodegradation of PET: Current Status and Application Aspects. *ACS Catal.* **2019**, *9*, 4089−4105.
(87) Kawai, F.; Kawabata, T.; Oda, M. Current State and Perspectives Related to the Polyethylene Terephthalate Hydrolases Available for Biorecycling. *ACS Sustain. Chem. Eng.* **2020**, *8*, 8894−8908.
(88) Magalhães, R. P.; Cunha, J. M.; Sousa, S. F. Perspectives on the Role of Enzymatic Biocatalysis for the Degradation of Plastic Pet. *Int. J. Mol. Sci.* **2021**, *22*, 11257.
(89) Chen, Y.; Black, D. S.; Reilly, P. J. Carboxylic Ester Hydrolases: Classification and Database Derived from Their Primary, Secondary, and Tertiary Structures. *Protein Sci.* **2016**, *25* (11), 1942−1953.
(90) Yoshida, S.; Hiraga, K.; Takehana, T.; Taniguchi, I.; Yamaji, H.; Maeda, Y.; Toyohara, K.; Miyamoto, K.; Kimura, Y.; Oda, K. A Bacterium That Degrades and Assimilates Poly(Ethylene Terephthalate). *Science (80-.).* **2016**, *351*, 1196−1199.
(91) Kawai, F. Emerging Strategies in Polyethylene Terephthalate Hydrolase Research for Biorecycling. *ChemSusChem* **2021**, *14*, 4115−4122.
(92) Dresler, K.; Van Den Heuvel, J.; Müller, R. J.; Deckwer, W. D. Production of a Recombinant Polyester-Cleaving Hydrolase from *Thermobifida Fusca* in *Escherichia Coli*. *Bioprocess Biosyst. Eng.* **2006**, *29*, 169−183.
(93) Then, J.; Wei, R.; Oeser, T.; Barth, M.; Belisário-Ferrari, M. R.; Schmidt, J.; Zimmermann, W. Ca2+ and Mg2+ Binding Site Engineering Increases the Degradation of Polyethylene Terephthalate Films by Polyester Hydrolases from Thermobifida Fusca. *Biotechnol. J.* **2015**, *10*, 592−598.
(94) Lykidis, A.; Mavromatis, K.; Ivanova, N.; Anderson, I.; Land, M.; DiBartolo, G.; Martinez, M.; Lapidus, A.; Lucas, S.; Copeland, A.; Richardson, P.; Wilson, D. B.; Kyrpides, N. Genome Sequence and Analysis of the Soil Cellulolytic Actinomycete *Thermobifida Fusca* YX. *J. Bacteriol.* **2007**, *189*, 2477−2486.
(95) Chen, S.; Tong, X.; Woodard, R. W.; Du, G.; Wu, J.; Chen, J. Identification and Characterization of Bacterial Cutinase. *J. Biol. Chem.* **2008**, *283*, 25854−25862.
(96) Herrero Acero, E.; Ribitsch, D.; Steinkellner, G.; Gruber, K.; Greimel, K.; Eiteljoerg, I.; Trotscha, E.; Wei, R.; Zimmermann, W.; Zinn, M.; Cavaco-Paulo, A.; Freddi, G.; Schwab, H.; Guebitz, G. Enzymatic Surface Hydrolysis of PET: Effect of Structural Diversity on Kinetic Properties of Cutinases from Thermobifida. *Macromolecules* **2011**, *44*, 4632−4640.
(97) Huang, Y. C.; Chen, G. H.; Chen, Y. F.; Chen, W. L.; Yang, C. H. Heterologous Expression of Thermostable Acetylxylan Esterase Gene from Thermobifida Fusca and Its Synergistic Action with Xylanase for the Production of Xylooligosaccharides. *Biochem. Biophys. Res. Commun.* **2010**, *400*, 718−723.
(98) Ribitsch, D.; Acero, E. H.; Greimel, K.; Eiteljoerg, I.; Trotscha, E.; Freddi, G.; Schwab, H.; Guebitz, G. M. Characterization of a New Cutinase from *Thermobifida Alba* for PET-Surface Hydrolysis. *Biocatal. Biotransformation* **2012**, *30*, 2−9.
(99) Bååth, J. A.; Borch, K.; Jensen, K.; Brask, J.; Westh, P. Comparative Biochemistry of Four Polyester (PET) Hydrolases**. *ChemBioChem.* **2021**, *22*, 1627−1637.
(100) Hu, X.; Thumarat, U.; Zhang, X.; Tang, M.; Kawai, F. Diversity of Polyester-Degrading Bacteria in Compost and Molecular Analysis of a Thermoactive Esterase from *Thermobifida Alba* AHK119. *Appl. Microbiol. Biotechnol.* **2010**, *87*, 771−779.
(101) Thumarat, U.; Nakamura, R.; Kawabata, T.; Suzuki, H.; Kawai, F. Biochemical and Genetic Analysis of a Cutinase-Type Polyesterase from a Thermophilic *Thermobifida Alba* AHK119. *Appl. Microbiol. Biotechnol.* **2012**, *95*, 419−430.
(102) Ribitsch, D.; Herrero Acero, E.; Greimel, K.; Dellacher, A.; Zitzenbacher, S.; Marold, A.; Rodriguez, R. D.; Steinkellner, G.; Gruber, K.; Schwab, H.; Guebitz, G. M. A New Esterase from *Thermobifida Halotolerans* Hydrolyses Polyethylene Terephthalate (PET) and Polylactic Acid (PLA). *Polymers (Basel).* **2012**, *4*, 617−629.
(103) *SignalP-5.0 Signal Peptide and Cleavage Sites in Gram+, Gram- and Eukaryotic Amino Acid Sequences*; DTU Health Tech: Lyngby, Denmark, 2023; https://services.healthtech.dtu.dk/service.php?SignalP-5.0.
(104) Kleeberg, I.; Welzel, K.; VandenHeuvel, J.; Müller, R. J.; Deckwer, W. D. Characterization of a New Extracellular Hydrolase from *Thermobifida Fusca* Degrading Aliphatic-Aromatic Copolyesters. *Biomacromolecules* **2005**, *6*, 262−270.
(105) Su, L.; Woodard, R. W.; Chen, J.; Wu, J. Extracellular Location of *Thermobifida Fusca* Cutinase Expressed in Escherichia Coli BL21(DE3) without Mediation of a Signal Peptide. *Appl. Environ. Microbiol.* **2013**, *79*, 4192−4198.
(106) Hegde, K.; Veeranki, V. D. Production Optimization and Characterization of Recombinant Cutinases from *Thermobifida Fusca* Sp. NRRL B-8184. *Appl. Biochem. Biotechnol.* **2013**, *170*, 654−675.
(107) Thumarat, U.; Kawabata, T.; Nakajima, M.; Nakajima, H.; Sugiyama, A.; Yazaki, K.; Tada, T.; Waku, T.; Tanaka, N.; Kawai, F.

https://doi.org/10.1021/acs.chemrev.2c00644
Chem. Rev. XXXX, XXX, XXX−XXX

Comparison of Genetic Structures and Biochemical Properties of Tandem Cutinase-Type Polyesterases from *Thermobifida Alba* AHK119. *J. Biosci. Bioeng.* **2015**, *120*, 491−497.
(108) Chertkov, O.; Sikorski, J.; Nolan, M.; Lapidus, A.; Lucas, S.; del Rio, T. G.; Tice, H.; Cheng, J. F.; Goodwin, L.; Pitluck, S.; et al. Complete Genome Sequence of *Thermomonospora Curvata* Type Strain (B9 T). *Stand. Genomic Sci.* **2011**, *4*, 13−22.
(109) Wei, R.; Oeser, T.; Zimmermann, W. *Synthetic Polyester-Hydrolyzing Enzymes from Thermophilic Actinomycetes*; Elsevier, 2014; Vol *89*.
(110) Kawai, F.; Oda, M.; Tamashiro, T.; Waku, T.; Tanaka, N.; Yamamoto, M.; Mizushima, H.; Miyakawa, T.; Tanokura, M. A Novel Ca2+-Activated, Thermostabilized Polyesterase Capable of Hydrolyzing Polyethylene Terephthalate from *Saccharomonospora Viridis* AHK190. *Appl. Microbiol. Biotechnol.* **2014**, *98*, 10053−10064.
(111) Oda, M.; Yamagami, Y.; Inaba, S.; Oida, T.; Yamamoto, M.; Kitajima, S.; Kawai, F. Enzymatic Hydrolysis of PET: Functional Roles of Three Ca2+ Ions Bound to a Cutinase-like Enzyme, Cut190*, and Its Engineering for Improved Activity. *Appl. Microbiol. Biotechnol.* **2018**, *102*, 10067−10077.
(112) Oren, A.; Garrity, G. M. Valid Publication of the Names of Forty-Two Phyla of Prokaryotes. *Int. J. Syst. Evol. Microbiol.* **2021**, *71*, 005056.
(113) Wei, R.; Oeser, T.; Then, J.; Kühn, N.; Barth, M.; Schmidt, J.; Zimmermann, W. Functional Characterization and Structural Modeling of Synthetic Polyester-Degrading Hydrolases from *Thermomonospora Curvata*. *AMB Express* **2014**, *4*, 1−10.
(114) Danso, D.; Schmeisser, C.; Chow, J.; Zimmermann, W.; Wei, R.; Leggewie, C.; Li, X.; Hazen, T.; Streit, W. R. New Insights into the Function and Global Distribution of Polyethylene Terephthalate (PET)-Degrading Bacteria and Enzymes in Marine and Terrestrial Metagenomes. *Appl. Environ. Microbiol.* **2018**, *84*, No. e02773-17.
(115) Lombard, V.; Golaconda Ramulu, H.; Drula, E.; Coutinho, P. M.; Henrissat, B. The Carbohydrate-Active Enzymes Database (CAZy) in 2013. *Nucleic Acids Res.* **2014**, *42*, D490−D495.
(116) Novy, V.; Carneiro, L. V.; Shin, J. H.; Larsbrink, J.; Olsson, L. Phylogenetic Analysis and In-Depth Characterization of Functionally and Structurally Diverse CE5 Cutinases. *J. Biol. Chem.* **2021**, *297*, 101302.
(117) Danso, D.; Chow, J.; Streit, W. R. Plastics: Environmental and Biotechnological Perspectives on Microbial Degradation. *Appl. Environ. Microbiol.* **2019**, *85*, e02095-19.
(118) Gan, Z.; Zhang, H. PMBD: A Comprehensive Plastics Microbial Biodegradation Database. *Database (Oxford).* **2019**, *2019*, 1−11.
(119) Ahmaditabatabaei, S.; Kyazze, G.; Iqbal, H. M. N.; Keshavarz, T. Fungal Enzymes as Catalytic Tools for Polyethylene Terephthalate (PET) Degradation. *J. Fungi* **2021**, *7*, 931.
(120) Zimmermann, W.; Billig, S. Enzymes for the Biofunctionalization of Poly(ethylene terephthalate). In *Advances in Biochemical Engineering/Biotechnology*; Book Series (ABE, Volume 125); Springer-Verlag: Berlin, Heidelberg, 2011; Vol *125*, pp 97−120.
(121) Bauer, T. L.; Buchholz, P. C. F.; Pleiss, J. The Modular Structure of α/β-Hydrolases. *FEBS J.* **2020**, *287* (5), 1035−1053.
(122) Ronkvist, Å. M.; Xie, W.; Lu, W.; Gross, R. A. Cutinase-Catalyzed Hydrolysis of Poly(Ethylene Terephthalate). *Macromolecules* **2009**, *42*, 5128−5138.
(123) Carniel, A.; Valoni, É.; Nicomedes, J.; Gomes, A. da C.; Castro, A. M. de. Lipase from Candida Antarctica (CALB) and Cutinase from *Humicola Insolens* Act Synergistically for PET Hydrolysis to Terephthalic Acid. *Process Biochem.* **2017**, *59*, 84−90.
(124) Alisch-Mark, M.; Herrmann, A.; Zimmermann, W. Increase of the Hydrophilicity of Polyethylene Terephthalate Fibres by Hydrolases from *Thermomonospora Fusca* and *Fusarium Solani* f. Sp. Pisi. *Biotechnol. Lett.* **2006**, *28*, 681−685.
(125) Dimarogona, M.; Nikolaivits, E.; Kanelli, M.; Christakopoulos, P.; Sandgren, M.; Topakas, E. Structural and Functional Studies of a Fusarium Oxysporum Cutinase with Polyethylene Terephthalate Modification Potential. *Biochim. Biophys. Acta - Gen. Subj.* **2015**, *1850*, 2308−2317.
(126) Brueckner, T.; Eberl, A.; Heumann, S.; Rabe, M.; Guebitz, G. M. Enzymatic and Chemical Hydrolysis of Poly(Ethylene Terephthalate) Fabrics. *J. Polym. Sci. Part A Polym. Chem.* **2008**, *46*, 6435−6443.
(127) Weinberger, S.; Beyer, R.; Schüller, C.; Strauss, J.; Pellis, A.; Ribitsch, D.; Guebitz, G. M. High Throughput Screening for New Fungal Polyester Hydrolyzing Enzymes. *Front. Microbiol.* **2020**, *11* (April), 1−8.
(128) Ribitsch, D.; Heumann, S.; Trotscha, E.; Herrero Acero, E.; Greimel, K.; Leber, R.; Birner-Gruenberger, R.; Deller, S.; Eiteljoerg, I.; Remler, P.; et al. Hydrolysis of Polyethyleneterephthalate by P-Nitrobenzylesterase from *Bacillus Subtilis*. *Biotechnol. Prog.* **2011**, *27*, 951−960.
(129) Perz, V.; Baumschlager, A.; Bleymaier, K.; Zitzenbacher, S.; Hromic, A.; Steinkellner, G.; Pairitsch, A.; Łyskowski, A.; Gruber, K.; Sinkel, C.; et al. Hydrolysis of Synthetic Polyesters by *Clostridium Botulinum* Esterases. *Biotechnol. Bioeng.* **2016**, *113*, 1024−1034.
(130) Sulaiman, S.; Yamato, S.; Kanaya, E.; Kim, J. J.; Koga, Y.; Takano, K.; Kanaya, S. Isolation of a Novel Cutinase Homolog with Polyethylene Terephthalate-Degrading Activity from Leaf-Branch Compost by Using a Metagenomic Approach. *Appl. Environ. Microbiol.* **2012**, *78*, 1556−1562.
(131) Kato, S.; Sakai, S.; Hirai, M.; Tasumi, E.; Nishizawa, M.; Suzuki, K.; Takai, K. Long-Term Cultivation and Metagenomics Reveal Ecophysiology of Previously Uncultivated Thermophiles Involved in Biogeochemical Nitrogen Cycle. *Microbes Environ.* **2018**, *33*, 107−110.
(132) Xi, X.; Ni, K.; Hao, H.; Shang, Y.; Zhao, B.; Qian, Z. Secretory Expression in *Bacillus Subtilis* and Biochemical Characterization of a Highly Thermostable Polyethylene Terephthalate Hydrolase from Bacterium HR29. *Enzyme Microb. Technol.* **2021**, *143*, 109715.
(133) Zhou, Z.; Liu, Y.; Xu, W.; Pan, J.; Luo, Z.-H.; Li, M. Genome- and Community-Level Interaction Insights into Carbon Utilization and Element Cycling Functions of Hydrothermarchaeota in Hydrothermal Sediment. *mSystems* **2020**, *5*, No. e00795-19.
(134) Joo, S.; Cho, I. J.; Seo, H.; Son, H. F.; Sagong, H. Y.; Shin, T. J.; Choi, S. Y.; Lee, S. Y.; Kim, K. J. Structural Insight into Molecular Mechanism of Poly(Ethylene Terephthalate) Degradation. *Nat. Commun.* **2018**, *9*, 382.
(135) Sagong, H. Y.; Son, H. F.; Seo, H.; Hong, H.; Lee, D.; Kim, K. J. Implications for the PET Decomposition Mechanism through Similarity and Dissimilarity between PETases from *Rhizobacter Gummiphilus* and *Ideonella Sakaiensis*. *J. Hazard. Mater.* **2021**, *416*, 126075.
(136) Bollinger, A.; Thies, S.; Knieps-Grünhagen, E.; Gertzen, C.; Kobus, S.; Höppner, A.; Ferrer, M.; Gohlke, H.; Smits, S. H. J.; Jaeger, K. E. A Novel Polyester Hydrolase From the Marine Bacterium *Pseudomonas Aestusnigri* - Structural and Functional Insights. *Front. Microbiol.* **2020**, *11*, 114.
(137) Blázquez-Sánchez, P.; Engelberger, F.; Cifuentes-Anticevic, J.; Sonnendecker, C.; Griñén, A.; Reyes, J.; Díez, B.; Guixé, V.; Richter, P. K.; Zimmermann, W.; Ramírez-Sarmiento, C. A. Antarctic Polyester Hydrolases Degrade Aliphatic and Aromatic Polyesters at Moderate Temperatures. *Appl. Environ. Microbiol.* **2022**, *88*, No. e01842-21.
(138) Zhang, H.; Perez-Garcia, P.; Dierkes, R. F.; Applegate, V.; Schumacher, J.; Chibani, C. M.; Sternagel, S.; Preuss, L.; Weigert, S.; Schmeisser, C.; Danso, D.; Pleiss, J.; Almeida, A.; Höcker, B.; Hallam, S. J.; Schmitz, R. A.; Smits, S. H. J.; Chow, J.; Streit, W. R. The Bacteroidetes Aequorivita Sp. and *Kaistella Jeonii* Produce Promiscuous Esterases With PET-Hydrolyzing Activity. *Front. Microbiol.* **2022**, *12*, 803896.
(139) Sonnendecker, C.; Oeser, J.; Richter, P. K.; Hille, P.; Zhao, Z.; Fischer, C.; Lippold, H.; Blázquez-Sánchez, P.; Engelberger, F.; Ramírez-Sarmiento, C. A.; Oeser, T.; Lihanova, Y.; Frank, R.; Jahnke, H.-G.; Billig, S.; Abel, B.; Sträter, N.; Matysik, J.; Zimmermann, W. Low Carbon Footprint Recycling of Post-Consumer PET Plastic with

https://doi.org/10.1021/acs.chemrev.2c00644
Chem. Rev. XXXX, XXX, XXX−XXX

a Metagenomic Polyester Hydrolase. *ChemSusChem* **2021**, *15*, e202101062.
(140) Nakamura, A.; Kobayashi, N.; Koga, N.; Iino, R. Positive Charge Introduction on the Surface of Thermostabilized PET Hydrolase Facilitates PET Binding and Degradation. *ACS Catal.* **2021**, *11*, 8550−8564.
(141) Pfaff, L.; Gao, J.; Li, Z.; Jäckering, A.; Weber, G.; Mican, J.; Chen, Y.; Dong, W.; Han, X.; Feiler, C. G.; et al. Multiple Substrate Binding Mode-Guided Engineering of a Thermophilic PET Hydrolase. *ACS Catal.* **2022**, *12*, 9790−9800.
(142) Kawai, F. The Current State of Research on PET Hydrolyzing Enzymes Available for Biorecycling. *Catalysts* **2021**, *11*, 206.
(143) Fecker, T.; Galaz-Davison, P.; Engelberger, F.; Narui, Y.; Sotomayor, M.; Parra, L. P.; Ramírez-Sarmiento, C. A. Active Site Flexibility as a Hallmark for Efficient PET Degradation by *I. Sakaiensis* PETase. *Biophys. J.* **2018**, *114*, 1302−1312.
(144) Austin, H. P.; Allen, M. D.; Donohoe, B. S.; Rorrer, N. A.; Kearns, F. L.; Silveira, R. L.; Pollard, B. C.; Dominick, G.; Duman, R.; El Omari, K.; et al. Characterization and Engineering of a Plastic-Degrading Aromatic Polyesterase. *Proc. Natl. Acad. Sci. U. S. A.* **2018**, *115*, E4350−E4357.
(145) Berselli, A.; Ramos, M. J.; Menziani, M. C. Novel Pet-Degrading Enzymes: Structure-Function from a Computational Perspective. *ChemBioChem.* **2021**, *22*, 2032−2050.
(146) Kumar, S.; Stecher, G.; Li, M.; Knyaz, C.; Tamura, K. MEGA X: Molecular Evolutionary Genetics Analysis across Computing Platforms. *Mol. Biol. Evol.* **2018**, *35*, 1547−1549.
(147) Robert, X.; Gouet, P. Deciphering Key Features in Protein Structures with the New ENDscript Server. *Nucleic Acids Res.* **2014**, *42* (W1), 320−324.
(148) Chen, C. C.; Dai, L.; Ma, L.; Guo, R. T. Enzymatic Degradation of Plant Biomass and Synthetic Polymers. *Nat. Rev. Chem.* **2020**, *4*, 114−126.
(149) Oh, C.; Doohun Kim, T.; Kim, K. K. Carboxylic Ester Hydrolases in Bacteria: Active Site, Structure, Function and Application. *Crystals* **2019**, *9*, 597.
(150) Ge, B. K.; Hu, G. M.; Chen, C. M. Plastic Bioconversion: Reaction Mechanism of PETases. *Chin. J. Phys.* **2021**, *73* (April), 331−339.
(151) Rauwerdink, A.; Kazlauskas, R. J. How the Same Core Catalytic Machinery Catalyzes 17 Different Reactions: The Serine-Histidine-Aspartate Catalytic Triad of α/β- Hydrolase Fold Enzymes. *ACS Catal.* **2015**, *5*, 6153−6161.
(152) Han, X.; Liu, W.; Huang, J. W.; Ma, J.; Zheng, Y.; Ko, T. P.; Xu, L.; Cheng, Y. S.; Chen, C. C.; Guo, R. T. Structural Insight into Catalytic Mechanism of PET Hydrolase. *Nat. Commun.* **2017**, *8*, 2106.
(153) Dimitriou, P. S.; Denesyuk, A. I.; Nakayama, T.; Johnson, M. S.; Denessiouk, K. Distinctive Structural Motifs Co-Ordinate the Catalytic Nucleophile and the Residues of the Oxyanion Hole in the Alpha/Beta-Hydrolase Fold Enzymes. *Protein Sci.* **2019**, *28* (2), 344−364.
(154) Wei, R.; Breite, D.; Song, C.; Gräsing, D.; Ploss, T.; Hille, P.; Schwerdtfeger, R.; Matysik, J.; Schulze, A.; Zimmermann, W. Biocatalytic Degradation Efficiency of Postconsumer Polyethylene Terephthalate Packaging Determined by Their Polymer Microstructures. *Adv. Sci.* **2019**, *6*, 1900491.
(155) Thomsen, T. B.; Hunt, C. J.; Meyer, A. S. Influence of Substrate Crystallinity and Glass Transition Temperature on Enzymatic Degradation of Polyethylene Terephthalate (PET). *N. Biotechnol.* **2022**, *69*, 28.
(156) Wei, R.; Song, C.; Gräsing, D.; Schneider, T.; Bielytskyi, P.; Böttcher, D.; Matysik, J.; Bornscheuer, U. T.; Zimmermann, W. Conformational Fitting of a Flexible Oligomeric Substrate Does Not Explain the Enzymatic PET Degradation. *Nat. Commun.* **2019**, *10* (1), 3−6.
(157) Guo, B.; Vanga, S. R.; Lopez-Lorenzo, X.; Saenz-Mendez, P.; Ericsson, S. R.; Fang, Y.; Ye, X.; Schriever, K.; Bäckström, E.; Biundo, A.; et al. Conformational Selection in Biocatalytic Plastic Degradation by PETase. *ACS Catal.* **2022**, *12*, 3397−3409.
(158) Pirillo, V.; Pollegioni, L.; Molla, G. Analytical Methods for the Investigation of Enzyme-Catalyzed Degradation of Polyethylene Terephthalate. *FEBS J.* **2021**, *288*, 4730−4745.
(159) Arnling Bååth, J.; Novy, V.; Carneiro, L. V.; Guebitz, G. M.; Olsson, L.; Westh, P.; Ribitsch, D. Structure-Function Analysis of Two Closely Related Cutinases from *Thermobifida Cellulosilytica*. *Biotechnol. Bioeng.* **2021**, *119*, 470−481.
(160) Palm, G. J.; Reisky, L.; Böttcher, D.; Müller, H.; Michels, E. A. P.; Walczak, M. C.; Berndt, L.; Weiss, M. S.; Bornscheuer, U. T.; Weber, G. Structure of the Plastic-Degrading *Ideonella Sakaiensis* MHETase Bound to a Substrate. *Nat. Commun.* **2019**, *10*, 1−10.
(161) Sagong, H. Y.; Seo, H.; Kim, T.; Son, H. F.; Joo, S.; Lee, S. H.; Kim, S.; Woo, J. S.; Hwang, S. Y.; Kim, K. J. Decomposition of the PET Film by MHETase Using Exo-PETase Function. *ACS Catal.* **2020**, *10* (8), 4805−4812.
(162) Knott, B. C.; Erickson, E.; Allen, M. D.; Gado, J. E.; Graham, R.; Kearns, F. L.; Pardo, I.; Topuzlu, E.; Anderson, J. J.; Austin, H. P.; et al. Characterization and Engineering of a Two-Enzyme System for Plastics Depolymerization. *Proc. Natl. Acad. Sci. U. S. A.* **2020**, *117*, 25476−25485.
(163) Meyer-Cifuentes, I. E.; Werner, J.; Jehmlich, N.; Will, S. E.; Neumann-Schaal, M.; Öztürk, B. Synergistic Biodegradation of Aromatic-Aliphatic Copolyester Plastic by a Marine Microbial Consortium. *Nat. Commun.* **2020**, *11*, 5790.
(164) Meyer-Cifuentes, I. E.; Öztürk, B. Mle046 Is a Marine Mesophilic MHETase-Like Enzyme. *Front. Microbiol.* **2021**, *12* (July), 1−9.
(165) Gamerith, C.; Vastano, M.; Ghorbanpour, S. M.; Zitzenbacher, S.; Ribitsch, D.; Zumstein, M. T.; Sander, M.; Acero, E. H.; Pellis, A.; Guebitz, G. M. Enzymatic Degradation of Aromatic and Aliphatic Polyesters by P. Pastoris Expressed Cutinase 1 from *Thermobifida Cellulosilytica*. *Front. Microbiol.* **2017**, *8*, 938.
(166) Furukawa, M.; Kawakami, N.; Tomizawa, A.; Miyamoto, K. Efficient Degradation of Poly(Ethylene Terephthalate) with *Thermobifida Fusca* Cutinase Exhibiting Improved Catalytic Activity Generated Using Mutagenesis and Additive-Based Approaches. *Sci. Rep.* **2019**, *9*, 1−9.
(167) Yang, S.; Xu, H.; Yan, Q.; Liu, Y.; Zhou, P.; Jiang, Z. A Low Molecular Mass Cutinase of *Thielavia Terrestris* Efficiently Hydrolyzes Poly(Esters). *J. Ind. Microbiol. Biotechnol.* **2013**, *40* (2), 217−226.
(168) Nyyssölä, A.; Pihlajaniemi, V.; Häkkinen, M.; Kontkanen, H.; Saloheimo, M.; Nakari-Setälä, T. Cloning and Characterization of a Novel Acidic Cutinase from *Sirococcus Conigenus*. *Appl. Microbiol. Biotechnol.* **2014**, *98*, 3639−3650.
(169) Nyyssölä, A.; Pihlajaniemi, V.; Järvinen, R.; Mikander, S.; Kontkanen, H.; Kruus, K.; Kallio, H.; Buchert, J. Screening of Microbes for Novel Acidic Cutinases and Cloning and Expression of an Acidic Cutinase from *Aspergillus Niger* CBS 513.88. *Enzyme Microb. Technol.* **2013**, *52*, 272−278.
(170) Boneta, S.; Arafet, K.; Moliner, V. QM/MM Study of the Enzymatic Biodegradation Mechanism of Polyethylene Terephthalate. *J. Chem. Inf. Model.* **2021**, *61*, 3041−3051.
(171) Zheng, M.; Li, Y.; Dong, W.; Feng, S.; Zhang, Q.; Wang, W. Computational Biotransformation of Polyethylene Terephthalate by Depolymerase: A QM/MM Approach. *J. Hazard. Mater.* **2022**, *423* (PA), 127017.
(172) Pinto, A. V.; Ferreira, P.; Neves, R. P. P.; Fernandes, P. A.; Ramos, M. J.; Magalhães, A. L. Reaction Mechanism of MHETase, a PET Degrading Enzyme. *ACS Catal.* **2021**, *11*, 10416−10428.
(173) Jerves, C.; Neves, R. P. P.; Ramos, M. J.; Da Silva, S.; Fernandes, P. A. Reaction Mechanism of the PET Degrading Enzyme PETase Studied with DFT/MM Molecular Dynamics Simulations. *ACS Catal.* **2021**, *11*, 11626−11638.
(174) Wei, Y.; Swenson, L.; Castro, C.; Derewenda, U.; Minor, W.; Arai, H.; Aoki, J.; Inoue, K.; Servin-Gonzalez, L.; Derewenda, Z. S. Structure of a Microbial Homologue of Mammalian Platelet-Activating Factor Acetylhydrolases: *Streptomyces Exfoliatus* Lipase at 1.9 Å Resolution. *Structure* **1998**, *6*, 511−519.

https://doi.org/10.1021/acs.chemrev.2c00644
Chem. Rev. XXXX, XXX, XXX−XXX

(175) Ollis, D. L.; Carr, P. D. Alpha/Beta Hydrolase Fold: An Update. *Protein Pept. Lett.* **2009**, *16*, 1137−1148.
(176) Nardini, M.; Dijkstra, B. W. α/β Hydrolase Fold Enzymes: The Family Keeps Growing. *Curr. Opin. Struct. Biol.* **1999**, *9*, 732−737.
(177) Chen, S.; Su, L.; Chen, J.; Wu, J. Cutinase: Characteristics, Preparation, and Application. *Biotechnol. Adv.* **2013**, *31*, 1754−1767.
(178) Zeng, W.; Li, X.; Yang, Y.; Min, J.; Huang, J.-W.; Liu, W.; Niu, D.; Yang, X.; Han, X.; Zhang, L.; Dai, L.; Chen, C.-C.; Guo, R.-T. Substrate-Binding Mode of a Thermophilic PET Hydrolase and Engineering the Enzyme to Enhance the Hydrolytic Efficacy. *ACS Catal.* **2022**, *12*, 3033−3040.
(179) Roth, C.; Wei, R.; Oeser, T.; Then, J.; Föllner, C.; Zimmermann, W.; Sträter, N. Structural and Functional Studies on a Thermostable Polyethylene Terephthalate Degrading Hydrolase from *Thermobifida Fusca*. *Appl. Microbiol. Biotechnol.* **2014**, *98*, 7815−7823.
(180) Santacruz-Juárez, E.; Buendia-Corona, R. E.; Ramírez, R. E.; Sánchez, C. Fungal Enzymes for the Degradation of Polyethylene: Molecular Docking Simulation and Biodegradation Pathway Proposal. *J. Hazard. Mater.* **2021**, *411*, 125118.
(181) da Costa, C. H. S.; dos Santos, A. M.; Alves, C. N.; Martí, S.; Moliner, V.; Santana, K.; Lameira, J. Assessment of the PETase Conformational Changes Induced by Poly(Ethylene Terephthalate) Binding. *Proteins: Struct. Funct. Bioinform.* **2021**, *89*, 1340−1352.
(182) Qi, X.; Yan, W.; Cao, Z.; Ding, M.; Yuan, Y. Current Advances in the Biodegradation and Bioconversion of Polyethylene Terephthalate. *Microorganisms* **2022**, *10*, 39−42.
(183) Charlier, C.; Gavalda, S.; Borsenberger, V.; Duquesne, S.; Marty, A.; Tournier, V.; Lippens, G. Article An NMR Look at an Engineered PET Depolymerase. *Biophysj* **2022**, *121*, 2882−2894.
(184) Dong, Q.; Yuan, S.; Wu, L.; Su, L.; Zhao, Q.; Wu, J.; Huang, W.; Zhou, J. Structure-Guided Engineering of a *Thermobifida Fusca* Cutinase for Enhanced Hydrolysis on Natural Polyester Substrate. *Bioresour. Bioprocess.* **2020**, *7*, 37.
(185) Ribitsch, D.; Hromic, A.; Zitzenbacher, S.; Zartl, B.; Gamerith, C.; Pellis, A.; Jungbauer, A.; Łyskowski, A.; Steinkellner, G.; Gruber, K.; et al. Small Cause, Large Effect: Structural Characterization of Cutinases from *Thermobifida Cellulosilytica*. *Biotechnol. Bioeng.* **2017**, *114*, 2481−2488.
(186) Kitadokoro, K.; Thumarat, U.; Nakamura, R.; Nishimura, K.; Karatani, H.; Suzuki, H.; Kawai, F. Crystal Structure of Cutinase Est119 from *Thermobifida Alba* AHK119 That Can Degrade Modified Polyethylene Terephthalate at 1.76 Å Resolution. *Polym. Degrad. Stab.* **2012**, *97* (5), 771−775.
(187) Kitadokoro, K.; Kakara, M.; Matsui, S.; Osokoshi, R.; Thumarat, U.; Kawai, F.; Kamitani, S. Structural Insights into the Unique Polylactate-Degrading Mechanism of *Thermobifida Alba* Cutinase. *FEBS J.* **2019**, *286*, 2087−2098.
(188) Miyakawa, T.; Mizushima, H.; Ohtsuka, J.; Oda, M.; Kawai, F.; Tanokura, M. Structural Basis for the Ca2+-Enhanced Thermostability and Activity of PET-Degrading Cutinase-like Enzyme from *Saccharomonospora Viridis* AHK190. *Appl. Microbiol. Biotechnol.* **2015**, *99*, 4297−4307.
(189) Numoto, N.; Kamiya, N.; Bekker, G. J.; Yamagami, Y.; Inaba, S.; Ishii, K.; Uchiyama, S.; Kawai, F.; Ito, N.; Oda, M. Structural Dynamics of the PET-Degrading Cutinase-like Enzyme from *Saccharomonospora Viridis* AHK190 in Substrate-Bound States Elucidates the Ca2+-Driven Catalytic Cycle. *Biochemistry* **2018**, *57*, 5289−5300.
(190) Senga, A.; Numoto, N.; Yamashita, M.; Iida, A.; Ito, N.; Kawai, F.; Oda, M. Multiple Structural States of Ca2+-Regulated PET Hydrolase, Cut190, and Its Correlation with Activity and Stability. *J. Biochem.* **2021**, *169*, 207−213.
(191) Emori, M.; Numoto, N.; Senga, A.; Bekker, G. J.; Kamiya, N.; Kobayashi, Y.; Ito, N.; Kawai, F.; Oda, M. Structural Basis of Mutants of PET-Degrading Enzyme from *Saccharomonospora Viridis* AHK190 with High Activity and Thermal Stability. *Proteins Struct. Funct. Bioinforma.* **2021**, *89*, 502−511.
(192) Sulaiman, S.; You, D. J.; Kanaya, E.; Koga, Y.; Kanaya, S. Crystal Structure and Thermodynamic and Kinetic Stability of Metagenome-Derived LC-Cutinase. *Biochemistry* **2014**, *53*, 1858−1869.
(193) Liu, B.; He, L.; Wang, L.; Li, T.; Li, C.; Liu, H.; Luo, Y.; Bao, R. Protein Crystallography and Site-Direct Mutagenesis Analysis of the Poly(Ethylene Terephthalate) Hydrolase PETase from *Ideonella Sakaiensis*. *ChemBioChem* **2018**, *19*, 1471−1475.
(194) Son, H. F.; Cho, I. J.; Joo, S.; Seo, H.; Sagong, H. Y.; Choi, S. Y.; Lee, S. Y.; Kim, K. J. Rational Protein Engineering of Thermo-Stable PETase from *Ideonella Sakaiensis* for Highly Efficient PET Degradation. *ACS Catal.* **2019**, *9*, 3519−3526.
(195) Liu, C.; Shi, C.; Zhu, S.; Wei, R.; Yin, C. C. Structural and Functional Characterization of Polyethylene Terephthalate Hydrolase from *Ideonella Sakaiensis*. *Biochem. Biophys. Res. Commun.* **2019**, *508*, 289−294.
(196) Cui, Y.; Chen, Y.; Liu, X.; Dong, S.; Tian, Y.; Qiao, Y.; Mitra, R.; Han, J.; Li, C.; Han, X.; et al. Computational Redesign of a PETase for Plastic Biodegradation under Ambient Condition by the GRAPE Strategy. *ACS Catal.* **2021**, *11*, 1340−1350.
(197) Chen, K.; Hu, Y.; Dong, X.; Sun, Y. Molecular Insights into the Enhanced Performance of EKylated PETase Toward PET Degradation. *ACS Catal.* **2021**, *11*, 7358−7370.
(198) Erickson, E.; Shakespeare, T. J.; Bratti, F.; Buss, B. L.; Graham, R.; Hawkins, M. A.; König, G.; Michener, W. E.; Miscall, J.; Ramirez, K. J.; et al. Comparative Performance of PETase as a Function of Reaction Conditions, Substrate Properties, and Product Accumulation. *ChemSusChem* **2022**, *15*, 1−12.
(199) Lu, H.; Diaz, D. J.; Czarnecki, N. J.; Zhu, C.; Kim, W.; Shroff, R.; Acosta, D. J.; Alexander, B. R.; Cole, H. O.; Zhang, Y.; et al. Machine Learning-Aided Engineering of Hydrolases for PET Depolymerization. *Nature* **2022**, *604*, 662−667.
(200) Bell, E. L.; Smithson, R.; Kilbride, S.; Foster, J.; Hardy, F.; Ramachandran, S.; Tedstone, A. B.; Haigh, S. J.; Garforth, A. B.; Day, P. J. R.; et al. Directed Evolution of an Efficient and Thermostable PET Depolymerase. *Nature Catal.* **2022**, *5*, 673−681.
(201) Singh, A.; Rorrer, N. A.; Nicholson, S. R.; Erickson, E.; DesVeaux, J. S.; Avelino, A. F. T.; Lamers, P.; Bhatt, A.; Zhang, Y.; Avery, G.; et al. Techno-Economic, Life-Cycle, and Socioeconomic Impact Analysis of Enzymatic Recycling of Poly(Ethylene Terephthalate). *Joule* **2021**, *5*, 2479−2503.
(202) Chen, H.; Cebe, P. Vitrification and Devitrification of Rigid Amorphous Fraction of PET during Quasi-Isothermal Cooling and Heating. *Macromolecules* **2009**, *42*, 288−292.
(203) Castro, A. M. de.; Carniel, A.; Stahelin, D.; Chinelatto Junior, L. S.; Honorato, H. de A.; de Menezes, S. M. C. High-Fold Improvement of Assorted Post-Consumer Poly(Ethylene Terephthalate) (PET) Packages Hydrolysis Using *Humicola Insolens* Cutinase as a Single Biocatalyst. *Process Biochem.* **2019**, *81*, 85−91.
(204) Gamerith, C.; Zartl, B.; Pellis, A.; Guillamot, F.; Marty, A.; Acero, E. H.; Guebitz, G. M. Enzymatic Recovery of Polyester Building Blocks from Polymer Blends. *Process Biochem.* **2017**, *59*, 58−64.
(205) Brizendine, R. K.; Erickson, E.; Haugen, S. J.; Ramirez, K. J.; Miscall, J.; Salvachúa, D.; Pickford, A. R.; Sobkowicz, M. J.; Mcgeehan, J. E.; Beckham, G. T. Particle Size Reduction of Poly(Ethylene Terephthalate) Increases the Rate of Enzymatic Depolymerization But Does Not Increase the Overall Conversion Extent. *ACS Sustain. Chem. Eng.* **2022**, *10*, 9131−9140.
(206) Rezazadeh, A.; Thomsen, K.; Gavala, H. N.; Skiadas, I. V.; Fosbøl, P. L. Solubility and Freezing Points of Disodium Terephthalate in Water-Ethylene Glycol Mixtures. *J. Chem. Eng. Data* **2021**, *66*, 2143−2152.
(207) Mueller, R. J. Biological Degradation of Synthetic Polyesters-Enzymes as Potential Catalysts for Polyester Recycling. *Process Biochem.* **2006**, *41*, 2124−2128.
(208) Zhang, W.; Yan, Q.; Ye, K.; Zhang, Q.; Chen, W.; Meng, L.; Chen, X.; Wang, D.; Li, L. The Effect of Water Absorption on Stretch-Induced Crystallization of Poly(Ethylene Terephthalate): An in Situ

https://doi.org/10.1021/acs.chemrev.2c00644
Chem. Rev. XXXX, XXX, XXX−XXX

Synchrotron Radiation Wide Angle X-Ray Scattering Study. *Polymer* **2019**, *162*, 91−99.
(209) Langevin, D.; Grenet, J.; et Saiter, J. M. Moisture Sorption in Pet Influence on the Thermokinetic Parameters. *Eur. Polym. J.* **1994**, *30*, 339−345.
(210) Levine, H.; Slade, L. *Water as a Plasticizer: Physico-Chemical Aspects of Low-Moisture Polymeric Systems* **1988**, 79.
(211) Keller, B. A.; Lester, G. R. Crystallization Phenomena in Polymers - Preliminary Investigation of the Crystallization Characteristics of Polyethylene Terephthalate. *Philos. Trans. R. Soc. London, Ser. A* **1954**, *247*, 1−12.
(212) Shieh, Y.-T.; Lin, Y.-S.; Twu, Y.-K.; Tsai, H.-B.; Lin, R.-H. Effect of Crystallinity on Enthalpy Recovery Peaks and Cold-Crystallization Peaks in PET via TMDSC and DMA Studies. *J. Appl. Polym. Sci.* **2010**, *116*, 1334−1341.
(213) Zhang, J.; Wang, X.; Gong, J.; Gu, Z. A Study on the Biodegradability of Polyethylene Terephthalate Fiber and Diethylene Glycol Terephthalate. *J. Appl. Polym. Sci.* **2004**, *93*, 1089−1096.
(214) Kondratowicz, F.; Ukielski, R. Synthesis and Hydrolytic Degradation of Poly(Ethylene Succinate) and Poly(Ethylene Terephthalate) Copolymers. *Polym. Degrad. Stab.* **2009**, *94*, 375−382.
(215) Wallace, N. E.; Adams, M. C.; Chafin, A. C.; Jones, D. D.; Tsui, C. L.; Gruber, T. D. The Highly Crystalline PET Found in Plastic Water Bottles Does Not Support the Growth of the PETase-Producing Bacterium Ideonella Sakaiensis. *Environ. Microbiol. Rep.* **2020**, *12*, 578−582.
(216) Rodríguez-Hernández, A. G.; Muñoz-Tabares, J. A.; Aguilar-Guzmán, J. C.; Vazquez-Duhalt, R. A Novel and Simple Method for Polyethylene Terephthalate (PET) Nanoparticle Production. *Environ. Sci. Nano* **2019**, *6*, 2031−2036.
(217) Wei, R.; Oeser, T.; Barth, M.; Weigl, N.; Lübs, A.; Schulz-Siegmund, M.; Hacker, M. C.; Zimmermann, W. Turbidimetric Analysis of the Enzymatic Hydrolysis of Polyethylene Terephthalate Nanoparticles. *J. Mol. Catal. B Enzym.* **2014**, *103*, 72−78.
(218) Pütz, A. Isolierung, Identifizierung Und Biochemische Charakterisierung Dialkylphthalat Spaltender Esterasen. Ph.D. Thesis. Institut für Molekulare Enzymtechnologie der Heinrich-Heine-Universität Düsseldorf. 2006.
(219) de Castro, A. M.; Carniel, A.; Nicomedes Junior, J.; da Conceição Gomes, A.; Valoni, É. Screening of Commercial Enzymes for Poly(Ethylene Terephthalate) (PET) Hydrolysis and Synergy Studies on Different Substrate Sources. *J. Ind. Microbiol. Biotechnol.* **2017**, *44*, 835−844.
(220) Falkenstein, P.; Gräsing, D.; Bielytskyi, P.; Zimmermann, W.; Matysik, J.; Wei, R.; Song, C. UV Pretreatment Impairs the Enzymatic Degradation of Polyethylene Terephthalate. *Front. Microbiol.* **2020**, *11* (April), 1−10.
(221) Maurya, A.; Bhattacharya, A.; Khare, S. K. Enzymatic Remediation of Polyethylene Terephthalate (PET)-Based Polymers for Effective Management of Plastic Wastes: An Overview. *Front. Bioeng. Biotechnol.* **2020**, *8*, 602325.
(222) Desrousseaux, M.-L.; Texier, H.; Duquesne, S.; Marty, A.; Aloui Dalibey, M.; Chateau, M. A Process for Degrading Plastic Products, WO 2017198786, 2017.
(223) Nelson, D. L.; Cox, M. M. *Lehninger Principles of Biochemistry*, 7th ed.; W. H. Freeman, New York, 2017.
(224) Wei, R.; von Haugwitz, G.; Pfaff, L.; Mican, J.; Badenhorst, C. P. S.; Liu, W.; Weber, G.; Austin, H. P.; Bednar, D.; Damborsky, J.; et al. Mechanism-Based Design of Efficient PET Hydrolases. *ACS Catal.* **2022**, *12*, 3382−3396.
(225) Zhu, B.; Wang, D.; Wei, N. Enzyme Discovery and Engineering for Sustainable Plastic Recycling. *Trends Biotechnol.* **2022**, *40* (1), 22−37.
(226) Herrero Acero, E.; Ribitsch, D.; Dellacher, A.; Zitzenbacher, S.; Marold, A.; Steinkellner, G.; Gruber, K.; Schwab, H.; Guebitz, G. M. Surface Engineering of a Cutinase from *Thermobifida Cellulosilytica* for Improved Polyester Hydrolysis. *Biotechnol. Bioeng.* **2013**, *110*, 2581−2590.
(227) Furukawa, M.; Kawakami, N.; Oda, K.; Miyamoto, K. Acceleration of Enzymatic Degradation of Poly(Ethylene Terephthalate) by Surface Coating with Anionic Surfactants. *ChemSusChem* **2018**, *11*, 4018−4025.
(228) Parrott, M. C.; DeSimone, J. M. Relieving PEGylation. *Nat. Chem.* **2012**, *4*, 13−14.
(229) Szkolar, L.; Guilbaud, J. B.; Miller, A. F.; Gough, J. E.; Saiani, A. Enzymatically Triggered Peptide Hydrogels for 3D Cell Encapsulation and Culture. *J. Pept. Sci.* **2014**, *20*, 578−584.
(230) Biundo, A.; Ribitsch, D.; Steinkellner, G.; Gruber, K.; Guebitz, G. M. Polyester Hydrolysis Is Enhanced by a Truncated Esterase: Less Is More. *Biotechnol. J.* **2017**, *12*, 450.
(231) Armenta, S.; Moreno-Mendieta, S.; Sánchez-Cuapio, Z.; Sánchez, S.; Rodríguez-Sanoja, R. Advances in Molecular Engineering of Carbohydrate-Binding Modules. *Proteins Struct. Funct. Bioinforma.* **2017**, *85* (9), 1602−1617.
(232) Weber, J.; Petrović, D.; Strodel, B.; Smits, S. H. J.; Kolkenbrock, S.; Leggewie, C.; Jaeger, K. E. Interaction of Carbohydrate-Binding Modules with Poly(Ethylene Terephthalate). *Appl. Microbiol. Biotechnol.* **2019**, *103*, 4801−4812.
(233) Zhang, Y.; Chen, S.; Xu, M.; Cavoco-Paulo, A. P.; Wu, J.; Chen, J. Characterization of *Thermobifida Fusca* Cutinase-Carbohydrate-Binding Module Fusion Proteins and Their Potential Application in Bioscouring∇. *Appl. Environ. Microbiol.* **2010**, *76*, 6870−6876.
(234) Zhang, Y.; Wang, L.; Chen, J.; Wu, J. Enhanced Activity toward PET by Site-Directed Mutagenesis of *Thermobifida Fusca* Cutinase-CBM Fusion Protein. *Carbohydr. Polym.* **2013**, *97*, 124−129.
(235) Ribitsch, D.; Yebra, A. O.; Zitzenbacher, S.; Wu, J.; Nowitsch, S.; Steinkellner, G.; Greimel, K.; Doliska, A.; Oberdorfer, G.; Gruber, C. C.; Gruber, K.; Schwab, H.; Stana-Kleinschek, K.; Acero, E. H.; Guebitz, G. M. Fusion of Binding Domains to *Thermobifida Cellulosilytica* Cutinase to Tune Sorption Characteristics and Enhancing PET Hydrolysis. *Biomacromolecules* **2013**, *14*, 1769−1776.
(236) Dai, L.; Qu, Y.; Huang, J. W.; Hu, Y.; Hu, H.; Li, S.; Chen, C. C.; Guo, R. T. Enhancing PET Hydrolytic Enzyme Activity by Fusion of the Cellulose-Binding Domain of Cellobiohydrolase I from *Trichoderma Reesei*. *J. Biotechnol.* **2021**, *334* (March), 47−50.
(237) Zhang, A.; He, Y.; Wei, G.; Zhou, J.; Dong, W.; Chen, K.; Ouyang, P. Molecular Characterization of a Novel Chitinase CmChi1 from *Chitinolyticbacter Meiyuanensis* SYBC-H1 and Its Use in N-Acetyl-d-Glucosamine Production. *Biotechnol. Biofuels* **2018**, *11*, 1−14.
(238) Xue, R.; Chen, Y.; Rong, H.; Wei, R.; Cui, Z.; Zhou, J.; Dong, W.; Jiang, M. Fusion of Chitin-Binding Domain From *Chitinolyticbacter Meiyuanensis* SYBC-H1 to the Leaf-Branch Compost Cutinase for Enhanced PET Hydrolysis. *Front. Bioeng. Biotechnol.* **2021**, *9*, 762854.
(239) Oliveira, C.; Carvalho, V.; Domingues, L.; Gama, F. M. Recombinant CBM-Fusion Technology - Applications Overview. *Biotechnol. Adv.* **2015**, *33*, 358−369.
(240) Ribitsch, D.; Acero, E. H.; Przylucka, A.; Zitzenbacher, S.; Marold, A.; Gamerith, C.; Tscheließnig, R.; Jungbauer, A.; Rennhofer, H.; Lichtenegger, H.; et al. Enhanced Cutinase-Catalyzed Hydrolysis of Polyethylene Terephthalate by Covalent Fusion to Hydrophobins. *Appl. Environ. Microbiol.* **2015**, *81*, 3586−3592.
(241) Islam, S.; Apitius, L.; Jakob, F.; Schwaneberg, U. Targeting Microplastic Particles in the Void of Diluted Suspensions. *Environ. Int.* **2019**, *123*, 428−435.
(242) Berger, B. W.; Sallada, N. D. Hydrophobins: Multifunctional Biosurfactants for Interface Engineering. *J. Biol. Eng.* **2019**, *13* (1), 1−8.
(243) Wösten, H. A. B.; Scholtmeijer, K. Applications of Hydrophobins: Current State and Perspectives. *Appl. Microbiol. Biotechnol.* **2015**, *99*, 1587−1597.
(244) Espino-Rammer, L.; Ribitsch, D.; Przylucka, A.; Marold, A.; Greimel, K. J.; Herrero Acero, E.; Guebitz, G. M.; Kubicek, C. P.; Druzhinina, I. S. Two Novel Class Ii Hydrophobins from *Trichoderma*

https://doi.org/10.1021/acs.chemrev.2c00644
Chem. Rev. XXXX, XXX, XXX−XXX

Spp. Stimulate Enzymatic Hydrolysis of Poly(Ethylene Terephthalate) When Expressed as Fusion Proteins. *Appl. Environ. Microbiol.* **2013**, *79*, 4230−4238.
(245) Puspitasari, N.; Tsai, S. L.; Lee, C. K. Class I Hydrophobins Pretreatment Stimulates PETase for Monomers Recycling of Waste PETs. *Int. J. Biol. Macromol.* **2021**, *176*, 157−164.
(246) Puspitasari, N.; Tsai, S. L.; Lee, C. K. Fungal Hydrophobin RolA Enhanced PETase Hydrolysis of Polyethylene Terephthalate. *Appl. Biochem. Biotechnol.* **2021**, *193*, 1284−1295.
(247) Rübsam, K.; Stomps, B.; Böker, A.; Jakob, F.; Schwaneberg, U. Anchor Peptides: A Green and Versatile Method for Polypropylene Functionalization. *Polymer (Guildf).* **2017**, *116*, 124−132.
(248) Büscher, N.; Sayoga, G. V.; Rübsam, K.; Jakob, F.; Schwaneberg, U.; Kara, S.; Liese, A. Biocatalyst Immobilization by Anchor Peptides on an Additively Manufacturable Material. *Org. Process Res. Dev.* **2019**, *23* (9), 1852−1859.
(249) Liu, Z.; Zhang, Y.; Wu, J. Enhancement of PET Biodegradation by Anchor Peptide-Cutinase Fusion Protein. *Enzyme Microb. Technol.* **2022**, *156*, 110004.
(250) Apitius, L.; Rübsam, K.; Jakesch, C.; Jakob, F.; Schwaneberg, U. Ultrahigh-Throughput Screening System for Directed Polymer Binding Peptide Evolution. *Biotechnol. Bioeng.* **2019**, *116*, 1856−1867.
(251) Fersht, A. *Structure and Mechanism in Protein Science: A Guide to Enzyme Catalysis and Protein Folding, Series in Structural Biology*; World Scientific, 2017.
(252) Sabatier, P. *La Catalyse En Chimie Organique*; Nouveau Monde, 2013.
(253) Arnling Bååth, J.; Jensen, K.; Borch, K.; Westh, P.; Kari, J. Sabatier Principle for Rationalizing Enzymatic Hydrolysis of a Synthetic Polyester. *JACS Au* **2022**, *2*, 1223−1231.
(254) Dai, L.; Qu, Y.; Hu, Y.; Min, J.; Yu, X.; Chen, C. C.; Huang, J. W.; Guo, R. T. Catalytically Inactive Lytic Polysaccharide Monooxygenase PcAA14A Enhances the Enzyme-Mediated Hydrolysis of Polyethylene Terephthalate. *Int. J. Biol. Macromol.* **2021**, *190*, 456−462.
(255) Couturier, M.; Ladevèze, S.; Sulzenbacher, G.; Ciano, L.; Fanuel, M.; Moreau, C.; Villares, A.; Cathala, B.; Chaspoul, F.; Frandsen, K. E.; Labourel, A.; Herpoël-Gimbert, I.; Grisel, S.; Haon, M.; Lenfant, N.; Rogniaux, H.; Ropartz, D.; Davies, G. J.; et al. Lytic Xylan Oxidases from Wood-Decay Fungi Unlock Biomass Degradation. *Nat. Chem. Biol.* **2018**, *14*, 306−310.
(256) Gercke, D.; Furtmann, C.; Tozakidis, I. E. P.; Jose, J. Highly Crystalline Post-Consumer PET Waste Hydrolysis by Surface Displayed PETase Using a Bacterial Whole-Cell Biocatalyst. *ChemCatChem.* **2021**, *13*, 3479−3489.
(257) Nielsen, A. D.; Arleth, L.; Westh, P. Analysis of Protein-Surfactant Interactions - A Titration Calorimetric and Fluorescence Spectroscopic Investigation of Interactions between *Humicola Insolens* Cutinase and an Anionic Surfactant. *Biochim. Biophys. Acta - Proteins Proteomics* **2005**, *1752*, 124−132.
(258) Nielsen, A. D.; Borch, K.; Westh, P. Thermal Stability of *Humicola Insolens* Cutinase in Aqueous SDS. *J. Phys. Chem. B* **2007**, *111*, 2941−2947.
(259) Kjølbye, L. R.; Laustsen, A.; Vestergaard, M.; Periole, X.; De Maria, L.; Svendsen, A.; Coletta, A.; Schiøtt, B. Molecular Modeling Investigation of the Interaction between *Humicola Insolens* Cutinase and SDS Surfactant Suggests a Mechanism for Enzyme Inactivation. *J. Chem. Inf. Model.* **2019**, *59*, 1977−1987.
(260) Weiland, M. H. Enzymatic Biodegradation by Exploring the Rational Protein Engineering of the Polyethylene Terephthalate Hydrolyzing Enzyme PETase from *Ideonella Sakaiensis* 201-F6. *ACS Symp. Ser.* **2020**, *1357*, 161−174.
(261) Gao, R.; Pan, H.; Lian, J. Enzyme and Microbial Technology Recent Advances in the Discovery, Characterization, and Engineering of Poly (Ethylene Terephthalate) (PET) Hydrolases. *Enzyme Microb. Technol.* **2021**, *150* (July), 109868.
(262) Oda, M. Structural Basis for Ca^{2+}-Dependent Catalysis of a Cutinase-like Enzyme and Its Engineering: Application to Enzymatic PET Depolymerization. *Biophys. Physicobiology* **2021**, *18*, 168−176.
(263) Shirke, A. N.; White, C.; Englaender, J. A.; Zwarycz, A.; Butterfoss, G. L.; Linhardt, R. J.; Gross, R. A. Stabilizing Leaf and Branch Compost Cutinase (LCC) with Glycosylation: Mechanism and Effect on PET Hydrolysis. *Biochemistry* **2018**, *57*, 1190−1200.
(264) Shirke, A. N.; Su, A.; Jones, J. A.; Butterfoss, G. L.; Koffas, M. A. G.; Kim, J. R.; Gross, R. A. Comparative Thermal Inactivation Analysis of *Aspergillus Oryzae* and *Thiellavia Terrestris* Cutinase: Role of Glycosylation. *Biotechnol. Bioeng.* **2017**, *114*, 63−73.
(265) Shirke, A. N.; Basore, D.; Holton, S.; Su, A.; Baugh, E.; Butterfoss, G. L.; Makhatadze, G.; Bystroff, C.; Gross, R. A. Influence of Surface Charge, Binding Site Residues and Glycosylation on *Thielavia Terrestris* Cutinase Biochemical Characteristics. *Appl. Microbiol. Biotechnol.* **2016**, *100*, 4435−4446.
(266) Then, J.; Wei, R.; Oeser, T.; Gerdts, A.; Schmidt, J.; Barth, M.; Zimmermann, W. A Disulfide Bridge in the Calcium Binding Site of a Polyester Hydrolase Increases Its Thermal Stability and Activity against Polyethylene Terephthalate. *FEBS Open Bio* **2016**, *6*, 425−432.
(267) Brott, S.; Pfaff, L.; Schuricht, J.; Schwarz, J. N.; Böttcher, D.; Badenhorst, C. P. S.; Wei, R.; Bornscheuer, U. T. Engineering and Evaluation of Thermostable IsPETase Variants for PET Degradation. *Eng. Life Sci.* **2022**, *22*, 192−203.
(268) André, I.; Tournier, V.; Gilles, A.; Duquesne, S. Novel Esterases and Uses Thereof. WO 2020021117, 2019.
(269) Cui, Y.; Chen, Y.; Liu, X.; Dong, S.; Tian, Y.; Qiao, Y.; Mitra, R.; Han, J.; Li, C.; Han, X.; et al. Computational Redesign of a PETase for Plastic Biodegradation under Ambient Condition by the GRAPE Strategy. *ACS Catal.* **2021**, *11*, 1340−1350.
(270) Li, Q.; Zheng, Y.; Su, T.; Wang, Q.; Liang, Q.; Zhang, Z.; Qi, Q.; Tian, J. Computational Design of a Cutinase for Plastic Biodegradation by Mining Molecular Dynamics Simulations Trajectories. *Comput. Struct. Biotechnol. J.* **2022**, *20*, 459−470.
(271) Bava, K. A.; Gromiha, M. M.; Uedaira, H.; Kitajima, K.; Sarai, A. ProTherm, Version 4.0: Thermodynamic Database for Proteins and Mutants. *Nucleic Acids Res.* **2004**, *32*, D120−D121.
(272) Kumar, M. D. S.; Bava, K. A.; Gromiha, M. M.; Prabakaran, P.; Kitajima, K.; Uedaira, H.; Sarai, A. ProTherm and ProNIT: Thermodynamic Databases for Proteins and Protein-Nucleic Acid Interactions. *Nucleic Acids Res.* **2006**, *34*, D204−D206.
(273) Nikam, R.; Kulandaisamy, A.; Harini, K.; Sharma, D.; Gromiha, M. M. ProThermDB: Thermodynamic Database for Proteins and Mutants Revisited after 15 Years. *Nucleic Acids Res.* **2021**, *49*, D420−D424.
(274) Zumstein, M. T.; Rechsteiner, D.; Roduner, N.; Perz, V.; Ribitsch, D.; Guebitz, G. M.; Kohler, H. P. E.; McNeill, K.; Sander, M. Enzymatic Hydrolysis of Polyester Thin Films at the Nanoscale: Effects of Polyester Structure and Enzyme Active-Site Accessibility. *Environ. Sci. Technol.* **2017**, *51*, 7476−7485.
(275) Araújo, R.; Silva, C.; O'Neill, A.; Micaelo, N.; Guebitz, G.; Soares, C. M.; Casal, M.; Cavaco-Paulo, A. Tailoring Cutinase Activity towards Polyethylene Terephthalate and Polyamide 6,6 Fibers. *J. Biotechnol.* **2007**, *128*, 849−857.
(276) Kawabata, T.; Oda, M.; Kawai, F. Mutational Analysis of Cutinase-like Enzyme, Cut190, Based on the 3D Docking Structure with Model Compounds of Polyethylene Terephthalate. *J. Biosci. Bioeng.* **2017**, *124*, 28−35.
(277) Zou, Y.; Xue, M.; Wang, W.; Cai, L.; Chen, L.; Liu, J.; Wang, P. G.; Shen, J.; Chen, M. One-Pot Three-Enzyme Synthesis of UDP-Glc, UDP-Gal, and Their Derivatives. *Carbohydr. Res.* **2013**, *373*, 76−81.
(278) Ma, Y.; Yao, M.; Li, B.; Ding, M.; He, B.; Chen, S.; Zhou, X.; Yuan, Y. Enhanced Poly(Ethylene Terephthalate) Hydrolase Activity by Protein Engineering. *Engineering* **2018**, *4* (6), 888−893.
(279) Silva, C.; Da, S.; Silva, N.; Matamá, T.; Araújo, R.; Martins, M.; Chen, S.; Chen, J.; Wu, J.; Casal, M.; Cavaco-Paulo, A. Engineered *Thermobifida Fusca* Cutinase with Increased Activity on Polyester Substrates. *Biotechnol. J.* **2011**, *6*, 1230−1239.
(280) Chen, C. C.; Han, X.; Li, X.; Jiang, P.; Niu, D.; Ma, L.; Liu, W.; Li, S.; Qu, Y.; Hu, H.; Min, J.; Yang, Y.; Zhang, L.; Zeng, W.;

https://doi.org/10.1021/acs.chemrev.2c00644
Chem. Rev. XXXX, XXX, XXX−XXX

Huang, J. W.; Dai, L.; Guo, R. T. General Features to Enhance Enzymatic Activity of Poly(Ethylene Terephthalate) Hydrolysis. *Nat. Catal.* **2021**, *4*, 425−430.
(281) de Queiros Eugenio, E.; SSampaio Pereira Campisano, I.; Machado de Castro, A.; Zarur Coelho, M. A.; Pereira Langone, M. A. Kinetic Modeling of the Post-Consumer Poly(Ethylene Terephthalate) Hydrolysis Catalyzed by Cutinase from Humicola Insolens. *J. Polym. Environ.* **2022**, *30*, 1627−1637.
(282) Wallace, P. W.; Haernvall, K.; Ribitsch, D.; Zitzenbacher, S.; Schittmayer, M.; Steinkellner, G.; Gruber, K.; Guebitz, G. M.; Birner-Gruenberger, R. PpEst Is a Novel PBAT Degrading Polyesterase Identified by Proteomic Screening of Pseudomonas Pseudoalcaligenes. *Appl. Microbiol. Biotechnol.* **2017**, *101*, 2291−2303.
(283) Barth, M.; Oeser, T.; Wei, R.; Then, J.; Schmidt, J.; Zimmermann, W. Effect of Hydrolysis Products on the Enzymatic Degradation of Polyethylene Terephthalate Nanoparticles by a Polyester Hydrolase from *Thermobifida Fusca*. *Biochem. Eng. J.* **2015**, *93*, 222−228.
(284) Groß, C.; Hamacher, K.; Schmitz, K.; Jager, S. Cleavage Product Accumulation Decreases the Activity of Cutinase during PET Hydrolysis. *J. Chem. Inf. Model.* **2017**, *57*, 243−255.
(285) Barth, M.; Wei, R.; Oeser, T.; Then, J.; Schmidt, J.; Wohlgemuth, F.; Zimmermann, W. Enzymatic Hydrolysis of Polyethylene Terephthalate Films in an Ultrafiltration Membrane Reactor. *J. Membr. Sci.* **2015**, *494*, 182−187.
(286) Wei, R.; Oeser, T.; Schmidt, J.; Meier, R.; Barth, M.; Then, J.; Zimmermann, W. Engineered Bacterial Polyester Hydrolases Efficiently Degrade Polyethylene Terephthalate Due to Relieved Product Inhibition. *Biotechnol. Bioeng.* **2016**, *113*, 1658−1665.
(287) Barth, M.; Honak, A.; Oeser, T.; Wei, R.; Belisário-Ferrari, M. R.; Then, J.; Schmidt, J.; Zimmermann, W. A Dual Enzyme System Composed of a Polyester Hydrolase and a Carboxylesterase Enhances the Biocatalytic Degradation of Polyethylene Terephthalate Films. *Biotechnol. J.* **2016**, *11*, 1082−1087.
(288) Sales, J. C. S.; Santos, A. G.; de Castro, A. M.; Coelho, M. A. Z. A Critical View on the Technology Readiness Level (TRL) of Microbial Plastics Biodegradation. *World J. Microbiol. Biotechnol.* **2021**, *37*, 1−15.
(289) Thiyagarajan, S.; Maaskant-Reilink, E.; Ewing, T. A.; Julsing, M. K.; van Haveren, J. Back-to-Monomer Recycling of Polycondensation Polymers: Opportunities for Chemicals and Enzymes. *RSC Adv.* **2021**, *12* (2), 947−970.
(290) Merchan, A. L.; Fischöder, T.; Hee, J.; Lehnertz, M. S.; Osterthun, O.; Pielsticker, S.; Schleier, J.; Tiso, T.; Blank, L. M.; Klankermayer, J.; Kneer, R.; Quicker, P.; Walther, G.; Palkovits, R. Chemical Recycling of Bioplastics: Technical Opportunities to Preserve Chemical Functionality as Path towards a Circular Economy. *Green Chem.* **2022**, *24*, 9428−9449.
(291) Subramanian, M. R.; Talluri, S.; Christopher, L. P. Production of Lactic Acid Using a New Homofermentative Enterococcus Faecalis Isolate. *Microboial Biotechnol.* **2015**, *8*, 221−229.
(292) *Poly(Lactic Acid) Science and Technology: Processing, Properties, Additives and Applications*; Jiménez, A., Peltzer, M., Ruseckaite, R., Eds.; Royal Society of Chemistry, 2015.
(293) Castro-Aguirre, E.; Iñiguez-Franco, F.; Samsudin, H.; Fang, X.; Auras, R. Poly(Lactic Acid)—Mass Production, Processing, Industrial Applications, and End of Life. *Adv. Drug Delivery Rev.* **2016**, *107*, 333−366.
(294) Garlotta, D. A Literature Review of Poly(Lactic Acid). *J. Polym. Environ.* **2001**, *9*, 63−84.
(295) *European Bioplastics e.V.*; European Bioplastics e.V., 2022; https://www.european-bioplastics.org/market/ (accessed 2022-04-07).
(296) Pretula, J.; Slomkowski, S.; Penczek, S. Polylactides—Methods of Synthesis and Characterization. *Adv. Drug Delivery Rev.* **2016**, *107*, 3−16.
(297) Naser, A. Z.; Deiab, I.; Darras, B. M. Poly(Lactic Acid) (PLA) and Polyhydroxyalkanoates (PHAs), Green Alternatives to Petroleum-Based Plastics: A Review. *RSC Adv.* **2021**, *11*, 17151−17196.
(298) Cunha, B. L. C.; Bahú, J. O.; Xavier, L. F.; Crivellin, S.; de Souza, S. D. A.; Lodi, L.; Jardini, A. L.; Maciel Filho, R.; Schiavon, M. I. R. B.; Cárdenas Concha, V. O.; Severino, P.; Souto, E. B. Lactide: Production Routes, Properties, and Applications. *Bioengineering* **2022**, *9*, 164.
(299) Tábi, T.; Ageyeva, T.; Kovács, J. G. Improving the Ductility and Heat Deflection Temperature of Injection Molded Poly(Lactic Acid) Products: A Comprehensive Review. *Polym. Test.* **2021**, *101*, 107282.
(300) Martin, O.; Avérous, L. Poly(Lactic Acid): Plasticization and Properties of Biodegradable Multiphase Systems. *Polymer (Guildf).* **2001**, *42*, 6209−6219.
(301) Jacobsen, S.; Fritz, H. G. Plasticizing Polylactide - the Effect of Different Plasticizers on the Mechanical Properties. *Polym. Eng. Sci.* **1999**, *39*, 1303−1310.
(302) Singh, S.; Maspoch, M. Ll.; Oksman, K. Crystallization of Triethyl-Citrate-Plasticized Poly(Lactic Acid) Induced by Chitin Nanocrystals. *J. Appl. Polym. Sci.* **2019**, *136*, 47936.
(303) Chaos, A.; Sangroniz, A.; Fernández, J.; del Río, J.; Iriarte, M.; Sarasua, J. R.; Etxeberria, A. Plasticization of Poly(Lactide) with Poly(Ethylene Glycol): Low Weight Plasticizer vs Triblock Copolymers. Effect on Free Volume and Barrier Properties. *J. Appl. Polym. Sci.* **2020**, *137*, 48868.
(304) Kopinke, F. D.; Remmler, M.; Mackenzie, K.; Möder, M.; Wachsen, O. Thermal Decomposition of Biodegradable Polyesters - II. Poly(Lactic Acid). *Polym. Degrad. Stab.* **1996**, *53*, 329−342.
(305) Lim, L. T.; Auras, R.; Rubino, M. Processing Technologies for Poly(Lactic Acid). *Prog. Polym. Sci.* **2008**, *33*, 820−852.
(306) Lajus, S.; Dusséaux, S.; Verbeke, J.; Rigouin, C.; Guo, Z.; Fatarova, M.; Bellvert, F.; Borsenberger, V.; Bressy, M.; Nicaud, J. M.; et al. Engineering the Yeast *Yarrowia Lipolytica* for Production of Polylactic Acid Homopolymer. *Front. Bioeng. Biotechnol.* **2020**, *8*, 954.
(307) Jung, Y. K.; Kim, T. Y.; Park, S. J.; Lee, S. Y. Metabolic Engineering of *Escherichia Coli* for the Production of Polylactic Acid and Its Copolymers. *Biotechnol. Bioeng.* **2010**, *105*, 161−171.
(308) Jung, Y. K.; Lee, S. Y. Efficient Production of Polylactic Acid and Its Copolymers by Metabolically Engineered Escherichia Coli. *J. Biotechnol.* **2011**, *151*, 94−101.
(309) Kricheldorf, H. R.; Kreiser-Saunders, I.; Jurgens, C.; Wolter, D. Polylactides-synthesis, characterization and medical application. *Macromol. Symp.* **1996**, *103*, 85−I02.
(310) Ajioka, M.; Enomoto, K.; Suzuki, K.; Yamaguchi, A. The Basic Properties of Poly(Lactic Acid) Produced by the Direct Condensation Polymerization of Lactic Acid. *J. Environ. Polym. Degrad.* **1995**, *3*, 225−234.
(311) Stanford, M. J.; Dove, A. P. Stereocontrolled Ring-Opening Polymerisation of Lactide. *Chem. Soc. Rev.* **2010**, *39*, 486−494.
(312) Carothers, W. H.; Dorough, G.; Natta, F. V. Studies of Polymerization and Ring Formation. *J. Am. Chem. Soc.* **1932**, *54*, 761−772.
(313) Chisholm, M. H. Concerning the Ring-Opening Polymerization of Lactide and Cyclic Esters by Coordination Metal Catalysts. *Pure Appl. Chem.* **2010**, *82*, 1647−1662.
(314) Zhu, J. B.; Chen, E. Y. X. From Meso-Lactide to Isotactic Polylactide: Epimerization by B/N Lewis Pairs and Kinetic Resolution by Organic Catalysts. *J. Am. Chem. Soc.* **2015**, *137*, 12506−12509.
(315) Guillaume, S. M. Organic Catalysis for the Polymerization of Lactide and Related Cyclic Diesters. In *Organic Catalysis for Polymerization*; Dove, A., Sardon, H., Naumann, S., Eds.; Royal Society of Chemistry, 2018; pp 224−273.
(316) Tschan, M. J. L.; Gauvin, R. M.; Thomas, C. M. Controlling Polymer Stereochemistry in Ring-Opening Polymerization: A Decade of Advances Shaping the Future of Biodegradable Polyesters. *Chem. Soc. Rev.* **2021**, *50*, 13587−13608.
(317) Samantaray, P. K.; Little, A.; Wemyss, A. M.; Iacovidou, E.; Wan, C. Design and Control of Compostability in Synthetic Biopolyesters. *ACS Sustain. Chem. Eng.* **2021**, *9*, 9151−9164.
(318) *EPA, Advancing Sustainable Materials Management*: U.S. Environmental Protection Agency, 2013; https://www.epa.gov/

https://doi.org/10.1021/acs.chemrev.2c00644
Chem. Rev. XXXX, XXX, XXX−XXX

sites/default/files/2015-09/documents/2013_advncng_smm_fs.pdf (accessed 2015-09-14).
(319) Rossi, V.; Cleeve-Edwards, N.; Lundquist, L.; Schenker, U.; Dubois, C.; Humbert, S.; Jolliet, O. Life Cycle Assessment of End-of-Life Options for Two Biodegradable Packaging Materials: Sound Application of the European Waste Hierarchy. *J. Clean. Prod.* **2015**, *86*, 132−145.
(320) Chariyachotilert, C.; Joshi, S.; Selke, S. E.; Auras, R. Assessment of the Properties of Poly(L-Lactic Acid) Sheets Produced with Differing Amounts of Postconsumer Recycled Poly(L-Lactic Acid). *J. Plast. Film Sheeting* **2012**, *28* (4), 314−335.
(321) Tiso, T.; Winter, B.; Wei, R.; Hee, J.; de Witt, J.; Wierckx, N.; Quicker, P.; Bornscheuer, U. T.; Bardow, A.; Nogales, J.; Blank, L. M. The Metabolic Potential of Plastics as Biotechnological Carbon Sources - Review and Targets for the Future. *Metab. Eng.* **2022**, *71*, 77−98.
(322) Satti, S. M.; Shah, A. A.; Auras, R.; Marsh, T. L. Isolation and Characterization of Bacteria Capable of Degrading Poly(Lactic Acid) at Ambient Temperature. *Polym. Degrad. Stab.* **2017**, *144*, 392−400.
(323) Palsikowski, P. A.; Roberto, M. M.; Sommaggio, L. R. D.; Souza, P. M. S.; Morales, A. R.; Marin-Morales, M. A. Ecotoxicity Evaluation of the Biodegradable Polymers PLA, PBAT and Its Blends Using Allium Cepa as Test Organism. *J. Polym. Environ.* **2018**, *26*, 938−945.
(324) Satti, S. M.; Shah, A. A.; Marsh, T. L.; Auras, R. Biodegradation of Poly(Lactic Acid) in Soil Microcosms at Ambient Temperature: Evaluation of Natural Attenuation, Bio-Augmentation and Bio-Stimulation. *J. Polym. Environ.* **2018**, *26*, 3848−3857.
(325) Kliem, S.; Kreutzbruck, M.; Bonten, C. Review on the Biological Degradation of Polymers in Various Environments. *Materials.* **2020**, *13*, 4586.
(326) Satti, S. M.; Shah, A. A. Polyester-Based Biodegradable Plastics: An Approach towards Sustainable Development. *Lett. Appl. Microbiol.* **2020**, *70*, 413−430.
(327) Brodhagen, M.; Peyron, M.; Miles, C.; Inglis, D. A. Biodegradable Plastic Agricultural Mulches and Key Features of Microbial Degradation. *Appl. Microbiol. Biotechnol.* **2015**, *99*, 1039−1056.
(328) Madhavan Nampoothiri, K.; Nair, N. R.; John, R. P. An Overview of the Recent Developments in Polylactide (PLA) Research. *Bioresour. Technol.* **2010**, *101*, 8493−8501.
(329) Zaaba, N. F.; Jaafar, M. A Review on Degradation Mechanisms of Polylactic Acid: Hydrolytic, Photodegradative, Microbial, and Enzymatic Degradation. *Polym. Eng. Sci.* **2020**, *60*, 2061−2075.
(330) *About PlasticDB*; PlasticDB: Auckland, New Zealand, 2022; http://plasticdb.org (accessed 2022-07-15.
(331) Butbunchu, N.; Pathom-Aree, W. Actinobacteria as Promising Candidate for Polylactic Acid Type Bioplastic Degradation. *Front. Microbiol.* **2019**, *10*, 2834.
(332) Kamarudin, N. H. A.; Noor, D.; Raja Abd Rahman, R. N Z. Microbial Degradation Of Polylactic Acid Bioplastic. *J. Sustain. Sci. Manage.* **2021**, *16*, 299−317.
(333) Pranamuda, H.; Tokiwa, Y. Degradation of Poly(L-Lactide) by Strains Belonging to Genus Amycolatopsis. *Biotechnol. Lett.* **1999**, *21* (10), 901−905.
(334) Penkhrue, W.; Khanongnuch, C.; Masaki, K.; Pathom-aree, W.; Punyodom, W.; Lumyong, S. Isolation and Screening of Biopolymer-Degrading Microorganisms from Northern Thailand. *World J. Microbiol. Biotechnol.* **2015**, *31*, 1431−1442.
(335) Yagi, H.; Ninomiya, F.; Funabashi, M.; Kunioka, M. Mesophilic Anaerobic Biodegradation Test and Analysis of Eubacteria and Archaea Involved in Anaerobic Biodegradation of Four Specified Biodegradable Polyesters. *Polym. Degrad. Stab.* **2014**, *110*, 278−283.
(336) Pranamuda, H.; Tokiwa, Y.; Tanaka, H. Polylactide Degradation by an Amycolatopsis Sp. *Appl. Environ. Microbiol.* **1997**, *63*, 1637−1640.
(337) Ikura, Y.; Kudo, T. Isolation of a Microorganism Capable of Degrading Poly-(L-Lactide). *J. Gen. Appl. Microbiol.* **1999**, *45*, 247−251.
(338) Tokiwa, Y.; Konno, M.; Nishida, H. Isolation of Silk Degrading Microorganisms and Its Poly(L-Lactide) Degradability. *Chem. Lett.* **1999**, *28*, 355−356.
(339) Pranamuda, H.; Tsuchii, A.; Tokiwa, Y. Poly (L-Lactide)-Degrading Enzyme Produced by Amycolatopsis Sp. *Macromol. Biosci.* **2001**, *1*, 25−29.
(340) Nakamura, K.; Tomita, T.; Abe, N.; Kamio, Y. Purification and Characterization of an Extracellular Poly(L-Lactic Acid) Depolymerase from a Soil Isolate, Amycolatopsis Sp. Strain K104−1. *Appl. Environ. Microbiol.* **2001**, *67*, 345−353.
(341) Jarerat, A.; Tokiwa, Y.; Tanaka, H. Production of Poly(L-Lactide)-Degrading Enzyme by Amycolatopsis Orientalis for Biological Recycling of Poly(L-Lactide). *Appl. Microbiol. Biotechnol.* **2006**, *72*, 726−731.
(342) Li, F.; Wang, S.; Liu, W.; Chen, G. Purification and Characterization of Poly(l-Lactic Acid)-Degrading Enzymes from Amycolatopsis Orientalis Ssp. Orientalis. *FEMS Microbiol. Lett.* **2008**, *282*, 52−58.
(343) Jarerat, A.; Pranamuda, H.; Tokiwa, Y. Poly(L-lactide)-Degrading Activity in Various Actinomycetes. *Macromol. Biosci.* **2002**, *2*, 420.
(344) Chomchoei, A.; Pathom-Aree, W.; Yokota, A.; Kanongnuch, C.; Lumyong, S. Amycolatopsis Thailandensis Sp. Nov., a Poly(L-Lactic Acid)-Degrading Actinomycete, Isolated from Soil. *Int. J. Syst. Evol. Microbiol.* **2011**, *61*, 839−843.
(345) Decorosi, F.; Exana, M. L.; Pini, F.; Adessi, A.; Messini, A.; Giovannetti, L.; Viti, C. The Degradative Capabilities of New Amycolatopsis Isolates on Polylactic Acid. *Microorganisms* **2019**, *7*, 590.
(346) Jarerat, A.; Tokiwa, Y.; Tanaka, H. Microbial Poly(L-Lactide)-Degrading Enzyme Induced by Amino Acids, Peptides, and Poly(L-Amino Acids). *J. Polym. Environ.* **2004**, *12*, 139−146.
(347) Konkit, M.; Jarerat, A.; Kamongnuch, C.; Lumyong, S.; Pathom-aree, W. Poly(lactide) Degradation By Pseudonocardia Alni. *Chiang Mai J. Sci.* **2012**, *39*, 128−132.
(348) Apinya, T.; Sombatsompop, N.; Prapagdee, B. Selection of a Pseudonocardia Sp. RM423 That Accelerates the Biodegradation of Poly(Lactic) Acid in Submerged Cultures and in Soil Microcosms. *Int. Biodeterior. Biodegrad.* **2015**, *99*, 23−30.
(349) Sangwan, P.; Wu, D. Y. New Insights into Polylactide Biodegradation from Molecular Ecological Techniques. *Macromol. Biosci.* **2008**, *8*, 304−315.
(350) Sukkhum, S.; Tokuyama, S.; Tamura, T.; Kitpreechavanich, V. A Novel Poly (L-Lactide) Degrading Actinomycetes Isolated from Thai Forest Soil, Phylogenic Relationship and the Enzyme Characterization. *J. Gen. Appl. Microbiol.* **2009**, *55*, 459−467.
(351) Sriyapai, P.; Chansiri, K.; Sriyapai, T. Isolation and Characterization of Polyester-Based Plastics-Degrading Bacteria from Compost Soils. *Microbiology (Russian Fed.)* **2018**, *87*, 290−300.
(352) Husárová, L.; Pekařová, S.; Stloukal, P.; Kucharzcyk, P.; Verney, V.; Commereuc, S.; Ramone, A.; Koutny, M. Identification of Important Abiotic and Biotic Factors in the Biodegradation of Poly(l-Lactic Acid). *Int. J. Biol. Macromol.* **2014**, *71*, 155−162.
(353) Yottakot, S.; Leelavatcharamas, V. Isolation and Optimisation of Polylactic Acid (PLA)-Packaging-Degrading Actinomycete for PLA-Packaging Degradation. *Pertanika J. Trop. Agric. Sci.* **2019**, *42*, 1111−1129.
(354) Hajighasemi, M.; Nocek, B. P.; Tchigvintsev, A.; Brown, G.; Flick, R.; Xu, X.; Cui, H.; Hai, T.; Joachimiak, A.; Golyshin, P. N.; Savchenko, A.; Edwards, E. A.; Yakunin, A. F. Biochemical and Structural Insights into Enzymatic Depolymerization of Polylactic Acid and Other Polyesters by Microbial Carboxylesterases. *Biomacromolecules* **2016**, *17*, 2027−2039.
(355) Nawaz, A.; Hasan, F.; Shah, A. A. Degradation of Poly(ε-Caprolactone) (PCL) by a Newly Isolated Brevundimonas Sp. Strain MRL-AN1 from Soil. *FEMS Microbiol. Lett.* **2015**, *362*, 1−7.

https://doi.org/10.1021/acs.chemrev.2c00644
Chem. Rev. XXXX, XXX, XXX−XXX

(356) Nair, N. R.; Sekhar, V. C.; Nampoothiri, K. M. Augmentation of a Microbial Consortium for Enhanced Polylactide (PLA) Degradation. *Indian J. Microbiol.* **2016**, *56*, 59−63.
(357) Tchigvintsev, A.; Tran, H.; Popovic, A.; Kovacic, F.; Brown, G.; Flick, R.; Hajighasemi, M.; Egorova, O.; Somody, J. C.; Tchigvintsev, D.; Khusnutdinova, A.; Chernikova, T. N.; Golyshina, O. V.; Yakimov, M. M.; Savchenko, A.; Golyshin, P. N.; Jaeger, K. E.; Yakunin, A. F. The Environment Shapes Microbial Enzymes: Five Cold-Active and Salt-Resistant Carboxylesterases from Marine Metagenomes. *Appl. Microbiol. Biotechnol.* **2015**, *99*, 2165−2178.
(358) Urbanek, A. K.; Rymowicz, W.; Strzelecki, M. C.; Kociuba, W.; Franczak, Ł.; Mirończuk, A. M. Isolation and Characterization of Arctic Microorganisms Decomposing Bioplastics. *AMB Express* **2017**, *7*, 148.
(359) Wang, Z.; Wang, Y.; Guo, Z.; Li, F.; Chen, S. Purification and Characterization of Poly(L-Lactic Acid) Depolymerase From Pseudomonas Sp. Strain DS04-T. *Polym. Eng. Sci.* **2011**, *51*, 454−459.
(360) Liang, T. W.; Jen, S. N.; Nguyen, A. D.; Wang, S. L. Application of Chitinous Materialss in Production and Purification of a Poly(L-Lactic Acid) Depolymerase from *Pseudomonas Tamsuii* TKU015. *Polymers (Basel).* **2016**, *8*, 98.
(361) Kim, M. Y.; Kim, C.; Moon, J.; Heo, J.; Jung, S. P.; Kim, J. R. Polymer Film-Based Screening and Isolation of Polylactic Acid (PLA)-Degrading Microorganisms. *J. Microbiol. Biotechnol.* **2017**, *27*, 342−349.
(362) Bubpachat, T.; Sombatsompop, N.; Prapagdee, B. Isolation and Role of Polylactic Acid-Degrading Bacteria on Degrading Enzymes Productions and PLA Biodegradability at Mesophilic Conditions. *Polym. Degrad. Stab.* **2018**, *152*, 75−85.
(363) Shah, A. A.; Nawaz, A.; Kanwal, L.; Hasan, F.; Khan, S.; Badshah, M. Degradation of Poly(ε-Caprolactone) by a Thermophilic Bacterium Ralstonia Sp. Strain MRL-TL Isolated from Hot Spring. *Int. Biodeterior. Biodegrad.* **2015**, *98*, 35−42.
(364) Kim, M. N.; Park, S. T. Degradation of Poly(L-lactide) by a Mesophilic Bacterium. *J. Appl. Polym. Sci.* **2010**, *117*, 67−74.
(365) Prema, S.; Devi, U. M.; Pallempalli. Degradation of Polylactide Film by Depolymerase from Bacillus Amyloliquefaciens. *Int. J. Sci. Eng. Res.* **2015**, *5*, 520−525.
(366) Sakai, K.; Kawano, H.; Iwami, A.; Nakamura, M.; Moriguchi, M. Isolation of a Thermophilic Poly-L-Lactide Degrading Bacterium from Compost and Its Enzymatic Characterization. *J. Biosci. Bioeng.* **2001**, *92*, 298−300.
(367) Arena, M.; Abbate, C.; Fukushima, K.; Gennari, M. Degradation of Poly (Lactic Acid) and Nanocomposites by *Bacillus licheniformis*. *Environ. Sci. Pollut. Res.* **2011**, *18*, 865−870.
(368) Prema, S.; Palempalli, U. M. D. Degradation of Polylactide Plastic by PLA Depolymerase Isolated From Thermophilic Bacillus. *Int. J. Curr. Microbiol. Appl. Sci.* **2015**, *4*, 645−654.
(369) Kim, M. N.; Kim, W. G.; Weon, H. Y.; Lee, S. H. Poly(L-lactide)-Degrading Activity of a Newly Isolated Bacterium. *J. Appl. Polym. Sci.* **2008**, *109*, 234−239.
(370) Tomita, K.; Tsuji, H.; Nakajima, T.; Kikuchi, Y.; Ikarashi, K.; Ikeda, N. Degradation of Poly(D-Lactic Acid) by a Thermophile. *Polym. Degrad. Stab.* **2003**, *81*, 167−171.
(371) Oda, Y.; Yonetsu, A.; Urakami, T.; Tonomura, K. Degradation of Polylactide by Commercial Proteases. *J. Polym. Environ.* **2000**, *8*, 29−32.
(372) Castro-Aguirre, E.; Auras, R.; Selke, S.; Rubino, M.; Marsh, T. Enhancing the Biodegradation Rate of Poly(Lactic Acid) Films and PLA Bio-Nanocomposites in Simulated Composting through Bioaugmentation. *Polym. Degrad. Stab.* **2018**, *154*, 46−54.
(373) Tomita, K.; Nakajima, T.; Kikuchi, Y.; Miwa, N. Degradation of Poly(L-Lactic Acid) by a Newly Isolated Thermophile. *Polym. Degrad. Stab.* **2004**, *84*, 433−438.
(374) Chaisu, K.; Charles, A. L.; Guu, Y. K.; Chiu, C. H. Microbial Degradation of Poly Lactic Acid (PLA) by Aneurinibacillus Aneurinilyticus. *J. Biobased Mater. Bioenergy* **2013**, *7*, 509−511.
(375) Tomita, K.; Kuroki, Y.; Nagai, K. Isolation of Thermophiles Degrading Poly(L-Lactic Acid). *J. Biosci. Bioeng.* **1999**, *87*, 752−755.
(376) Akutsu-Shigeno, Y.; Teeraphatpornchai, T.; Teamtisong, K.; Nomura, N.; Uchiyama, H.; Nakahara, T.; Nakajima-Kambe, T. Cloning and Sequencing of a Poly(DL-Lactic Acid) Depolymerase Gene from *Paenibacillus amylolyticus* Strain TB-13 and Its Functional Expression in Escherichia Coli. *Appl. Environ. Microbiol.* **2003**, *69*, 2498−2504.
(377) Hanphakphoom, S.; Maneewong, N.; Sukkhum, S.; Tokuyama, S.; Kitpreechavanich, V. Characterization of Poly(L-Lactide)-Degrading Enzyme Produced by Thermophilic Filamentous Bacteria *Laceyella sacchari* LP175. *J. Gen. Appl. Microbiol.* **2014**, *60*, 13−22.
(378) Masaki, K.; Kamini, N. R.; Ikeda, H.; Iefuji, H. Cutinase-like Enzyme from the Yeast Cryptococcus Sp. Strain S-2 Hydrolyzes Polylactic Acid and Other Biodegradable Plastics. *Appl. Environ. Microbiol.* **2005**, *71*, 7548−7550.
(379) Watanabe, T.; Suzuki, K.; Shinozaki, Y.; Yarimizu, T.; Yoshida, S.; Sameshima-Yamashita, Y.; Koitabashi, M.; Kitamoto, H. K. A UV-Induced Mutant of *Cryptococcus Flavus* GB-1 with Increased Production of a Biodegradable Plastic-Degrading Enzyme. *Process Biochem.* **2015**, *50*, 1718−1724.
(380) Suzuki, K.; Sakamoto, H.; Shinozaki, Y.; Tabata, J.; Watanabe, T.; Mochizuki, A.; Koitabashi, M.; Fujii, T.; Tsushima, S.; Kitamoto, H. K. Affinity Purification and Characterization of a Biodegradable Plastic-Degrading Enzyme from a Yeast Isolated from the Larval Midgut of a Stag Beetle, *Aegus Laevicollis*. *Appl. Microbiol. Biotechnol.* **2013**, *97*, 7679−7688.
(381) Shinozaki, Y.; Morita, T.; Cao, X. H.; Yoshida, S.; Koitabashi, M.; Watanabe, T.; Suzuki, K.; Sameshima-Yamashita, Y.; Nakajima-Kambe, T.; Fujii, T.; Kitamoto, H. K. Biodegradable Plastic-Degrading Enzyme from Pseudozyma Antarctica: Cloning, Sequencing, and Characterization. *Appl. Microbiol. Biotechnol.* **2013**, *97*, 2951−2959.
(382) Antipova, T. V.; Zhelifonova, V. P.; Zaitsev, K. V.; Nedorezova, P. M.; Aladyshev, A. M.; Klyamkina, A. N.; Kostyuk, S. V.; Danilogorskaya, A. A.; Kozlovsky, A. G. Biodegradation of Poly-ε-Caprolactones and Poly-l-Lactides by Fungi. *J. Polym. Environ.* **2018**, *26*, 4350−4359.
(383) Maeda, H.; Yamagata, Y.; Abe, K.; Hasegawa, F.; Machida, M.; Ishioka, R.; Gomi, K.; Nakajima, T. Purification and Characterization of a Biodegradable Plastic-Degrading Enzyme from Aspergillus Oryzae. *Appl. Microbiol. Biotechnol.* **2005**, *67*, 778−788.
(384) Karamanlioglu, M.; Houlden, A.; Robson, G. D. Isolation and Characterisation of Fungal Communities Associated with Degradation and Growth on the Surface of Poly(Lactic) Acid (PLA) in Soil and Compost. *Int. Biodeterior. Biodegrad.* **2014**, *95* (PB), 301−310.
(385) Torres, A.; Li, S. M.; Roussos, S.; Vert, M. Screening of Microorganisms for Biodegradation of Poly(Lactic Acid) and Lactic Acid-Containing Polymers. *Appl. Environ. Microbiol.* **1996**, *62*, 2393−2397.
(386) Pellis, A.; Acero, E. H.; Weber, H.; Obersriebnig, M.; Breinbauer, R.; Srebotnik, E.; Guebitz, G. M. Biocatalyzed Approach for the Surface Functionalization of Poly(L-Lactic Acid) Films Using Hydrolytic Enzymes. *Biotechnol. J.* **2015**, *10*, 1739−1749.
(387) Williams, D. F. Enzymic Hydrolysis of Polylactic Acid. *Eng. Med.* **1981**, *10*, 5−7.
(388) Lipsa, R.; Tudorachi, N.; Darie-Nita, R. N.; Oprică, L.; Vasile, C.; Chiriac, A. Biodegradation of Poly(Lactic Acid) and Some of Its Based Systems with *Trichoderma Viride*. *Int. J. Biol. Macromol.* **2016**, *88*, 515−526.
(389) Suzuki, K.; Noguchi, M. T.; Shinozaki, Y.; Koitabashi, M.; Sameshima-Yamashita, Y.; Yoshida, S.; Fujii, T.; Kitamoto, H. K. Purification, Characterization, and Cloning of the Gene for a Biodegradable Plastic-Degrading Enzyme from Paraphoma-Related Fungal Strain B47−9. *Appl. Microbiol. Biotechnol.* **2014**, *98*, 4457−4465.
(390) Zrimec, J.; Kokina, M.; Jonasson, S.; Zorrilla, F.; Zelezniak, A. Plastic-Degrading Potential across the Global Microbiome Correlates with Recent Pollution Trends. *MBio* **2021**, *12* (5), No. e0215521.

https://doi.org/10.1021/acs.chemrev.2c00644
Chem. Rev. XXXX, XXX, XXX−XXX

(391) Mayumi, D.; Akutsu-Shigeno, Y.; Uchiyama, H.; Nomura, N.; Nakajima-Kambe, T. Identification and Characterization of Novel Poly(DL-Lactic Acid) Depolymerases from Metagenome. *Appl. Microbiol. Biotechnol.* **2008**, *79*, 743−750.
(392) Matsuda, E.; Abe, N.; Tamakawa, H.; Kaneko, J.; Kamio, Y. Gene Cloning and Molecular Characterization of an Extracellular Poly(L-Lactic Acid) Depolymerase from Amycolatopsis Sp. Strain K104−1. *J. Bacteriol.* **2005**, *187*, 7333−7340.
(393) Emadian, S. M.; Onay, T. T.; Demirel, B. Biodegradation of Bioplastics in Natural Environments. *Waste Manag.* **2017**, *59*, 526−536.
(394) Jarerat, A.; Tokiwa, Y. Degradation of Poly(L-Lactide) by a Fungus. *Macromol. Biosci.* **2001**, *1*, 136−140.
(395) Pattanasuttichonlakul, W.; Sombatsompop, N.; Prapagdee, B. Accelerating Biodegradation of PLA Using Microbial Consortium from Dairy Wastewater Sludge Combined with PLA-Degrading Bacterium. *Int. Biodeterior. Biodegrad.* **2018**, *132* (May), 74−83.
(396) Saadi, Z.; Rasmont, A.; Cesar, G.; Bewa, H.; Benguigui, L. Fungal Degradation of Poly(l-Lactide) in Soil and in Compost. *J. Polym. Environ.* **2012**, *20*, 273−282.
(397) Copinet, A.; Bertrand, C.; Govindin, S.; Coma, V.; Couturier, Y. Effects of Ultraviolet Light (315 Nm), Temperature and Relative Humidity on the Degradation of Polylactic Acid Plastic Films. *Chemosphere* **2004**, *55* (5), 763−773.
(398) Isono, Y.; Hoshino, A. Method for Degrading Polylactic Acid. JP 2001178483, 1999.
(399) Zhang, M.; Jia, H.; Li, C. The Polylactic Acid Degradation Bacteria and Its Application of One Plant of Production Protease. CN 110317762A, 2019.
(400) Tokiwa, Y.; Amunatto, J.; Tsuchiya, A. Method for Polylactic Acid Splitting Enzyme and/or Proteinase k-like Protease Production. JP 2003009855A, 2001.
(401) Sukhumaporn, S.; Shinji, T.; Prachumporn, K.; Tomohiko, T.; Yuumi, I.; Vichien, K. A Novel Poly (L-Lactide) Degrading Thermophilic Actinomycetes, *Actinomadura Keratinilytica* Strain T16−1 and Pla Sequencing. *African J. Microbiol. Res.* **2011**, *5*, 2575−2582.
(402) Lim, H. A.; Raku, T.; Tokiwa, Y. Hydrolysis of Polyesters by Serine Proteases. *Biotechnol. Lett.* **2005**, *27*, 459−464.
(403) Fukuzaki, H.; Yoshida, M.; Asano, M.; Kumakura, M. Synthesis of Copoly(D,L-Lactic Acid) with Relatively Low Molecular Weight and in Vitro Degradation. *Eur. Polym. J.* **1989**, *25*, 1019−1026.
(404) Reeve, M. S.; McCarthy, S. P.; Downey, M. J.; Gross, R. A. Polylactide Stereochemistry: Effect on Enzymic Degradability. *Macromolecules* **1994**, *27*, 825−831.
(405) Hoshino, A.; Isono, Y. Degradation of Aliphatic Polyester Films by Commercially Available Lipases with Special Reference to Rapid and Complete Degradation of Poly(L-Lactide) Film by Lipase PL Derived from Alcaligenes Sp. *Biodegradation* **2002**, *13*, 141−147.
(406) Vichaibun, V.; Chulavatnatol, M. A New Assay for the Enzymatic Degradation of Polylactic Acid. *ScienceAsia* **2003**, *29*, 297−300.
(407) Kawai, F.; Nakadai, K.; Nishioka, E.; Nakajima, H.; Ohara, H.; Masaki, K.; Iefuji, H. Different Enantioselectivity of Two Types of Poly(Lactic Acid) Depolymerases toward Poly(l-Lactic Acid) and Poly(d-Lactic Acid). *Polym. Degrad. Stab.* **2011**, *96*, 1342−1348.
(408) Miksch, L.; Gutow, L.; Saborowski, R. PH-Stat Titration: A Rapid Assay for Enzymatic Degradability of Bio-Based Polymers. *Polymers (Basel).* **2021**, *13*, 860.
(409) Noor, H.; Satti, S. M.; Din, S. ud; Farman, M.; Hasan, F.; Khan, S.; Badshah, M.; Shah, A. A. Insight on Esterase from *Pseudomonas Aeruginosa* Strain S3 That Depolymerize Poly(Lactic Acid) (PLA) at Ambient Temperature. *Polym. Degrad. Stab.* **2020**, *174* (2020), 109096.
(410) Kodama, Y.; Masaki, K.; Kondo, H.; Suzuki, M.; Tsuda, S.; Nagura, T.; Shimba, N.; Suzuki, E. I.; Iefuji, H. Crystal Structure and Enhanced Activity of a Cutinase-like Enzyme from Cryptococcus Sp. Strain S-2. *Proteins Struct. Funct. Bioinforma.* **2009**, *77*, 710−717.
(411) Shinozaki, Y.; Kikkawa, Y.; Sato, S.; Fukuoka, T.; Watanabe, T.; Yoshida, S.; Nakajima-Kambe, T.; Kitamoto, H. K. Enzymatic Degradation of Polyester Films by a Cutinase-like Enzyme from Pseudozyma Antarctica: Surface Plasmon Resonance and Atomic Force Microscopy Study. *Appl. Microbiol. Biotechnol.* **2013**, *97* (19), 8591−8598.
(412) Lomthong, T.; Guicherd, M.; Cioci, G.; Duquesne, S.; Marty, A.; Lumyong, S.; Kitpreechavanich, V. Poly(L-Lactide)-Degrading Enzyme from *Laceyella Sacchari* LP175: Cloning, Sequencing, Expression, Characterization and Its Hydrolysis of Poly(L-Lactide) Polymer. *Chiang Mai J. Sci.* **2019**, *46*, 417−430.
(413) Popovic, A.; Hai, T.; Tchigvintsev, A.; Hajighasemi, M.; Nocek, B.; Khusnutdinova, A. N.; Brown, G.; Glinos, J.; Flick, R.; Skarina, T.; Chernikova, T. N.; Yim, V.; Brüls, T.; Paslier, D. Le; Yakimov, M. M.; Joachimiak, A.; Ferrer, M.; Golyshina, O. V.; Savchenko, A.; Golyshin, P. N.; Yakunin, A. F. Activity Screening of Environmental Metagenomic Libraries Reveals Novel Carboxylesterase Families. *Sci. Rep.* **2017**, *7* (March), 1−15.
(414) Hajighasemi, M.; Tchigvintsev, A.; Nocek, B.; Flick, R.; Popovic, A.; Hai, T.; Khusnutdinova, A. N.; Brown, G.; Xu, X.; Cui, H.; Anstett, J.; et al. Screening and Characterization of Novel Polyesterases from Environmental Metagenomes with High Hydrolytic Activity against Synthetic Polyesters. *Environ. Sci. Technol.* **2018**, *52*, 12388−12401.
(415) Alvarez, P.; Amilastre, E.; Duquesne, S.; Marty, A. Polypeptide Having a Polyester Degrading Activity and Uses Thereof. WO 2016062695, 2014.
(416) Marty, A.; Duquesne, S.; Guicherd, M.; Gueroult, M.; André, I. Patents Novel Proteases and Uses Thereof. WO 2019122308, 2017.
(417) Marty, A.; Duquesne, S.; Guicherd, M.; Vuillemin, M.; Ben Khaled, M. Improved Plastic Degrading Proteases. WO 2018109183, 2016.
(418) *MEROPS, The Peptidase Database*; EMBL-EBI, 2021https://www.ebi.ac.uk/merops/.
(419) Rawlings, N. D.; Barrett, A. J.; Thomas, P. D.; Huang, X.; Bateman, A.; Finn, R. D. The MEROPS Database of Proteolytic Enzymes, Their Substrates and Inhibitors in 2017 and a Comparison with Peptidases in the PANTHER Database. *Nucleic Acids Res.* **2018**, *46* (D1), D624−D632.
(420) Gouda, M. K.; Kleeberg, I.; Van den Heuvel, J.; Müller, R. J.; Deckwer, W. D. Production of a Polyester Degrading Extracellular Hydrolase from *Thermomonospora Fusca*. *Biotechnol. Prog.* **2002**, *18*, 927−934.
(421) Youngpreda, A.; Panyachanakul, T.; Kitpreechavanich, V.; Sirisansaneeyakul, S.; Suksamrarn, S.; Tokuyama, S.; Krajangsang, S. Optimization of Poly(Dl-Lactic Acid) Degradation and Evaluation of Biological Re-Polymerization. *J. Polym. Environ.* **2017**, *25*, 1131−1139.
(422) Sukkhum, S.; Tokuyama, S.; Kitpreechavanich, V. Development of Fermentation Process for PLA-Degrading Enzyme Production by a New Thermophilic Actinomadura Sp. T16−1. *Biotechnol. Bioprocess Eng.* **2009**, *14*, 302−306.
(423) Lomthong, T.; Hanphakphoom, S.; Kongsaeree, P.; Srisuk, N.; Guicherd, M.; Cioci, G.; Duquesne, S.; Marty, A.; Kitpreechavanich, V. Enhancement of Poly(L-Lactide)-Degrading Enzyme Production by Laceyella Sacchari LP175 Using Agricultural Crops as Substrates and Its Degradation of Poly(L-Lactide) Polymer. *Polym. Degrad. Stab.* **2017**, *143*, 64−73.
(424) Sameshima-Yamashita, Y.; Koitabashi, M.; Tsuchiya, W.; Suzuki, K.; Watanabe, T.; Shinozaki, Y.; Yamamoto-Tamura, K.; Yamazaki, T.; Kitamoto, H. Enhancement of Biodegradable Plastic-Degrading Enzyme Production from Paraphoma-like Fungus, Strain B47−9. *J. Oleo Sci.* **2016**, *65* (3), 257−262.
(425) Betzel, C.; Klupsch, S.; Papendorf, G.; Hastrup, S.; Branner, S.; Wilson, K. S. Crystal Structure of the Alkaline Proteinase Savinase™ from *Bacillus Lentus* at 1.4 Å Resolution. *J. Mol. Biol.* **1992**, *223*, 427−445.

https://doi.org/10.1021/acs.chemrev.2c00644
Chem. Rev. XXXX, XXX, XXX−XXX

(426) Alden, R. A.; Birktoft, J. J.; Kraut, J.; Robertus, J. D.; Wright, C. S. Atomic Coordinates for Subtilisin BPN′ (or Novo). *Biochem. Biophys. Res. Commun.* **1971**, *45*, 337−344.
(427) Bode, W.; Papamokos, E.; Musil, D. The High-resolution X-ray Crystal Structure of the Complex Formed between Subtilisin Carlsberg and Eglin c, an Elastase Inhibitor from the Leech Hirudo Medicinalis Structural Analysis, Subtilisin Structure and Interface Geometry. *Eur. J. Biochem.* **1987**, *166*, 673−692.
(428) Betzel, C.; Pal, G. P.; Saenger, W. Three-dimensional Structure of Proteinase K at 0.15-nm Resolution. *Eur. J. Biochem.* **1988**, *178*, 155−171.
(429) Kold, D.; Dauter, Z.; Laustsen, A. K.; Brzozowski, A. M.; Turkenburg, J. P.; Nielsen, A. D.; Koldsø, H.; Petersen, E.; Schiøtt, B.; De Maria, L.; Wilson, K. S.; Svendsen, A.; Wimmer, R. Thermodynamic and Structural Investigation of the Specific SDS Binding of Humicola Insolens Cutinase. *Protein Sci.* **2014**, *23*, 1023−1035.
(430) Munro, G. K. L.; McHale, R. H.; Saul, D. J.; Reeves, R. A.; Bergquist, P. L. A Gene Encoding a Thermophilic Alkaline Serine Proteinase from Thermos Sp. Strain Rt41A and Its Expression in *Escherichia Coli*. *Microbiology* **1995**, *141*, 1731−1738.
(431) Peek, K.; Daniel, R. M.; Monk, C.; Parker, L.; Coolbear, T. Purification and Characterization of a Thermostable Proteinase Isolated from Thermus Sp. Strain Rt41A. *Eur. J. Biochem.* **1992**, *207*, 1035−1044.
(432) Panyachanakul, T.; Sorachart, B.; Lumyong, S.; Lorliam, W.; Kitpreechavanich, V.; Krajangsang, S. Development of Biodegradation Process for Poly(DL-Lactic Acid)Degradation by Crude Enzyme Produced by *Actinomadura Keratinilytica* Strain T16−1. *Electron. J. Biotechnol.* **2019**, *40*, 52−57.
(433) Ohtaki, S.; Maeda, H.; Takahashi, T.; Yamagata, Y.; Hasegawa, F.; Gomi, K.; Nakajima, T.; Abe, K. Novel Hydrophobic Surface Binding Protein, HsbA, Produced by Aspergillus Oryzae. *Appl. Environ. Microbiol.* **2006**, *72*, 2407−2413.
(434) Takahashi, T.; Maeda, H.; Yoneda, S.; Ohtaki, S.; Yamagata, Y.; Hasegawa, F.; Gomi, K.; Nakajima, T.; Abe, K. The Fungal Hydrophobin RolA Recruits Polyesterase and Laterally Moves on Hydrophobic Surfaces. *Mol. Microbiol.* **2005**, *57*, 1780−1796.
(435) MacDonald, R. T.; McCarthy, S. P.; Gross, R. A. Enzymatic Degradability of Poly(Lactide): Effects of Chain Stereochemistry and Material Crystallinity. *Macromolecules* **1996**, *29*, 7356−7361.
(436) Makino, K.; Arakawa, M.; Kondo, T. Preparation and in Vitro Degradation Properties of Polylactide Microcapsules. *Chem. Pharm. Bull.* **1985**, *33*, 1195−1201.
(437) Chinaglia, S.; Tosin, M.; Degli-Innocenti, F. Biodegradation Rate of Biodegradable Plastics at Molecular Level. *Polym. Degrad. Stab.* **2018**, *147*, 237−244.
(438) Tsuji, H.; Miyauchi, S. Poly(L-Lactide): VI. Effects of Crystallinity on Enzymatic Hydrolysis of Poly(L-Lactide) without Free Amorphous Region. *Polym. Degrad. Stab.* **2001**, *71*, 415−424.
(439) Muller, A.; Hinrichs, W.; Wolf, W. M.; Saenger, W. Crystal Structure of Calcium-Free Proteinase K at 1.5-Å Resolution. *J. Biol. Chem.* **1994**, *269*, 23108−23111.
(440) Nakajima-Kambe, T.; Edwinoliver, N. G.; Maeda, H.; Thirunavukarasu, K.; Gowthaman, M. K.; Masaki, K.; Mahalingam, S.; Kamini, N. R. Purification, Cloning and Expression of an Aspergillus Niger Lipase for Degradation of Poly(Lactic Acid) and Poly(ε-Caprolactone). *Polym. Degrad. Stab.* **2012**, *97*, 139−144.
(441) Li, S.; Girard, A.; Garreau, H.; Vert, M. Enzymatic Degradation of Polylactide Stereocopolymers with Predominant D-Lactyl Contents. *Polym. Degrad. Stab.* **2000**, *71*, 61−67.
(442) Li, S.; Tenon, M.; Garreau, H.; Braud, C.; Vert, M. Enzymatic Degradation of Stereocopolymers Derived from L-, DL- and Meso-Lactides. *Polym. Degrad. Stab.* **2000**, *67*, 85−90.
(443) Nilsson, F.; Lan, X.; Gkourmpis, T.; Hedenqvist, M. S.; Gedde, U. W. Modelling Tie Chains and Trapped Entanglements in Polyethylene. *Polymer (Guildf).* **2012**, *53*, 3594−3601.
(444) Tsuji, H.; Ikada, Y. Properties and Morphologies of Poly(l-Lactide): 1. Annealing Condition Effects on Properties and Morphologies of Poly(l-Lactide). *Polymer (Guildf).* **1995**, *36*, 2709−2716.
(445) Kikkawa, Y.; Abe, H.; Iwata, T.; Inoue, Y.; Doi, Y. Crystallization, Stability, and Enzymatic Degradation of Poly(L-Lactide) Thin Film. *Biomacromolecules* **2002**, *3*, 350−356.
(446) Iwata, T.; Doi, Y. Morphology and Enzymatic Degradation of Poly(L-Lactic Acid) Single Crystals. *Macromolecules* **1998**, *31*, 2461−2467.
(447) Tsuji, H.; Miyauchi, S. Poly(L-Lactide): 7. Enzymatic Hydrolysis of Free and Restricted Amorphous Regions in Poly(L-Lactide) Films with Different Crystallinities and a Fixed Crystalline Thickness. *Polymer (Guildf).* **2001**, *42*, 4463−4467.
(448) Cai, H.; Dave, V.; Gross, R. A.; McCarthy, S. P. Effects of Physical Aging, Crystallinity, and Orientation on the Enzymatic Degradation of Poly(Lactic Acid). *J. Polym. Sci., Part B: Polym. Phys.* **1996**, *34*, 2701−2708.
(449) Li, S.; McCarthy, S. Influence of Crystallinity and Stereochemistry on the Enzymatic Degradation of Poly(Lactide)S. *Macromolecules* **1999**, *32*, 4454−4456.
(450) Nofar, M.; Sacligil, D.; Carreau, P. J.; Kamal, M. R.; Heuzey, M. C. Poly (Lactic Acid) Blends: Processing, Properties and Applications. *Int. J. Biol. Macromol.* **2019**, *125*, 307−360.
(451) Jang, W. Y.; Shin, B. Y.; Lee, T. J.; Narayan, R. Thermal Properties and Morphology of Biodegradable PLA/Starch Compatibilized Blends. *J. Ind. Eng. Chem.* **2007**, *13*, 457−464.
(452) Gattin, R.; Copinet, A.; Bertrand, C.; Couturier, Y. Biodegradation Study of a Starch and Poly(Lactic Acid) Co-Extruded Material in Liquid, Composting and Inert Mineral Media. *Int. Biodeterior. Biodegrad.* **2002**, *50*, 25−31.
(453) Yang, S.; Madbouly, S. A.; Schrader, J. A.; Srinavasan, G.; Grewell, D.; McCabe, K. G.; Kessler, M. R.; Graves, W. R. Characterization and biodegradation behavior of bio-based poly(lactic acid) and soy protein blends for sustainable horticultural applications. *Green Chem.* **2015**, *17*, 380.
(454) Wu, C. S. Renewable Resource-Based Composites of Recycled Natural Fibers and Maleated Polylactide Bioplastic: Characterization and Biodegradability. *Polym. Degrad. Stab.* **2009**, *94*, 1076−1084.
(455) Weng, Y.; Wang, L.; Zhang, M.; Wang, X.; Wang, Y. Biodegradation Behavior of P (3HB, 4HB)/ PLA Blends in Real Soil Environments. *Polym. Test.* **2013**, *32*, 60−70.
(456) Zhang, M. I. N.; Thomas, N. L. Blending Polylactic Acid with Polyhydroxybutyrate : The Effect on Thermal, Mechanical, and Biodegradation Properties. *Adv. Polym. Technol.* **2010**, *30*, 67−79.
(457) Kikkawa, Y.; Suzuki, T.; Kanesato, M.; Doi, Y.; Abe, H. Effect of Phase Structure on Enzymatic Degradation in Poly(L-Lactide)/ Atactic Poly(3-Hydroxybutyrate) Blends with Different Miscibility. *Biomacromolecules* **2009**, *10*, 1013−1018.
(458) Jeszeová, L.; Puškárová, A.; Bučková, M.; Kraková, L.; Grivalský, T.; Danko, M.; Mosnáčková, K.; Chmela, Š.; Pangallo, D. Microbial Communities Responsible for the Degradation of Poly-(Lactic Acid)/Poly(3-Hydroxybutyrate) Blend Mulches in Soil Burial Respirometric Tests. *World J. Microbiol. Biotechnol.* **2018**, *34*, 0.
(459) Wang, S.; Ma, P.; Wang, R.; Wang, S.; Zhang, Y.; Zhang, Y. Mechanical, Thermal and Degradation Properties of Poly(d,l-Lactide)/Poly(Hydroxybutyrate-Co-Hydroxyvalerate)/Poly(Ethylene Glycol) Blend. *Polym. Degrad. Stab.* **2008**, *93*, 1364−1369.
(460) Arrieta, M. P.; López, J.; Rayón, E.; Jiménez, A. Disintegrability under Composting Conditions of Plasticized PLA-PHB Blends. *Polym. Degrad. Stab.* **2014**, *108*, 307−318.
(461) Sheth, M.; Kumar, R. A.; Dave, V.; Gross, R. A.; McCarthy, S. P. Biodegradable Polymer Blends of Poly (Lactic Acid) and Poly (Ethylene Glycol). *J. Appl. Polym. Sci.* **2008**, *66*, 1495−1505.
(462) Nair, N. R.; Nampoothiri, K. M.; Pandey, A. Preparation of Poly(l-Lactide) Blends and Biodegradation by Lentzea Waywayandensis. *Biotechnol. Lett.* **2012**, *34*, 2031−2035.
(463) Liu, L.; Li, S.; Garreau, H.; Vert, M. Selective Enzymatic Degradation of Poly (L-lactide) and Poly(ε-caprolactone) Blend Films. *Biomacromolecules* **2000**, *1*, 350−359.

https://doi.org/10.1021/acs.chemrev.2c00644
Chem. Rev. XXXX, XXX, XXX−XXX

(464) Sivalingam, G.; Vijayalakshmi, S. P.; Madras, G. Enzymatic and Thermal Degradation of Poly (E-Caprolactone), Poly (D,L-Lactide), and Their Blends. *Ind. Eng. Chem. Res.* **2004**, *43*, 7702−7709.
(465) Van Cong, D.; Hoang, T.; Giang, N. V.; Ha, N. T.; Lam, T. D.; Sumita, M. A Novel Enzymatic Biodegradable Route for PLA/EVA Blends under Agricultural Soil of Vietnam. *Mater. Sci. Eng., C* **2012**, *32*, 558−563.
(466) Gajria, A. M.; Davé, V.; Gross, R. A.; McCarthy, S. P. Miscibility and Biodegradability of Blends of Poly(lactic acid) and Poly(vinyl acetate). *Polymer* **1996**, *37*, 437−444.
(467) Mahalik, J. P.; Madras, G. Enzymatic Degradation of Poly(D,L-Lactide) and Its Blends with Poly(Vinyl Acetate). *J. Appl. Polym. Sci.* **2006**, *101*, 675−680.
(468) Cheng, Y.; Deng, S.; Chen, P.; Ruan, R. Polylactic Acid (PLA) Synthesis and Modifications: A Review. *Front. Chem. China* **2009**, *4*, 259−264.
(469) Castro-Aguirre, E.; Auras, R.; Selke, S.; Rubino, M.; Marsh, T. Impact of Nanoclays on the Biodegradation of Poly(Lactic Acid) Nanocomposites. *Polymers (Basel).* **2018**, *10*, 202.
(470) Malwela, T.; Ray, S. S. Enzymatic Degradation Behavior of Nanoclay Reinforced Biodegradable PLA/PBSA Blend Composites. *Int. J. Biol. Macromol.* **2015**, *77*, 131−142.
(471) Tolga, S.; Kabasci, S.; Duhme, M. Progress of Disintegration of Polylactide (PLA)/Poly(Butylene Succinate) (PBS) Blends Containing Talc and Chalk Inorganic Fillers under Industrial Composting Conditions. *Polymers (Basel).* **2020**, *13*, 10.
(472) Katayama, T. Method for Decomposition of Biodegradable Resin. RU 2016116270, 2014.
(473) Katayama, T. Method for Degrading Biodegradable Resin. CA 02924964, 2018.
(474) Katayama, T.; Yoshikawa, S.; Kogure, M. Method for Treating Biodegradable Resin. JP 2011157483, 2010.
(475) Matsumura, S. Enzymatic Depolymerization Method of Polylactic Acid and Method for Producing Polylactic Acid Using Depolymerization Product. WO 2004013217, 2004.
(476) Ganesh, M.; Dave, R. N.; L'Amoreaux, W.; Gross, R. A. Embedded Enzymatic Biomaterial Degradation. *Macromolecules* **2009**, *42*, 6836−6839.
(477) Ganesh, M.; Gross, R. A. Embedded Enzymatic Biomaterial Degradation: Flow Conditions & Relative Humidity. *Polymer (Guildf).* **2012**, *53*, 3454−3461.
(478) DelRe, C.; Jiang, Y.; Kang, P.; Kwon, J.; Hall, A.; Jayapurna, I.; Ruan, Z.; Ma, L.; Zolkin, K.; Li, T.; Scown, C. D.; Ritchie, R. O.; Russell, T. P.; Xu, T. Near-Complete Depolymerization of Polyesters with Nano-Dispersed Enzymes. *Nature* **2021**, *592*, 558−563.
(479) Greene, A. F.; Vaidya, A.; Collet, C.; Wade, K. R.; Patel, M.; Gaugler, M.; West, M.; Petcu, M.; Parker, K. 3D-Printed Enzyme-Embedded Plastics. *Biomacromolecules* **2021**, *22*, 1999−2009.
(480) Huang, Q.; Hiyama, M.; Kabe, T.; Kimura, S.; Iwata, T. Enzymatic Self-Biodegradation of Poly(l -Lactic Acid) Films by Embedded Heat-Treated and Immobilized Proteinase K. *Biomacromolecules* **2020**, *21*, 3301−3307.
(481) Panda, P.; Appalashetti, M.; Judeh, Z. M. A. Phenylpropanoid Sucrose Esters: Plant-Derived Natural Products as Potential Leads for New Therapeutics. *Curr. Med. Chem.* **2011**, *18*, 3234−3251.
(482) Kind, S.; Neubauer, S.; Becker, J.; Yamamoto, M.; Völkert, M.; von Abendroth, G.; Zelder, O.; Wittmann, C. From Zero to Hero - Production of Bio-Based Nylon from Renewable Resources Using Engineered Corynebacterium Glutamicum. *Metab. Eng.* **2014**, *25*, 113−123.
(483) *Global Nylon Industry*; ReportLinker, 2021; https://www.reportlinker.com/P03993523/global-nylon-industry.html.
(484) Turk, S. C. H. J.; Kloosterman, W. P.; Ninaber, D. K.; Kolen, K. P. A. M.; Knutova, J.; Suir, E.; Schürmann, M.; Raemakers-Franken, P. C.; Müller, M.; De Wildeman, S. M. A.; Raamsdonk, L. M.; Van Der Pol, R.; Wu, L.; Temudo, M. F.; Van Der Hoeven, R. A. M.; Akeroyd, M.; Van Der Stoel, R. E.; Noorman, H. J.; Bovenberg, R. A. L.; Trefzer, A. C. Metabolic Engineering toward Sustainable Production of Nylon-6. *ACS Synth. Biol.* **2016**, *5*, 65−73.
(485) Yamano, N.; Kawasaki, N.; Ida, S.; Nakayama, A. Biodegradation of Polyamide 4 in Seawater. *Polym. Degrad. Stab.* **2019**, *166*, 230−236.
(486) *Aquafil*; Aquafil SpA, 2022; www.aquafil.com.
(487) Robello, R.; Calenti, F.; Jahic, D.; Mikuz, M. Method of Polyamide Fiber Recycling from Elastomeric Fabrics. WO 2013032408A1, 2013.
(488) Karasiak, W.; Karasiak, D. Method and Device for Treating Polymers. WO 2014072483A1, 2012.
(489) Kumar, A.; Von Wolff, N.; Rauch, M.; Zou, Y. Q.; Shmul, G.; Ben-David, Y.; Leitus, G.; Avram, L.; Milstein, D. Hydrogenative Depolymerization of Nylons. *J. Am. Chem. Soc.* **2020**, *142*, 14267−14275.
(490) Bonaldi, R. R.; Gorescu, G.; Pak, P. H.; Macret, R. Biodegradable Polyamide Fiber, Process for Obtaining Such Fiber and Polyamide Article Made Therefrom. WO 2016079724A2, 2016.
(491) Ragupathy, L.; Ziener, U.; Dyllick-Brenzinger, R.; Von Vacano, B.; Landfester, K. Enzyme-Catalyzed Polymerizations at Higher Temperatures: Synthetic Methods to Produce Polyamides and New Poly(Amide-Co-Ester)S. *J. Mol. Catal. B Enzym.* **2012**, *76*, 94−105.
(492) Negoro, S.; Kato, D.-i.; Ohki, T.; Yasuhira, K.; Kawashima, Y.; Nagai, K.; Takeo, M.; Shibata, N.; Kamiya, K.; Shigeta, Y. *Structural and Functional Characterization of Nylon Hydrolases*, 1st ed.; Elsevier, 2021; Vol *648*.
(493) Negoro, S. Biodegradation of Nylon Oligomers. *Appl. Microbiol. Biotechnol.* **2000**, *54*, 461−466.
(494) Heumann, S.; Eberl, A.; Pobeheim, H.; Liebminger, S.; Fischer-Colbrie, G.; Almansa, E.; Cavaco-Paulo, A.; Gübitz, G. M. New Model Substrates for Enzymes Hydrolysing Polyethyleneterephthalate and Polyamide Fibres. *J. Biochem. Biophys. Methods* **2006**, *69*, 89−99.
(495) Yasuhira, K.; Uedo, Y.; Takeo, M.; Kato, D. I.; Negoro, S. Genetic Organization of Nylon-Oligomer-Degrading Enzymes from Alkalophilic Bacterium, Agromyces Sp. KY5R. *J. Biosci. Bioeng.* **2007**, *104* (6), 521−524.
(496) Tomita, K.; Ikeda, N.; Ueno, A. Isolation and Characterization of a Thermophilic Bacterium, Geobacillus Thermocatenulatus, Degrading Nylon 12 and Nylon 66. *Biotechnol. Lett.* **2003**, *25*, 1743−1746.
(497) Almansa, E.; Heumann, S.; Eberl, A.; Kaufmann, F.; Cavaco-paulo, A.; Gübitz, G. M. Surface Hydrolysis of Polyamide with a New Polyamidase from Beauveria Brongniartii. *Biocatal. Biotransformation* **2008**, *26*, 371−377.
(498) Smith, R.; Oliver, C.; Williams, D. F. The enzymatic degradation of polymers in vitro. *J. Biomed. Mater. Res.* **1987**, *21*, 991−1003.
(499) Miettinen-Oinonen, A.; Puolakka, A.; Buchert, J. Method for Modifying Polyamide. WO 2005121438A2, 2004.
(500) Kanelli, M.; Vasilakos, S.; Ladas, S.; Symianakis, E.; Christakopoulos, P.; Topakas, E. Surface Modification of Polyamide 6.6 Fibers by Enzymatic Hydrolysis. *Process Biochem.* **2017**, *59*, 97−103.
(501) Parvinzadeh, M.; Assefipour, R.; Kiumarsi, A. Biohydrolysis of Nylon 6,6 Fiber with Different Proteolytic Enzymes. *Polym. Degrad. Stab.* **2009**, *94*, 1197−1205.
(502) Silva, C.; Araújo, R.; Casal, M.; Gübitz, G. M.; Cavaco-Paulo, A. Influence of Mechanical Agitation on Cutinases and Protease Activity towards Polyamide Substrates. *Enzyme Microb. Technol.* **2007**, *40*, 1678−1685.
(503) Silva, C.; Cavaco-Paulo, A. Monitoring Biotransformations in Polyamide Fibres. *Biocatal. Biotransformation* **2004**, *22*, 357−360.
(504) Silva, C. M.; Carneiro, F.; O'Neill, A.; Fonseca, L. P.; Cabral, J. S. M.; Guebitz, G.; Cavaco-Paulo, A. Cutinase - A New Tool for Biomodification of Synthetic Fibers. *J. Polym. Sci. Part A Polym. Chem.* **2005**, *43*, 2448−2450.

https://doi.org/10.1021/acs.chemrev.2c00644
Chem. Rev. XXXX, XXX, XXX−XXX

(505) Biundo, A.; Ribitsch, D.; Syren, P.-O.; Guebitz, G. M. Increasing Amide Acceptance on a Polyester-Hydrolyzing Enzyme. *N. Biotechnol.* **2016**, *33* (2016), S105.
(506) Negoro, S.; Taniguchi, T.; Kanaoka, M.; Kimura, H.; Okada, H. Plasmid-Determined Enzymatic Degradation of Nylon Oligomers. *J. Bacteriol.* **1983**, *155*, 22−31.
(507) Negoro, S.; Ohki, T.; Shibata, N.; Mizuno, N.; Wakitani, Y.; Tsurukame, J.; Matsumoto, K.; Kawamoto, I.; Takeo, M.; Higuchi, Y. X-Ray Crystallographic Analysis of 6-Aminohexanoate-Dimer Hydrolase: Molecular Basis for the Birth of a Nylon Oligomer-Degrading Enzyme. *J. Biol. Chem.* **2005**, *280*, 39644−39652.
(508) Negoro, S.; Ohki, T.; Shibata, N.; Sasa, K.; Hayashi, H.; Nakano, H.; Yasuhira, K.; Kato, D.-I.; Takeo, M.; Higuchi, Y. Nylon-Oligomer Degrading Enzyme/Substrate Complex: Catalytic Mechanism of 6-Aminohexanoate-Dimer Hydrolase. *J. Mol. Biol.* **2007**, *370*, 142−156.
(509) Yasuhira, K.; Shibata, N.; Mongami, G.; Uedo, Y.; Atsumi, Y.; Kawashima, Y.; Hibino, A.; Tanaka, Y.; Lee, Y. H.; Kato, D. I.; Takeo, M.; Higuchi, Y.; Negoro, S. X-Ray Crystallographic Analysis of the 6-Aminohexanoate Cyclic Dimer Hydrolase: Catalytic Mechanism and Evolution of an Enzyme Responsible for Nylon-6 Byproduct Degradation. *J. Biol. Chem.* **2010**, *285*, 1239−1248.
(510) Takehara, I.; Fujii, T.; Tanimoto, Y.; Kato, D. I.; Takeo, M.; Negoro, S. Correction to: Metabolic Pathway of 6-Aminohexanoate in the Nylon Oligomer-Degrading Bacterium Arthrobacter Sp. KI72: Identification of the Enzymes Responsible for the Conversion of 6-Aminohexanoate to Adipate (Applied Microbiology and Biotechnology, (201. *Appl. Microbiol. Biotechnol.* **2018**, *102*, 815.
(511) Negoro, S. *Biodegradation of Nylon and Other Synthetic Polyamides.*; Steinbuechel, Ed.; Springer-Verlag: Berlin, 2002.
(512) Negoro, S.; Shibata, N.; Tanaka, Y.; Yasuhira, K.; Shibata, H.; Hashimoto, H.; Lee, Y. H.; Oshima, S.; Santa, R.; Mochiji, K.; et al. Three-Dimensional Structure of Nylon Hydrolase and Mechanism of Nylon-6 Hydrolysis. *J. Biol. Chem.* **2012**, *287*, 5079−5090.
(513) Crouzet, J.; Faucher, D.; Favre-Bulle, O.; Jourdat, C.; Petre, D.; Pierrard, J.; Thibaut, D.; Guitton, C. Enzymes and Micro-Organisms with Amidase Activity Which Hydrolyses Polyamides. WO 1997004083A1, 1995.
(514) Crouzet, J.; Favre-Bulle, O.; Jourdat, C.; Coq, A.-M. Le; Petre, D. Enzymes and Microorganisms Having Amidase Activity for Hydrolysing Polyamides. WO 1997004084A1, 1995.
(515) Heumann, S.; Eberl, A.; Fischer-Colbrie, G.; Pobeheim, H.; Kaufmann, F.; Ribitsch, D.; Cavaco-Paulo, A.; Guebitz, G. M. A Novel Aryl Acylamidase from Nocardia Farcinica Hydrolyses Polyamide. *Biotechnol. Bioeng.* **2009**, *102*, 1003−1011.
(516) Acero, E. H.; Ribitsch, D.; Rodriguez, R. D.; Dellacher, A.; Zitzenbacher, S.; Marold, A.; Greimel, K. J.; Schroeder, M.; Kandelbauer, A.; Heumann, S.; Nyanhongo, G. S.; Schwab, H.; Guebitz, G. M. Two-Step Enzymatic Functionalisation of Polyamide with Phenolics. *J. Mol. Catal. B Enzym.* **2012**, *79*, 54−60.
(517) Ohtaki, S.; Takahashi, T.; Tanaka, T.; Fujita, H.; Yamagata, Y.; Abe, K.; Hasegawa, F.; Gomi, K. Novel Ceramidase and Use Thereof. WO 2007029630A1, 2006.
(518) Kamiya, K.; Baba, T.; Boero, M.; Matsui, T.; Negoro, S.; Shigeta, Y. Nylon-Oligomer Hydrolase Promoting Cleavage Reactions in Unnatural Amide Compounds. *J. Phys. Chem. Lett.* **2014**, *5*, 1210−1216.
(519) Baba, T.; Boero, M.; Kamiya, K.; Ando, H.; Negoro, S.; Nakano, M.; Shigeta, Y. Unraveling the Degradation of Artificial Amide Bonds in Nylon Oligomer Hydrolase: From Induced-Fit to Acylation Processes. *Phys. Chem. Chem. Phys.* **2015**, *17*, 4492−4504.
(520) Deguchi, T.; Kakezawa, M.; Nishida, T. Nylon Biodegradation by Lignin-Degrading Fungi. *Appl. Environ. Microbiol.* **1997**, *63*, 329−331.
(521) Deguchi, T.; Kitaoka, Y.; Kakezawa, M.; Nishida, T. Purification and Characterization of a Nylon-Degrading Enzyme Purification and Characterization of a Nylon-Degrading Enzyme. *Appl. Environ. Microbiol.* **1998**, *64*, 1366−1371.
(522) Nomura, N.; Deguchi, T.; Shigeno-Akutsu, Y.; Nakajima-Kambe, T.; Nakahara, T. Gene Structures and Catalytic Mechanisms of Microbial Enzymes Able to Blodegrade the Synthetic Solid Polymers Nylon and Polyester Polyurethaoe. *Biotechnology and Genetic Engineering Reviews* **2001**, *18*, 125−147.
(523) Fujisawa, M.; Hirai, H.; Nishida. Degradation of Polyethylene and Nylon-66 by the Laccase-Mediator System. *J. Polym. Environ.* **2001**, *9*, 103−108.
(524) Uesono, Y.; Deguchi, T.; Nishida, T.; Takahara, Y.; Katayama, Y. Method for Decomposing Polyamide-Based Polymer Compound. JP 5304968A, 1991.
(525) Deguchi, T.; Nishida, T.; Takahara, Y. Method for Decomposing Synthetic High-Molecular Compound by Enzyme. JP 6296949A, 1993.
(526) Nishida, T.; Deguchi, T.; Takahara, Y. Method of Enzymatically Degrading Synthetic Polymer. WO1996011972A1, 1994.
(527) Nishida, T.; Kahata, M. Method for Decomposing Polyamide Resin. JP 2003128836A, 2001.
(528) *Optimizing a Microbial Platform to Break Down and Valorize Waste Plastic*; Open Plastic: Kingston, Ontario, 2022; www.openplastic.com.
(529) Takami, M. Biodegradable Polymer Composition and Molded Article. JP 6322263A, 1993.
(530) Eling, B.; Tomović, Ž.; Schädler, V. Current and Future Trends in Polyurethanes: An Industrial Perspective. *Macromol. Chem. Phys.* **2020**, *221*, 2000114.
(531) *The Polyurethanes*; Randall, D., Lee, S., Eds.; Wiley, 2003.
(532) Owen, S.; Otani, T.; Masaoka, S.; Ohe, T. The Biodegradation of Low-Molecular-Weight Urethane Compounds by a Strain of Exophiala Jeanselmei. *Biosci. Biotechnol. Biochem.* **1996**, *60*, 244−248.
(533) Akutsu-Shigeno, Y.; Adachi, Y.; Yamada, C.; Toyoshima, K.; Nomura, N.; Uchiyama, H.; Nakajima-Kambe, T. Isolation of a Bacterium That Degrades Urethane Compounds and Characterization of Its Urethane Hydrolase. *Appl. Microbiol. Biotechnol.* **2006**, *70*, 422−429.
(534) Howard, G. T. Microbial Biodegradation of Polyurethane. In *Recent Developments in Polymer Recycling*, 2011; Vol *661*, Chapter 7, pp 215−238.
(535) Magnin, A.; Pollet, E.; Perrin, R.; Ullmann, C.; Persillon, C.; Phalip, V.; Avérous, L. Enzymatic Recycling of Thermoplastic Polyurethanes: Synergistic Effect of an Esterase and an Amidase and Recovery of Building Blocks. *Waste Manag.* **2019**, *85*, 141−150.
(536) Liu, J.; He, J.; Xue, R.; Xu, B.; Qian, X.; Xin, F.; Blank, L. M.; Zhou, J.; Wei, R.; Dong, W.; Jiang, M. Biodegradation and Up-Cycling of Polyurethanes: Progress, Challenges, and Prospects. *Biotechnol. Adv.* **2021**, *48*, 107730.
(537) Howard, G. T.; Norton, W. N.; Burks, T. Growth of *Acinetobacter Gerneri* P7 on Polyurethane and the Purification and Characterization of a Polyurethanase Enzyme. *Biodegradation* **2012**, *23*, 561−573.
(538) Gautam, R.; Bassi, A. S.; Yanful, E. K. *Candida Rugosa* Lipase-Catalyzed Polyurethane Degradation in Aqueous Medium. *Biotechnol. Lett.* **2007**, *29*, 1081−1086.
(539) Biffinger, J. C.; Barlow, D. E.; Cockrell, A. L.; Cusick, K. D.; Hervey, W. J.; Fitzgerald, L. A.; Nadeau, L. J.; Hung, C. S.; Crookes-Goodson, W. J.; Russell, J. N. The Applicability of Impranil® DLN for Gauging the Biodegradation of Polyurethanes. *Polym. Degrad. Stab.* **2015**, *120*, 178−185.
(540) Álvarez-Barragán, J.; Domínguez-Malfavón, L.; Vargas-Suárez, M.; González-Hernández, R.; Aguilar-Osorio, G.; Loza-Tavera, H. Biodegradative Activities of Selected Environmental Fungi on a Polyester Polyurethane Varnish and Polyether Polyurethane Foams. *Appl. Environ. Microbiol.* **2016**, *82*, 5225−5235.
(541) Osman, M.; Satti, S. M.; Luqman, A.; Hasan, F.; Shah, Z.; Shah, A. A. Degradation of Polyester Polyurethane by Aspergillus Sp. Strain S45 Isolated from Soil. *J. Polym. Environ.* **2018**, *26*, 301−310.
(542) Vargas-Suárez, M.; Savín-Gámez, A.; Domínguez-Malfavón, L.; Sánchez-Reyes, A.; Quirasco-Baruch, M.; Loza-Tavera, H. Exploring the Polyurethanolytic Activity and Microbial Composition

https://doi.org/10.1021/acs.chemrev.2c00644
Chem. Rev. XXXX, XXX, XXX−XXX

of Landfill Microbial Communities. *Appl. Microbiol. Biotechnol.* **2021**, *105*, 7969−7980.
(543) Schmidt, J.; Wei, R.; Oeser, T.; Dedavid e Silva, L. A.; Breite, D.; Schulze, A.; Zimmermann, W. Degradation of Polyester Polyurethane by Bacterial Polyester Hydrolases. *Polymers (Basel).* **2017**, *9*, 65.
(544) El-Sayed, A. H. M. M.; Mahmoud, W. M.; Davis, E. M.; Coughlin, R. W. Biodegradation of Polyurethane Coatings by Hydrocarbon-Degrading Bacteria. *Int. Biodeterior. Biodegrad.* **1996**, *37*, 69−79.
(545) Oceguera-Cervantes, A.; Carrillo-García, A.; López, N.; Bolaños-Nuñez, S.; Cruz-Gómez, M. J.; Wacher, C.; Loza-Tavera, H. Characterization of the Polyurethanolytic Activity of Two Alicycliphilus Sp. Strains Able to Degrade Polyurethane and N-Methylpyrrolidone. *Appl. Environ. Microbiol.* **2007**, *73*, 6214−6223.
(546) Ruiz, C.; Howard, G. T. Nucleotide Sequencing of a Polyurethanase Gene (PulA) from *Pseudomonas Fluorescens*. *Int. Biodeterior. Biodegrad.* **1999**, *44*, 127−131.
(547) Russell, J. R.; Huang, J.; Anand, P.; Kucera, K.; Sandoval, A. G.; Dantzler, K. W.; Hickman, D. S.; Jee, J.; Kimovec, F. M.; Koppstein, D.; Marks, D. H.; Mittermiller, P. A.; Núñez, S. J.; Santiago, M.; Townes, M. A.; Vishnevetsky, M.; Williams, N. E.; Vargas, M. P. N.; Boulanger, L. A.; Bascom-Slack, C.; Strobel, S. A. Biodegradation of Polyester Polyurethane by Endophytic Fungi. *Appl. Environ. Microbiol.* **2011**, *77*, 6076−6084.
(548) Crabbe, J. R.; Campbell, J. R.; Thompson, L.; Walz, S. L.; Schultz, W. W. Biodegradation of a Colloidal Ester-Based Polyurethane by Soil Fungi. *Int. Biodeterior. Biodegrad.* **1994**, *33*, 103−113.
(549) Mathur, G.; Prasad, R. Degradation of Polyurethane by *Aspergillus Flavus* (ITCC 6051) Isolated from Soil. *Appl. Biochem. Biotechnol.* **2012**, *167*, 1595−1602.
(550) Peng, Y. H.; Shih, Y.-h.; Lai, Y. C.; Liu, Y. Z.; Liu, Y. T.; Lin, N. C. Degradation of Polyurethane by Bacterium Isolated from Soil and Assessment of Polyurethanolytic Activity of a *Pseudomonas Putida* Strain. *Environ. Sci. Pollut. Res.* **2014**, *21*, 9529−9537.
(551) Ruiz, C.; Main, T.; Hilliard, N. P.; Howard, G. T. Purification and Characterization of Two Polyurethanase Enzymes from *Pseudomonas Chlororaphis*. *Int. Biodeterior. Biodegrad.* **1999**, *43*, 43−47.
(552) Howard, G. T.; Crother, B.; Vicknair, J. Cloning, Nucleotide Sequencing and Characterization of a Polyurethanase Gene (PueB) from *Pseudomonas Chlororaphis*. *Int. Biodeterior. Biodegrad.* **2001**, *47*, 141−149.
(553) Stern, R. V.; Howard, G. T. The Polyester Polyurethanase Gene (PueA) from *Pseudomonas Chlororaphis* Encodes a Lipase. *FEMS Microbiol. Lett.* **2000**, *185*, 163−168.
(554) Howard, G. T.; Mackie, R. I.; Cann, I. K. O.; Ohene-Adjei, S.; Aboudehen, K. S.; Duos, B. G.; Childers, G. W. Effect of Insertional Mutations in the PueA and PueB Genes Encoding Two Polyurethanases in *Pseudomonas Chlororaphis* Contained within a Gene Cluster. *J. Appl. Microbiol.* **2007**, *103*, 2074−2083.
(555) Gautam, R.; Bassi, A. S.; Yanful, E. K.; Cullen, E. Biodegradation of Automotive Waste Polyester Polyurethane Foam Using *Pseudomonas Chlororaphis* ATCC55729. *Int. Biodeterior. Biodegrad.* **2007**, *60*, 245−249.
(556) Montgomery, M. T.; Campbell, J. R.; Crabbe, J. R.; Walz, S. E.; Thompson, L. Pseudomonas Chlororaphis Microorganism Polyurethane Degrading Enzyme Obtained Therefrom and Method of Using Enzyme. US 5714378A, 1995.
(557) Biffinger, J. C.; Barlow, D. E.; Pirlo, R. K.; Babson, D. M.; Fitzgerald, L. A.; Zingarelli, S.; Nadeau, L. J.; Crookes-Goodson, W. J.; Russell, J. N. A Direct Quantitative Agar-Plate Based Assay for Analysis of *Pseudomonas Protegens* Pf-5 Degradation of Polyurethane Films. *Int. Biodeterior. Biodegrad.* **2014**, *95* (PB), 311−319.
(558) Hung, C. S.; Zingarelli, S.; Nadeau, L. J.; Biffinger, J. C.; Drake, C. A.; Crouch, A. L.; Barlow, D. E.; Russell, J. N.; Crookes-Goodson, W. J. Carbon Catabolite Repression and Impranil Polyurethane Degradation in Pseudomonas Protegens Strain Pf-5. *Appl. Environ. Microbiol.* **2016**, *82*, 6080−6090.
(559) Zha, D. M.; Wang, X. L.; Xiao, X. H.; Shi, H. Q.; Yang, Y. W.; Shi, X.; Kang, Y. B. Two Polyurethanases PueA and PueB Are Major Extracellular Lipases Partly Secreted by the Mediation of Their Cognate ABC Exporter AprDEF in *Pseudomonas Protegens* Pf-5. *Lett. Appl. Microbiol.* **2021**, *73*, 652−657.
(560) do Canto, V. P.; Thompson, C. E.; Netz, P. A. Computational Studies of Polyurethanases from Pseudomonas. *J. Mol. Model.* **2021**, *27*, 1−8.
(561) Nakajima-Kambe, T.; Onuma, F.; Kimpara, N.; Nakahara, T. Isolation and Characterization of a Bacterium Which Utilizes Polyester Polyurethane as a Sole Carbon and Nitrogen Source. *FEMS Microbiol. Lett.* **1995**, *129*, 39−42.
(562) Akutsu, Y.; Nakajima-Kambe, T.; Nomura, N.; Nakahara, T. Purification and Properties of a Polyester Polyurethane-Degrading Enzyme from *Comamonas Acidovorans* TB-35. *Appl. Environ. Microbiol.* **1998**, *64*, 62−67.
(563) Nomura, N.; Shigeno-Akutsu, Y.; Nakajima-Kambe, T.; Nakahara, T. Cloning and Sequence Analysis of a Polyurethane Esterase of *Comamonas Acidovorans* TB-35. *J. Ferment. Bioeng.* **1998**, *86*, 339−345.
(564) Naidu, R. B.; Ramesh, R.; Oliver, N. G. E.; Prasad D, P. S. A Novel Esterase and a Process for Preparation Thereof. IN 201101937I1, 2011.
(565) Festel, G.; Haensel, E.; Klein, H.; Koch, R.; Lund, H. Process for Enzymatic Decomposition of Biodegradable Adhesives for the Cleaning of Vessels, Workplaces and Equipment, Using an Aqueous Solution Containing One or More Lipases or Cutinases. DE 19834359A1, 1998.
(566) Koch, R.; Lund, H. Decomposition de Polymeres Biodegradables Avec Des Enzymes. WO 1998036086A1, 1997.
(567) Di Bisceglie, F.; Quartinello, F.; Vielnascher, R.; Guebitz, G. M.; Pellis, A. Cutinase-Catalyzed Polyester-Polyurethane Degradation: Elucidation of the Hydrolysis Mechanism. *Polymers (Basel).* **2022**, *14*, 411.
(568) Magnin, A.; Pollet, E.; Avérous, L. Characterization of the Enzymatic Degradation of Polyurethanes. *Methods Enzymol.* **2021**, *648*, 317−336.
(569) Magnin, A.; Entzmann, L.; Pollet, E.; Avérous, L. Breakthrough in Polyurethane Bio-Recycling: An Efficient Laccase-Mediated System for the Degradation of Different Types of Polyurethanes. *Waste Manage.* **2021**, *132*, 23−30.
(570) Santerre, J. P.; Labow, R. S.; Duguay, D. G.; Erfle, D.; Adams, G. A. Biodegradation Evaluation of Polyether and Polyester-urethanes with Oxidative and Hydrolytic Enzymes. *J. Biomed. Mater. Res.* **1994**, *28*, 1187−1199.
(571) Ufarté, L.; Laville, E.; Duquesne, S.; Morgavi, D.; Klopp, C.; Rizzo, A.; Pizzut-Serin, S.; Potocki-Veronese, G. Discovery of Carbamate Degrading Enzymes by Functional Metagenomic. *PLoS One* **2017**, *12*, No. e0189201.
(572) Ibrahim, I. N.; Maraqa, A.; Hameed, K. M.; Saadoun, I. M.; Maswadeh, H. M.; Nakajima-Kambe, T. Polyester-Polyurethane Biodegradation by Alternaria Solani, Isolated from Northern Jordan. *Adv. Environ. Biol.* **2009**, *2*, 62−170.
(573) Phua, S. K.; Castillo, E.; Anderson, J. M.; Hiltner, A. Biodegradation of a Polyurethane in Vitro. *J. Biomed. Mater. Res.* **1987**, *21*, 231−246.
(574) Labow, R. S.; Erfle, D. J.; Santerre, J. P. Elastase-Induced Hvdrolvsis of Synthetic Solid Sub & Rate & Poly (Ester-Urea-Urethane) and Poly(Ether-Urea-Urethane). *Biomaterials* **1996**, *17*, 2381−2388.
(575) Yamamoto, N.; Nakayama, A.; Oshima, M.; Kawasaki, N.; Aiba, S.-i. Enzymatic Hydrolysis of Lysine Diisocyanate Based Polyurethanes and Segmented Polyurethane Ureas by Various Proteases. *React. Funct. Polym.* **2007**, *67*, 1338−1345.
(576) Campiñez, M. D.; Aguilar-De-Leyva, Á.; Ferris, C.; De Paz, M. V.; Galbis, J. A.; Caraballo, I. Study of the Properties of the New Biodegradable Polyurethane PU (TEG-HMDI) as Matrix Forming Excipient for Controlled Drug Delivery. *Drug Dev. Ind. Pharm.* **2013**, *39*, 1758−1764.

https://doi.org/10.1021/acs.chemrev.2c00644
Chem. Rev. XXXX, XXX, XXX−XXX

(577) Wlodawer, A.; Li, M.; Dauter, Z.; Gustchina, A.; Uchida, K.; Oyama, H.; Dunn, B.; Oda, K. Carboxyl Proteinase from Pseudomonas Defines a Novel Family of Subtilisin-like Enzymes. *Nat. Struct. Biol.* **2001**, *8*, 442−446.
(578) Gamerith, C.; Herrero Acero, E.; Pellis, A.; Ortner, A.; Vielnascher, R.; Luschnig, D.; Zartl, B.; Haernvall, K.; Zitzenbacher, S.; Strohmeier, G.; et al. Improving Enzymatic Polyurethane Hydrolysis by Tuning Enzyme Sorption. *Polym. Degrad. Stab.* **2016**, *132*, 69−77.
(579) Jansen, B.; Schumacher-Perdreau, F.; Peters, G.; Pulverer, G. Evidence for Degradation of Synthetic Polyurethanes by *Staphylococcus Epidermidis*. *Zentralblatt fur Bakteriol.* **1991**, *276*, 36−45.
(580) Ignat, L.; Ignat, M.; Ciobanu, C.; Doroftei, F.; Popa, V. I. Effects of Flax Lignin Addition on Enzymatic Oxidation of Poly(Ethylene Adipate) Urethanes. *Ind. Crops Prod.* **2011**, *34*, 1017−1028.
(581) Magnin, A.; Entzmann, L.; Bazin, A.; Pollet, E.; Avérous, L. Green Recycling Process for Polyurethane Foams by a Chem-Biotech Approach. *ChemSusChem* **2021**, *14*, 4234−4241.
(582) Branson, A. Y.; Söltl, S.; Buchmann, C.; Wei, R.; Schaffert, L.; Badenhorst, C. P. S.; Reisky, L.; Bornscheuer, U. Urethanases for the enzymatic hydrolysis of low molecular weight carbamates and the recycling of polyurethanes. *Angew. Chem. Int Ed.* **2023**, e202216220.
(583) Sangale, M. K. A Review on Biodegradation of Polythene: The Microbial Approach. *J. Bioremediation Biodegrad.* **2012**, *03*, 164.
(584) Ojeda, T.; Freitas, A.; Birck, K.; Dalmolin, E.; Jacques, R.; Bento, F.; Camargo, F. Degradability of Linear Polyolefins under Natural Weathering. *Polym. Degrad. Stab.* **2011**, *96*, 703−707.
(585) Mohanan, N.; Montazer, Z.; Sharma, P. K.; Levin, D. B. Microbial and Enzymatic Degradation of Synthetic Plastics. *Front. Microbiol.* **2020**, *11*, 580709.
(586) Auta, H. S.; Emenike, C. U.; Fauziah, S. H. Distribution and Importance of Microplastics in the Marine EnvironmentA Review of the Sources, Fate, Effects, and Potential Solutions. *Environ. Int.* **2017**, *102*, 165−176.
(587) Pramila, R.; Ramesh, K. V. Biodegradation of Low Density Polyethylene (LDPE) by Fungi Isolated from Marine Water- a SEM Analysis. *African J. Microbiol. Res.* **2011**, *5*, 5013−5018.
(588) Usha, R.; Sangeetha, T.; Palaniswamy, M. Screening of Polyethylene Degrading Microorganisms from Garbage Soil. *Libyan Agric. Res. Cent. J. Int.* **2011**, *2*, 200−204.
(589) Satlewal, A.; Soni, R.; Zaidi, M.; Shouche, Y.; Goel, R. Comparative Biodegradation of HDPE and LDPE Using an Indigenously Developed Microbial Consortium. *J. Microbiol. Biotechnol.* **2008**, *18*, 477−482.
(590) Restrepo-Flórez, J. M.; Bassi, A.; Thompson, M. R. Microbial Degradation and Deterioration of Polyethylene - A Review. *Int. Biodeterior. Biodegrad.* **2014**, *88*, 83−90.
(591) Deepika, S.; Madhuri, R. J. Biodegradation of Low Density Polyethylene by Micro-Organisms from Garbage Soil. *J. Exp. Biol. Agric. Sci.* **2015**, *3*, 15−21.
(592) Paço, A.; Duarte, K.; da Costa, J. P.; Santos, P. S. M.; Pereira, R.; Pereira, M. E.; Freitas, A. C.; Duarte, A. C.; Rocha-Santos, T. A. P. Biodegradation of Polyethylene Microplastics by the Marine Fungus Zalerion Maritimum. *Sci. Total Environ.* **2017**, *586*, 10−15.
(593) Muhonja, C. N.; Makonde, H.; Magoma, G.; Imbuga, M. Biodegradability of Polyethylene by Bacteria and Fungi from Dandora Dumpsite Nairobi-Kenya. *PLoS One* **2018**, *13*, e0198446.
(594) DSouza, G. C.; Sheriff, R. S.; Ullanat, V.; Shrikrishna, A.; Joshi, A. V.; Hiremath, L.; Entoori, K. Fungal Biodegradation of Low-Density Polyethylene Using Consortium of Aspergillus Species under Controlled Conditions. *Heliyon* **2021**, *7*, No. e07008.
(595) Singh, R.; Pant, D. Polyvinyl Chloride Degradation by Hybrid (Chemical and Biological) Modification. *Polym. Degrad. Stab.* **2016**, *123*, 80−87.
(596) Dang, T. C. H.; Nguyen, D. T.; Thai, H.; Nguyen, T. C.; Hien Tran, T. T.; Le, V. H.; Nguyen, V. H.; Tran, X. B.; Thao Pham, T. P.; Nguyen, T. G.; Nguyen, Q. T. Plastic Degradation by Thermophilic Bacillus Sp. BCBT21 Isolated from Composting Agricultural Residual in Vietnam. *Adv. Nat. Sci. Nanosci. Nanotechnol.* **2018**, *9*, 015014.
(597) Kowalczyk, A.; Chyc, M.; Ryszka, P.; Latowski, D. Achromobacter Xylosoxidans as a New Microorganism Strain Colonizing High-Density Polyethylene as a Key Step to Its Biodegradation. *Environ. Sci. Pollut. Res.* **2016**, *23*, 11349−11356.
(598) Ojha, N.; Pradhan, N.; Singh, S.; Barla, A.; Shrivastava, A.; Khatua, P.; Rai, V.; Bose, S. Evaluation of HDPE and LDPE Degradation by Fungus, Implemented by Statistical Optimization. *Sci. Rep.* **2017**, *7*, 39515.
(599) Goel, R.; Sah, A.; Negi, H.; Kapri, A. Process for the Preparation of Talc Based Formulation for LDPE-Degrading Bacterial Consortia. US 20120196351A1, 2011.
(600) Cheung, L. Methods and Compositions for Degrading Polymeric Compounds. US 20020123130A1, 2001.
(601) Tanaka, K.; Shigeta, T.; Kikkawa, N.; Kumura, N.; Ono, K. Method of Producing Decomposable Resin Moldings. US 3909468, 1973.
(602) Jie, Z.; Guocai, Z.; Binsong, W.; Yujie, G.; Changli, L.; Mingyan, C.; Kongli, H.; Shanshan, W.; Xinxin, D.; Yanfei, J.; Chao, G. Method for Producing Alkane from Strain of Pichia Guilliermondii by Degrading Polyethylene. CN 110283853, 2019.
(603) Jie, Z.; Changli, L.; Binsong, W.; Guocai, Z.; Shanshan, W.; Mingyan, C.; Kongli, H.; Xinxin, D.; Yanfei, J.; Chao, G.; Tianshun, W. Method for Biodegrading Polyethylene by Utilizing Serratia Marcescens. CN 111084957, 2020.
(604) Xia, L.; Wenjie, G.; Shaohai, Y.; Hangtao, W.; Peizhi, X.; Yusheng, L.; Kaizhi, X.; Lili, S. Penicillium Citrinum Fungus for Thin Film Degradation and Application Thereof. CN 107354101, 2019.
(605) Yan, N. Recycling Plastic Using a Hybrid Process. *Science (80-.).* **2022**, *378*, 132−133.
(606) Sullivan, K. P.; Werner, A. Z.; Ramirez, K. J.; Ellis, L. D.; Bussard, J. R.; Black, B. A.; Brandner, D. G.; Bratti, F.; Buss, B. L.; Dong, X.; Haugen, S. J.; et al. Mixed Plastics Waste Valorization through Tandem Chemical Oxidation and Biological Funneling. *Science (80-.).* **2022**, *378*, 207−211.
(607) Cacciari, I.; Quatrini, P.; Zirletta, G.; Mincione, E.; Vinciguerra, V.; Lupattelli, P.; Sermanni, G. G. Isotactic Polypropylene Biodegradation by a Microbial Community: Physicochemical Characterization of Metabolites Produced. *Appl. Environ. Microbiol.* **1993**, *59*, 3695−3700.
(608) Skariyachan, S.; Taskeen, N.; Kishore, A. P.; Krishna, B. V. Recent Advances in Plastic Degradation- From Microbial Consortia-Based Methods to Data Sciences and Computational Biology Driven Approaches. *J. Hazard. Mater.* **2021**, *426*, 128086.
(609) Frederico, T. D.; Peixoto, J.; Fernandes de Sousa, J.; Vizzotto, C. S.; Steindorff, A. S.; Bezerra Pinto, O. H.; Kruger, R. H. Draft Genome Sequence of *Stenotrophomonas Maltophilia* Strain PE591, a Polyethylene-Degrading Bacterium Isolated from Savanna Soil. *Microbiol. Resour. Announc.* **2020**, *10*, e00490-21.
(610) Furlan, J. P. R.; Lopes, R.; Stehling, E. G. Whole-Genome Sequence-Based Analysis of the Paenibacillus Aquistagni Strain DK1, a Polyethylene-Degrading Bacterium Isolated from Landfill. *World J. Microbiol. Biotechnol.* **2021**, *37*, 1−9.
(611) Gravouil, K.; Ferru-Clément, R.; Colas, S.; Helye, R.; Kadri, L.; Bourdeau, L.; Moumen, B.; Mercier, A.; Ferreira, T. Transcriptomics and Lipidomics of the Environmental Strain *Rhodococcus Ruber* Point out Consumption Pathways and Potential Metabolic Bottlenecks for Polyethylene Degradation. *Environ. Sci. Technol.* **2017**, *51*, 5172−5181.
(612) Zampolli, J.; Orro, A.; Manconi, A.; Ami, D.; Natalello, A.; Di Gennaro, P. Transcriptomic Analysis of *Rhodococcus Opacus* R7 Grown on Polyethylene by RNA-Seq. *Sci. Rep.* **2021**, *11*, 1−14.
(613) Gao, R.; Liu, R.; Sun, C. A Marine Fungus *Alternaria Alternata* FB1 Efficiently Degrades Polyethylene. *J. Hazard. Mater.* **2022**, *431*, 128617.
(614) Brandon, A. M.; Gao, S. H.; Tian, R.; Ning, D.; Yang, S. S.; Zhou, J.; Wu, W. M.; Criddle, C. S. Biodegradation of Polyethylene and Plastic Mixtures in Mealworms (Larvae of *Tenebrio Molitor*) and

https://doi.org/10.1021/acs.chemrev.2c00644
Chem. Rev. XXXX, XXX, XXX−XXX

Effects on the Gut Microbiome. *Environ. Sci. Technol.* **2018**, *52*, 6526−6533.
(615) Yang, S. S.; Ding, M. Q.; Zhang, Z. R.; Ding, J.; Bai, S. W.; Cao, G. L.; Zhao, L.; Pang, J. W.; Xing, D. F.; Ren, N. Q.; Wu, W. M. Confirmation of Biodegradation of Low-Density Polyethylene in Dark- versus Yellow- Mealworms (Larvae of Tenebrio Obscurus versus Tenebrio Molitor) via. Gut Microbe-Independent Depolymerization. *Sci. Total Environ.* **2021**, *789*, 147915.
(616) Kundungal, H.; Gangarapu, M.; Sarangapani, S.; Patchaiyappan, A.; Devipriya, S. P. Efficient Biodegradation of Polyethylene (HDPE) Waste by the Plastic-Eating Lesser Waxworm (Achroia Grisella). *Environ. Sci. Pollut. Res.* **2019**, *26*, 18509−18519.
(617) Peng, B. Y.; Chen, Z.; Chen, J.; Yu, H.; Zhou, X.; Criddle, C. S.; Wu, W. M.; Zhang, Y. Biodegradation of Polyvinyl Chloride (PVC) in *Tenebrio Molitor* (*Coleoptera: Tenebrionidae*) Larvae. *Environ. Int.* **2020**, *145* (July), 106106.
(618) Pivato, A. F.; Miranda, G. M.; Prichula, J.; Lima, J. E. A.; Ligabue, R. A.; Seixas, A.; Trentin, D. S. Hydrocarbon-Based Plastics: Progress and Perspectives on Consumption and Biodegradation by Insect Larvae. *Chemosphere* **2022**, *293*, 133600.
(619) Bulak, P.; Proc, K.; Pytlak, A.; Puszka, A.; Gawdzik, B.; Bieganowski, A. Biodegradation of Different Types of Plastics by *Tenebrio Molitor* Insect. *Polymers (Basel).* **2021**, *13*, 3508.
(620) Bombelli, P.; Howe, C. J.; Bertocchini, F. Polyethylene Bio-Degradation by Caterpillars of the Wax Moth *Galleria Mellonella*. *Curr. Biol.* **2017**, *27* (8), R292−R293.
(621) Billen, P.; Khalifa, L.; Van Gerven, F.; Tavernier, S.; Spatari, S. Technological Application Potential of Polyethylene and Polystyrene Biodegradation by Macro-Organisms Such as Mealworms and Wax Moth Larvae. *Sci. Total Environ.* **2020**, *735*, 139521.
(622) Zhong, Z.; Nong, W.; Xie, Y.; Hui, J. H. L.; Chu, L. M. Long-Term Effect of Plastic Feeding on Growth and Transcriptomic Response of Mealworms (*Tenebrio Molitor L.*). *Chemosphere* **2022**, *287* (P1), 132063.
(623) Yang, G.; Ding, Y. Recent Advances in Biocatalyst Discovery, Development and Applications. *Bioorg. Med. Chem.* **2014**, *22*, 5604−5612.
(624) Ren, L.; Men, L.; Zhang, Z.; Guan, F.; Tian, J.; Wang, B.; Wang, J.; Zhang, Y.; Zhang, W. Biodegradation of Polyethylene by Enterobacter Sp. D1 from the Guts Ofwax Moth *Galleria Mellonella*. *Int. J. Environ. Res. Public Health* **2019**, *16*, 1941.
(625) Montazer, Z.; Habibi Najafi, M. B.; Levin, D. B. In Vitro Degradation of Low-Density Polyethylene by New Bacteria from Larvae of the Greater Wax Moth, *Galleria Mellonella*. *Can. J. Microbiol.* **2021**, *67* (3), 249−258.
(626) Yin, C. F.; Xu, Y.; Zhou, N. Y. Biodegradation of Polyethylene Mulching Films by a Co-Culture of Acinetobacter Sp. Strain NyZ450 and Bacillus Sp. Strain NyZ451 Isolated from Tenebrio Molitor Larvae. *Int. Biodeterior. Biodegrad.* **2020**, *155* (July), 105089.
(627) Luo, L.; Wang, Y.; Guo, H.; Yang, Y.; Qi, N.; Zhao, X.; Gao, S.; Zhou, A. Biodegradation of Foam Plastics by *Zophobas Atratus* Larvae (*Coleoptera: Tenebrionidae*) Associated with Changes of Gut Digestive Enzymes Activities and Microbiome. *Chemosphere* **2021**, *282*, 131006.
(628) Latour, S.; Noel, G.; Serteyn, L.; Sare, A. R.; Massart, S.; Delvigne, F.; Francis, F. Multi-Omics Approach Reveals New Insights into the Gut Microbiome of Galleria Mellonella (Lepidoptera:Pyralidae) Exposed to Polyethylene Diet. *bioRxiv* 2021, 2021.06.04.446152.
(629) Cheng, J.; Suh, D. Microorganism Isolated from Tenebrio Molitor Larva and Having Plastic Degrading Activity, and Method for Degrading Plastic Using Same. WO 2018143750A1, 2018.
(630) El-Shafei, H. A.; Abd El-Nasser, N. H.; Kansoh, A. L.; Ali, A. M. Biodegradation of Disposable Polyethylene by Fungi and Streptomyces Species. *Polym. Degrad. Stab.* **1998**, *62*, 361−365.
(631) Eubeler, J. P.; Bernhard, M.; Knepper, T. P. Environmental Biodegradation of Synthetic Polymers II. Biodegradation of Different Polymer Groups. *TrAC - Trends Anal. Chem.* **2010**, *29*, 84−100.
(632) Sanluis-Verdes, A.; Colomer-Vidal, P.; Rodriguez-Ventura, F.; Bello-Villarino, M.; Spinola-Amilibia, M.; Ruiz-Lopez, E.; Illanes-Vicioso, R.; Castroviejo, P.; Aiese Cigliano, R.; Montoya, M.; et al. Wax Worm Saliva and the Enzymes Therein Are the Key to Polyethylene Degradation by *Galleria Mellonella*. *Nat. Commun.* **2022**, *13*, 5568.
(633) Claus, H. Laccases: Structure, Reactions, Distribution. *Micron* **2004**, *35*, 93−96.
(634) Cañas, A. I.; Camarero, S. Laccases and Their Natural Mediators: Biotechnological Tools for Sustainable Eco-Friendly Processes. *Biotechnol. Adv.* **2010**, *28*, 694−705.
(635) Santo, M.; Weitsman, R.; Sivan, A. The Role of the Copper-Binding Enzyme - Laccase - in the Biodegradation of Polyethylene by the Actinomycete *Rhodococcus Ruber*. *Int. Biodeterior. Biodegrad.* **2013**, *84*, 204−210.
(636) Span, E.; Hattendorf, D. Methods for Enzymatic and Microbial Degradation of Polyethylene. WO 2021183867A1, 2021.
(637) Krueger, M. C.; Seiwert, B.; Prager, A.; Zhang, S.; Abel, B.; Harms, H.; Schlosser, D. Degradation of Polystyrene and Selected Analogues by Biological Fenton Chemistry Approaches: Opportunities and Limitations. *Chemosphere* **2017**, *173*, 520−528.
(638) Uzan, E.; Nousiainen, P.; Balland, V.; Sipila, J.; Piumi, F.; Navarro, D.; Asther, M.; Record, E.; Lomascolo, A. High Redox Potential Laccases from the Ligninolytic Fungi *Pycnoporus Coccineus* and *Pycnoporus Sanguineus* Suitable for White Biotechnology: From Gene Cloning to Enzyme Characterization and Applications. *J. Appl. Microbiol.* **2010**, *108*, 2199−2213.
(639) Mateljak, I.; Rice, A.; Yang, K.; Tron, T.; Alcalde, M. The Generation of Thermostable Fungal Laccase Chimeras by SCHEMA-RASPP Structure-Guided Recombination in Vivo. *ACS Synth. Biol.* **2019**, *8*, 833−843.
(640) Pometto, A. L.; Lee, B.; Johnson, K. E. Production of an Extracellular Polyethylene-Degrading Enzyme(s) by *Streptomyces Species*. *Appl. Environ. Microbiol.* **1992**, *58*, 731−733.
(641) Iiyoshi, Y.; Tsutsumi, Y.; Nishida, T. Polyethylene Degradation by Lignin-Degrading Fungi and Manganese Peroxidase. *J. Wood Sci.* **1998**, *44*, 222−229.
(642) Ehara, K.; Iiyoshi, Y.; Tsutsumi, Y.; Nishida, T. Polyethylene Degradation by Manganese Peroxidase in the Absence of Hydrogen Peroxide. *J. Wood Sci.* **2000**, *46*, 180−183.
(643) Nathan, J. L.; Kell, D. B. Enzymatic degradation of plastic polyalkene polymers by KatG enzyme. WO 2021205160A1, 2021.
(644) Zhao, J.; Guo, Z.; Ma, X.; Liang, G.; Wang, J. Novel Surface Modification of High-Density Polyethylene Films by Using Enzymatic Catalysis. *J. Appl. Polym. Sci.* **2004**, *91*, 3673−3678.
(645) Zhang, H.; Kong, D.; Wang, L.; Xia, W.; Yao, C.; Wu, J. Degradation of UV-Pretreated Polyolefins by Latex Clearing Protein from Streptomyces Sp. Strain K30. *Sci. Total Environ.* **2022**, *806*, 150779.
(646) Ho, B. T.; Roberts, T. K.; Lucas, S. An Overview on Biodegradation of Polystyrene and Modified Polystyrene: The Microbial Approach. *Crit. Rev. Biotechnol.* **2018**, *38*, 308−320.
(647) Kim, H.-W.; Jo, J. H.; Kim, Y.-B.; Le, T. K.; Cho, C.-W.; Yun, C.-H.; Chi, W. S.; Yeom, S.-J. Biodegradation of Polystyrene by Bacteria from the Soil in Common Environments. *J. Hazard. Mater.* **2021**, *416*, 126239.
(648) Savoldelli, J.; Tomback, D.; Savoldelli, H. Breaking down Polystyrene through the Application of a Two-Step Thermal Degradation and Bacterial Method to Produce Usable Byproducts. *Waste Manag.* **2017**, *60*, 123−126.
(649) Lu, Y.; Zhang, Y.; Deng, Y.; Jiang, W.; Zhao, Y.; Geng, J.; Ding, L.; Ren, H. Uptake and Accumulation of Polystyrene Microplastics in Zebrafish (*Danio Rerio*) and Toxic Effects in Liver. *Environ. Sci. Technol.* **2016**, *50*, 4054−4060.
(650) Hou, L.; Majumder, E. L.-W. Potential for and Distribution of Enzymatic Biodegradation of Polystyrene by Environmental Microorganisms. *Materials (Basel)* **2021**, *14*, 503.
(651) Nakamiya, K.; Sakasita, G.; Ooi, T.; Kinoshita, S. Enzymatic Degradation of Polystyrene by Hydroquinone Peroxidase of

https://doi.org/10.1021/acs.chemrev.2c00644
Chem. Rev. XXXX, XXX, XXX−XXX

Azotobacter Beijerinckii HM121. *J. Ferment. Bioeng.* **1997**, *84*, 480−482.
(652) Yang, Y.; Yang, J.; Wu, W. M.; Zhao, J.; Song, Y.; Gao, L.; Yang, R.; Jiang, L. Biodegradation and Mineralization of Polystyrene by Plastic-Eating Mealworms: Part 1. Chemical and Physical Characterization and Isotopic Tests. *Environ. Sci. Technol.* **2015**, *49*, 12080−12086.
(653) Xu, S.; Hui, X. Degradation Method of Plastic Foam. CN 103141445A, 2013.
(654) Kim, H. R.; Lee, H. M.; Yu, H. C.; Jeon, E.; Lee, S.; Li, J.; Kim, D. H. Biodegradation of Polystyrene by Pseudomonas Sp. Isolated from the Gut of Superworms (Larvae of *Zophobas Atratus*). *Environ. Sci. Technol.* **2020**, *54*, 6987−6996.
(655) Jiang, S.; Su, T.; Zhao, J.; Wang, Z. Biodegradation of Polystyrene by Tenebrio Molitor, Galleria Mellonella, and Zophobas Atratus Larvae and Comparison of Their Degradation Effects. *Polymers (Basel).* **2021**, *13*, 3539.
(656) Song, Y.; Qiu, R.; Hu, J.; Li, X.; Zhang, X.; Chen, Y.; Wu, W. M.; He, D. Biodegradation and Disintegration of Expanded Polystyrene by Land Snails *Achatina Fulica*. *Sci. Total Environ.* **2020**, *746*, 141289.
(657) Sun, J.; Prabhu, A.; Aroney, S. T. N.; Rinke, C. Insights into Plastic Biodegradation: Community Composition and Functional Capabilities of the Superworm (*Zophobas Morio*) Microbiome in Styrofoam Feeding Trials. *Microb. Genomics* **2022**, *8*, 1−19.
(658) Whitney, P. J. A Comparison of Two Methods for Testing Defined Formulations of PVC for Resistance to Fungal Colonisation with Two Methods for the Assessment of Their Biodegradation. *Int. Biodeterior. Biodegrad.* **1996**, *37*, 205−213.
(659) Das, G.; Bordoloi, N. K.; Rai, S. K.; Mukherjee, A. K.; Karak, N. Biodegradable and Biocompatible Epoxidized Vegetable Oil Modified Thermostable Poly(Vinyl Chloride): Thermal and Performance Characteristics Post Biodegradation with *Pseudomonas Aeruginosa* and Achromobacter Sp. *J. Hazard. Mater.* **2012**, *209−210*, 434−442.
(660) Shah, A. A.; Kato, S.; Shintani, N.; Kamini, N. R.; Nakajima-Kambe, T. Microbial Degradation of Aliphatic and Aliphatic-Aromatic Co-Polyesters. *Appl. Microbiol. Biotechnol.* **2014**, *98*, 3437−3447.
(661) Sumathi, T.; Viswanath, B.; Lakshmi, A. S.; SaiGopal, D. V. R. Production of Laccase by Cochliobolus Sp. Isolated Low Molecular Weight PVC. *Biochem. Res. Int.* **2016**, *2016*, 9519527.
(662) Giacomucci, L.; Raddadi, N.; Soccio, M.; Lotti, N.; Fava, F. Polyvinyl Chloride Biodegradation by *Pseudomonas Citronellolis* and *Bacillus Flexus*. *N. Biotechnol.* **2019**, *52*, 35−41.
(663) Giacomucci, L.; Raddadi, N.; Soccio, M.; Lotti, N.; Fava, F. Biodegradation of Polyvinyl Chloride Plastic Films by Enriched Anaerobic Marine Consortia. *Mar. Environ. Res.* **2020**, *158*, 104949.
(664) Patil, R. Isolation of Polyvinyl Chloride Degrading Bacterial Strains from Environmental Samples Using Enrichment Culture Technique. *African J. Biotechnol.* **2012**, *11*, 7947−7956.
(665) Anwar, M. S.; Kapri, A.; Chaudhry, V.; Mishra, A.; Ansari, M. W.; Souche, Y.; Nautiyal, C. S.; Zaidi, M. G. H.; Goel, R. Response of Indigenously Developed Bacterial Consortia in Progressive Degradation of Polyvinyl Chloride. *Protoplasma* **2016**, *253*, 1023−1032.

https://doi.org/10.1021/acs.chemrev.2c00644
Chem. Rev. XXXX, XXX, XXX−XXX